Programa de Doctorado en Tecnologías Industriales y Materiales

Escuela de Doctorado de la Universitat Jaume I

Alternative refrigerant mixtures to Isobutane (R-600a): energy efficiency enhancement and flammability reduction

A dissertation presented by Daniel Calleja Anta for the Degree of Doctor of Philosophy from the Universitat Jaume I

Daniel Calleja Anta

DANIEL|CALLEJA|ANTA

Firmado digitalmente por DANIEL|CALLEJA|ANTA
Nombre de reconocimiento (DN): cn=DANIEL|CALLEJA|ANTA, serialNumber=20911665L, givenName=DANIEL, sn=CALLEJA ANTA, ou=CIUDADANOS, o=ACCV, c=ES
Fecha: 2024.05.24 12:33:42 +02'00'

Rodrigo Llopis Doménech

Daniel Sánchez García-Vacas

RODRIGO|LLOPIS|DOMENECH

Firmado digitalmente por RODRIGO|LLOPIS|DOMENECH
Nombre de reconocimiento (DN): cn=RODRIGO|LLOPIS|DOMENECH, serialNumber=73391682Q, givenName=RODRIGO, sn=LLOPIS DOMENECH, ou=CIUDADANOS, o=ACCV, c=ES
Fecha: 2024.05.24 11:53:39 +02'00'

20473834 Q

Firmado digitalmente porSANCHEZ GARCIA-VACAS DANIEL - 20473834Q
Fecha:2024-05-24 11:39+02:00

Castelló de la Plana, May 2024

UNIVERSITAT
JAUME•I

Programa de Doctorado en Tecnologías Industriales y Materiales

Escuela de Doctorado de la Universitat Jaume I

Mezclas de refrigerantes alternativas al isobutano (R-600a): mejora de la eficiencia energética y reducción de la inflamabilidad

Memoria presentada por Daniel Calleja Anta **para optar al grado de doctor/a por la Universitat Jaume I**

Daniel Calleja Anta

Rodrigo Llopis Doménech

Daniel Sánchez García-Vacas

DANIEL|
CALLEJ
A|ANTA

Firmado digitalmente por DANIEL|
CALLEJA|ANTA
Nombre de reconocimiento (DN):
cn=DANIEL|CALLEJA|ANTA,
serialNumber=20911665L,
givenName=DANIEL, sn=CALLEJA
ANTA, ou=CIUDADANOS, o=ACCV,
c=ES
Fecha: 2024.05.24 12:34:25 +02'00'

RODRIGO
|LLOPIS|
DOMENE
CH

Firmado digitalmente por
RODRIGO|LLOPIS|
DOMENECH
Nombre de reconocimiento
(DN): cn=RODRIGO|LLOPIS|
DOMENECH,
serialNumber=73391682Q,
givenName=RODRIGO,
sn=LLOPIS DOMENECH,
ou=CIUDADANOS, o=ACCV,
c=ES
Fecha: 2024.05.24 11:12:02
+02'00'

20473834 Q

Firmado
digitalmente
porSANCHEZ
GARCIA-VAC
AS DANIEL -
20473834Q
Fecha:2024-0
5-24
11:39+02:00

Castelló de la Plana, Mayo 2024

Funding

Predoctoral contract:

- Subvenciones del Programa para la promoción de la investigación científica, el desarrollo tecnológico y la innovación en la Comunitat Valenciana. (project AICO/2018/058).
  1st November 2019 – 31st December 2020

- Ayudas predoctorales para la formación de personal investigador, Acción 3.1 del Pla de Promoción de la Investigación de la UJI para el año 2019 (Ref. PREDOC/2019/19).
  1st July 2020 – 30th June 2024

Research stays:

- Dipartimento di Ingegneria Industriale dell'Università degli Studi di Napoli Federico Università degli Studi di Napoli Federico II, Fisciano, Italy.
  6th February 2023 – 8th May 2023
  Financed by becas para realizar estancias temporales en otros centros de investigación, para el personal docente e investigador de la Universitat Jaume I, 2022 (Ref. E-2022-47).

Economic support:

- Conselleria d'Educació, Investigació, Cultura i Esport de la Generalitat Valenciana (project AICO/2018/058).
- Ministry of Science, Innovation and Universities of Spain (RTI2018-093501-B-C21).
- Jaume I University (project UJI-B2021-10).
- Ministerio de Ciencia e Innovación of Spain (project PID2021-126926OB-C21)
- Ministerio de Ciencia e Innovación of Spain (TED2021-130162B-I00)

Thesis by compendium of publications

- Calleja-Anta, D., Nebot-Andrés, L., Catalán-Gil, J., Sánchez, D., Cabello, R., Llopis, R., Thermodynamic screening of alternative refrigerants for R290 and R600a (2020) Results in Engineering, 5, art. no. 100081. DOI: 10.1016/j.rineng.2019.100081
  Journal Citation Indicator QUARTILE: Q1 (2021 quartile).
  Cited 41 times.
  DOCUMENT TYPE: Article
- Calleja-Anta, D., Nebot-Andrés, L., Cabello, R., Sánchez, D., Llopis, R., A3 and A2 refrigerants: Border determination and hunt for A2 low-GWP blends (2022) International Journal of Refrigeration, 134, 86-94. DOI: 10.1016/j.ijrefrig.2021.11.012
  Journal Impact Factor QUARTILE: Q2.
  Cited 6 times.
  DOCUMENT TYPE: Article
- Calleja-Anta, D., Nebot-Andrés, L., Sánchez, D., Cabello, R., Llopis, R., Drop-in substitutes for R-600a. Experimental evaluation and optimization of a commercial fridge (2022) Applied thermal Engineering, 211, art. no. 118490. DOI: 10.1016/j.applthermaleng.2022.118490
  Journal Impact Factor QUARTILE: Q1.
  Cited 3 times.
  DOCUMENT TYPE: Article
- Calleja-Anta, D., Sánchez, D., Nebot-Andrés, L., Cabello, R., Llopis, R., Alternative mixtures to R-600a. Theoretical assessment and experimental energy evaluation of binary mixtures in a commercial cooler (2023) International Journal of Refrigeration, 152, 83-92. DOI: 10.1016/j.ijrefrig.2023.05.009
  Journal Impact Factor QUARTILE: Q2 (2022 quartile).
  Cited 1 times.
  DOCUMENT TYPE: Article
- Calleja-Anta, D., Martínez-Angeles, M., Nebot-Andrés, L., Sánchez, D., Llopis, R., Optimizing R152a/R600 and R290/R600 Mixtures for Superior Energy Performance in Vapor Compression Systems: Promising Alternatives to Isobutane (R600a) (2023), Applied Thermal Engineering, art. no. 247, 123070. DOI: 10.1016/j.applthermaleng.2024.123070
  Journal Impact Factor QUARTILE: Q1 (2022 quartile).
  Cited 0 times.
  DOCUMENT TYPE: Article

“This thesis has been accepted by the co-authors of the publications listed above that have waved the right to present them as a part of another PhD thesis”

Abstract

This doctoral thesis addresses the search for alternative refrigerant mixtures to isobutane (R-600a) in vapor compression systems for refrigeration production, with the aim of improving energy efficiency and reducing its flammability.

Isobutane has been widely used in Europe in domestic and low-capacity commercial refrigeration installations due to its low global warming potential (GWP) and good energy properties. However, its high flammability imposes limitations on the maximum refrigerant charge and thus on the cooling capacity that systems can satisfy.

At the beginning of the PhD thesis it was observed, based on previous research, that there were real possibilities to go beyond the energy efficiencies achieved with pure hydrocarbons, and that refrigerant blends can be a viable solution that achieves a good balance between energy efficiency, volumetric capacity, low GWP and flammability.

This context motivated the research carried out in this PhD thesis, which focuses on the search for refrigerant blends that not only improve energy efficiency compared to R-600a, but also reduce its flammability classification. The aim is to identify new alternatives that overcome the limitations of isobutane and offer more efficient and safer solutions for refrigeration systems.

The study begins with a comprehensive thermodynamic analysis of 120 ternary blends of 10 refrigerants, revealing promising blends with significant COP increases compared to R-600a. In particular, blends such as R-1270/R-600, R-152a/R-600, R-1234yf/R-600, R-1234ze(E)/R-600 and R-290/R-600 show promise in improving energy efficiency.

It then focuses on the extension of a method that allows theoretical prediction of the flammable class of newly developed refrigerant blends. Using this method, the limiting compositions of binary hydrocarbon mixtures are calculated, highlighting the limited ability to reduce the flammability classification of hydrocarbons by mixing them with less flammable refrigerants.

Experimental tests are then carried out with the adaptation and instrumentation of domestic and commercial refrigeration units, demonstrating the energy consumption savings with the identified blends compared to R-600a. In the domestic refrigerator, the blends R-1234yf/R-600a (7.5/92.5)%, R-1234ze(E)/R-600 (10.5/89.5)% and R-290/R-600 (11/89)% show energy reductions of 2.15%, 3. 84% and 1.31% respectively; while in the commercial unit, R-1234ze(E)/R-600 (8/92)% and R-152a/R-600 (8/92)% mixtures show energy reductions of 2.69% and 5.04% respectively.

Finally, in order to directly measure the thermodynamic properties of the mixtures and experimentally determine the optimum composition of the R-152a/R-600 and R-290/R-600 mixtures, a test bench is constructed with a vapour compression cycle fitted with sensors, concluding that the optimum composition for both mixtures is 10/90%, obtaining average COP increases of 7.3% and 10.3% respectively.

In conclusion, this thesis identifies four binary blends as energy-efficient alternatives to isobutane, offering promising avenues to enhance refrigeration system performance. These blends exhibit operating parameters and thermodynamic properties akin to R-600a, obviating the need for system redesign and additional safety considerations. Additionally, it establishes that no binary refrigerant mixtures can achieve simultaneous reductions in flammability, increased energy efficiency, and low Global Warming Potential (GWP).

Resumen

Esta tesis doctoral aborda la búsqueda de mezclas de refrigerantes alternativas al isobutano (R-600a) en sistemas de compresión de vapor para la producción de frío, con el objetivo de mejorar la eficiencia energética y de reducir su inflamabilidad.

El isobutano ha sido ampliamente utilizado en Europa en instalaciones de refrigeración domésticas y comerciales de baja potencia debido a su bajo potencial de calentamiento global (GWP) y buenas propiedades energéticas. Sin embargo, su alta inflamabilidad impone limitaciones en la carga máxima de refrigerante y, por ende, en la capacidad frigorífica que los sistemas pueden satisfacer.

Al inicio de la tesis doctoral se observó, en base a investigaciones previas, que existían posibilidades reales de ir más allá de los rendimientos energéticos conseguidos con hidrocarburos puros, y que las mezclas de refrigerantes pueden ser una solución viable que logre un buen equilibrio entre eficiencia energética, capacidad volumétrica, bajo GWP e inflamabilidad.

Este contexto motivó la investigación llevada a cabo en esta tesis doctoral, que se centra en la búsqueda de mezclas de refrigerantes que no solo mejoraran la eficiencia energética en comparación con el R-600a, sino que también redujeran su clasificación inflamable. El objetivo es la identificación de nuevas alternativas que superen las limitaciones del isobutano y ofrezcan soluciones más eficientes y seguras para sistemas de refrigeración.

El estudio comienza con un análisis termodinámico exhaustivo de 120 mezclas ternarias de 10 refrigerantes, que revela mezclas prometedoras con aumentos significativos del COP en comparación con el R-600a. En particular, mezclas como R-1270/R-600, R-152a/R-600, R-1234yf/R-600, R-1234ze(E)/R-600 y R-290/R-600 aparecen como prometedoras en la mejora del rendimiento energético.

Posteriormente se centra en la extensión de un método que permita la predicción teórica de la clase inflamable de mezclas de refrigerantes de nueva creación. Utilizando este método, se calculan las composiciones límite de las mezclas binarias de hidrocarburos, poniendo de relieve la limitada capacidad de reducir el índice de inflamabilidad de los hidrocarburos mezclándolos con refrigerantes menos inflamables.

A continuación, se realizan ensayos experimentales con la adaptación e instrumentación de unidades de refrigeración domésticas y comerciales, demostrando el ahorro de consumo energético con las mezclas identificadas en comparación con el R-600a. En el frigorífico doméstico, las mezclas R-1234yf/R-600a (7.5/92.5)%, R-1234ze(E)/R-600

(10.5/89.5)% y R-290/R-600 (11/89)% muestran reducciones energéticas del 2.15%, 3.84% y 1.31% respectivamente; mientras que en el mueble comercial, las mezclas R-1234ze(E)/R-600 (8/92)% y R-152a/R-600 (8/92)% muestran reducciones energéticas del 2.69% y 5.04%.

Por último, con el objetivo de medir directamente las propiedades termodinámicas de las mezclas y determinar experimentalmente la composición óptima de las mezclas R-152a/R-600 y R-290/R-600, se construye un banco de pruebas con un ciclo de compresión de vapor provisto de sensores, concluyendo que la composición óptima para ambas mezclas es del 10/90%, obteniendo incrementos medios de COP del 7.3% y del 10.3% respectivamente.

En conclusión, esta tesis identifica cuatro mezclas binarias como alternativas al isobutano energéticamente eficientes, que ofrecen soluciones prometedoras para mejorar el rendimiento de los sistemas de refrigeración. Las mezclas presentan parámetros de funcionamiento y propiedades termodinámicas comparables a las del R-600a, lo que evita la necesidad de rediseñar los sistemas y de tener en cuenta consideraciones de seguridad adicionales. Además, establece que ninguna mezcla binaria de refrigerantes puede lograr simultáneamente reducciones de la inflamabilidad, una mayor eficiencia energética y un bajo Potencial de Calentamiento Global.

Resum

Aquesta tesi doctoral aborda la recerca de mescles de refrigerants alternatives al isobutano (R-600a) en sistemes de compressió de vapor per a la producció de fred, amb l'objectiu de millorar l'eficiència energètica i de reduir la seua inflamabilitat.

El isobutà s'ha utilitzat àmpliament a Europa en instal·lacions de refrigeració domèstiques i comercials de baixa potència a causa del seu baix potencial d'escalfament global (GWP) i bones propietats energètiques. No obstant això, la seua alta inflamabilitat imposa limitacions en la càrrega màxima de refrigerant i, per tant, en la capacitat frigorífica que els sistemes poden satisfer.

A l'inici de la tesi doctoral es va observar, sobre la base de recerques prèvies, que existien possibilitats reals d'anar més enllà dels rendiments energètics aconseguits amb hidrocarburs purs, i que les mescles de refrigerants poden ser una solució viable que aconseguisca un bon equilibri entre eficiència energètica, capacitat volumètrica, baix GWP i inflamabilitat.

Aquest context va motivar la recerca duta a terme en aquesta tesi doctoral, que se centra en la cerca de mescles de refrigerants que no sols milloraren l'eficiència energètica en comparació amb el R-600a, sinó que també reduïren la seua classificació inflamable. L'objectiu és la identificació de noves alternatives que superen les limitacions del isobutà i oferisquen solucions més eficients i segures per a sistemes de refrigeració.

L'estudi comença amb una anàlisi termodinàmica exhaustiva de 120 mescles ternàries de 10 refrigerants, que revela mescles prometedores amb augments significatius del COP en comparació amb el R-600a. En particular, mescles com a R-1270/R-600, R-152a/R-600, R-1234yf/R-600, R-1234ze(E)/R-600 i R-290/R-600 apareixen com a prometedores en la millora del rendiment energètic.

Posteriorment se centra en l'extensió d'un mètode que permeta la predicció teòrica de la classe inflamable de mescles de refrigerants de nova creació. Utilitzant aquest mètode, es calculen les composicions límit de les mescles binàries d'hidrocarburs, posant en relleu la limitada capacitat de reduir l'índex d'inflamabilitat dels hidrocarburs barrejant-los amb refrigerants menys inflamables.

A continuació, es realitzen assajos experimentals amb l'adaptació i instrumentació d'unitats de refrigeració domèstiques i comercials, demostrant l'estalvi de consum energètic amb les mescles identificades en comparació amb el R-600a. En el frigorífic domèstic, les barreges R-1234yf/R-*600a (7.5/92.5)%, R-1234ze(E)/R-600 (10.5/89.5)%

i R-290/R-600 (11/89)% mostren reduccions energètiques del 2.15%, 3.84% i 1.31% respectivament; mentre que en el moble comercial, les barreges R-1234ze(E)/R-600 (8/92)% i R-152a/R-600 (8/92)% mostren reduccions energètiques del 2.69% i 5.04%.

Finalment, amb l'objectiu de mesurar directament les propietats termodinàmiques de les mescles i determinar experimentalment la composició òptima de les mescles R-152a/R-600 i R-290/R-600, es construeix un banc de proves amb un cicle de compressió de vapor proveït de sensors, concloent que la composició òptima per a totes dues mescles és del 10/90%, obtenint increments mitjans de COP del 7.3% i del 10.3% respectivament.

En conclusió, aquesta tesi identifica quatre mescles binàries com a alternatives al isobutà energèticament eficients, que ofereixen solucions prometedores per a millorar el rendiment dels sistemes de refrigeració. Les mescles presenten paràmetres de funcionament i propietats termodinàmiques comparables a les del R-600a, la qual cosa evita la necessitat de redissenyar els sistemes i de tenir en compte consideracions de seguretat addicionals. A més, estableix que cap mescla binària de refrigerants pot aconseguir simultàniament reduccions de la inflamabilitat, una major eficiència energètica i un baix Potencial d'Escalfament Global.

Acknowledgments

I cannot begin this section of acknowledgments in any other way than by naming Rodrigo Llopis, my director, tutor and whom I am lucky to call a friend. Thank you for everything Rodri, from the first day I stepped into the lab for the first time in a not so distant February 2018 to do my internship for my degree in mechanical engineering, to then continue with the final degree project, final master project and to this day after 4 years of PhD. It was you who encouraged me to start my thesis and transmitted to me your love for research. It has been more than 6 years in which I have learned a lot from you, not only professionally but also personally, and in which sometimes you have done things that go far beyond the functions required of a thesis supervisor. Thank you for everything.

Of course, I must also dedicate some lines of thanks to Daniel Sánchez, also tutor of this thesis. Thank you for always being available and for helping me whenever I needed it. I have been lucky to have been able to learn with you and to be able to talk about any subject when I needed to, whether it was a Monday or a Sunday when we met in the lab without either of us expecting it.

To Laura Nebot, my office colleague and one of the people I am most happy to have met. What a great time we have had both inside and outside the university and what we still have left. To Manel Martínez, office and lab colleague, who, although you have been here for a short time, it seems like you have been here since the beginning.

I would also like to mention all the members of the GIT over the years, Ramón, Jesús, Fran, Rafa, who have made the hours in the lab and offices more entertaining.

Thanks to Professor William Mauro for giving me the opportunity to do my PhD at the Università degli Studi di Napoli, as well as to all his team, Alice, Giovanni and Francesco, who made me feel like one of them from the first day.

Doing the thesis has not only made me learn a lot about refrigerants, but I have also been able to meet a lot of people. Although I can't mention them all, I would like to highlight three of them. Nuria, part of my little social bubble during COVID. Gabriele, ustia! what a great time we had and what a great friend you have become. Dela, what a great time we've had over the years and how glad I am to have met you.

I also want to thank my friends, ‘Los Papus’. Saúl, Pablo, Padi, Balfa and Moncho. Thank you for being my support outside the university, for all the laughs, the good times and for always being there. I am so glad to have you as friends.

Finally, to my family. To my sister Irene, who has the ability to spread your joy wherever you go. To my grandmother Carmina, how I love you. And the most important people of all: my parents. Thank you, Dad and Mum, for everything. For being the people around whom my life has orbited, for giving me the financial support I needed to be able to study, for having supported me in all my decisions and for being the way you are. How lucky I am.

I have always said that the important thing in life is not the place you get to, but the road you travel and wow... what a road. Thank you all for making it possible.

Agradecimientos

No puedo empezar esta sección de agradecimientos de otra forma que no sea empezar nombrando Rodrigo Llopis, mi director, tutor y al que tengo la suerte de también poderle llamar amigo. Gracias por todo Rodri, desde el primer día que pise por primera vez el laboratorio en un no tan lejano febrero de 2018 para hacer las prácticas del grado de ingeniería mecánica, para después seguir con el TFG, TFM y hasta el día de hoy después de 4 años de doctorado. Fuiste tú quien me animo a empezar la tesis y me contagió su amor hacia la investigación. Han sido más de 6 años en los que he aprendido mucho de ti, no solo a nivel profesional si no también personal, y en los que a veces has hecho cosas que van mucho más allá de las funciones que se le piden a un director de tesis. Gracias por todo.

Como no, también tengo que dedicar unas líneas de agradecimiento a Daniel Sánchez, también tutor de esta tesis. Gracias por estar siempre disponible y por ayudarme siempre que lo he necesitado. Es una suerte poder haber aprendido contigo y poder charlar de cualquier tema cuando lo he necesitado, ya sea un lunes o algún domingo que nos hemos encontrado por el laboratorio sin que ninguno de los dos se lo esperase.

A Laura Nebot, mi compañera de despacho y una de las personas que más me alegro de haber conocido. Que bien lo hemos pasado tanto fuera como dentro de la uni y lo que aún nos queda. A Manel Martínez, compañero de despacho y laboratorio y que, aunque lleves poco tiempo, parece que estes aquí desde el principio.

Mencionar también a todos los miembros que han pasado por el GIT a lo largo de estos años, Ramón, Jesús, Fran, Rafa, y que han hecho las horas por el laboratorio y despachos más entretenidas.

Gracias al profesor William Mauro por darme la oportunidad de hacer la estancia del doctorado en la Università degli Studi di Napoli, así como a todo su equipo de trabajo, Alice, Giovanni y Francesco, que me hicieron sentir como uno más desde el primer día.

Hacer la tesis no solo me ha hecho aprender mucho de refrigerantes, también he podido conocer a muchas personas. Aunque a todas no puedo mencionarlas, me gustaría destacar a tres. Nuria, parte de mi pequeña burbuja social en época COVID. Gabriele, ustia! que bien que nos lo hemos pasado y que gran amigo te has vuelto. Dela, anda que no lo hemos pasado bien estos años y como me alegro de haberte conocido.

También tengo que agradecer a mis amigos, “Los Papus”. A Saúl, Pablo, Padi, Balfa y Moncho. Gracias por ser mi apoyo fuera de la universidad, por todas las risas, los buenos momentos y por estar siempre. Como me alegro de teneros como amigos.

Para acabar, a mi familia. A mi hermana Irene, que tienes la capacidad de contagiar tu alegría allí donde vas. A mi abuela Carmina, que como te quiero. Y las personas más importantes de todas: mis padres. Gracias Papá y Mamá por todo. Por ser las personas sobre la que ha orbitado mi vida, por darme el apoyo económico necesario para poder estudiar, por haberme apoyado en todas mis decisiones y por ser como sois. Que suerte que tengo.

Siempre he dicho que lo importante en vida no es el sitio al que llegues, si no el camino que recorres y vaya… que camino. Gracias a todos por hacerlo posible.

Contents

List of figures

List of tables

CHAPTER 1.
INTRODUCTION.

1 INTRODUCTION

1.1 Context

Global average temperatures have risen by 1.1ºC since the 19th century [1], with the five warmest years on record occurring from 2015 to 2019 [2]. This climate change, primarily caused by anthropogenic greenhouse gas emissions [3], threatens to push global temperatures up to 4.4ºC by the end of the century if current trends continue [4].

The refrigeration, air-conditioning and heat pump (RACHP) sector is one of the sectors that has the most significant impact on climate change. RACHP systems are crucial to understanding modern society. Refrigeration and air conditioning systems are essential for food preservation, air quality control, and various industrial applications. The International Institute of Refrigeration (IIR) reports that there are approximately 5 billion such systems in operation worldwide, including 2.6 billion air conditioning units and 2 billion domestic refrigerators and freezers [5]. The RACHP sector currently consumes around 20% of the world's electrical energy, and this figure is expected to double by 2050. However, the intensive use of energy in this sector comes at an environmental cost. According to IIR [6], approximately 7.8% of greenhouse gas emissions are a direct result of this industry.

Demand for cooling services is growing rapidly, driven by population growth, economic booms and rising global average temperatures. Refrigeration is essential for sustainable development, but growing demand in this sector would further accelerate climate change, leading to a vicious circle of increasing demand for cooling and higher greenhouse gas emissions.

In addition to the above, there is the scarcity of fossil resources to which Europe is subject and the fact that since Russia's invasion of Ukraine there has been a clear energy crisis due to Europe's dependence on Russian gas. To this end, in order to make Europe less energy dependent and more economically competitive, it is necessary to improve energy efficiency across the continent.

Thus, under the current paradigm, the refrigeration sector is subject to various regulations to make it more environmentally sustainable and energy efficient. At the European level, these regulations have started to become tangible as of 2014, with the European Council's target to reduce the EU's greenhouse gas emissions by at least 40% by 2030 compared to 1990 levels [7], and more recently by the REPowerEU plan, which has made this reduction more ambitious at 45% [8].

To meet this target, the refrigeration sector can contribute by reducing its emissions from direct sources through the use of refrigerants with low global warming potential (GWP), and from indirect sources by improving its energy efficiency, thereby reducing the emissions associated with the generation of the energy consumed. The following sections detail the regulations that have been adopted to achieve each of these objectives.

1.2 Evolution of the refrigerants and current status

The vast majority of refrigeration systems use vapor compression cycles based on the compression and expansion of a fluid and the exchange of heat with the environment. These fluids, commonly referred to as refrigerants, have evolved over time in response to the needs of society, the evolution of technology and environmental regulations.

The first fluids used were the substances available that met the minimum requirements for the proper functioning of machines, even if they had inherent dangers in their use. This period lasted from 1830 to 1930 and included solvents and volatile fluids such as ethers, ammonia, hydrocarbons, etc.

The next era, which began in 1931, was that of chlorofluorocarbons (CFCs) and hydrochlorofluorocarbons (HCFCs), refrigerants characterized by their stability and safety. However, in 1974, Molina and Rowland [9] discovered that these refrigerants had a high ozone depletion potential (ODP). This discovery was further affirmed by Chubachi [10] in 1983 through the measurement of the weakening of the ozone layer. As a result, HCFCs were gradually banned of HCFCs by the Montreal Protocol [11] from 1990 onwards.

The next family is hydrofluorocarbons (HFCs), which were safe and stable substances with low or zero ODP. However, they were not environmentally friendly due to their high global warming potential. It was therefore necessary to regulate and limit their use. The Kigali Amendment to the Montreal Protocol [12] established a phase-out schedule for reducing the use of HFCs worldwide. However, the European Union had already legislated in this regard through EU Regulation No. 517/2014 [13]. This regulation, commonly referred to as “F-Gas”, was the last major refrigerant revolution at the European level, as it restricts the use of HFCs in two ways. On the one hand, it establishes a maximum GWP for refrigerants to be used in new equipment, setting the limit at 150 for most applications from January 2022, although in other cases the limit is higher. This reduction has resulted in the elimination of most of the old refrigerants. Additionally, the regulation sets a timetable for reducing the use of HFCs by allocating trading quotas of 21% of the average amount traded between 2009 and 2012 in 2030.

Due to the above-mentioned restrictions, since the mid-2010s we have been immersed in the new generation of refrigerants, the so-called low GWP generation. These refrigerants are mainly natural refrigerants, mainly isobutane, propane, ammonia and carbon dioxide; and unsaturated halogenated hydrocarbon molecules (HFOs, HCFOs and HCOs), which are atmospherically unstable molecules, which means that they have a short lifetime and therefore very low GWP and ODP. This generation also includes refrigerant blends with a resulting GWP below the F-Gas threshold of 150.

However, recent studies have shown that certain current and alternative synthetic refrigerants (particularly HFOs) can produce significant amounts of trifluoroacetic acid (TFA) when they break down in the atmosphere. TFA is a persistent and long-lived chemical with potentially harmful (toxic) effects on animals, plants and humans. There are currently large uncertainties associated with TFA concentrations, so the environmental and safety acceptability of HFOs may be re-evaluated in the coming years [14, 15].

It should also be noted that in October 2023, F-Gas was revised and an agreement was reached in the European Parliament [16] which repeals Regulation (EU) No. 517/2014 and drastically accelerates the timetable for reducing the use of FGGs (Fluorinated Greenhouse Gases), allowing a maximum quota of 5.2% of 2009-2012 levels to be placed on the market from 2030, with a total phase-out in 2050. This means the virtual elimination of all FGG refrigerants in the near future, giving rise to a new generation: the generation of carbon-neutral refrigerants.

1.3 Sealed domestic and commercial refrigeration appliances

The sealed domestic and commercial refrigeration subsector is one of the most important subsectors within the refrigeration industry in terms of total electricity consumption, number of units in stock and annual sales. Depending on the use of these appliances, a distinction is made between:

- Domestic appliances: Comprises appliances widely used for domestic purposes, such as refrigerators, freezers and combined refrigerator-freezers. It is estimated that there is a total stock of 2 billion such units, to which must be added 200 million units sold annually (worth €35-50 billion). In 2019, this sector consumed approximately 4% of the world's electricity [5].
- Stand-alone commercial equipment: These include all stand-alone refrigeration equipment and cover a wide range of typologies: beverage coolers, ice-cream freezers, vending machines, water coolers, ice machines and professional

refrigeration cabinets. According to the IIR [5], in 2019 the stock of these appliances was estimated at 120 million units.

With the aim of reducing direct and indirect emissions, the European Union has implemented two regulations affecting this sub-sector, which have led to a complete overhaul:

- Directive 2009/125/EC of the European Parliament and of the Council of 21 October 2009 establishing a framework for the setting of ecodesign requirements for energy-related products [17]. Directive 2009/125/EC is transposed in different regulations (Regulation (EU) 2019/2019 [18] for household refrigeration products and EC 1095/2015 [19] for commercial refrigeration products), which set the minimum ecodesign requirements for energy-using products, prohibiting the placing on the market or putting into service of refrigeration equipment with an energy efficiency index below the limit set by these regulations. Furthermore, an energy label is proposed to visually categorize the energy efficiency of each product (Regulation (EU) 2019/2016 [20] for domestic refrigeration and Regulation (EU) 2015/1094 [21] for commercial refrigeration).
- Regulation EU 517/2014 of the European Parliament and of the Council of 16 April 2014 on fluorinated greenhouse gases [13], already discussed in the previous section.

These directives affect the design options as follows:

- Use of refrigerants with a GWP below 150.
- Compliance with a minimum annual energy efficiency index (EEI) of 100 for domestic appliances (<1500 liters) and 85 for commercial appliances.

With these restrictions, there are few refrigerants available that can meet the requirements, and almost all of them (with the exception of CO_2, which is not competitive in terms of energy efficiency in this type of applications) are flammable to a greater or lesser degree. This fact leads to additional safety regulations that limit the maximum refrigerant charge that can be used in each refrigerant circuit of an installation. Specifically, for domestic refrigeration the limit is 150 g according to IEC 60335-2-24:2022 [22] and for commercial units it is limited to 13 times the LFL with a maximum of 1 kg according to IEC 60335-2-89:2022 (which in practice means around 500 g for HCs and 1 kg for less flammable refrigerants). This limit is directly related to the maximum cooling capacity that these systems can handle.

Figure 1.1 outlines the rules and regulations for designing low or medium capacity stand-alone cooling systems for domestic applications, while Figure 1.2 outlines the same for commercial applications.

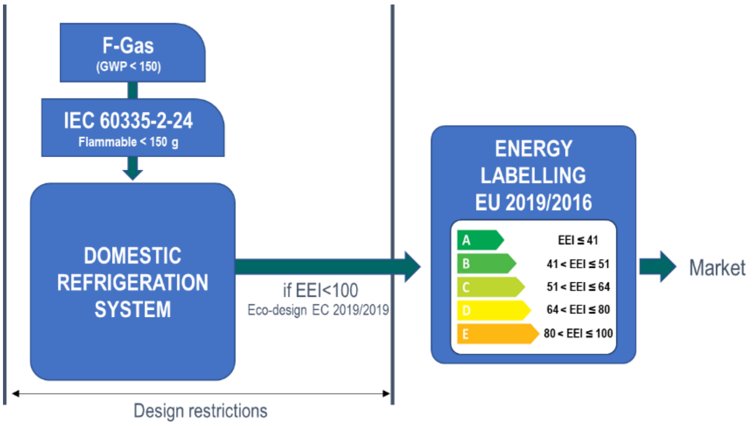

Figure 1.1. Regulations regarding the design of domestic refrigeration systems.

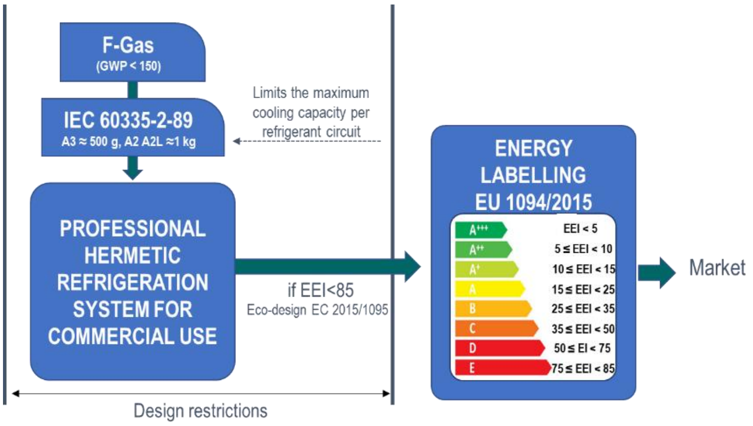

Figure 1.2. Regulations regarding the design of professional refrigeration systems.

With these restrictions, only a few refrigerants are available to meet the requirements. For domestic appliances, isobutane (R-600a) has clearly established itself as a long-term option and is currently the standard in Europe, with around 800 million units currently using this refrigerant [15]. For commercial refrigeration, there are more alternatives, but propane (R-290) predominates in the vast majority of applications, although there are some low-capacity units using R-600a.

These refrigerants have prevailed because of their almost negligible GWP and good energy efficiency, which allows them to comply with eco-design directives, although they have the disadvantage of being highly flammable. The 500 g load limit set by the

IEC for commercial appliances has a direct impact on the maximum cooling capacity that these systems can handle, which is estimated to be between 1095 and 710 W for R-600a [23, 24] and between 7350 and 3470 W for R-290 [25, 26]. Although these cooling capacities may be sufficient for most applications, achieving them with 500 g requires the use of advanced heat exchangers configurations that minimise refrigerant charge and add cost to the installation. Alternatively, to reach or even surpass this cooling capacity limit, the standard also allows the use of independent circuits, each with a maximum of 500 g, but this also represents an additional cost. The use of a refrigerant with a less flammable classification would allow to reduce costs or increase the maximum cooling capacity.

1.4 Previous investigations to the doctoral thesis

R-600a and R-290 are the standard pure refrigerants in Europe for sealed refrigeration appliances since the beginning of the 2010s. They have been demonstrated as valid refrigerants in the current context. However, at the beginning of the thesis, the idea of exploring refrigerants or mixtures of refrigerants that could improve the energetic and flammable characteristics of these refrigerants was raised.

Various studies, including those conducted by McLinden, et al. [27], McLinden, et al. [28], and Domanski, et al. [29], have demonstrated that the potential for discovering new pure refrigerants that meet current regulations is severely limited and that refrigerant mixtures may be a viable solution that achieves a good balance between Coefficient Of Performance (COP), volumetric capacity (VCC), low-GWP, and flammability.

At the beginning of the thesis, there were already proven possibilities of improving machine performance by considering the use of refrigerant mixtures. This can lead to COP increases of up to 11% and, in some cases, simultaneously reduce refrigerant flammability. Table 1.1 summarizes the most relevant research on alternative fluids to R-290 and R-600a based on refrigerant mixtures.

It should be noted that these mixtures were not specifically studied as alternatives to the two hydrocarbons but rather as alternatives to previous generation refrigerants. Along with these mixtures, in some articles R-290 and R-600a were also tested, enabling a comparative analysis. These studies incidentally suggested potential alternatives to R-290 and R-600a. However, the authors do not provide the reasons behind the chosen mixtures, focusing only on the experimental results. There has not been comprehensive research in this area.

Table 1.1. Previous research to the doctoral thesis on alternative mixtures to R-290.

Authors	Mixture or fluids	System	Results
Jung, et al. [30]	R290/R600a (mixtures with different proportions)	Single-evaporator domestic refrigerator	R290/R600a (60, 40% mass) showed 2-4% increase in energy efficiency.
Wongwises and Chimres [31]	R290, R600, R600a, R134a (mixtures with different proportions)	Household refrigerator for fresh and frozen food	R290/R600 (60, 40% mass) is the most appropriate alternative.
Mohanraj, et al. [32]	R290/R600a (45.2/54.8 % mass)	Single-evaporator domestic refrigerator	Energy consumption reduction of 11.1% respect R-134a. COP increased 3.6%.
Rasti, et al. [33]	R436A (R600a/R290 46/54% mass)	Single-evaporator vertical household refrigerator	Energy consumption reduction of 8% respect R-600a.
Yu and Teng [34]	R290/R600a (different proportions)	Vertical single-evaporator with two compartments	Energy factors of HCs mixtures increased in 9.1% and 12.2% respect R-134a.
Aprea, et al. [35]	R-1234yf/R-134a, 90/10%	Domestic refrigerator with freezer compartment	Non-flammable mixture. Energy savings 14% respect R-134a.
Abou-Ziyan and Fatouh [36]	R-290/R600/R600a	Domestic refrigerator with freezer compartment	Optimization of charge and capillary tube length. Energy savings during cycling of 38.8%.

On the subject of flammability, a study done by Linteris, et al. [37] opened up the possibility of predicting the flammability of refrigerant mixtures in a relatively straightforward manner. This allowed for the determination of the flammable class to which they belong according to ASHRAE 34. Based on the calculation method used in that study, Bell, et al. [38] conducted a comprehensive search for non-flammable refrigerant blends and concluded that there were no refrigerant blends that simultaneously had good energy efficiency, low GWP, and were non-flammable. Therefore, it is necessary to search for refrigerants with reduced flammability levels instead of non-flammable ones. However, Linteris, et al. [37]methodology only predicts whether a refrigerant is flammable or not, without reference to other flammable classes.

1.5 Identified gaps

At the beginning of the doctoral thesis, it was observed from previous research that there were real possibilities of going beyond the energy yields achieved with pure hydrocarbons, fundamentally from the combination of low GWP fluids to achieve mixtures with optimized thermophysical properties for each of the types of refrigeration machines. However, it was observed that an exhaustive search was not carried out to determine which mixtures can offer greater energy performance, have a lower flammable classification and, furthermore, if possible, can combine both characteristics. This lack of research was specifically pronounced with R-600a.

1.6 Objectives of the thesis

The primary objective of this doctoral thesis is to explore and investigate alternative refrigerant mixtures that enhance the properties of isobutane as a refrigerant fluid in vapor compression installations for cold production.

To achieve this aim, two general sub-objectives have been established:

i) **Subobjective 1**: Search for alternative refrigerant mixtures that provide better energy performance than R-600a in terms of COP and energy consumption, resulting in a lower environmental impact and improved energy labelling for facilities that use it.
ii) **Subobjective 2:** Search for refrigerant mixtures with a lower flammability class according to ASHRAE 34, allowing for a higher refrigerant charge according to the IEC 60335-2-89:2022 safety standard.

To do this, the following items are marked:

- **Item 1:** Conduct a theoretical screening in which all possible ternary combinations of a large number of refrigerants are considered to obtain the most promising refrigerant mixtures in comparison to R-600a and R-290.
- **Item 2:** Extend and explore a generic methodology that enables the identification of the flammable classification to which a refrigerant mixture belongs.
- **Item 3:** Determine the A3/A2 limit composition (according to ASHRAE 34) for binary mixtures of highly flammable refrigerants with other of lower flammability.
- **Item 4:** Adapt real refrigeration appliances to carry out experimental tests that quantify the energy savings that alternative refrigerant mixtures could offer in comparison to isobutane.

- **Item 5:** Construction of an experimental plant that allows the COP to be measured experimentally, as well as the direct measurement of various thermodynamic parameters.
- **Item 6:** Obtain experimentally the optimal composition that maximizes the performance of the alternative refrigerants previously identified as the most promising and measure their parameters.

A scheme of the objectives of the thesis can be seen in the Figure 1.3.

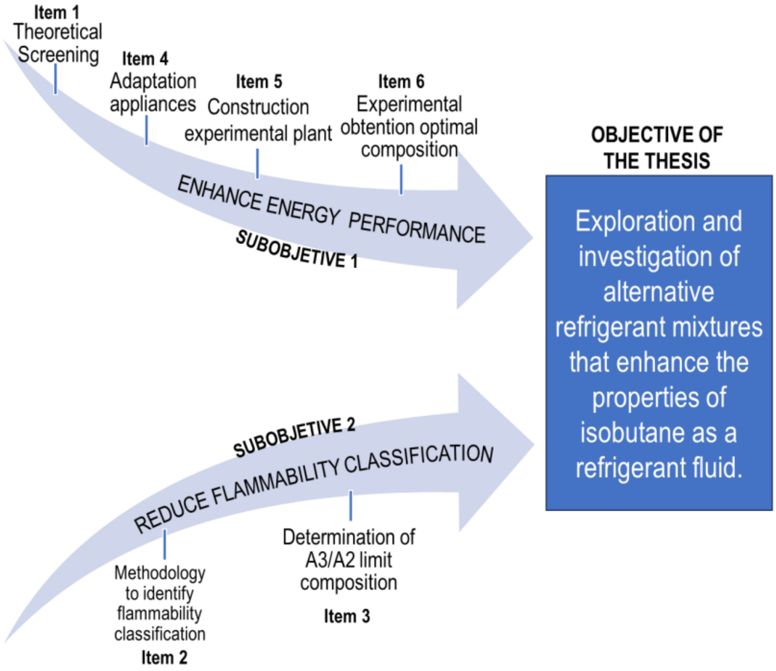

Figure 1.3. Objectives of the thesis.

1.7 Structure of the thesis

This thesis is divided into eight chapters. The **first chapter** is the chapter where the state of the art, the objectives and the general structure of the thesis are presented. The **second chapter** presents the methodology used in both the theoretical studies and the experimental tests, which involved the adaptation of two sealed refrigeration systems and the design and construction of a laboratory test plant. **Chapters 3 to 7** form the main body of the document, presenting the research results, organized according to the objectives of the thesis and adapted from articles published in high-impact journals. **Chapter 8** contains the main conclusions drawn from the research and future research avenues.

It is important to note that the structure of each chapter corresponds to the structure of the published article, although they have been adapted to the format of the present document. Each chapter specifies the journal of publication and the co-authors who contributed to the work.

Chapter 3 presents a theoretical study aimed at identifying alternative mixtures to R-600a and R-290 that can improve the energy performance of the systems. A thermodynamic screening is carried out to analyze all possible ternary combinations of 10 refrigerants, including R-290, R-600a, R-600, R-1270, R-152a, R-32, R-1234yf, R-1234ze(E), R-1233zd, R-744, and R-134a. The analysis includes all possible combinations in mass steps of 5%, resulting in the analysis of 27480 different mixtures. The mixtures are analyzed in four different conditions, considering various types of machines and evaporation temperatures. The study revealed the existence of several mixtures that could enhance the COP of R-600a.

Chapter 4 explores the potential of obtaining mixtures with a lower flammable classification according to ASHRAE 34 (class A2 or lower) to increase the cooling capacity of a system by allowing for higher refrigerant charges.

The chapter begins by extending a method that enables the theoretical prediction of the flammable class of a newly created refrigerant mixture, thus avoiding the need for large experimental campaigns to evaluate new refrigerant mixtures. The method is based on analysing the adiabatic flame temperature and the F/F+H ratio of the mixtures present in ASHRAE 34. It is completed by a thermodynamic screening to search for mixtures with an HOC of approximately 19000 kJ/kg.

Using this method, the limiting compositions of binary hydrocarbon mixtures were calculated, highlighting the limited ability to reduce the flammability rating of HCs by mixing them with less flammable refrigerants.

Chapter 5 investigates the experimental reduction of energy consumption in a domestic refrigerator with some of the alternative mixtures identified in chapter 3. The plant was equipped with various measuring instruments and tested according to the IEC 62552:2015 standard, recording the energy consumption of the mixtures for 24 hours. The mixtures tested in this chapter include R-1234yf/R-600a (7.5/92.5)%, R-1234ze(E)/R-600 (10.5/89.5)%, R-290/R-600 (11.0/89.0)%, and R-1270/R-600 (15.5/84.5)%.

In **Chapter 6**, a new theoretical study and experimental campaign were conducted on a sealed stand-alone commercial appliance. The theoretical study once again aimed to identify mixtures with superior energy performance than R-600a, but this time it was done by adapting the theoretical model to the operating parameters of the machine where they will be tested.

Unlike the previous machine, this experimental plant has an electronic expansion valve that can adjust its operation to each of the mixtures tested. The experimental plant was fully instrumented, and tests were conducted in accordance with ISO 23953-2:2023, recording its energy consumption for 16 hours. The mixtures analysed were R-1234ze(E)/R-600 (8/92%), R-152a/R-600 (8/92%), and R-32/R-600 (2/98%).

Chapter 7 presents an experimental investigation into the optimization of the composition of the R-152a/R-600 and R-290/R-600 mixtures in a single-stage vapor compression cycle. The chapter begins by describing the experimental plant, which was designed and built as part of the author's doctoral thesis. The plant features a novel typology of heat exchangers that allows for high sensorization throughout its entire geometry, enabling direct evaluation of temperature evolution throughout the phase change region. The plant enables direct measurement of energy and thermodynamic parameters, avoiding the need for indirect measurements.

Composition optimization is achieved by testing different compositions under steady-state conditions and selecting the composition that provides the best balance between COP, VCC, and $\dot{Q}_o$ parameters. Once the optimum composition was identified, an analysis was conducted at various phase change temperatures for each of mixture.

Chapter 8 outlines the primary conclusions and contributions to the scientific field derived from this thesis, as well as potential future research.

1.8 Nomenclature

CFCs	Chlorofluorocarbons
COP	Coefficient Of Performance
EEI	Energy Efficiency Index
F	Number of fluorine atoms
FGGs	Fluorinated Greenhouse Gases
GWP	Global Warming Potential
H	Number of hydrogen atoms
HCFCs	Hydrochlorofluorocarbons
HCs	Hydrocarbons
HCFOs	Hydrochlorofluoroolefyns
HCOs	Hydrochloroolefyns
HFCs	Hydrofluorocarbons
HFOs	Hydrofluoroolefyns
HOC	Heat of Combustion
LFL	Lower Flammability Limit
ODP	Ozone Depletion Potential
$\dot{Q}_o$	Cooling Capacity
RACHP	Refrigeration, Air-Conditioning and Heat Pump
TFA	Trifluoroacetic Acid

1.9 References

[1] IPCC, Climate Change 2023: Synthesis Report. Contribution of Working Groups I, II and III to the Sixth Assessment Report of the Intergovernmental Panel on Climate Change [Core Writing Team, H. Lee and J. Romero (eds.)]. IPCC, Geneva, Switzerland, pp. 35-115, (2023) DOI: 10.59327/IPCC/AR6-9789291691647.

[2] W.M.O. (WMO), State of the Global Climate 2020 (WMO-No. 1264), in, 2021.

[3] IPCC, Global Warming of 1.5°C. An IPCC Special Report on the impacts of global warming of 1.5°C above pre-industrial levels and related global greenhouse gas emission pathways, in the context of strengthening the global response to the threat of climate change, sustainable development, and efforts to eradicate poverty, in, 2018, DOI: 10.1017/9781009157940.008.

[4] IPCC, Climate Change 2021: The Physical Science Basis. Contribution of Working Group I to the Sixth Assessment Report of the Intergovernmental Panel on Climate Change, in, 2021, DOI: 10.1017/9781009157896.

[5] International Institute of Refrigeration, 38th Note on Refrigeration Technologies. The Role of Refrigeration in the Global Economy (2019). in, International Institute of Refrigeration, 2019, DOI: 10.18462/iif.NItec38.06.2019.

[6] International Institute of Refrigeration, 35th Informatory note on Refrigeration Technologies. The impact of the refrigeration sector on climate change, in, IIR, France, 2017.

[7] E. Council, EUCO 169/14, in, 2014.

[8] E. Commission, REPowerEU: A plan to rapidly reduce dependence on Russian fossil fuels and fast forward the green transition, in, 2022.
[9] M.J. Molina, F.S. Rowland, Stratospheric sink for chlorofluoromethanes: chlorine atom-catalysed destruction of ozone, Nature, 249 (1974) 810-812 DOI: 10.1038/249810a0.
[10] S. Chubachi, A Special Ozone Observation at Syowa Station, Antarctica from February 1982 to January 1983, in: Zerefos, Springer, Dordrecht, 1983, DOI: doi.org/10.1007/978-94-009-5313-0_58.
[11] U.N. (UN), Montreal Protocol on Substances That Deplete the Ozone Layer, 1987, in, Montreal, 1987.
[12] U.N. (UN), Amendment to the Montreal Protocol on Substances that Deplete the Ozone Layer, in, Kigali, 2016.
[13] European Commission, Regulation (EU) No 517/2014 of the European Parliament and of the Council of 16 April 2014 on fluorinated greenhouse gases and repealing Regulation (EC) No 842/2006., in: E. Commission (ed.), Official Journal of the European Union, 2014.
[14] UNEP, Environmental Effects of Stratospheric Ozone Depletion, UV Radiation, and Interactions with Climate Change, in, 2022.
[15] UNEP, Refrigeration, Air Conditioning and Heat Pumps Technical Options Committee. 2022 Assessment Report, in, United Nations Environment Programme, 2022.
[16] T.E.P.a.t.c.o.t.E. Union, REGULATION (EU) …/… OF THE EUROPEAN PARLIAMENT AND OF THE COUNCIL of … on fluorinated greenhouse gases, amending Directive (EU) 2019/1937 and repealing Regulation (EU) No 517/2014, in, 2023.
[17] European Commission, Directiva 2009/125/EC del Parlamento Europeo y del Consejo del 21 de Octubre de 2009 que establece un marco para el establecimiento de requerimientos de ecodiseño para productos relacionados con la energía, in, 2009.
[18] European Commission, Commission Regulation (EU) 2019/2019 of 1 October 2019 laying down ecodesign requirements for refrigerating appliences pursuant to Directive 2009/125/EC of the European Parliament and of the Council and repealing Commission Regulation (EC) No 643/2009, in, 2019.
[19] European Commission, COMMISSION REGULATION (EU) 2015/1095 of 5 May 2015 implementing Directive 2009/125/EC of the European Parliament and of the Council with regard to ecodesign requirements for professional refrigerated storage cabinets, blast cabinets, condensing units and process chillers., in, 2015.
[20] E. Commission, Commission Delegated Regulation (EU) 2019/2016 of 11 March 2019 supplementing Regulation (EU) 2017/1369 of the European Parliament and of the Council with regard to energy labelling of refrigerating appliances and repealing Commission Delegated Regulation (EU) No 1060/2010 (Text with EEA relevance.) in, 2019.
[21] European Commission, COMMISSION DELEGATED REGULATION (EU) 2015/1094 of 5 May 2015 supplementing Directive 2010/30/EU of the European Parliament and

of the Council with regard to the energy labelling of professional refrigerated storage cabinets., in, 2015.

[22] E.I. 60335-2-24:2022, Household and similar electrical appliances - Safety - Part 2-24: Particular requirements for refrigerating appliances, ice-cream appliances and ice makers, in, 2022.

[23] W. Cho, D.S. Jang, S.H. Lee, S. Yun, Y. Kim, Refrigerant charge reduction in R600a domestic refrigerator-freezer by optimizing hot-wall condenser geometry, International Journal of Refrigeration, 117 (2020) 295-306 DOI: 10.1016/j.ijrefrig.2020.05.012.

[24] W. Zhou, X. Bi, Z. Gan, Performance investigation of a domestic freezer with micro-bare-tube evaporators, Applied Thermal Engineering, 174 (2020) DOI: 10.1016/j.applthermaleng.2020.115306.

[25] W. Zhou, Z. Gan, A potential approach for reducing the R290 charge in air conditioners and heat pumps, International Journal of Refrigeration, 101 (2019) 47-55 DOI: 10.1016/j.ijrefrig.2019.02.030.

[26] A. Pisano, S. Martínez-Ballester, J.M. Corberán, A.W. Mauro, Optimal design of a light commercial freezer through the analysis of the combined effects of capillary tube diameter and refrigerant charge on the performance, International Journal of Refrigeration, 52 (2015) 1-10 DOI: 10.1016/j.ijrefrig.2014.12.023.

[27] M.O. McLinden, A.F. Kazakov, J. Steven Brown, P.A. Domanski, A thermodynamic analysis of refrigerants: Possibilities and tradeoffs for Low-GWP refrigerants, International Journal of Refrigeration, 38 (2014) 80-92 DOI: 10.1016/j.ijrefrig.2013.09.032.

[28] M.O. McLinden, J.S. Brown, R. Brignoli, A.F. Kazakov, P.A. Domanski, Limited options for low-global-warming-potential refrigerants, Nat Commun, 8 (2017) 14476 DOI: 10.1038/ncomms14476.

[29] P.A. Domanski, R. Brignoli, J.S. Brown, A.F. Kazakov, M.O. McLinden, Low-GWP refrigerants for medium and high-pressure applications, International Journal of Refrigeration, 84 (2017) 198-209 DOI: 10.1016/j.ijrefrig.2017.08.019.

[30] D. Jung, C.B. Kim, K. Song, B. Park, Testing of propane/isobutane mixture in domestic refrigerators, International Journal of Refrigeration, 23 (2000) 517-527 DOI: 10.1016/S0140-7007(99)00084-5.

[31] S. Wongwises, N. Chimres, Experimental study of hydrocarbon mixtures to replace HFC-134a in a domestic refrigerator, Energy Conversion and Management, 46 (2005) 85-100 DOI: 10.1016/j.enconman.2004.02.011.

[32] M. Mohanraj, S. Jayaraj, C. Muraleedharan, P. Chandrasekar, Experimental investigation of R290/R600a mixture as an alternative to R134a in a domestic refrigerator, International Journal of Thermal Sciences, 48 (2009) 1036-1042 DOI: 10.1016/j.ijthermalsci.2008.08.001.

[33] M. Rasti, S. Aghamiri, M.-S. Hatamipour, Energy efficiency enhancement of a domestic refrigerator using R436A and R600a as alternative refrigerants to R134a, International Journal of Thermal Sciences, 74 (2013) 86-94 DOI: http://dx.doi.org/10.1016/j.ijthermalsci.2013.07.009.

[34] C.C. Yu, T.P. Teng, Retrofit assessment of refrigerator using hydrocarbon refrigerants, Applied Thermal Engineering, 66 (2014) 507-518 DOI: 10.1016/j.applthermaleng.2014.02.050.

[35] C. Aprea, A. Greco, A. Maiorino, An experimental investigation of the energetic performances of HFO1234yf and its binary mixtures with HFC134a in a household refrigerator, International Journal of Refrigeration, 76 (2017) 109-117 DOI: 10.1016/j.ijrefrig.2017.02.005.

[36] H. Abou-Ziyan, M. Fatouh, Transient and cyclic characteristics of a household refrigerator using ternary hydrocarbon mixture – An experimental investigation, Applied Thermal Engineering, 129 (2018) 446-462 DOI: https://doi.org/10.1016/j.applthermaleng.2017.09.076.

[37] G.T. Linteris, I.H. Bell, M.O. McLinden, An empirical model for refrigerant flammability based on molecular structure and thermodynamics, International Journal of Refrigeration, 104 (2019) 144-150 DOI: 10.1016/j.ijrefrig.2019.05.006.

[38] I. Bell, P.A. Domanski, M. McLinden, G. Linteris, The hunt for nonflammable refrigerant blends to replace R-134a, International Journal of Refrigeration, 104 (2019) 484-495 DOI: 10.1016/j.ijrefrig.2019.05.035.

CHAPTER 2.
METHODOLOGY.

2 METHODOLOGY

This chapter outlines the methodology used in this doctoral thesis to achieve the established objectives. The text presents the methodological framework for the theoretical simulations in two key components. Firstly, the thermodynamic model is presented, which is used to derive the most alternatives substitute mixtures for isobutane and propane. Secondly, the flammability model is articulated, which is used to predict whether a given mixture aligns with the A3 or A2 safety classification of ASHRAE 34. The following section presents the experimental setups and their respective test procedures. Three different setups were used, including a domestic plant, a commercial plant, and a laboratory test bench.

The software used during this PhD are Refprop v.10.0 [1], for the thermodynamic properties calculations; Refleak v.5.1 [2], for the leakage simulation; and Cantera [3], for the chemical properties calculation.

2.1 Theoretical simulations

2.1.1 Mixtures Identification

The initial step in this thesis involves conducting a thermodynamic screening to theoretically identify alternative mixtures to isobutane and propane that have the potential to enhance its energy efficiency. This step aims to fulfil Subobjective 1 and item 1.

Thermodynamic screening involves a comprehensive theoretical evaluation of all possible combinations between a varied group of refrigerants, considering a significant range of compositions for each combination. The text describes the simulation of the thermodynamic and energetic behaviour of each possible mixture to obtain the composition that optimizes and maximizes the COP.

Figure 2.1 shows the thermodynamic screening scheme. A matrix of combinations is made for each trio of refrigerants, considering increments and decrements of a 5% variation, resulting in a total of 229 different compositions. The energy behaviour of each combination is simulated by considering its operation in a simple vapour compression cycle. This involves an isentropic compression, an isobaric transformation in the exchangers, and an isenthalpic transformation in the capillary tube. The simulation is carried out for each mix in four different scenarios:

- M1: Conditions for the preservation of fresh product, with non-adiabatic capillary tube. t_o = -10 ºC, t_k= 40 ºC, ε_{cap}=80 %, SH=4 K, SUB=1 K.
- M2: Conditions for the preservation of fresh product, with adiabatic capillary tube. t_o = -10 ºC, t_k= 40 ºC, ε_{cap}=0 %, SH=4 K, SUB=1 K.
- L1: Conditions for the preservation of frozen product, with non-adiabatic capillary tube. t_o = -30 ºC, t_k= 40 ºC, ε_{cap}=80 %, SH=4 K, SUB=1 K.
- L2: Conditions for the preservation of frozen product, with adiabatic capillary tube. t_o = -30 ºC, t_k= 40 ºC, ε_{cap}=0 %, SH=4 K, SUB=1 K.

The evaporating pressure (p_o), corresponding to the evaporating temperature level, was calculated by an iterative method using the mean enthalpy in the evaporator, as determined by Eq.(2.1) and Eq.(2.2). This criterion is the most recommended for the evaluation of refrigerant mixtures, as suggested by Radermacher and Hwang [4].

$$h_m = \left(\frac{h_{O,in}+h_{O,out}}{2}\right) \qquad \text{Eq.(2.1)}$$

$$p_O = f(t_O, h_m) \qquad \text{Eq.(2.2)}$$

The condensing pressure (p_k) was calculated according to Eq.(2.3) which assumes that the medium enthalpy corresponds to 50% vapour quality (x_v) in the condenser.

$$p_k = f(t_k, x_v = 0.5) \qquad \text{Eq.(2.3)}$$

The evaluation of suction temperature and enthalpy took into account the capillary tube's role as an internal heat exchanger with defined thermal effectiveness, as expressed by Eq.(2.4) to Eq.(2.6). The evaporator inlet enthalpy was determined through the heat balance in the capillary tube.

$$t_{suc} = t_{O,out} + \varepsilon_{ihx} \cdot (t_{K,out} - t_{O,out}) \qquad \text{Eq.(2.4)}$$

$$h_{suc} = f(t_{suc}, p_O) \qquad \text{Eq.(2.5)}$$

$$h_{O,in} = h_{K,out} - h_{suc} + h_{O,out} \qquad \text{Eq.(2.6)}$$

The process includes certain conditions for filtering mixtures. Mixtures with a GWP greater than 150 are excluded as they do not meet the requirements of the F-Gas Regulation. Similarly, mixtures with an effective glide ($Glide_O$) in the evaporator greater than 10 K and a total glide in the condenser ($Glide_k$) greater than 20 K are also excluded as it has been proven that large glides degrade heat transfer. Additionally, a discharge temperature limit of 70 ºC was established. The formulas used to calculate the mentioned parameters are indicated in Eq.(2.7), Eq.(2.8) y Eq.(2.9).

$$GWP = \sum_i^n (m_i \cdot GWP_i) \qquad \text{Eq.(2.7)}$$

$$Glide_O = t(p_O, x_v = 1) \ - t\left(p_O, x_{v,O,in}\right) \qquad \text{Eq.(2.8)}$$

$$Glide_K = t(p_K, x_v = 1) - t(p_K, x_v = 0) \qquad \text{Eq.(2.9)}$$

Considered mixtures are those with a Volumetric Cooling Capacity (VCC) between ±30% of isobutane, as compatibility with R-600a compressors is aimed for, and those with a COP higher than isobutane but not exceeding 15% improvement, since those that exceed this percentage are considered unreliable due to limitations in the mixing rules available in Refprop 10. COP and VCC are evaluated using Eq.(2.10) and Eq.(2.11).

$$VCC = \frac{h_{O,out} - h_{O,in}}{v_{suc}} \qquad \text{Eq.(2.10)}$$

$$COP = \frac{h_{O,out} - h_{O,in}}{h_{dis,S}(p_K, s_{suc}) - h_{suc}} \qquad \text{Eq.(2.11)}$$

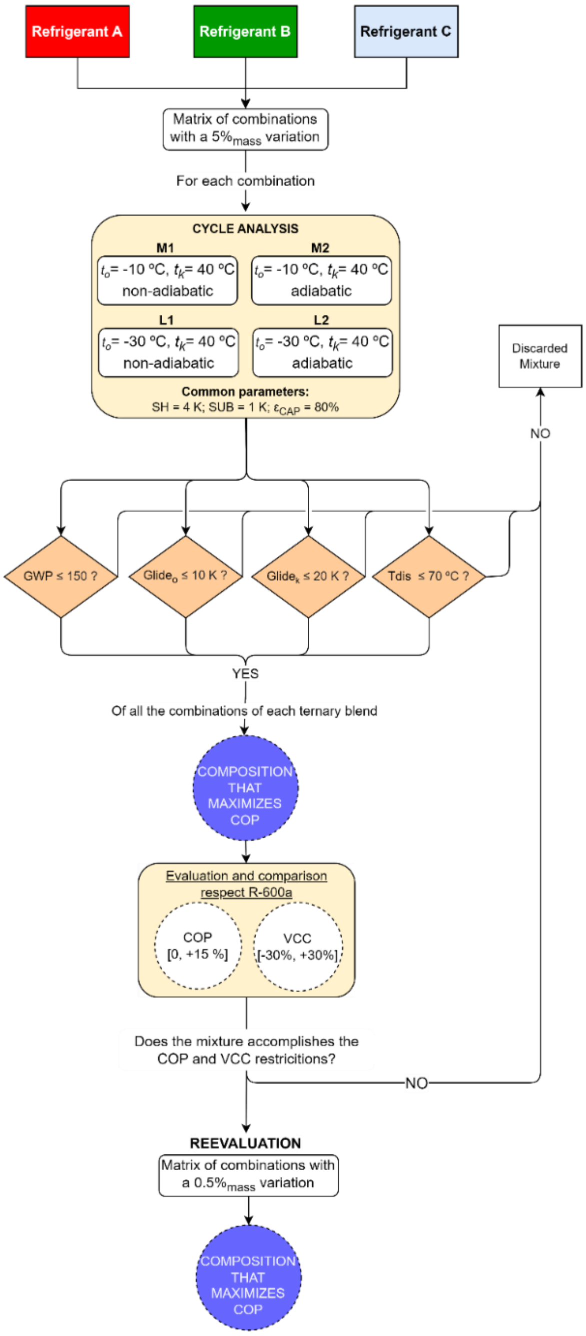

Figure 2.1. Scheme of the methodology used in the thermodynamic screening for the alternative mixtures identification.

All mixtures within the acceptance range marked by COP and VCC are re-evaluated taking into account a 0.5% variation in order to re-select the composition that maximizes the COP.

In total, 27480 different mixtures are evaluated.

The research, with the detailed methodology and the results can be found in CHAPTER 3.

2.1.2 Method to predict the flammability classification

Subobjective 2 of this thesis is to search for flammable refrigerant blends that have a lower flammability rating than isobutane according to ASHRAE 34, allowing a higher refrigerant charge considering the restrictions imposed by the IEC 60335-2-89:2022 Regulation. To this end, a theoretical methodology must first be developed to theoretically identify the flammability classification to which a mixture belongs (item 2).

The methodology developed by Linteris, et al. [5] to identify whether a mixture belongs to an A3 or A2 flammability class is based on the evaluation of the adiabatic flame temperature (T_{ad}) and the ratio of fluorine and hydrogen (F/F+H) of all mixtures composed of HFCs, HFOs and HCs present in ASHRAE 34. Placing the refrigerants on a graph with the origin at 1600 K T_{ad} and evaluating the angle they form (Π) according to Eq.(2.12) would result in an arrangement as shown in Figure 2.2. Linteris, et al. [5] identified the boundary angles between the A1 and A2L regions as $\Pi = 36^{\text{o}}$ and between the A2L and A2 regions as $\Pi = 60^{\text{o}}$, but the boundary angle between the A3 and A2 regions was not identified. The angles are delimited according to the spatial arrangement of the refrigerants within the graph.

Therefore, we are attempting to extend the methodology developed by Linteris et al. to include the A3/A2 boundary angle.

$$\Pi = \mathrm{arctan2}\left\{\left[\frac{\mathrm{T_{ad}}-1600}{2500-1600}\right],\left[\frac{\mathrm{F}}{\mathrm{F+H}}\right]\right\}\cdot\left(\frac{1800}{\pi}\right) \qquad \text{Eq.(2.12)}$$

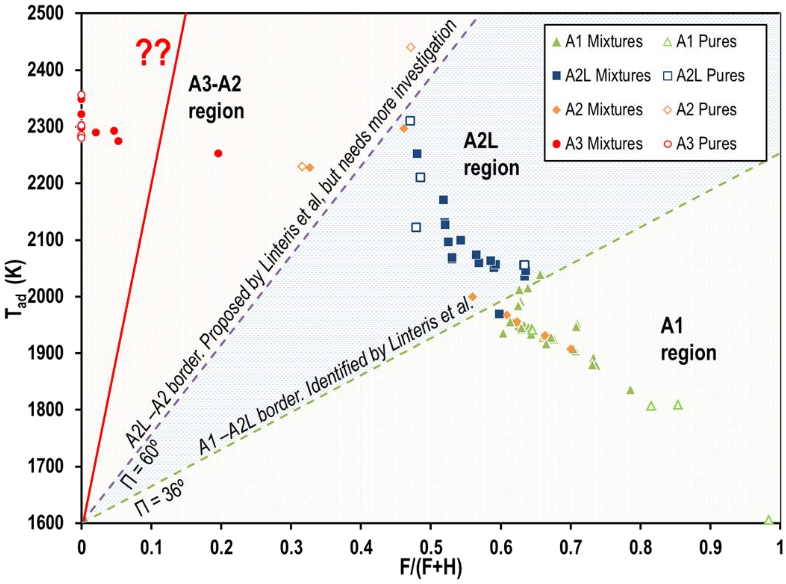

Figure 2.2. Refrigerants present in ASHRAE 34 after evaluation of T_{ad} and F/F+H proposed by Linteris et. al.

The methodology used to determine the A3/A2 threshold angle is described in Figure 2.3. It must first be understood that the classification of a refrigerant mixture is not defined by its nominal composition, but by its Worst Case of Fractionation for Flammability (WCFF), which is the most flammable of all the resulting compositions that may occur when a mixture is exposed to different adverse scenarios in which a leak may occur. Depending on the conditions under which the leak occurs and the volatility of the components, the resulting mixture composition can be very different. This fractionation process has been simulated using the REFLEAK software [2].

First, all A3 and A2 refrigerants present in ASHRAE 34 and its addenda are identified. For each refrigerant mixture, all possible Worst Case of Formulation for Flammability (WCF) cases are identified according to the composition mass tolerances of each mixture as registered in the ASHRAE 34. Once identified, for each WCF, a fractionation study considering possible leakages must be performed to find its WCFF. Three different conditions must be considered: leaks under storage/shipping conditions (two different temperatures), leaks from equipments (two different temperatures) and leak/recharge test. In the first two conditions, the resulting vapour/liquid mixture must be tested at 2% leakage, at 10% leakage and in successive ranges from 10% to no liquid or 1 atm pressure or 95%. In the last condition, only the resulting vapour mixture is analysed at the end of each recharging, for a total of 5 recharges. In total, for a mixture with two WCFs, 186 different compositions have to be analysed to identify the WCFF and the most flammable of them (WCFF) has to be decided according to the angle Π they form. The T_{ad} evaluation was done with the software Cantera [3].

Once the WCFF of the less flammable A3 and the more flammable A2 have been determined, it was found that the formation angles were 77.1º and 67.37º respectively, creating a zone of uncertainty. To overcome this, it was decided to carry out a screening of ternary mixtures of refrigerants, varying their composition to calculate the heat of combustion according to the enthalpy of formation of the reactants and products. The compositions with an HOC (heat of combustion) ≈ 19000 kJ/kg (which is the boundary between zone A3 and A2) were recorded and then the T_{ad} and F/F+H were calculated. It was concluded that the angle defining the boundary between the two flammability classifications is 67.37º.

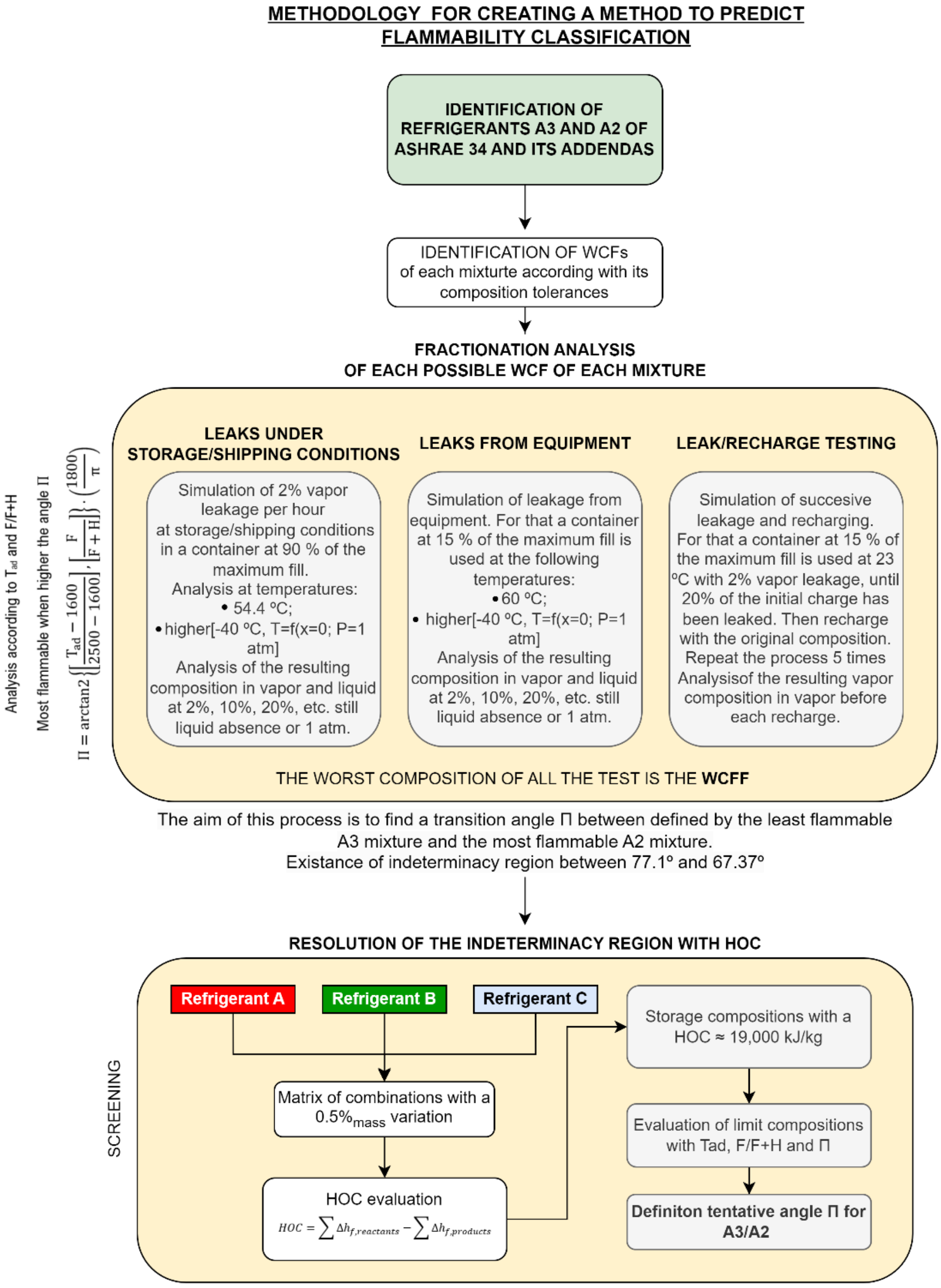

Figure 2.3. Scheme of the methodology used for creating the method to predict if a mixture pertains to a security classification A3/A2.

For a mixture of refrigerants, the combustion reaction must not be evaluated as three independent reactions, but as a single reaction involving a hypothetical molecule consisting of all the atoms of each refrigerant multiplied by its molecular weight. As an example, Figure 2.4 shows the resulting molecule in the mixture R-600a /R-152a /R-1234yf (21 /16 /63 %mass). Once formed, the reactants are obtained according to the formation rules explained in Figure 2.5.

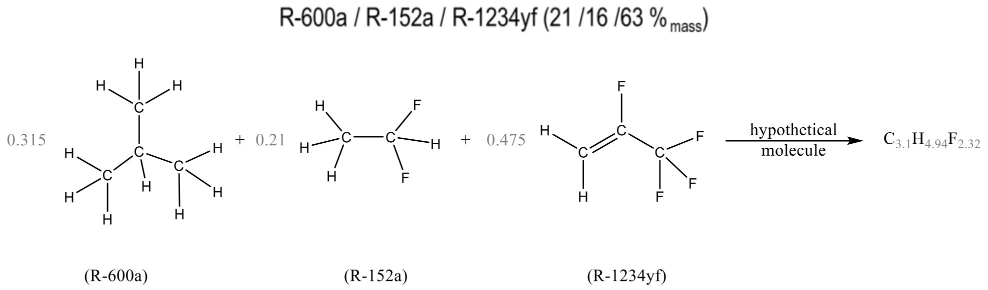

Figure 2.4. Formation of the hypothetical molecule.

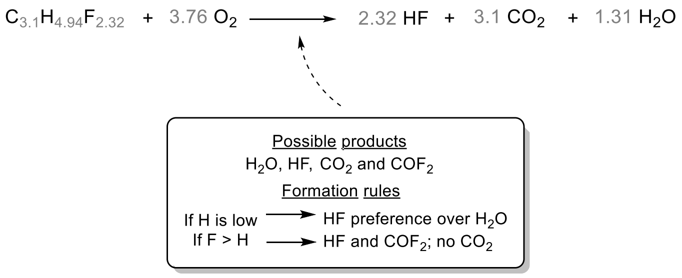

Figure 2.5. Products and reactants from the combustion process.

Lastly, the HOC is calculated from the sum of the enthalpies of formation of the reactants minus the sum of the enthalpies of formation of the products, as shown in Figure 2.3.

Finally, to meet subobjective 1, item 3, the limiting compositions of binary blends of A3 refrigerants with other refrigerants of lower flammability classification were analysed. They were analysed considering the previously identified angle, the HOC and the lower flammability limit (LFL).

The complete study, with a detailed description of the methodology and the results obtained, can be found in CHAPTER 4.

2.2 Experimental plants

This section describes the various experimental plants used during the development of this thesis and the contribution of each facility to the achievement of each of the subobjectives and items described. It includes a brief description of each installation, including the modifications made to adapt them to working research equipment, an outline of their main mechanical components, a description of the test methods used, and details of the measurement sensors integrated into these assemblies.

The first two installations presented are two sealed refrigeration appliances adapted for the purposes of this thesis, one being a domestic refrigerator and the other a stand-alone refrigerator for commercial applications. Both are designed for the preservation of fresh product. The last of the installations is a test rig specifically designed for laboratory purposes for the experimental identification of alternative blends to isobutane. The machine has been completely designed and constructed during the development of this thesis.

2.2.1 Sealed Domestic and Commercial Plant

Both the domestic and commercial machines share similarities in components, test methodology and objectives achieved, and are therefore described together in this subsection.

Domestic plant description

The first experimental setup used in this thesis was a commercially available single-compartment domestic refrigerator for the preservation of fresh product, with dimensions of 170 x 60 x 60 cm (Figure 2.6).

This appliance was selected from an extensive catalogue because its function conditions coincided with one of the scenarios simulated in the thermodynamic screening [scenario L2 (t_o = -30 ºC, adiabatic capillary)] to test the observed mixtures and fulfil subobjective 1 and item 4.

This facility was used to test the most promising refrigerant blends identified in the thermodynamic screening. Specifically, the blends R-1234yf / R-600a (7.5/92.5)%, R-1234ze(E) / R-600 (10.5/89.5)%, R-290 / R-600 (11/89)% and R-152a / R-600 (9.5/90.5)% were tested.

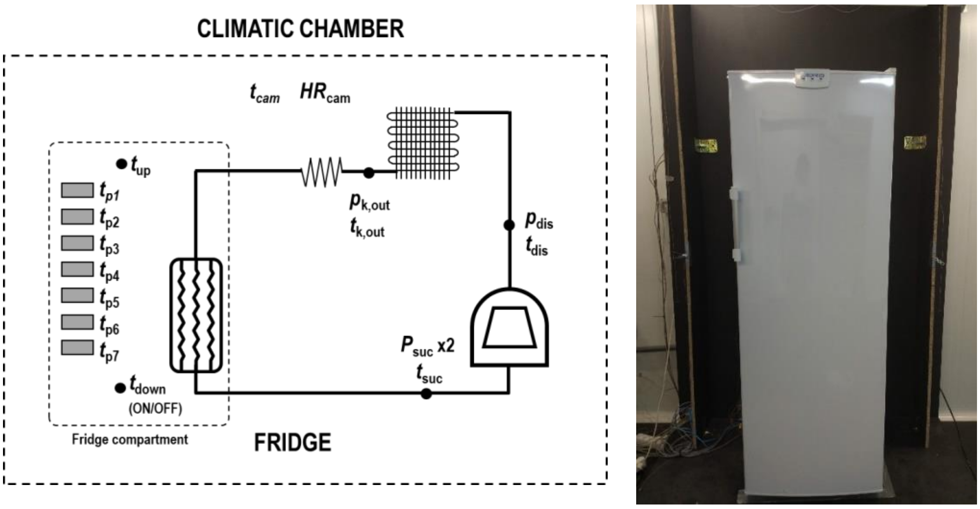

Figure 2.6. Refrigeration scheme (left) and frontal image of the domestic appliance (right).

The appliance operates through a simple vapor compression cycle with an adiabatic capillary tube, which is driven by a hermetic piston compressor, causing the refrigerant to flow through the rest of the system components. The heat is removed from the cycle using an air wired-tube heat exchanger placed in the system's rear part, while the expansion process is performed by an adiabatic capillary. Finally, the cooling effect in the fridge compartment is introduced through a roll bond evaporator. The appliance was instrumented with four pressure gauges and twelve thermocouples at the points show in Figure 2.6, together with a wattmeter to record the power consumption.

The system was modified as minimally as possible, only to adapt it for proper instrumentation, facilitate charging and discharging, and to ensure homogeneous operating conditions during the different tests carried out.

The only four minor modifications that were made are as follows:

1. Installation of pressure probes. The system had to be opened to weld different 'Ts' together with a male SAE thread where the probes are screwed in. Two pressure probes are placed in the high-pressure zone (at the compressor discharge and at the condenser outlet) and two in the low-pressure zone (at the compressor suction).
2. Installation of thermocouples inside the refrigerator compartment: A hole was made in the side of the refrigerator compartment for the internal installation of thermocouples to measure the temperature of the air inside the cabinet and the M packages placed to simulate fresh product. Subsequently, the hole was covered with thermal insulation material.
3. Installation of a refrigerant charging port: A SAE thread port is installed at the compressor suction to enable refrigerant charging and discharging.

4. Installation of an ON/OFF relay to command the system's start and stop: The machine was turned on and off with a relay activated by the data acquisition system, based on the value of the thermocouple positioned at the interior base of the cabinet (t_{down}). The system sets the desired set-point and hysteresis. The electrical schematic of the modification made can be observed in Figure 2.7.

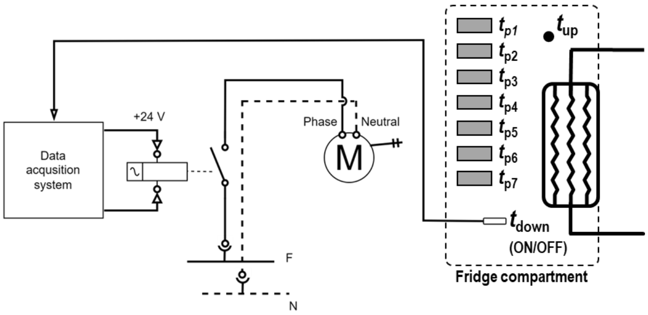

Figure 2.7. Electric scheme of the relay installation.

The refrigerator was tested in adherence to the IEC 62552:2015+AMD1:2020, which describes the test methods for households appliances [6]. It was placed inside a climatic chamber with controlled temperature and humidity and inside a structure made of wood to ensure a homogeneous air flow during the different tests. The geometry of the structure can be seen in Figure 2.8. In the figure can be seen the place of the thermocouples to measure the ambient temperature (T_a) which have to be encapsuled in a 25 g ± 5% copper cylinder. There are two at the laterals cylinders that serves to measure the ambient temperature (the average value between both) and one below the structure to verify that there is not a deviation higher than ± 1 K respect the upper thermocouples.

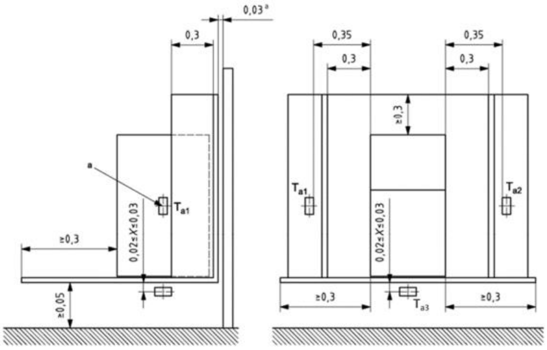

Figure 2.8. Wood structure, position of the appliance inside it and position of the temperature sensor (T_a).

All the mentioned modifications, as well as the wooden structure and the placement of temperature sensors, can be observed in Figure 2.9.

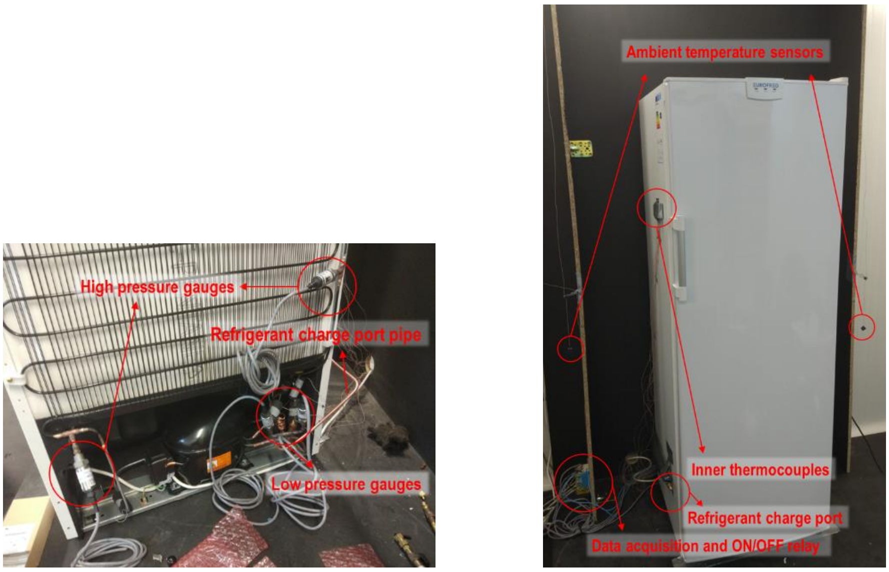

Figure 2.9. Modifications effectuated on the domestic appliance.

The detailed description of the components, sensor placement, and the testing methodology can be found in CHAPTER 5.

Commercial plant description

The second experimental installation used in this thesis is a commercial stand-alone beverage cooler with dimensions of 200 x 690 x 600 cm (Figure 2.10).

Like the previous installation, this machine is used to meet the requirements of subobjective 1 and item 4. However, unlike the previous installation, this unit has a higher refrigeration requirement, which makes it possible to obtain more stable test results, where external disturbances are of little importance. In addition, this unit is equipped with an electronic expansion valve capable of adapting its operation to the refrigerants tested, which allows a better adaptation of the system to the refrigerant. These two facts, which may seem insignificant, have a significant impact on the evaluation of alternative blends, as they allow us to better assess the real potential of the alternative blends analysed. The fluids tested in this system were R-1234ze(E)/R-600 (8/92)%, R-152a/R-600 (8/92)% and R-32/R-600 (2/98)% and isobutane (R-600a) as a reference.

The unit operates with a simple vapour compression cycle driven by a hermetic piston compressor designed for isobutane. Two condensers are connected in series to ensure full condensation of the refrigerant: the first is a wire-tube with natural convection and the second is a finned tube with forced convection. As expansion element, the system has an electronic valve whose driver can be configured according to the bubble line of each refrigerant tested. In addition, there was an intermediate heat exchanger between the vapour and liquid lines. The location of the measurement sensors is shown in Figure 2.10, together with a wattmeter that recorded all the energy consumed by the system.

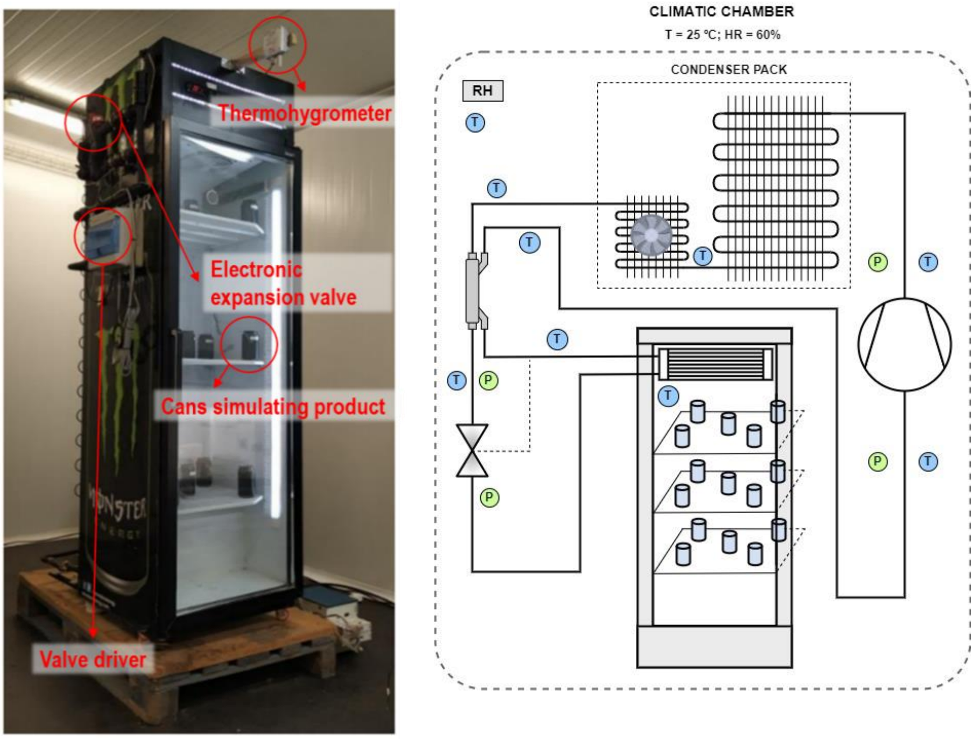

Figure 2.10. Commercial plant.

Unlike the previous installation, this one underwent further modifications to better adapt to the operation of each of the blends. The second condenser described above was added, the original thermostatic valve was replaced with an electronic one, and the system was opened to add the necessary pressure gauges.

The plant was controlled by an ON/OFF relay activated according to the temperature inside the cabinet.

The system was tested in accordance with ISO 23953-2:2023 [7], which specifies the requirements and test conditions for commercial refrigerated furniture. The unit should be tested at an ambient temperature of 25°C and a relative humidity of 60%, measured by a thermohygrometer placed on top of the unit at a distance of 25 cm. 15 cans filled with a water/propylene glycol mixture (67/33%$_v$) were evenly distributed over the three shelves of the cabinet, simulating the behaviour of fresh product.

A detailed description of the components, sensor placement and test methodology can be found in CHAPTER 6.

Methodology test of sealed plants

The test methodology, although described in more detail in CHAPTER 5 and CHAPTER 6 for each appliance, is summarised and described jointly in this subsection, as there are many similarities between the two appliances.

The tests consisted of recording the energy consumption, temperatures and pressures for 24 hours in the case of the domestic unit and 16 hours in the case of the commercial unit, with each refrigerant tested under homogeneous conditions. The data is collected every 5 seconds by the data acquisition system, which is connected to the computer. The main points of the test methodology are listed below:

- Homogeneous environmental conditions: The cabinet was installed in a climatic chamber at 25°C ambient temperature and a RH of 60% for the commercial cabinet and below 60% RH for the domestic cabinet.
- Constant product temperature: The set-point of the machine was varied with each test to ensure that the average product temperature (7 M-test packages in the refrigerator and 15 cans in the commercial cabinet) is 5.0 ºC for the fridge and 3.1 ºC for the beverage cooler.
- Refrigerant preparation: The refrigerant mixture was prepared in our laboratory with certified gases with a purity of 99.9%. The mixture was made in a third bottle of sufficient volume to ensure that the mixture was in the gas phase. The least volatile refrigerant (the one with the highest NBP) was charged first, followed by the one with the lowest NBP.
- Charge optimization: For each alternative mixture, as well as for each isobutane, different refrigerant charges were tested to find the one with the lowest energy consumption.

The test methodology is summarized in Figure 2.11.

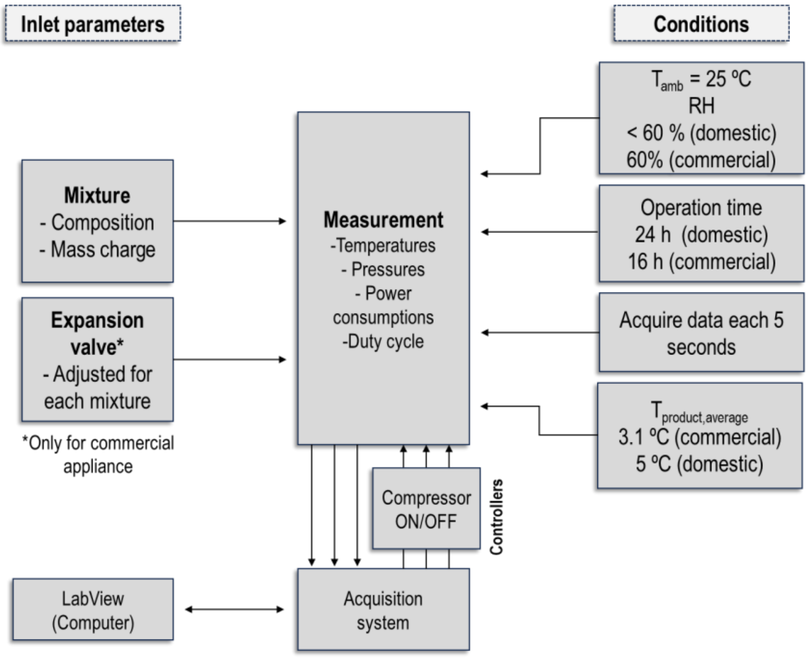

Figure 2.11. Test methodology for the sealed plants.

2.2.2 Test bench

The last experimental plant used in this thesis is a bench test with a simple vapour compression cycle, with the aim of obtaining tests under stationary conditions. The experimental plant is shown in Figure 2.12, together with its refrigeration diagram and the position of the various sensors installed. The experimental plant was conceived, designed and built as part of the thesis.

This facility was built with the aim of having a machine that could directly measure the thermodynamic properties of the desired refrigerants. Therefore, it fulfils subobjectives 1 and items 5 and 6. Using the test bench, the optimal compositions of the R-152a / R-600 and R-290 / R-600 refrigerant blends were determined according to thermodynamic screening.

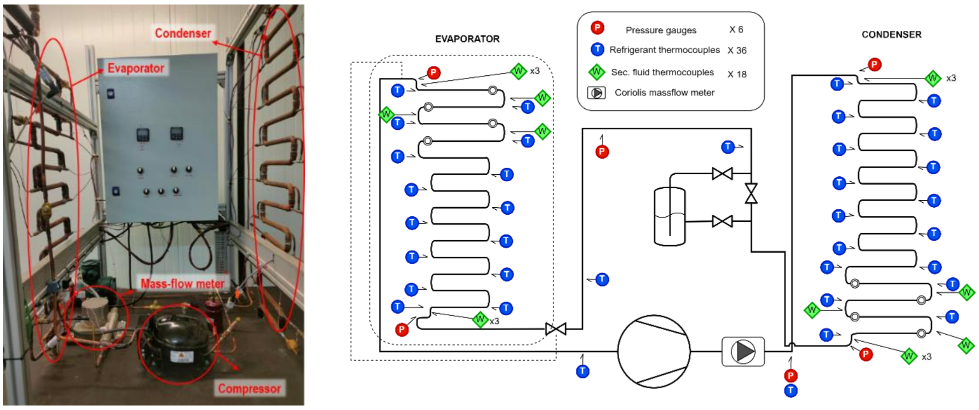

Figure 2.12. Experimental plant (left) and diagram (right).

The system has a variable speed hermetic piston compressor whose operating speed is controlled by a square wave sent by a function generator. The expansion element is an electronic expansion valve whose operating parameters are adjusted according to the ln(P)-T saturation curve of each refrigerant tested. A liquid receiver was added to the installation between the two exchangers of the unit. The evaporator and condenser are built according to a specific geometric layout based on a tube-in-tube configuration. Two concentric tubes in which the refrigerant flows through the inner tube and the secondary fluid flows through the outer tube in a countercurrent arrangement. The heat exchangers are divided into different sections, as shown in the figure, so that thermocouples can be fitted to measure the evolution of the refrigerant throughout the heat transfer process.

Secondary fluid loops

The evaporator and condenser exchange heat with two independent secondary circuits.

For the evaporator (Figure 2.13), the secondary liquid used is a propylene-glycol/water mixture (50/50$\%_{v}$) circulated through the circuit by a variable speed pump. The circuit has a 30 liter tank to store the liquid, a Coriolis mass flow meter and a flow control valve. The flow circulates through the outer tube of the heat exchanger described in the previous section.

Regarding the condenser, the secondary loop is similar but using distilled water. This loop has a volumetric flow meter, a 30-liter accumulator tank, and a condensing unit to remove the heat from the condenser.

To control the inlet temperature to the heat exchangers, an electric resistance of 1 kW is installed in both 30liter tanks controlled by two solid-state relays and two PIDs. In the case of the evaporator circuit, the resistor is responsible both for providing the necessary heat load and for regulating the temperature, while in the case of the condenser circuit, the function of the resistance is to regulate the water temperature.

All temperatures are measured by thermocouples, using three thermocouples at the inlet and outlet of the heat exchangers to reduce the measurement uncertainty by 43% compared to the equivalent of a single sensor. In addition, intermediate thermocouples (see Figure 2.12) are added to measure temperatures within the evaporating / condensing process.

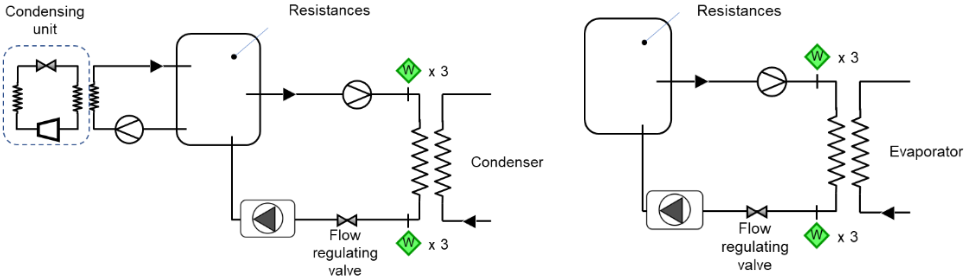

Figure 2.13. Scheme of the secondary loop for the condenser (left) and the evaporator (right).

Plant assembly

The entire plant was designed and assembled during the period of the thesis, including the assembly of the structure, the assembly of the refrigeration circuit, the assembly of the secondary fluid loops, the implementation of the electrical installation and the installation and calibration of the measurement elements together with the data acquisition system. Figure 2.14 shows two pictures of the plant assembly (left) and the electrical and data acquisition part (right).

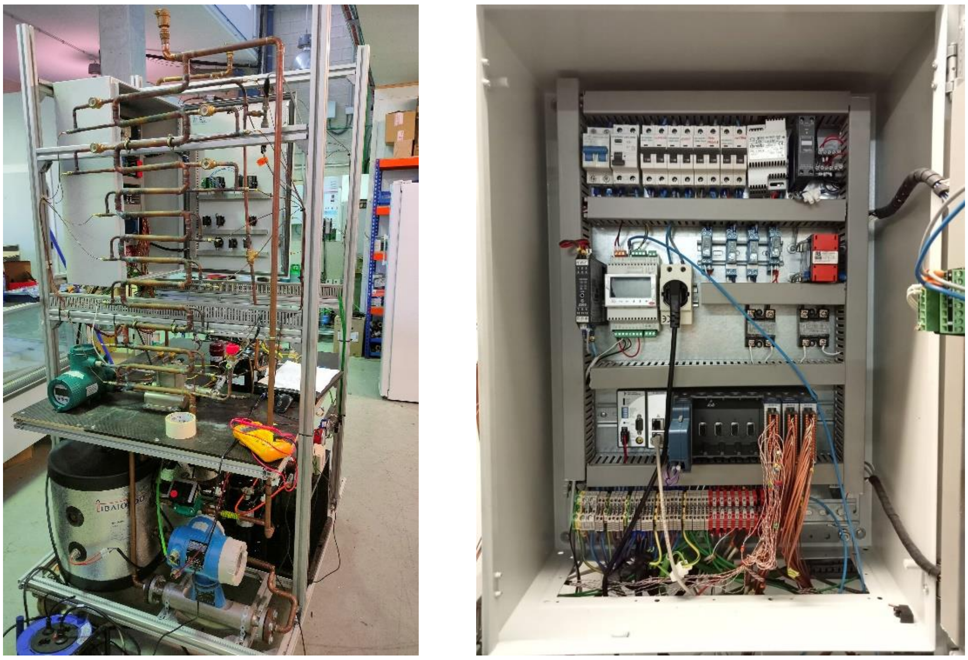

Figure 2.14. Picture of the plant assembly (left) and the electric installation (right).

Test bench methodology

The test methodology was based on progressively increasing the mass percentage of the lesser proportion refrigerant in the mixture until an optimum was identified for subsequent analysis over a wider range of phase-change temperatures. The acquisition time was 12 minutes once steady-state conditions were reached, with data acquired every 5 seconds. The summarized methodology is shown below:

- Gradual increment of the concentration of the refrigerant with the lower proportion in the mixture: The tests started with 97.5% butane and 2.5% of the second refrigerant, increasing the second refrigerant in 2.5% increments. Between charges, a complete vacuum of the system was done and recharged to avoid accumulating charging uncertainties. In addition, the expansion valve parameters were updated with each composition.

- Selection of the optimum composition: The optimum composition is selected based on the parameters COP, VCC y $\dot{Q}_o$.
- Evaluation of the optimum over a wide range of state change temperatures: the optimum composition was evaluated at different temperatures to assess its performance under different conditions.

The test methodology is summarized in Figure 2.15.

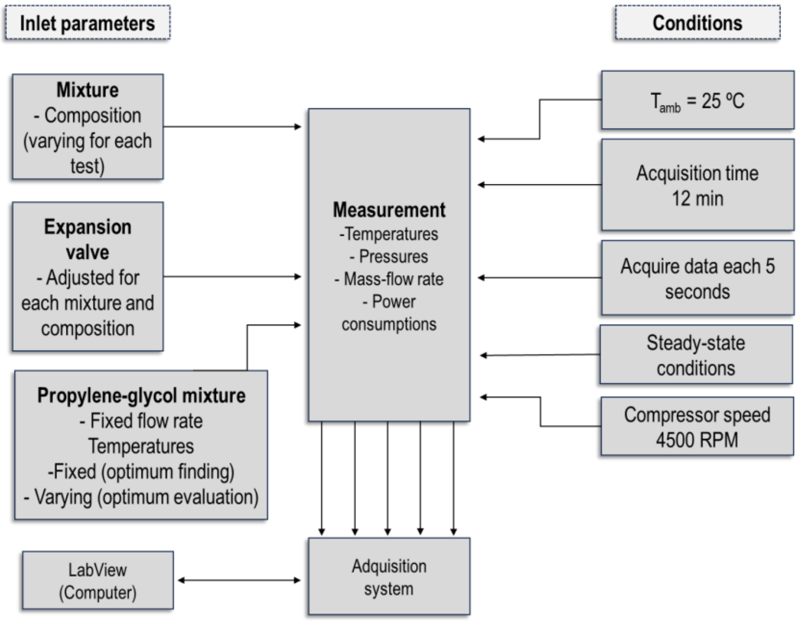

Figure 2.15. Test methodology for the test bench.

2.2.3 Measurement elements and data acquisition system

Five types of sensors were installed throughout the installations to measure the various parameters to be recorded: pressure gauges, thermocouples, thermohygrometers, mass and volume flow meters and wattmeters.

Pressure gauges

Pressure gauges are used to measure the pressure throughout the installed system, providing a 4-20 mA output signal over their measuring range depending on the absolute pressure. Three different range transducers were used, depending on whether the measurement is made in the low pressure part of the installation or in the high pressure part. In the low pressure part, probes with a measuring range of 0 to 9 bar were used, while in the high pressure part, probes with ranges of 0 to 16 bar and 1 to 31 bar were used.

To ensure correct measurement, the pressure probes were calibrated over their full range by recording their pressure with a calibrated absolute pressure transducer together with the electrical output signal at 10 different points. Two pictures of the calibration process are shown in Figure 2.16.

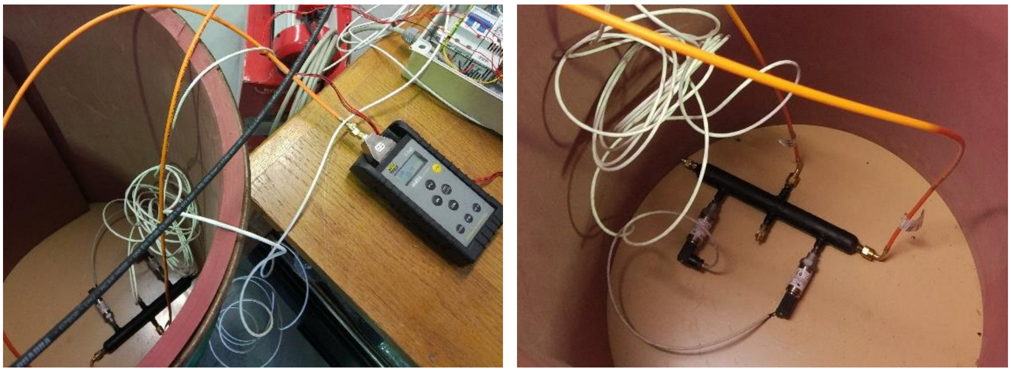

Figure 2.16. Calibration process of the pressure transducers.

Thermocouples

Temperature measurement is carried out using T-type thermocouples, whose range adjusts to registered temperatures. Two types of thermocouple are used depending on where they are located in the plant:

- Surface thermocouple: Attached to the outer part of the tube to avoid any type of modification of the cycle, it is used in all experimental facilities.
- Immersion thermocouple: This is a sheath that is inserted into the circuit and measures the temperature of the fluid directly. It is used in the test bench heat exchangers. A picture is shown in Figure 2.17.

Figure 2.17. Side view of a heat exchanger showing the immersion thermocouples along its entire length.

Combined thermohygrometer

This is a device that measures simultaneously the temperature and the relative humidity of the air in the climatic chamber where the described systems are tested.

Mass and volume flow meters

Due to the small capacity of the sealed plants, the circulating flow was measured only in the test bench. Specifically, three flow meters were used. Two Coriolis mass flow meter were installed for measuring the refrigerant and the water/propylene-glycol mixture mass flow rate. Moreover, a volumetric flow meter based on electromagnetic technology was used to determine the volumetric flow rate through the condenser.

Wattmeters

Digital wattmeters were used to measure the power consumption of the compressors. They provide an analogue output of 4 to 20 mA depending on the power consumption.

Accuracy

The sensors used in the different experimental machines, together with their measurement ranges and uncertainties, are listed in Table 2.1.

Table 2.1. Characteristics of the measurement systems

Measured variable	Measurement device	Range	Calibrated accuracy
Temperature (ºC)	T-type thermocouple	-40.0 to 145.0	± 0.5 K
Pressure (bar)	Pressure gauge (high pressure)	0.0 to 30.0	± 0.03 bar
Pressure (bar)	Pressure gauge (medium pressure)	0.0 to 16.0	± 0.016 bar
Pressure (bar)	Pressure gauge (low pressure)	0.0 to 9.0	± 0.009 bar
RH (%)	Thermohygrometer	0.0 to 100.0	± 2%
Refrigerant mass-flow (kg·s^{-1})	Coriolis mass flow meter	0.0 to 0.0028	± 0.1% of reading
Secondary fluid mass-flow (evaporator loop) (kg·s^{-1})	Coriolis mass flow meter	0.0 to 0.028	± 0.55% of reading
Secondary fluid mass-flow (condenser loop) (m^3·h^{-1})	Volumetric flow meter	0 to 0.1	± 2.1% of reading
Power consumption (kW)	Digital wattmeter	0.0 to 1.0	± 0.5% of reading

Data acquisition system

The system is equipped with measurement and control elements managed by an interface developed using LabView® software. This software makes it possible to visualize in real time the different parameters and control some operating parameters if needed, such as the activation and deactivation of the compressor via a relay and an analog output.

The sampling and conditioning of the electrical signals from the measuring elements is carried out by a National Instruments® acquisition system, model cRIO-9074, which is made up of various modules responsible for receiving and receiving the signals from the measuring elements. For this purpose, it has:

- Thermocouple input modules (NI 9213).
- Analogue Input Module (NI 9201).
- Analogue Output Module (NI 9263).

The signals from these modules are visualised in real time using the Labview® graphical user interface. The data is stored for later analysis and calculations using Microsoft® Excel® and Refprop libraries.

2.2.4 Data calculation and uncertainty analysis

As a general rule, in all the test facilities, a pressure gauge and a thermocouple were installed after each element, making it possible to calculate the specific enthalpy at each of the desired points. In general, the enthalpy is calculated as a function of pressure, temperature and the mass composition of the mixture tested [Eq. (2.13)].

$$h = f(P, T, M_{comp}) \qquad \text{Eq. (2.13)}$$

The only property calculated differently is the enthalpy at the evaporator inlet. The calculation is based on the assumption of an isenthalpic expansion through the expansion device, as shown in Eq. (2.14) to Eq. (2.16).

$$h_{o,in} = h_{exp,in} \qquad \text{Eq. (2.14)}$$

$$T_{o,in} = f(P_{o,in}, h_{o,in}, M_{comp}) \qquad \text{Eq. (2.15)}$$

$$x_{o,in} = f(P_{o,in}, h_{o,in}, M_{comp}) \qquad \text{Eq. (2.16)}$$

Figure 2.18 shows a scheme of the property calculation.

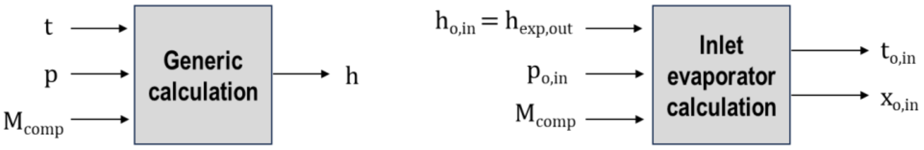

Figure 2.18. Properties calculation.

The calculation of the energy consumption ($\boldsymbol{E_i}$) during the test period in the sealed appliances is done according to Eq. (2.17), where $P_c(t)$ is the total power consumed by the test unit at time t.

$$E_i = \frac{1}{3600} \cdot \int_0^{24h/16h} P_c(t) \cdot dt = \frac{1}{3600} \cdot \sum_{j=1}^{24h/16h} \left\{ \left[\frac{P_c(j) + P_c(j-1)}{2} \right] \cdot [t(j) - t(j-1)] \right\} \qquad \text{Eq. (2.17)}$$

In the bench test, the calculation of the properties $\dot{Q}_o$, COP y VCC was carried out using the values of the secondary fluid, since, as explained in CHAPTER 7, Section 3, their calculation is more accurate than from the point of view of the refrigerant fluid. Therefore, the calculation is done according to Eq. (2.18) to Eq. (2.20).

$$\dot{Q}_o = \dot{m}_{gly} \cdot c_p \cdot (t_{o,in} - t_{o,out}) \quad \text{Eq. (2.18)}$$

$$COP = \frac{\dot{Q}_o}{P_c} \quad \text{Eq. (2.19)}$$

$$VCC = \frac{\dot{q}_o}{v_{suc}} = \frac{\dot{Q}_o / \dot{m}_{ref}}{v_{suc}} \quad \text{Eq. (2.20)}$$

The calculation of the phase-change temperatures differs between the sealed appliances and the bench test. For the sealed plants the calculation is done according to Eq. (2.21) and Eq. (2.22) using the average pressure during the phase-change. As mixtures have glide, phase-change temperature is calculated according to the criterion of the average enthalpy during the evaporation, which also coincides with a vapour quality of 50% in the condenser.

$$\bar{t}_o = f\left[\left(p_{o,in} + p_{asp}\right)/_2, \left(h_{o,in} + h_{sat,vap}\right)/_2 \right] \quad \text{Eq. (2.21)}$$

$$\bar{t}_k = f\left[\left(p_{des} + p_{exp}\right)/_2, x_v = 0.5 \right] \quad \text{Eq. (2.22)}$$

Regarding the bench test, since there are thermocouples distributed along both heat exchangers, the phase-change temperature is calculated directly, without the need to use calculations, considering it as the average of all the recorded values that are within the change of state, as seen in Eq. (2.23).

$$\bar{t} = \frac{\sum_i^n t_i}{n} \quad \text{Eq. (2.23)}$$

Uncertainty analysis

The measurement uncertainties associated with the measurement of each measurement element are given in Table 2.1. However, the propagation of the error in the calculation of variables (i.e. an indirect measurement), where several measurements are taken into account, is done according to Eq. (2.24) [8]. The equation is based on the square root of the sum of the squares of the partial derivatives of each variable involved in the formula and its multiplication by its measurement error.

$$\varepsilon(f) = \sqrt{\left(\frac{\partial f}{\partial x}\right)^2 [\varepsilon(x)]^2 + \left(\frac{\partial f}{\partial y}\right)^2 [\varepsilon(y)]^2 + \left(\frac{\partial f}{\partial z}\right)^2 [\varepsilon(z)]^2 + \cdots} \quad \text{Eq. (2.24)}$$

The most important variables calculated by indirect measurements in this thesis are E_i [Eq. (2.17)], $\dot{Q}_o$ [Eq. (2.18)], COP [Eq. (2.19)] and VCC [Eq. (2.20)]. Eq. (2.25) to Eq. (2.28) show the developed uncertainty calculation for each of them.

$$\varepsilon(E_i) = \frac{u(P_c)\cdot\Delta t}{\sqrt{2}\cdot 36\cdot 10^5}\cdot\sqrt{\sum_{i=1}^{n}[P_C(i)]^2} \qquad \text{Eq. (2.25)}$$

$$\varepsilon(\dot{Q}_o) = \sqrt{\left(c_p\cdot\left(t_{gly,o,in}-t_{gly,o,out}\right)\cdot\varepsilon\left(m_{gly}\right)\right)^2 + 2\cdot\left(c_p\cdot m_{gly}\cdot\frac{\varepsilon(t)}{\sqrt{3}}\right)^2} \qquad \text{Eq. (2.26)}$$

$$\varepsilon(COP) = \sqrt{\begin{gathered}\left(\frac{c_p\cdot\left(t_{gly,o,in}-t_{gly,o,out}\right)}{P_c}\cdot\varepsilon\left(m_{gly}\right)\right)^2 + \\ 2\cdot\left(\frac{c_p\cdot m_{gly}}{P_c}\cdot\frac{\varepsilon(t)}{\sqrt{3}}\right)^2 + \\ \left(\frac{-m_{gly}\cdot c_p\cdot\left(t_{gly,o,in}-t_{gly,o,out}\right)}{P_c^2}\cdot\varepsilon(P_C)\right)^2\end{gathered}} \qquad \text{Eq. (2.27)}$$

$$\varepsilon(VCC) = \sqrt{\begin{gathered}\left(\frac{c_p\cdot\left(t_{gly,o,in}-t_{gly,o,out}\right)}{m_{ref}}\cdot\varepsilon\left(m_{gly}\right)\right)^2 + \\ 2\cdot\left(\frac{c_p\cdot m_{gly}}{m_{ref}}\cdot\frac{\varepsilon(t)}{\sqrt{3}}\right)^2 + \\ \left(\frac{-m_{gly}\cdot c_p\cdot\left(t_{gly,o,in}-t_{gly,o,out}\right)}{{m_{ref}}^2}\cdot\varepsilon\left(m_{ref}\right)\right)^2\end{gathered}} \qquad \text{Eq. (2.28)}$$

2.3 Nomenclature

c_p	Specific heat capacity, $kJ \cdot kg^{-1} \cdot K^{-1}$
COP	Coefficient Of Performance
Ei	Energy consumption, $kW \cdot h^{-1}$
F	Number of fluorine atoms.
GWP	Global Warming Potential
h	Specific enthalpy, $kJ \cdot Kg^{-1}$
H	Number of hydrogen atoms
HOC	Heat Of Combustion, $kJ \cdot Kg^{-1}$
L1	Conditions for the preservation of frozen product, with non-adiabatic capillary tube.
L2	Conditions for the preservation of frozen product, with adiabatic capillary tube.
LFL	Lower Flammability Limit, $kg \cdot m^{-3}$
$\dot{m}$	Mass flow rate, $kg \cdot s^{-1}$
M1	Conditions for the preservation of fresh product, with non-adiabatic capillary tube.
M2	Conditions for the preservation of fresh product, with adiabatic capillary tube.
p	Pressure, bar
P_c	Total power consumed by the test unit at time t, kW
$\dot{Q}_o$	Cooling capacity, kW
$\dot{q}_o$	Specific cooling capacity, kJ·kg-1
RH	Relative Humidity, %
SH	Superheating, K
SUB	Subscooling, K
t	Temperature, ºC
Tad	Adiabatic Flame Temperature, ºC
VCC	Volumetric Cooling Capacity, $kJ \cdot m^{-3}$
v_{suc}	Suction volume, $m^3 \cdot kg^{-1}$
WCF	Worst Case of Formulation for Flammability
WCFF	Worst Case of Fractionation for Flammability
xv	Quality
ε	Thermal efficiency
Π	Angle for flammability classification (degrees)

Subscripts

a	ambient
cap	Relative to the capillary tube
dis	Relative to the discharge
down	Bottom position

gly	Relative to the water/propylene glycol mixture
ihx	Internal heat exchanger
in	inlet
k	Relative to the condensation
o	Relative to the evaporation
out	outlet
ref	Relative to the refrigerant
suc	suction

2.4 References

[1] Author, NIST Standard Reference Database 23: Reference Fluid Thermodynamic and Transport Properties-REFPROP, Version 10.0, National Institute of Standards and Technology, 2018 DOI: dx.doi.org/10.18434/T4JS3C.

[2] Author, REFLEAK: NIST Leak/Recharge Simulation Model for Refrigerant Blends, Version 5.1, National Institute of Standards and Technology Gaithersburg, MD, 2018 DOI: https://doi.org/10.6028/NIST.NSRDS.73-2018

[3] Author, Cantera: An object-oriented software toolkit for chemical kinetics, thermodynamics, and transport processes. , 2021 DOI: 10.5281/zenodo.4527812.

[4] R. Radermacher, Y. Hwang, Vapor compression heat pumps with refrigerant mixtures., CRC Press, Taylor & Francis, NW, 2005.

[5] G.T. Linteris, I.H. Bell, M.O. McLinden, An empirical model for refrigerant flammability based on molecular structure and thermodynamics, International Journal of Refrigeration, 104 (2019) 144-150 DOI: 10.1016/j.ijrefrig.2019.05.006.

[6] I. 62552-1:2015/AMD1:2020, Household refrigerating appliances - Characteristics and test methods - Part 1: General requirements, in, 2020.

[7] E.I. 23953-2:2023, Refrigerated display cabinets - Part 2: Classification, requirements and test conditions, in, 2023.

[8] R.J. Moffat, Describing the uncertainties in experimental results, Experimental Thermal and Fluid Science, 1 (1988) 3-17 DOI: 10.1016/0894-1777(88)90043-x.

CHAPTER 3.
THERMODYNAMIC SCREENING OF ALTERNATIVE REFRIGERANTS FOR R290 AND R600a.

Chapter adapted from the paper:

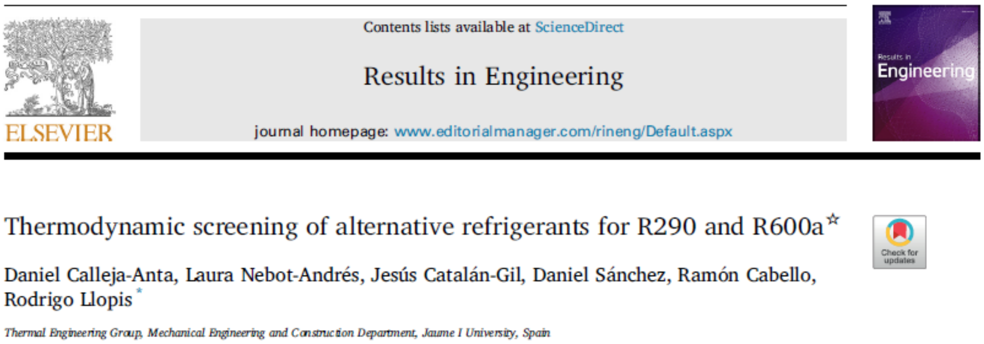

Contents lists available at ScienceDirect

Results in Engineering

journal homepage: www.editorialmanager.com/rineng/Default.aspx

Thermodynamic screening of alternative refrigerants for R290 and R600a☆

Daniel Calleja-Anta, Laura Nebot-Andrés, Jesús Catalán-Gil, Daniel Sánchez, Ramón Cabello, Rodrigo Llopis*

Thermal Engineering Group, Mechanical Engineering and Construction Department, Jaume I University, Spain

Calleja-Anta, D., Nebot-Andrés, L., Catalán-Gil, J., Sánchez, D., Cabello, R., Llopis, R., Thermodynamic screening of alternative refrigerants for R290 and R600a (2020) Results in Engineering, 5, art. no. 100081. DOI: 10.1016/j.rineng.2019.100081

Cited 41 times.

Journal Citation Indicator QUARTILE: Q1 (2021 quartile).

3 THERMODYNAMIC SCREENING OF ALTERNATIVE REFRIGERANTS FOR R290 AND R600a.

Daniel Calleja-Anta, Laura Nebot-Andrés, Jesús Catalán-Gil, Daniel Sánchez,
Ramón Cabello, Rodrigo Llopis

Thermal Engineering Group, Mechanical Engineering and Construction Department,
Jaume I University, Spain

Abstract

Due to Regulation EU 517/2014 (F-Gas), the use of refrigerants with GWP higher than 150 was limited from 2015 on in small capacity refrigeration systems in Europe. Although refrigerants that dominate are R600a and R290 nowadays, which are classified as A3 by ASHRAE 34, literature points out that some refrigerant mixtures exist that could offer benefits from the point of view of COP and VCC, especially mixtures of hydrocarbons.

This study tries to identify possible mixtures which could be used as alternatives to pure hydrocarbons, with the aim to increase the energetic behaviour of the systems and, if possible, to reduce the flammability characteristics. A thermodynamic screening of refrigerant mixtures (with the base refrigerants R290, R600a, R600, R1270, R152a, R32, R1234yf, R1234ze(E), R1233zd, R744 and R134a) is presented and detailed for two typologies of systems: single-stage systems with adiabatic capillary tube and single-stage systems with non-adiabatic capillary tube. The screening identifies the most promising refrigerant mixtures that will be tested later in experimental systems.

Keywords

Hydrocarbons, refrigerant, stand-alone systems, energy efficiency

3.1 Introduction

Energy use of refrigeration and air conditioning systems absorbed about 20 % of the total electricity produced in the World and it was responsible of 7.8 % of total greenhouse gas emissions in 2014, according to the International Institute of Refrigeration [1]. Inside this sector, the subgroup of domestic fridge/freezers and stand-alone commercial refrigeration appliances, with more than 1.5 billion units, absorbed a 15.4 % of the generated electricity, thus they accounted for approximately a 2.6 % of electricity produced in the world [2].

To reduce the environmental impact of the refrigeration sector globally, the World and especially the European Union have implemented different agreements and regulations that affect the refrigeration sector, such as the Kigali amendment to the Montreal Protocol [3] or the F-Gas Regulation [4]. However, specifically in relation to the domestic and stand-alone commercial systems and in addition to those mentioned previously, Europe has implemented two important regulations: The Eco-design directive [5] that establishes a minimum level of energy efficiency to be reached by the products that can be placed on the market; and the Energy labelling Regulation ([6] for domestic systems and [7] for commercial systems) which will classify them into efficiency groups.

Obviously, this segment of refrigeration appliances must meet many requirements, such as security, use of low-GWP (low Global Warming Potential) refrigerants and energy efficiency, being sometimes difficult to meet them all simultaneously. Nonetheless, what is clear is that the low-GWP refrigerants (HCs, and HFOs) will be the selected option [8]. Improve security and increase energy efficiency are the pending conditions. In the last two decades, refrigeration manufacturers expanded the use of hydrocarbons as refrigerants for equipment able to operate with maximum refrigerant charge of 150 g, R-600a dominates the domestic sector and R-290 the commercial one [9]. However, the recent modification of the IEC standard [10] will allow to increase the refrigerant charge with A3 refrigerants up to 500 g, thus, its use will be extended to larger systems. In relation to upgrade the performance of these systems, few efforts are being done to improve the performance of the refrigerant. But, literature reflects that there are some options that could enhance energy performance by the use of refrigerant mixtures, such as the mixture R-290/R600a ([11-13]) with energy consumption reduction in refrigerators between 2 to 4 %; the use of R-152a [14, 15] with energy improvements in a freezer of 7 %, or the mixture R-1234yf/R-134a with improvements in relation to R-134a between 14-16 % [16, 17].

Although not considered by the scientific community up to the moment, to the best knowledge of the authors, the search for alternative refrigerants to hydrocarbons has not been considered, but the experimental investigations found in literature indicate that there is room for improvement. Accordingly, the objective of this work is to present the results of a thermodynamic screening of refrigerant mixtures which could be '*better*' refrigerants or at least reduce the energy consumption of stand-alone systems based on R-600a or R-290 and to analyze if thermodynamically the hypothesis is possible. Thus, here, a systematic search based on thermodynamic models has been conducted by considering 120 possible ternary mixtures with 231 combinations in each one for 4 different working conditions, giving a total number of combinations of 27480. This screening has identified a small set of combinations, which, thermodynamically could offer energy benefits. Thus, this is the first stage of a new line of research, which will bring about the scientific community possibilities to test the proposed mixtures in real systems to obtain definite conclusions.

3.2 Refrigeration typologies and thermodynamic model

Simulations were carried out for the most common refrigeration typologies used in small capacity hermetic refrigeration systems: single-stage systems with adiabatic capillary tube (Figure 3.1) and single-stage systems with non-adiabatic capillary tube (Figure 3.2). The main difference between them is the heat transfer in the capillary tube. In the first one (Figure 3.1), the capillary is alone, whereas in the non-adiabatic layout (Figure 3.2) it is wrapped around the suction line, acting as a suction-line to liquid-line heat exchanger [18]. For simulations, both compression and expansion processes were considered as ideal (isentropic and isenthalpic respectively) and pressure drops and kinetic and potential variations were neglected.

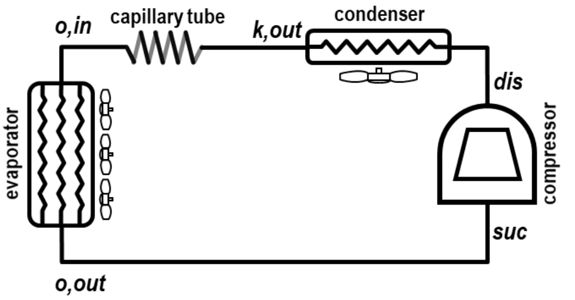

Figure 3.1. Single-stage cycle with adiabatic capillary tube

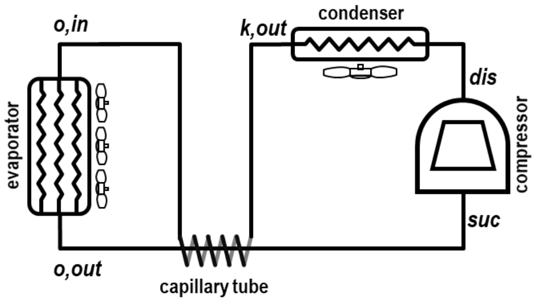

Figure 3.2. Single-stage cycle with non-adiabatic capillary tube

The refrigerants were evaluated and compared at fixed evaporating and condensing temperatures for the considered cycles (conditions are presented subsequently in Table 3.2). Evaporation pressure (p_o), corresponding to evaporating temperature level, was calculated with an iterative method by using the mean enthalpy in the evaporator, as stablished by Eq.(3.1 and Eq.(3.2). This criteria is the most recommended for the evaluation of refrigerant mixtures, as suggested by Radermacher and Hwang [19].

$$h_m = (\frac{h_{O,in}+h_{O,out}}{2}) \qquad \text{Eq.(3.1)}$$

$$p_O = f(t_O, h_m) \qquad \text{Eq.(3.2)}$$

Condensing pressure (p_k), following the same criteria, was calculated using Eq.(3.3), that considers that the medium enthalpy matches with 50 % vapour quality (x_v) in the condenser.

$$p_k = f(t_k, x_v = 0.5) \qquad \text{Eq.(3.3)}$$

Outlet temperature of evaporator and condenser were evaluated using Eq.(3.4) and Eq.(3.5) respectively, considering saturation temperatures at the corresponding pressure and the degree of superheat in the evaporator and degree of subcooling in the condenser.

$$t_{O,out} = f(t_{v,p_O} + RU, p_O) \qquad \text{Eq.(3.4)}$$

$$t_{K,out} = f(t_{l,Pk} - SUB, p_K) \qquad \text{Eq.(3.5)}$$

Suction temperature and enthalpy were evaluated considering that the capillary acts as an internal heat exchanger with defined thermal effectiveness, as expressed by Eq.(3.6) and Eq.(3.7). Finally, evaporator inlet enthalpy was obtained through the heat balance in the capillary tube.

$$t_{suc} = t_{O,out} + \varepsilon_{ihx} \cdot (t_{K,out} - t_{O,out}) \qquad \text{Eq.(3.6)}$$

$$h_{suc} = f(t_{suc}, p_O) \qquad \text{Eq.(3.7)}$$

$$h_{O,in} = h_{K,out} - h_{suc} + h_{O,out} \qquad \text{Eq.(3.8)}$$

With the thermodynamic states of the refrigerants through the cycles, the following parameters were considered to analyse the performance of the tested refrigerant mixtures:

- **Effective glide**: in evaporator and condenser, the effective glide corresponds to the temperature difference along the phase-change process at constant pressure, as defined by Eq.(3.9) for the evaporator and by Eq.(3.10) for the condenser.

$$Glide_O = t(p_O, x_v = 1) - t(p_O, x_{v,O,in}) \qquad \text{Eq.(3.9)}$$

$$Glide_K = t(p_K, x_v = 1) - t(p_K, x_v = 0) \qquad \text{Eq.(3.10)}$$

- **Volumetric Cooling Capacity (VCC) and Coefficient of Performance (COP)**, which were evaluated using Eq.(3.11) and Eq.(3.12), respectively.

$$VCC = \frac{h_{O,out} - h_{O,in}}{v_{suc}} \qquad \text{Eq.(3.11)}$$

$$COP = \frac{h_{O,out} - h_{O,in}}{h_{dis,S}(p_K, s_{suc}) - h_{suc}} \qquad \text{Eq.(3.12)}$$

- **Global warming potential (GWP)** of the mixture, which as evaluated using Eq.(3.13) as the sum of partial masses of each refrigerant multiplied by their GWP, these values being extracted from the 4th Assessment Report of the IPCC [20].

$$GWP = \sum_i^n (m_i \cdot GWP_i) \qquad \text{Eq.(3.13)}$$

It is important to mention that the model evaluated the thermodynamic properties of the mixtures using the most recent version of Refprop, version 10 [21], with the recommended mixing rules described in the file HMX.BNC version 4, although described later, in some cases the mixing rules provided incoherent results. Maltab 2016a was the platform used to perform the screening.

3.3 Boundary conditions and optimization process

Table 3.1 shows the refrigerants considered in the optimization process and their main properties. All of them have a GWP below 150, thus there is no limitation in the percentage that can be used in the mixture, except for the R-32, that only can be existing in a 22.1 % as maximum. According to Ashrae classification [22], all of them (except for the R-744) present flammable characteristics, however R-152a is classified as A2 and R-32, R-1234yf, R-1234ze and R-1233zd as A2L, so depending on the composition, the mixtures can present lower flammability characteristics than isobutane and propane, which are A3.

Table 3.1. Refrigerants considered in the screening and their properties.

	Family	NBP (ºC)	Critical temperature (ºC)	Critical pressure (bar)	GWP (AR4)	Safety Group
R-290	HC	-42.1	96.7	42.5	3	A3
R-600a	HC	-11.7	134.7	36.3	3	A3
R-600	HC	-0.5	152.0	38.0	3	A3
R-1270	HC	-47.7	92.4	46.6	1.8	A3
R-152a	HFC	-24.0	113.3	45.2	124	A2
R-32	HFC	-51.7	78.1	57.8	675	A2L
R-1234yf	HFO	-29.4	94.7	33.8	4	A2L
R-1234zeE	HFO	-19.0	109.4	36.3	6	A2L
R-1233zd	HCFO	18.3	116.5	36.2	1*	A2L
R-744	Natural	-78.4	31.0	73.8	1	A1

*Adapted from the 5th AR of the IPCC [23]

Two different applications are considered in the optimization process: conservation of fresh product and conservation of frozen product (with selected evaporation temperatures of -10 ºC and -30 ºC, respectively). For each application, calculations were conducted considering that the capillary was adiabatic or non-adiabatic, as described in Section 2. For the non-adiabatic case (Figure 3.2), an 80 % thermal efficiency was considered. Condensation temperature, superheating (SH) and subcooling (SUB) were maintained for all cases, taking values of 40 ºC, 4 K and 1 K, respectively. The working conditions are summarized in Table 3.2.

Table 3.2. Working conditions (M and L refer to “medium” and “low” temperature respectively).

Working conditions	
M1	t_o= -10 ºC, t_k= 40 ºC, non-adiabatic (ε=80 %), SH=4 K, SUB=1 K
M2	t_o= -10 ºC, t_k= 40 ºC, adiabatic, SH =4 K, SUB=1 K
L1	t_o= -30 ºC, t_k= 40 ºC, Non-adiabatic (ε=80 %), SH =4 K, SUB=1 K
L2	t_o= -30 ºC, t_k= 40 ºC, Non-adiabatic, SH =4 K, SUB=1 K

The purpose of the optimization process is to discover refrigerant mixtures with best energy indicators (COP, VCC) than isobutane (R-600a) and propane (R-290) in the four working conditions considered. For that purpose all possible combinations of three refrigerants of Table 3.1 were evaluated. Optimization was limited to three components at this moment due to the long-required computation time. For that end, three steps were carried out:

- Finding composition that maximizes COP for each combination of three refrigerants. In this process, the mixtures were formed by varying 5.0 % the mass percentage of each fluid.
- Filtering of results and election of mixtures with most suitable properties in terms of COP and VCC.
- Finding composition that maximizes COP for the selected mixtures. The mass variation for each refrigerant involved in the mixture was of 0.5 %.

To find the optimal composition, additional restrictions were imposed: To meet the requirements of the EU517/2014 [4], the maximum GWP of the mixture was set at 150. Mixtures exceeding this limit were discarded. The next step was to evaluate the energy parameters of the cycle for each working condition, with the model described in Section 2. As the fluids mixed may have very different Normal Boiling Point (NBP), the glide in the evaporator was a parameter that was controlled and restricted, since a huge glide affects significantly to the thermal performance of the heat exchangers. Therefore, the maximum effective glide allowed in evaporator was of 10 K, although larger values are found in commercial refrigerants [24]. Accordingly, mixtures that surpassed this value were discarded. Another parameter to focus on was the discharge temperature. As it was calculated assuming an isentropic process in the compressor, the restriction value should be moderated. When assuming adiabatic capillary, the limit value was fixed in 70 ºC, whereas when non-adiabatic capillary, the value was let free, since it was observed that 70 ºC was too restrictive. In that case, the results were analysed afterwards and filtered to discard any nonsense result. This process was carried out for all the possible combinations that each trio of refrigerants can offer. As a result, the combination with better COP was elected. The process is represented in Figure 3.3.

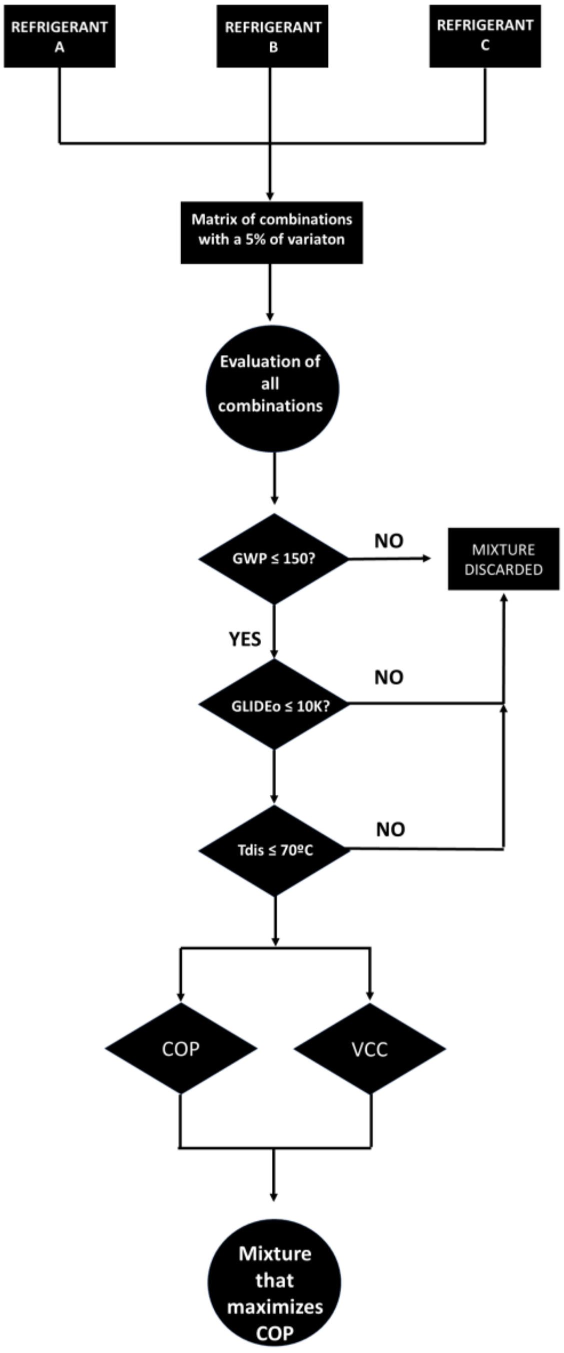

Figure 3.3. Scheme of optimization process.

3.4 Screening results

The number of evaluated mixtures were 27480, representing of 120 possible ternary mixtures, 231 combinations for each ternary mixture (5 % of mass variation) and 4 different working conditions. Section 4.1 presents the results of the optimization with 5 % percentage mass variation, section 4.2 the remaining mixtures when the compatibility restrictions were applied, and section 4.3 the fine optimization of the mixtures that fulfilled the restrictions.

3.4.1 First optimization process

Figure 3.4 and Figure 3.5 show, as an example, the result of the first optimization process for M1 and L1 working conditions, which consists in finding the optimal composition for each ternary mixture. As it can be observed, only mixtures with similar or higher COP than the base fluid are considered. Also, it can be observed that with some specific mixtures high COP values were predicted. Obviously, these large values could be associated to a fail of the mixing rules of the components of the database program. Accordingly, the optimal compositions were subjected to an acceptance data range, as explained in Section 3.4.2.

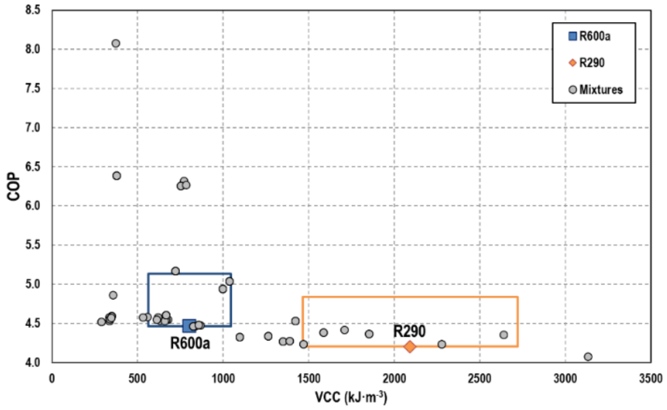

Figure 3.4. Resulting mixtures with t_0 =-10 ºC with non-adiabatic capillary.

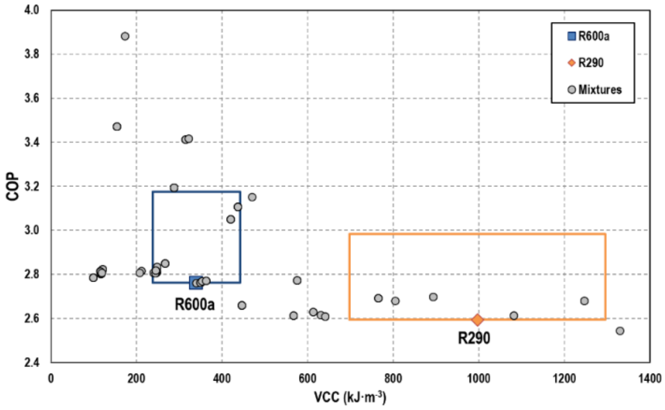

Figure 3.5. Resulting mixtures with t_0 =-30 ºC with non-adiabatic capillary.

3.4.2 Compatibility restrictions

Results obtained for all the possible ternary combinations were compared with reference to the COP and VCC calculated for R-600a and R-290 in each working condition, resulting in four scenarios for each base refrigerant. The considered acceptance range for each scenario was of ±30 % of the VCC of the base refrigerant (since for a correct operation of the compressor this value must be similar), and between 0 to +15 % of the base refrigerant COP. Higher COP increments were considered as a fail of the mixing rules available in Refprop 10 [21] and therefore the resulting mixtures were not considered as reliable.

Figure 3.6 represents all the refrigerant mixtures identified in the first optimization process in relation to R-600a, where it is represented the R-600a operating point in each working condition (Table 3.2) and the acceptance gap as defined previously. For the operation at medium evaporating conditions (condition M, Table 3.2), 10 binary and 2 ternary mixtures fulfilled the restrictions, with maximum COP increments in relation to R-600a up to 6.0 % and variations in the VCC between -24.5 to 11.5 %. At low evaporating levels (condition L, Table 3.2), only 8 binary blends were identified, with maximum COP increment up to 8.6 % and variations in the VCC between -28.0 % to 14.2 %.

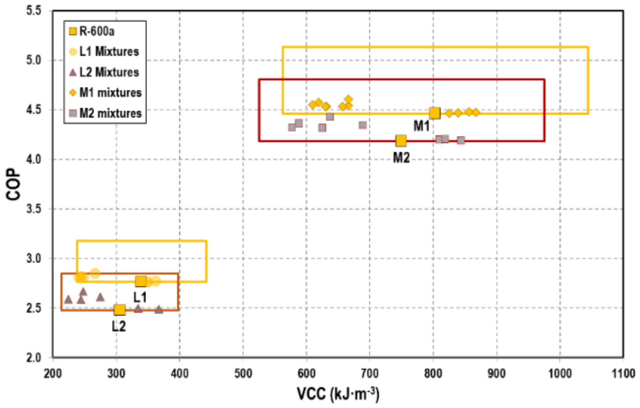

Figure 3.6. Alternative mixtures in the acceptance gap for R-600a.

Figure 3.7 depicts the refrigerant mixtures identified in the first process with R-290 as base refrigerant, as well as, its operating point and acceptance gap at each working condition. At medium temperature (condition M, Table 3.2), 5 binary and 2 ternary mixtures and 1 pure fluid were identified. R-152a, with reduction in VCC below -30 % was also considered because it provided an interesting COP increment. Maximum COP increments reached 11.3 % with variations in VCC between -24.5 to 11.5 %. At low evaporating level (condition L, Table 3.2). 6 binary and 1 ternary mixture were in agreement with the restrictions, as well as, one pure fluid. Additionally, R-744/R-290 blend and R-1234yf were also included because they were at the limit of the acceptance gap. For this condition, maximum COP increment was of 11.6 % and the variation of the VCC was between -27.5 to 25.8 %.

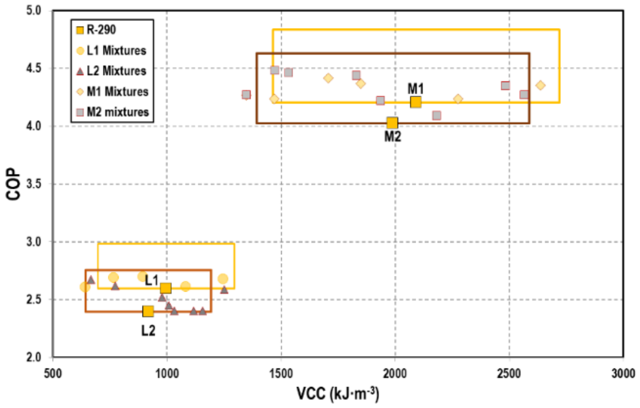

Figure 3.7. Alternative mixtures in the acceptance gap for R-290

3.4.3 Fine optimization process

Finally, mixtures identified in the first optimization process that fulfilled the compatibility restrictions were subjected to a fine optimization process, with the same calculation procedure described in Section 2, but considering 0.5 % of mass fraction variation of each component.

Alternative mixtures to R-600a

Figure 3.8 to Figure 3.11 represent the thermodynamic properties of alternative mixtures to R-600a in the four operating conditions considered (Table 3.2). It can be seen that the identified mixtures are mostly binary mixtures, mainly composed by R-600a (its composition varies between 96.5 % and 89.5 %) or R-600 (between 95.5 % and 84.5 %) with a small fraction of another fluid, although there are two ternary blends with a small fraction of a third component (below 1 %). All mixtures with R-600a achieve a slight increment in COP (between 0.1 % and 0.4 % for M1, 0.6 % and 0.3 % for M2, 0.3 % and 0.1 % for L1 and 0.8 % and 0.4 % for L2) and higher VCC (between 4.6 % and 8 % for M1, 6.4 % and 11.5 % for M2, 4.2 % and 6 % for L1 and 11.2 % and 14.2 % for L2). On the contrary, the mixtures composed by R600 achieve higher increments in COP (between 3.3 % and 1.6 % for M1, 6 % and 3.3 % for M2, 8.6 % and 1.7 % for L1 and 7.6 % and 4.3 % for L2), but the VCC decreases significantly (between -24.7 % and -16.4 % for M1, -22.7 % and -16.4 % for M2, -28.7 % and -24.6 % for L1 and -26.4 % and -10.8 % for L2). Another aspect to consider is the glide in the phase change processes, which is accentuated when the difference between the NBP of the refrigerants is greater, being higher with R-600.

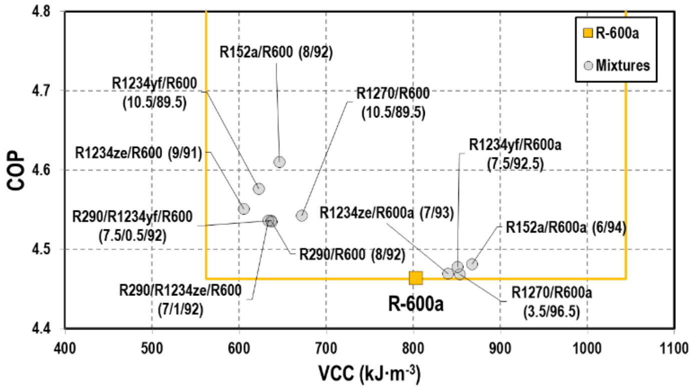

Figure 3.8. Mixtures in the acceptance gap for R-600a in M1 conditions

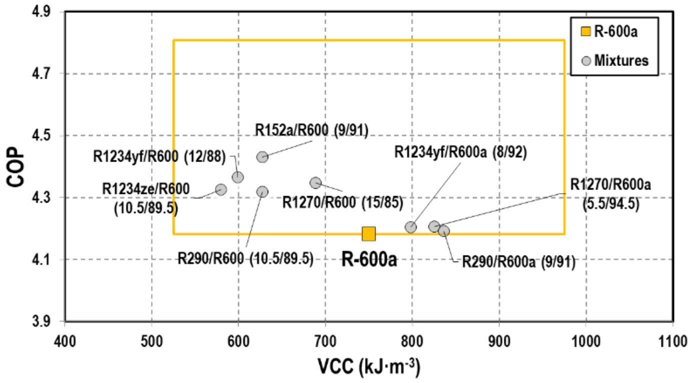

Figure 3.9. Mixtures in the acceptance gap for R-600a in M2 conditions

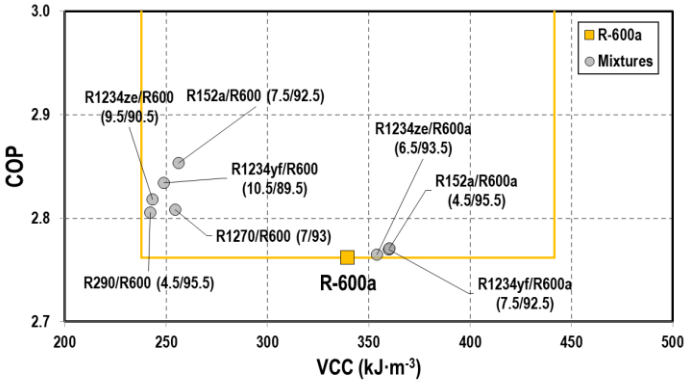

Figure 3.10. Mixtures in the acceptance gap for R-600a in L1 conditions

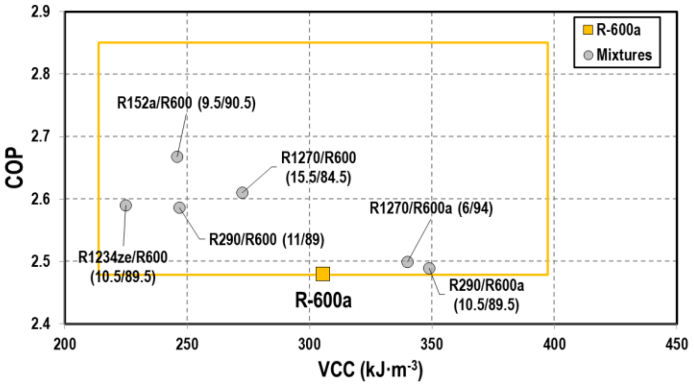

Figure 3.11. Mixtures in the acceptance gap for R-600a in L2 conditions

Alternative mixtures to R-290

Figure 3.12 to Figure 3.15 highlight the mixtures alternative to R-290 identified for all the operating conditions (Table 3.2). In this case the number of mixtures is shorter than for R-600a. For propane alternatives, two types of mixtures can be observed: mixtures composed by a low percentage of R-744 and another fluid (the R-744 increases the VCC of the mixture), and those constituted by R-290 as the main component with another refrigerant with low percentage. COP increases up to 5.1 % in M1 conditions, 11.7 % in M2, 4.1 % in L1 and 11.6 % in L2. It must be considered that the mixtures with R-744 have a significant glide, being around 10 K in the evaporator, which could lead into operational problems. It is important to mention that the pure fluids R-152 and R-1234yf are in the limit of the acceptance range. These fluids will provide small increments in COP in most of the cases but with a strong reduction in capacity.

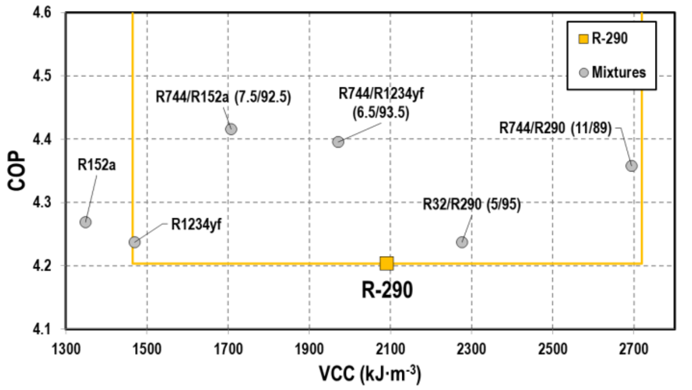

Figure 3.12. Mixtures in the acceptance gap for R-290 in M1 conditions.

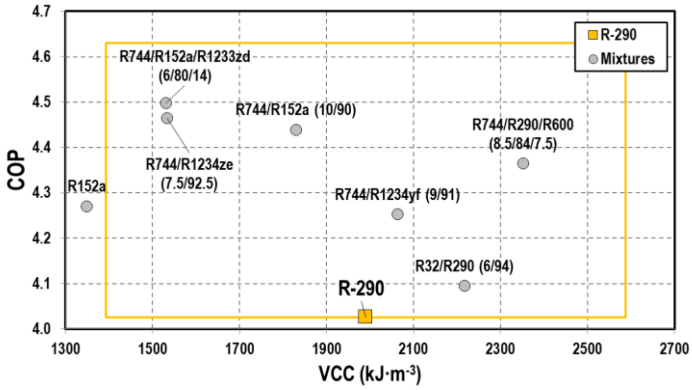

Figure 3.13. Mixtures in the acceptance gap for R-290 in M2 conditions.

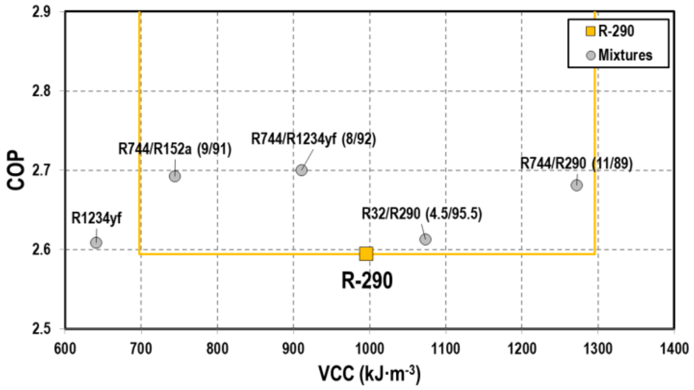

Figure 3.14. Mixtures in the acceptance gap for R-290 in L1 conditions.

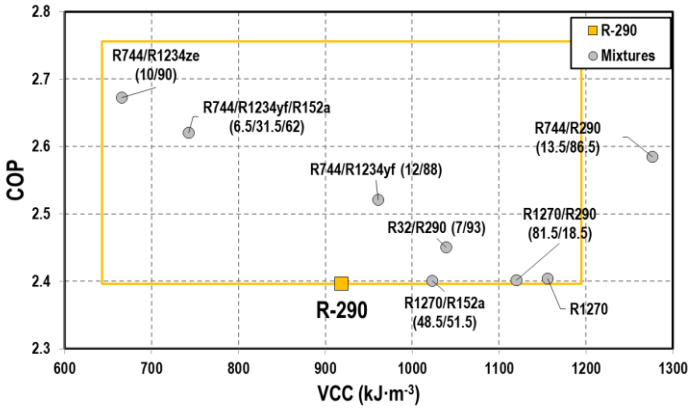

Figure 3.15. Mixtures in the acceptance gap for R-290 in L2 conditions.

3.5 Conclusions

A theoretical search for refrigerant mixtures that could provide energy improvements in relation to R-600a and R-290 for refrigeration systems was performed. Blends with a maximum of three components were subjected to a thermodynamic optimization process consisting on finding the optimal composition that maximizes COP subjected to different compatibility restrictions. The screening was focused on the application to two evaporating levels (-10 ºC and -30 ºC) for constant condensing temperature (40 ºC) for two types of typologies: single-stage systems with adiabatic capillary tube and single stage systems with non-adiabatic capillary tube.

In total, 27480 different refrigerant mixtures were evaluated to select the best candidates. Selection chose COP as optimizing parameter, but the blends were subjected to fulfil some compatibility restrictions that guarantee the experimental verification in real systems. Concretely, all the selected mixtures presented a GWP value below 150, operate with an effective glide in the evaporator of 10 K and present an isentropic discharge temperature below 70 ºC. From all mixtures fulfilling restrictions, the ones presenting theoretical COP increments from 0 to 15 % and variations in the volumetric cooling capacity (VCC) from -30 to 30 % in relation to R-600a and R-290 were selected. Finally, remaining mixtures were optimized again with a mass fraction variation of each component of 0.5 %.

Respect to possible alternatives to isobutane (R-600a), mixtures composed by R-1234yf/R-600a and R-1270/R-600a offer a slight increase in COP (between 0.3 % and 0.6 % and between 0.1 % and 0.8 % respectively) and a small increment in VCC (between 5.9 % and 6.4 % and between 6.3 % and 11.2 % respectively) respect R-600a, whereas mixtures form by R-1270/R-600, R-152a/R-600, R-1234yf/R-600, R-1234zeE/R-600 and R-290/R-600 achieve high increments of COP (between 1.7 % and 5.3 %, 3.3 % and 7.6 %, 2.5 % and 4.4 %, 2 % and 4.5 % and 1.6 % and 8.6 %) but the VCC is decreased significantly (between -25.1 % and -8.2 %, -24.6 % and -16.4 %, -24.6 % and -16.4 %, -28.4 % and -22.7 % and -28.4 % and -16.4 %, respectively) respect R-600a.

Respect to possible alternatives to propane (R-290), mixtures form by a small proportion of R-744 with R-290, R-1234yf, R-152a or R-1234ze(E) achieve high increments of COP (between 3.4 % and 7.9 %, 4.1 % and 5.6 %, 3.8 % and 10.3 % and 10.9 % and 11.6 %, respectively) but the VCC differs a lot between one mixture with each other (from 28.8 % and 38.9 %, -8.6 % and 3.7 %, -25.4 % and -8 %, -27.6 % and -23 % and 7.7 % and 13 %, respectively). It is also identified the mixture R-32/R-290, which accomplishes a raise of COP and VCC between 0.8% and 2.3% and 8.8% and 13%, respectively.

Accordingly, from the theoretical screening performed in this work, it is clear that there are some refrigerant mixtures which could be candidates to replace pure hydrocarbons in small systems, providing a slight increment in COP. This work constitutes an initial hypothesis, since experimental validation is needed to confirm the real possibilities of the identified mixtures.

3.6 Acknowledgements

Authors gratefully acknowledge Conselleria d’Educació, Investigació, Cultura i Esport de la Generalitat Valenciana (project AICO/2018/058) and the Ministry of Science, Innovation and Universities of Spain (RTI2018-093501-B-C21) for financing this research work.

3.7 Nomenclature

COP	coefficient of performance
GWP	global warming potential for 100 years (4th AR)
Glide	effective glide in heat exchanger, K
h	specific enthalpy, $kJ \cdot kg^{-1}$
HC	hydrocarbon
HCFO	hydroclorofluorocarbon
HFC	hydrofluorocarbon
HFO	hydrofluoroolefin
m	mass fraction, %
NBP	normal boiling point, ºC
p	absolute pressure, bar
S	specific entropy, $kJ \cdot kg^{-1}$
SH	degree of superheating in evaporator, K
SUB	degree of subcooling in condenser, K
t	temperature, ºC
VCC	volumetric cooling capacity, $kJ \cdot m^{-3}$
x_v	vapour quality

Greek symbols

ε	thermal effectiveness
v	specific volume, $m^3 \cdot kg^{-1}$

Subscripts

dis	compressor discharge
ihx	internal heat exchanger (non-adiabatic capillary)
in	inlet
K	condensing level
l	saturated liquid
m	average value
O	evaporating level
out	outlet
suc	compressor suction
v	saturated vapour

3.8 References

[1] International Institute of Refrigeration, 38th Note on Refrigeration Technologies. The Role of Refrigeration in the Global Economy (2019). in, International Institute of Refrigeration, 2019, DOI: 10.18462/iif.NItec38.06.2019.

[2] International Institute of Refrigeration, 35th Informatory note on Refrigeration Technologies. The impact of the refrigeration sector on climate change, in, IIR, France, 2017.

[3] UNEP, Report of the Twenty-Eighth Meeting of the Parties to the Montreal Protocol on Substances that Deplete the Ozone Layer, in, Kigali, Rwanda, 2016.

[4] European Commission, Regulation (EU) No 517/2014 of the European Parliament and of the Council of 16 April 2014 on fluorinated greenhouse gases and repealing Regulation (EC) No 842/2006., in: E. Commission (ed.), Official Journal of the European Union, 2014.

[5] European Commission, COMMISSION REGULATION (EU) 2015/1095 of 5 May 2015 implementing Directive 2009/125/EC of the European Parliament and of the Council with regard to ecodesign requirements for professional refrigerated storage cabinets, blast cabinets, condensing units and process chillers., in, 2015.

[6] European Commission, Commission delegated Regulation No 1060/2010 of 28 September 2010 supplementing Directive 2010/30/EU of the European Parliament and of the Council with regard to energy labelling of household refrigerating appliances, in, 2010.

[7] European Commission, COMMISSION DELEGATED REGULATION (EU) 2015/1094 of 5 May 2015 supplementing Directive 2010/30/EU of the European Parliament and of the Council with regard to the energy labelling of professional refrigerated storage cabinets., in, 2015.

[8] D. Sánchez, R. Cabello, R. Llopis, I. Arauzo, J. Catalán-Gil, E. Torrella, Energy performance evaluation of R1234yf, R1234ze(E), R600a, R290 and R152a as low-GWP R134a alternatives, International Journal of Refrigeration, 74 (2017) 269-282 DOI: http://dx.doi.org/10.1016/j.ijrefrig.2016.09.020.

[9] R. Llopis, D. Sánchez, R. Cabello, Refrigerants for vapor compression refrigeration systems a review on natural and artificial heat transfer fluids, in: Advances in New Heat Transfer Fluids: From Numerical to Experimental Techniques, 2017, pp. 463-522 DOI: 10.1201/9781315368184.

[10] International Electrotechnical Commission., IEC 60335-2-89:2019. Household and similar electrical appliances - Safety - Part 2-89: Particular requirements for commercial refrigerating appliances and ice-makers with an incorporated or remote refrigerant unit or motor-compressor, in, 2019.

[11] D. Jung, C.B. Kim, K. Song, B. Park, Testing of propane/isobutane mixture in domestic refrigerators, International Journal of Refrigeration, 23 (2000) 517-527 DOI: 10.1016/S0140-7007(99)00084-5.

[12] M. Mohanraj, S. Jayaraj, C. Muraleedharan, P. Chandrasekar, Experimental investigation of R290/R600a mixture as an alternative to R134a in a domestic

refrigerator, International Journal of Thermal Sciences, 48 (2009) 1036-1042 DOI: 10.1016/j.ijthermalsci.2008.08.001.
[13] M. Rasti, S. Aghamiri, M.-S. Hatamipour, Energy efficiency enhancement of a domestic refrigerator using R436A and R600a as alternative refrigerants to R134a, International Journal of Thermal Sciences, 74 (2013) 86-94 DOI: http://dx.doi.org/10.1016/j.ijthermalsci.2013.07.009.
[14] A. Maiorino, C. Aprea, M.G. Del Duca, R. Llopis, D. Sánchez, R. Cabello, R-152a as an alternative refrigerant to R-134a in domestic refrigerators: An experimental analysis, International Journal of Refrigeration, 96 (2018) 106-116 DOI: https://doi.org/10.1016/j.ijrefrig.2018.09.020.
[15] R. Cabello, D. Sánchez, R. Llopis, I. Arauzo, E. Torrella, Experimental comparison between R152a and R134a working in a refrigeration facility equipped with a hermetic compressor, International Journal of Refrigeration, 60 (2015) 92-105 DOI: http://dx.doi.org/10.1016/j.ijrefrig.2015.06.021.
[16] Allgood C. C., Hydutsky B., Leck T., Hughes J, Long Term Viability of HFO-1234yf in Stationary Refrigeration Systems – Multi-Year Evaluation of Refrigerant, Lubricant, and Compressor Performance in a Domestic Freezer, in: International Refrigeration and Air Conditioning Conference at Purdue, Purdue, EEUU, 2014.
[17] C. Aprea, A. Greco, A. Maiorino, An experimental investigation of the energetic performances of HFO1234yf and its binary mixtures with HFC134a in a household refrigerator, International Journal of Refrigeration, 76 (2017) 109-117 DOI: 10.1016/j.ijrefrig.2017.02.005.
[18] P.A. Domanski, Theoretical evaluation of the vapor compression cycle with a liquid-line/suction-line heat heat exchanger, economizer, and ejector, in: National Institute of Science and Technology, Interagency Report 5606., National Institute of Standards and Technology, Gaithersburg, MD., 1995.
[19] R. Radermacher, Y. Hwang, Vapor compression heat pumps with refrigerant mixtures., CRC Press, Taylor & Francis, NW, 2005.
[20] IPCC, Climate Change 2007: Synthesis Report. Contribution of Working Groups I, II and III to the Fourth Assessment Report of the Intergovernmental Panel on Climate Change [Core Writing Team, Pachauri, R.K and Reisinger, A. (eds.)]. IPCC, Geneva, Switzerland, 104 pp., in, 2007.
[21] Lemmon E. W., B. I.H., H.M. L., M.M. O., NIST Standard Reference Database 23: Reference Fluid Thermodynamic and Transport Properties-REFPROP, Version 10.0, National Institute of Standards and Technology, (2018) DOI: dx.doi.org/10.18434/T4JS3C.
[22] ASHRAE, ANSI/ASHRAE Standard 34-2016. Designation and safety classification of refrigerants, in, American Society of Heating, Refrigerating and Air-Conditioning Engineers, Inc., Atlanta, USA, 2016.
[23] IPCC, Climate Change 2013: The Physical Science Basis. Contribution of Working Group I to the Fifth Assessment Report of the Intergovernmental Panel on Climate Change [Stocker, T.F., D. Qin, G.-K. Plattner, M. Tignor, S.K. Allen, J. Boschung, A. Nauels, Y. Xia, V. Bex and P.M. Midgley (eds.)], in, Cambridge University Press, Cambridge, United Kingdom and New York, NY, USA, 1535 pp., 2013.

[24] R. Llopis, D. Calleja-Anta, D. Sánchez, L. Nebot-Andrés, J. Catalán-Gil, R. Cabello, R-454C, R-459B, R-457A and R-455A as low-GWP replacements of R-404A: Experimental evaluation and optimization, International Journal of Refrigeration, (2019) DOI: https://doi.org/10.1016/j.ijrefrig.2019.06.013.

CHAPTER 4.

A3 AND A2 REFRIGERANTS: BORDER DETERMINATION AND HUNT FOR A2 LOW-GWP BLENDS

Chapter adapted from the paper:

Contents lists available at ScienceDirect

International Journal of Refrigeration

journal homepage: www.elsevier.com/locate/ijrefrig

A3 and A2 refrigerants: Border determination and hunt for A2 low-GWP blends

Frigorigènes de classe A2 et A3 : détermination de la frontière et quête de mélanges A2 à faible PRP

Daniel Calleja-Anta [a,*], Laura Nebot-Andres [a], Ramón Cabello [a], Daniel Sánchez [a],
Rodrigo Llopis [a,*]

Calleja-Anta, D., Nebot-Andrés, L., Cabello, R., Sánchez, D., Llopis, R., A3 and A2 refrigerants: Border determination and hunt for A2 low-GWP blends (2022) International Journal of Refrigeration, 134, 86-94. DOI: 10.1016/j.ijrefrig.2021.11.012

Cited 6 times.

Journal Impact Factor QUARTILE: Q2.

4 A3 and A2 refrigerants: Border determination and hunt for A2 low-GWP blends

Daniel Calleja-Anta[1,*], Laura Nebot-Andres[1], Ramón Cabello[1], Daniel Sánchez[1], Rodrigo Llopis[1]

[1]Thermal Engineering Group, Mechanical Engineering and Construction Department, Jaume I University, Spain

Abstract

The hunt for new refrigerant blends has been concentrated to locate A1 refrigerants. However, the investigation for A2 or A2L blends to replace hydrocarbons (A3) has not attracted attention yet, although these mixtures will allow to increase the maximum charge of refrigeration systems from 500 g to 1200 g. This paper extends Linteris' et al. work to define, for first time, the frontier between A3 and A2 ASHRAE safety classifications with an approach that can avoid large experimental campaigns. Then, using the methodology, it determines the composition limits of possible A2 binary blends with hydrocarbons that have a GWP below 150. Only mixtures of hydrocarbons with A2 or A2L components meet the criteria, and the composition of the least flammable fluid is predominant. Proposed hypothesis, developed theoretically, should be completed in the future with experimentation, to quantify the energy performance of found blends.

Keywords

Hydrocarbons, R-152a, R-1234yf, R-1234ze(E), flammability

4.1 Introduction

Accelerated Planet global warming, which main cause is anthropogenic, requires that all industrial sectors quickly reduce their emissions of greenhouse gases (GHG). Refrigeration sector, responsible for 7.8% of overall GHG in 2018 [1], accelerated the phase-down of high global warming potential (GWP) fluids due to the entry into force of the F-Gas Regulation [2] in Europe, which was extended globally through the Kigali Amendment to the Montreal Protocol [3]. These agreements and prohibitions pushed the scientific community to search for reduced GWP alternatives to the most common used refrigerants.

The first intensive search was performed by McLinden et al. [4], who analyzed around 100 million known and unknown chemicals looking for low-GWP substances that could operate as refrigerants. They observed that only 62 pure substances had their critical temperature between 300-400 K, operating region of common refrigeration, air-conditioning and heat pumps. Following, McLinden et al. [5] and Domanski et al. [6] refined the search with screenings to find substitutes for R-410A and R-404A, concluding that there are few possible fluids and all of them are mildly flammable. Next, Bell et al. [7], using a similar approach, conducted an extensive search of blends up to four components (among HFOs, HFCs, CO_2) to find possible substitutes to R-134a. They identified 16 mixtures. However, they concluded that no mixture was a perfect substitute, since A1 mixtures with energy performance like R-134a were only able to reduce GWP by 54%, and blends with 99% GWP reduction showed flammability characteristics. Finally, Yu et al. [8] performed another theoretical search for low-GWP substitutes of R-410A for air-conditioning and heat pump applications considering blends from 12 pure fluids (among HFOs, HFCs, HCs, CO_2 and R13I1). They identified 34 low-GWP potential mixtures, all of them flammable, and concluded that only 4 mixtures matched R-410A vapour pressures but suffered from a COP decrease. The search for new refrigerant blends was taken a step forward by Calleja et al. [9], who established for the first time, a comprehensive screening to find alternative fluids to R-290 and R-600a. Through a vast thermodynamic screening limited by 150 GWP value and no flammability restrictions, they observed that there are 6 potential blends to substitute R-600a and 5 to replace R-290, all of them with flammable characteristics too.

The explorations for low-GWP substances indicate that stand-alone refrigeration systems (domestic and commercial), where the use of substances with a GWP value higher than 150 will be forbidden from 2022 on in Europe [2], unavoidably head towards a future based on flammable refrigerants. Although pure flammable fluids, especially R-290 and R-600a, have excellent thermodynamic properties and allow working with high COP values, they suffer from restrictions because their flammable characteristics. In fact, most of European countries have still the limit of 150 g as maximum refrigerant charge for A3, A2 and A2L refrigerants in a single circuit, although the update of the International Electrotechnical Standard has raised it to 1200 g for A2 and A2L refrigerants and 500 g for A3 ones [10]. In practice, this charge limit establishes the maximum capacity that a single cycle could satisfy. Attending to recent works devoted to minimizing the refrigerant charge (detailed in Table 4.1), it can be said that the maximum capacity of a single circuit using propane ranges from 1041 to 2200 W for a charge limit of 150 g, and when the IEC enters into force, it could be raised up to 3470 to 7350 W for a 500 g charge in a single circuit. For isobutane, the actual maximum capacity is between 213 to 328 W and soon from 710 to 1095 W. Although the needs of most domestic refrigeration requirements (with R-600a) could be generally satisfied using the maximum capacities detailed in Table 4.1, commercial refrigeration appliances, which standard refrigerant is propane, could not satisfy the cooling needs of all the equipment with a single circuit. For this equipment going to multiple circuits or using complex heat exchangers to minimize refrigerant charge, usually require an overrun that cannot be accommodated.

As mentioned, the recent version of the International Electrotechnical Standard [10], allows to use up to 1200 g of A2 or A2L refrigerants in a single circuit, therefore it creates a new opportunity for stand-alone refrigeration industry. If an A2 or A2L refrigerant with close thermodynamic properties to R-290 or R-600a is found, the range of capacity of systems that could be built with the maximum charge limit will rise. However, up to the moment and to the knowledge of authors, no systematic search has been performed to found A2 or A2L refrigerants that can be replacements of the current used hydrocarbons.

This work proposes a methodology (applied to binary mixtures but extendable to mixtures with more components) that determines the border between A3 and A2 ASHRAE 34 [11] safety classifications and then uses the proposed frontier, HOC and LFL parameters to determine the limit compositions of binary mixtures formed by propane, isobutane and propylene for building A2 refrigerant mixtures. It opens a new line of work, the hunt for A2/A2L refrigerants that could replace hydrocarbons having lower flammability.

4.2 A3/A2 flammability border location

Safety classification of a refrigerant is given by ASHRAE according to the Standard 34 [11]. If a blend, for a given nominal composition (NC), contains a flammable component, its classification is given by the worst case of formulation for flammability (WCF) and its worst case of fractionation for flammability (WCFF). First, for a mixture considering component tolerances, the worst case of formulation (WCF) is determined. Second, for this WCF, a fractionation analysis is done to evaluate the sensibility of the mixture to change its composition during leakages at different temperatures and in different conditions during the useful life. From that, the WCFF is determined, and it is which defines the safety classification of the nominal composition (NC) according to the following flammability terms (see Figure 4.1):

- A1 (non-flammable): The blend does not show flame propagation (FP) at its NC, WCF, and WCFF.
- A2 (lower flammability): The blend shows FP, a Lower Flammability Limit (LFL) > 0.1 kg·m^{-3} and Heat of Combustion (HOC) < 19000 kJ·kg^{-1} at its NC, WCF and WCFF. If a mixture meets these requirements, optionally, a burning velocity (S_u) test shall be conducted. If the result at the NC, WCF and WCFF is lower than 10 cm·s^{-1}, the blend shall be assigned to A2L class (mildly flammable).
- A3 (higher flammability): The blend shows FP, a LFL < 0,1 kg·m^{-3} or a HOC > 19000 kJ·kg^{-1} at its NC, WCF or WCFF.

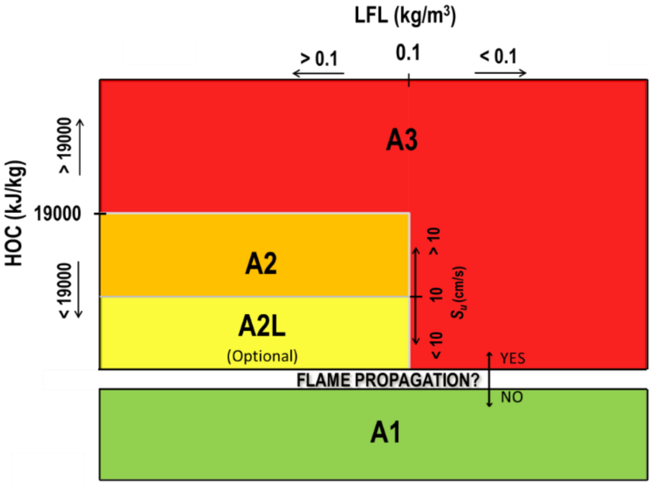

Figure 4.1. ASHRAE safety classifications according to HOC, LFL and burning velocity characteristics.

Flammability classification depends on four parameters: FP, LFL, HOC and, optionally, burning velocity. Of all of them, only HOC can be calculated theoretically from the enthalpies of formation of reactants and products. However, the FP and LFL should be determined experimentally in accordance with ASTM E681 methodology [12] and burning velocity can be determined with the method summarized by Clodic & Jabbour [13]. Some authors have proposed formulas to calculate theoretically lower and upper flammability limits of some materials [14-17], but they generally cannot be extended to other substances. Also, for burning velocity new methods have been proposed [18, 19], but they need more comprehensive research to be extended to other substances. The summary is that for classifying the safety of a refrigerant a great number of experimental tests should be performed and a methodology could be able to save time an effort to hunt for A2 or A2L blends.

Linteris et al. proposed a method to identify if a refrigerant presents flammability and proposed the location of the frontier between A1 and A2L blends in 2019 [20]. They proposed to evaluate the adiabatic flame temperature (T_{ad}) and the fluorine substitution ratio ($^F/_{F\,+\,H}$) for a substance. To calculate T_{ad}, combustion reaction Eq.(4.1) is used with the software Cantera® [21] and Matlab®. $\emptyset$ is the fuel-air equivalence ratio (<1 lean, >1 rich combustion), $Fuel$ is the blend composition multiplied by its molar mass and Γ is the molar oxygen required for stoichiometric combustion. X_{H_2O} is the molar proportion of water at 23 ºC and 50% RH (0.014 kmol·kmol^{-1}). T_{ad} is calculated over a range of $\emptyset$ between 0.5 and 2.0, from which the value that maximizes $\mathrm{T_{ad}}$ is taken. Fluorine substitution ratio is the molar ratio of F atoms to the sum of F and H atoms ($^F/_{F\,+\,H}$) in the reactants (consult reference [20] for further details).

$$\emptyset \cdot \mathrm{Fuel} + \Gamma\left[\mathrm{O_2} + 3.76\ \mathrm{N_2} + \frac{\mathrm{X_{H_2O}}}{(\frac{1.0}{4.76})(1-\mathrm{X_{H_2O}})}\mathrm{H_2O}\right] \qquad \text{Eq.(4.1)}$$

Linteris et al. proposed an angle (Π) to sum up both variables, as expressed by Eq.(4.2).

$$\Pi = \arctan2\left\{\left[\frac{\mathrm{T_{ad}}-1600}{2500-1600}\right],\left[\frac{\mathrm{F}}{\mathrm{F+H}}\right]\right\}\cdot\left(\frac{1800}{\pi}\right) \qquad \text{Eq.(4.2)}$$

Figure 4.2 represents the positions of nominal compositions of refrigerants and blends present in ASHRAE 34 standard (HFC, HFO, HC, CO_2 and DME and their mixtures). Origin is established at 0 fluorine substitution ratio and 1600 K, minimum adiabatic temperature observed for flammability. According to Linteris' et al., the angle defines different flammability regions. They identified 36º as the angle defining the border between A1-A2L regions ($\Pi_{A1-A2L} = 36º$). It was conservative, since some non-flammable mixtures are inside the A2L region, but no A2L blends appear in the A1 region. Authors performed fractionation analysis for these fluids, but no great scatter was produced near the A1-A2L border.

Also, Linteris's et al. proposed an angle of 60º to separate A2 and A2L regions, although they stated that more research is needed to determine it properly. However, they did not focus on the determination of the A3-A2 border, which is the first objective of this work.

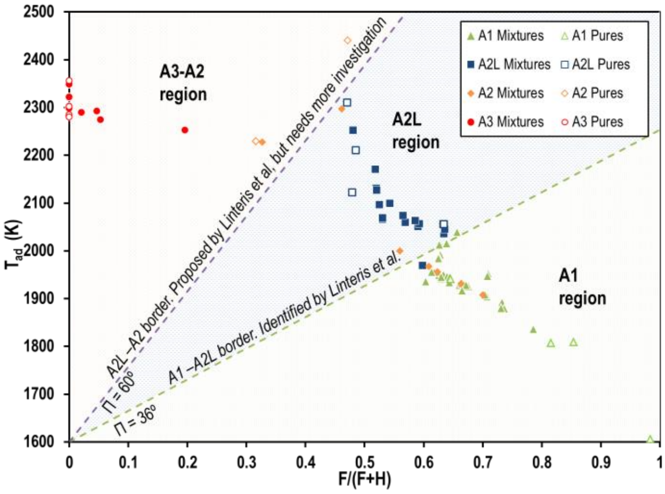

Figure 4.2. Application of Linteris' method to some ASHRAE 34 blends.

4.2.1 Empirical determination (from classified refrigerant mixtures)

To locate the A2-A3 border, we applied Linteris' et al. method [20] to A2 and A3 pure fluids and blends classified in ASHRAE 34, results being presented in Figure 4.3. All fluids onwards from R-439A to those included in the standard at the day of writing of this work (last is R-465A) were evaluated. Former fluids to R-439A were not considered, since the A2L classification still did not exist, and it is not possible to classify the blends into A2 or A2L groups. For each blend, we evaluated the properties for the NC (point to the right for each fluid) and for the different possibilities of fractionation. Fractionation analysis was performed using REFLEAK software [22] for all cases of WCF with the conditions defined in section B.2.4.1 and B.2.4.2 of Appendix B of the Standard 34. The WCFF is the point at the left for each fluid in Figure 4.3.

To illustrate the calculation process, Table 4.2 summarizes the fractionation analysis of R-465A (R-32/R-290/R-1234yf; 21.0/7.9/71.1 $\%_{mass}$). Two WCF are possible [R-32/R-290/R-1234yf; 21.5/8.0/70.5 $\%_{mass}$ and R-32/R-290/R-1234yf; 19.9/8.0/72.1 $\%_{mass}$], to which the fractionation during leakage under the scenarios established by ASHRAE standard were performed. The composition changes under different scenarios, as well as the T_{ad} and the ratio $\left({}^{F}/_{F+H}\right)$, are detailed in the table. For R-465A the WCFF, which establishes the safety classification of the blend, corresponds to the leak under storage/shipping conditions at -40 ºC. Final composition of the blend at the end of the leakage process results in (R-32/R-290/R-1234yf; 44.30/16.36/39.34 $\%_{mass}$). This WCFF has the highest angle, thus this is the most flammable fractionation condition.

Illustrated fractionation analysis was performed with A2 mixtures previously selected and to A3 mixtures containing HFC or HFO components, since for only-HC mixtures the fluorine substitution ratio is 0 and does not affect to the angle Π. Results are plotted in Figure 4.3 (all data is presented in supporting information). Dispersion for a blend is smaller when it is composed with one main fluid and small proportions of others, such as R-512A, and broader when there is no dominant component, such as R-439A. Mixtures with a value of $\left({}^{F}/_{F+H}\right)$ close to zero also present small scatter, since having small presence of fluorides in the nominal composition, the variation of this parameter is small during fractionation. In any case, it can be observed that the fractionation is very important when classifying a mixture.

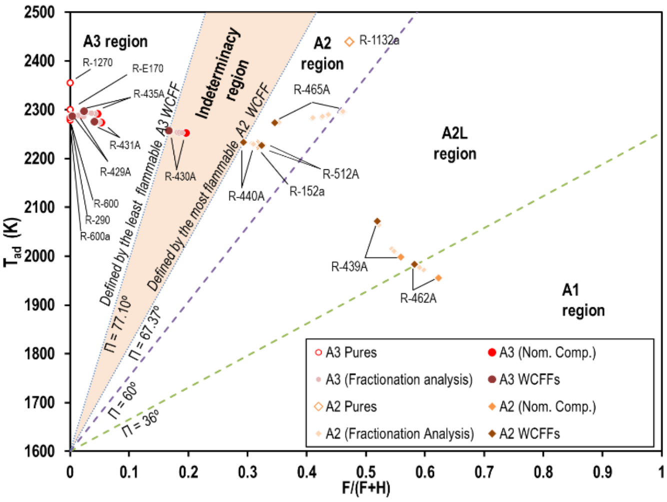

Figure 4.3. Application of Linteris' method to A2 and A3 ASHRAE 34 blends and their fractionation cases.

Our empirical determination defines the boundary between A3 and A2 safety classifications between the most flammable A2 WCFF (R-440A) and the least flammable A3 WCFF (R-430A). Fractionation analysis for these blends is detailed in Table 4.3, where it can be inferred that the A3/A2 boundary is located between the angles of 67.37° and 77.10°, resulting in an indeterminacy region. While in A1/A2L border identification [20] there was high density of blends around the boundary and a clear division between A1 and A2L classes could be seen, this does not occurs for the A3/A2 classes, because the efforts of refrigeration industry have been focused on developing A1 and A2L blends with the lowest possible GWP.

Overall, the conclusion that is extracted from the empirical determination is that border between A3 and A2 classes is within angles of 67.37° and 77.10°, but to identify it with more precision other approaches are needed.

4.2.2 Determination with Heat Of Combustion (HOC) index

If the HOC of a blend is higher than 19000 $kJ \cdot kg^{-1}$, its safety classification according to ASHRAE 34 standard is A3. The HOC, as specified in Appendix F of ASHRAE Standard 34, is calculated theoretically from a complete combustion of the refrigerants as the difference of the enthalpies of formation of the reactants (refrigerants and oxygen) minus the enthalpies of formation of the products according to Eq.(4.3).

$$HOC = \sum \Delta h_{f,reactants} - \sum \Delta h_{f,products} \qquad \text{Eq.(4.3)}$$

For a blend, the combustion reaction is evaluated as if the blend was a hypothetical molecule formed by the different atoms present in the components multiplied by the mole-fraction of each refrigerant ($x,\ y, \ldots$). Total oxygen required is given by the stoichiometric demands of each molecule ($\Gamma_1, \Gamma_2, \ldots$) multiplied by the molar fraction of each refrigerant. The hypothetical molecule formed for a general blend of two components is detailed by Eq.(4.4).

$$\begin{aligned} \mathrm{x} \cdot \left[\mathrm{C_iH_jF_kO_l} + \Gamma_1\mathrm{O_2}\right] + \mathrm{y} \cdot \left[\mathrm{C_mH_nF_pO_k} + \Gamma_2\mathrm{O_2}\right] \\ \rightarrow \mathrm{C_{i\cdot x+m\cdot y}H_{j\cdot x+n\cdot y}F_{k\cdot x+p\cdot y}O_{l\cdot x+l\cdot y}} + (\mathrm{x} \cdot \Gamma_1 + \mathrm{y} \cdot \Gamma_2)\mathrm{O_2} \end{aligned} \qquad \text{Eq.(4.4)}$$

Stoichiometric combustion reaction, expressed in a general form by Eq.(4.5), can have as products HF, COF_2, CO_2 and H_2O. Rules to define which product is formed are: if there is not enough hydrogen available for HF and H_2O formation, HF creation takes preference over H_2O formation; if there is more fluorine than hydrogen, HF is created and the remaining fluorine forms COF_2, having preference of the carbon over CO_2.

$$\mathrm{C_\alpha H_\beta F_\gamma O_\delta} + \Gamma \cdot \mathrm{O_2} = \zeta \cdot \mathrm{CO_2} + \eta \cdot \mathrm{COF_2} + \theta \cdot \mathrm{H_2O} + \lambda \cdot \mathrm{HF} \qquad \text{Eq.(4.5)}$$

We performed a wide screening of ternary mixtures to evaluate the limit composition of a blend that must be classified as A3 according to the HOC. Thirteen pure fluids were selected, including common components in blends (2 saturated HC, 1 unsaturated HC, 1 ether, 5 saturated HFC, 2 HFO, 1 FC, and 1 inorganic compound) with different flammability classifications (4 A3, 2 A2, 3 A2L and 4 A1). The screening included all possible combinations of three pure fluids (205 mixtures) with a molar composition step of 0.5% (20301 blends). Pure fluids, products, and their enthalpies of formation at 298 K are detailed in Table 4.4 (R-1234ze(E) was not included in the screening since the molecule is similar to R-1234yf).

The HOC was evaluated for each mixture and we selected the composition whose HOC was between 18990 and 19000 kJ·kg^{-1} to be at the limit between A3 and A2 safety classifications. The screening identified 1419 mixtures. For these, T_{ad} and $({}^{F}/_{F+H})$ were calculated and represented in Figure 4.4 (see supporting information for detailed data). In summary, 788 blends are composed by HFC-HFO-HC (grey dots), 473 with R-E170 as component (blue dots) and 158 with CO_2 presence (green dots). Mixtures of HFC-HC-HFO, organic compounds composed by C, H and F are concentrated around the same area. Blends with R-E170 and CO_2 present high scatter along the graph since their behaviour is quite different from the rest of substances: R-E170 presents an oxygen atom (boosts flammability) and CO_2 is a substance with a high power of inertization (limits flammability). Despite this, it has been observed that for molar quantities lower than 10% (of R-E170 and CO_2) and HOC between 18990 and 19000 kJ·kg^{-1}, those mixtures present similar location than to the HFC-HFO-HC ones. Therefore, a limit between A3 and A2 safety classifications is clearly identified, as observed in Figure 4.4. This tentative limit (Figure 4.4) is very close to 67.37º, which was the angle identified in Section 4.2.1. It must be highlighted that this angle is conservative, as probably some A2 mixtures may appear in the A3 region, but it is very unlikely to happen otherwise.

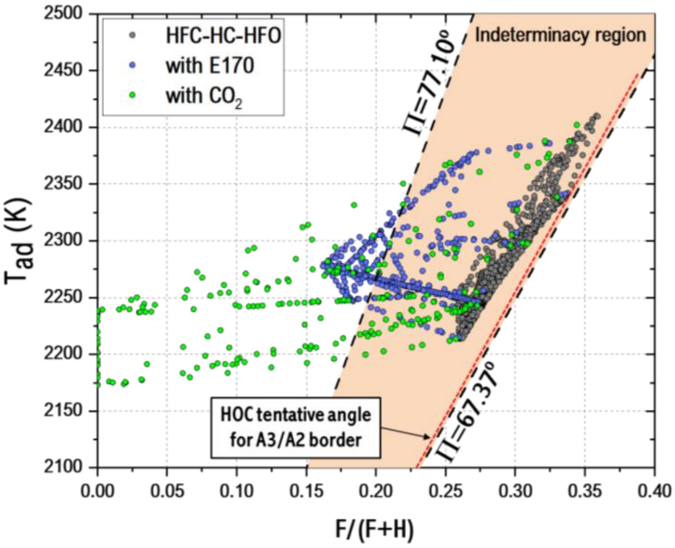

Figure 4.4. T_{ad} and fluorine substitution ratio of blends with HOC between 18990 and 19000 kJ·kg^{-1}

4.2.3 Definition of A3/A2 flammability border

Both empirical and HOC determinations coincide approximately in an angle of 67.37º as the frontier between A3 and A2 regions. Figure 4.4 shows that above grey dots A2 mixtures could not appear. However, it does not mean that below these points all mixtures will be A2, since ASHRAE Standard 34 also requires them to have a LFL below 0.1 $kg \cdot m^{-3}$. Although HOC and LFL are parameters generally correlated, as indicated by Kazakov et al. [23], our screening cannot be extended to the LFL parameter, since it is determined experimentally and no generalization method has been found. However, as the empirical determination (based on ASHRAE experimentation, and determined by the most flammable A2 blend, R-440A) is slightly more restrictive than the HOC determination, it can be concluded that the frontier between both safety classifications at an angle of 67.37º is consistent and it can be generalized. This angle is conservative, as some A2 mixtures may appear at the A3 region (near the border in any case) but it is very unlike that it could happen otherwise.

Nonetheless, in Section 4.1.3, the LFL criterion, when available, is also checked in the evaluation of binary mixtures.

4.3 Low-GWP A2 binary blends determination

The second objective of this work is to identify the composition limits of binary blends with reduced flammability in relation to HCs (R-600a, R-290 and R-1270) having at the same time a GWP below 150. These blends, that will have an A2 safety classification, will be subjected to 1200 g of maximum charge instead of 500 g (for A3 fluids), and thus it will offer larger capacities for stand-alone refrigeration systems.

Methodology used to determine the blends is sketched in Figure 4.5. For a blend of two components, first the WCFF is calculated. If experimental data of the LFL are available in literature, the WCFF is calculated setting the composition of the most flammable component to the limits established by ASHRAE for A2 classification (HOC or LFL); if data is not available the composition limit is calculated using an angle of 67.37º, as detailed in section 2. At this point, the WCFF that guarantees an A2 safety classification is obtained. The next step is to calculate the GWP of the WCFF. If GWP is higher than 150, it is not possible to obtain a WCF with a lower GWP, since the WCF is always going to have a higher presence of the component with a higher GWP. Therefore, no possible composition can meet the criteria. If the GWP of the WCFF is lower than 150, an iteration process with REFLEAK is performed to calculate the WCF that after fractionation will result in the previous WCFF. This process starts with low percentage of the most flammable component which is increased by 0.1%$_{\text{mass}}$ until the WCFF provided by REFLEAK coincides with the previous value. Considering that mass tolerances are neglected, WCF composition coincides with the NC of the blend that will be classified as A2.

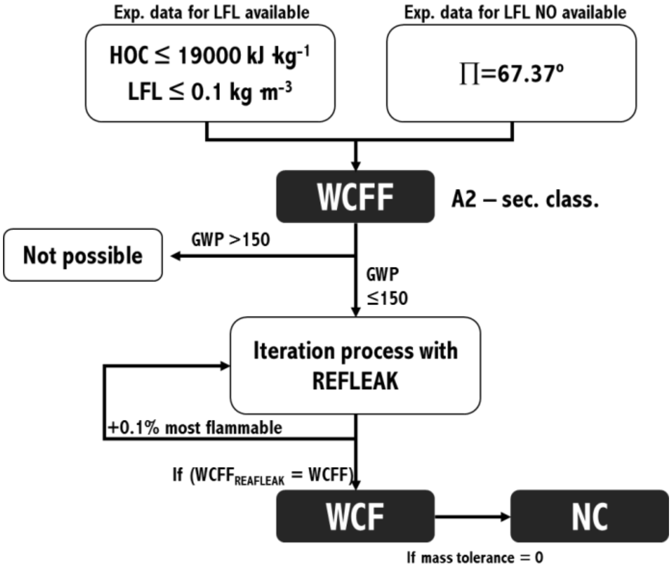

Figure 4.5. Method to determine composition limits for A2 blends with GWP < 150

4.3.1 Limit composition results

This methodology is used to evaluate binary blends resulting from mixing the reference HC fluid with fluids belonging to A2, A2L and A1 to reduce the flammable characteristics of the blend.

Table 4.5 reflects the pure fluids for the evaluation as well as their safety classification and GWP value.

Calculated nominal composition limits that guarantee an A2 classification and a GWP below 150 are summarized in Table 4.6 (right column), where the references used to calculate the LFL values and the ASHRAE leakage test that produces the WCFF are detailed.

For propane blends there are two sets of blends: mixtures of propane with A1 pure fluids, where to obtain an A2 classification the quantity of additive is too high that exceeds the GWP limit, therefore is not possible to formulate blends of propane with R-

143a, R-125, R-134a and R-218 meeting the criteria. This also happens for isobutane and propylene; thus, they have not been included in the table. The exception is the blend with R-744, that will provide an A2 classification for CO_2 proportions from 95.4% on. The second set corresponds to mixtures with propane with A2 and A2L fluids. For all of them, except for R-32 whose proportion for flammability reduction exceeds the GWP limit, is possible to obtain A2 blends meeting the criteria. But as observed after the fractionation analysis, the proportion of the A2 or A2L component is predominant. Except for the blend with R-1234yf, for which the proportion to get an A2 classification is of 89.0%, the rest of mixtures need at least 95.0% of the least flammable component to meet the criteria after fractionation of the NC.

Similar results have been obtained for mixtures of isobutane and propylene with other fluids. No possible formulations have been found with A1 fluids, except with R-744, and the mixtures with A2 and A2L components result in high proportions of the A2 and A2L fluids in the mixture. Again, the component with highest percentage is R-1234yf.

Conclusion obtained from this section is that it is possible to formulate low-GWP mixtures with A2 classification blending pure HC components. To do this, high proportions of A2 or A2L fluids need to be added to the blend, because the fractionation of the NC results in a WCFF with a higher proportion of the A3 component.

4.4 Further considerations and future investigation

At this point, the angle 67.37º has been proposed as the frontier between A3 and A2 safety classifications and has been used to identify the flammability limits of binary mixtures when LFL data is not available. As seen, literature provides experimental LFL data or formulas that can be used for a more or less broad group of binary mixtures. However, the available data diminish considerably for ternary mixtures or mixtures with a larger number of components. It is then when this angle becomes of great importance, since it allows predicting flammability without an extensive experimentation.

The study of mixtures with three or more components has not been addressed in this work, but could be of great interest. As can be seen in Table 4.6, when performing fractionation analysis on binary mixtures, the amount of HC in the composition varies greatly between the NC and the WCFF. In addition, it has been possible to observe a relation between the difference in NBPs that exists between the fluids that form the binary mixture and the reduction in the amount of HC between the composition of the WCFF and the NC. An example of this is the R-600a/R-744 mixture, where the amount of HC decreases by 97.72% between the WCFF (limited by the LFL) and the NC. This fact greatly limits the possibilities of the A2 binary mixtures. However, fractionation in ternary mixtures has not been studied. The behavior of fractionation in mixtures of three or more components may be key to achieve a higher HC presence in the NC. Studying how fractionation affects ternary mixtures could mitigate the large gap between the composition in the NC and the WCFF of HCs and thus increase the chances of A2 mixtures containing hydrocarbons.

To complete the search for alternative fluids to A3 refrigerants (R-290, R-600a and R-1270), composition limits detailed in this work (Table 6) can be used as reference, but this search must be supplemented with energy analysis. If any A2 blend, as defined in this work, can equal or has closer energy performance to the base fluids, then it could allow increasing the refrigerant charge limit and thus enhance the capacity that can be provided using a single circuit. Authors invite other researchers to perform theoretical and experimental analysis of the proposed mixtures with refrigeration systems to complete the hypothesis launched in this work.

4.5 Conclusions

Maximum allowed refrigerant charge with flammable refrigerants that can be used in a single circuit limits the capacity of the systems that can be built. A3 refrigerants are limited to 500 g and A2/A2L to 1200 g. Since most of stand-alone systems rely on pure HC refrigerants, belonging to an A3 safety classification, it is important to find new blends that, having close properties to the HC fluids, present at least an A2 safety classification.

This work has extended Linteris' et al. method to locate the border between A3 and A2 refrigerants as function of the fluorine substitution ratio and the adiabatic flame temperature. Border search has been performed using an empirical approach, from existing refrigerants in ASHRAE Standard 34, and has been completed with a wide screening based on the HOC index. It has been concluded that all the mixtures with an angle higher than 67.37º belong to an A3 safety classification.

The developed method has been used to determine blends of HC refrigerants (R-600a, R-290 and R-1270) with A1, A2 and A2L components that meet A2 safety classification and a GWP below 150. To find them out, the method determined the WCFF and with an iterative process using REFLEAK the NC of the blends that after fractionation result in the WCFF. It has been concluded that no blend with A1 fluids meet the criteria, because for inertization the quantity of A1 component makes the GWP value to exceed 150, and it is possible to create A2 blends mixing with A2 and A2L components. However, to decrease the flammability, the amount of A2 or A2L component is predominant, what limits the possibilities of the mixtures.

The work has established the NC of mixtures that will belong to an A2 security classification. However, in order to find substitutes to pure HC refrigerants, the energy performance of determined mixtures should be explored. Authors invite researchers to consider this possibility and perform experimental evaluations to validate the possibilities raised in this work.

4.6 Acknowledgements

Authors gratefully acknowledge Jaume I University (grant PREDOC/2019/19 and project UJI-B2019-56), Ministry of Science, Innovation and Universities of Spain (RTI2018-093501-B-C21) and Ministry of Education, Culture and Sport of Spain (grant FPU16/00151) for financing this research work.

4.7 Supporting information

In order to complete the information, supplementary material can be found attached to this paper. An excel file is available with the following data:

- Data of the fractionation analysis of the A3 and A2 ASHRAE 34 mixtures (see Fig. 3). Initial temperature and initial volumetric quality, as well as the details of the most unfavourable condition can be seen.
- Data with the results of the HOC screening (see Fig. 4). Mixtures obtained, HOC, F/F+H ratio, T_{ad}, and angle Π can be seen.

Supplementary material associated with this article can be found, in the online version, at doi: 10.1016/j.ijrefrig.2021.11.012.

4.8 Author contribution statements

D. C. developed idea and methods, performed simulations, and wrote the manuscript. R. Ll. developed the idea and supervised the work. D.S. helped to develop methods and supervised work. L. N. helped to develop the method and made final proofreading. R.C. helped to get funds.

4.9 Nomenclature

C	Carbon atom
DME	Dimethyl ether
F	Fluorine atom
FP	Flame Propagation
GHG	Greenhouse Gases
GWP	Global Warming Potential
H	Hydrogen atom
HC	Hydrocarbon
h_f	Enthalpy of formation, $kJ \cdot kmol^{-1}$
HFC	Hydrofluorocarbon
HFO	Hydrofluoroolefin
HOC	Heat Of Combustion, $kJ \cdot kg^{-1}$
IEC	International Electrotechnical Commission
LFL	Lower Flammability Limit, $kg \cdot m^{-3}$
NC	Nominal Composition
RH	Relative Humidity, %
S_u	Burning velocity, $cm \cdot s^{-1}$
T	Temperature, ºC
WCF	Worst Case of Formulation for Flammability
WCFF	Worst Case of Fractionation for Flammability
X_{H_2O}	molar proportion of water at 23ºC and 50% RH

Subscripts

ad	Adiabatic
i	Initial

Greek symbols

Δ	Increment
$\emptyset$	Fuel-air equivalence ratio
Γ	Molar oxygen required for stoichiometric combustion
Π	Flammability Angle

4.10 References

[1] International Institute of Refrigeration, 38th Note on Refrigeration Technologies. The Role of Refrigeration in the Global Economy (2019). in, International Institute of Refrigeration, 2019, DOI: 10.18462/iif.NItec38.06.2019.

[2] European Commission, Regulation (EU) No 517/2014 of the European Parliament and of the Council of 16 April 2014 on fluorinated greenhouse gases and repealing Regulation (EC) No 842/2006., in: E. Commission (ed.), Official Journal of the European Union, 2014.

[3] UNEP, Report of the Twenty-Eighth Meeting of the Parties to the Montreal Protocol on Substances that Deplete the Ozone Layer, in, Kigali, Rwanda, 2016.

[4] M.O. McLinden, A.F. Kazakov, J. Steven Brown, P.A. Domanski, A thermodynamic analysis of refrigerants: Possibilities and tradeoffs for Low-GWP refrigerants, International Journal of Refrigeration, 38 (2014) 80-92 DOI: 10.1016/j.ijrefrig.2013.09.032.

[5] M.O. McLinden, J.S. Brown, R. Brignoli, A.F. Kazakov, P.A. Domanski, Limited options for low-global-warming-potential refrigerants, Nat Commun, 8 (2017) 14476 DOI: 10.1038/ncomms14476.

[6] P.A. Domanski, R. Brignoli, J.S. Brown, A.F. Kazakov, M.O. McLinden, Low-GWP refrigerants for medium and high-pressure applications, International Journal of Refrigeration, 84 (2017) 198-209 DOI: 10.1016/j.ijrefrig.2017.08.019.

[7] I. Bell, P.A. Domanski, M. McLinden, G. Linteris, The hunt for nonflammable refrigerant blends to replace R-134a, International Journal of Refrigeration, 104 (2019) 484-495 DOI: 10.1016/j.ijrefrig.2019.05.035.

[8] B. Yu, H. Ouyang, J. Shi, W. Liu, J. Chen, Evaluation of low-GWP and mildly flammable mixtures as new alternatives for R410A in air-conditioning and heat pump system, International Journal of Refrigeration, 121 (2021) 95-104 DOI: 10.1016/j.ijrefrig.2020.09.018.

[9] D. Calleja-Anta, L. Nebot-Andres, J. Catalan-Gil, D. Sánchez, R. Cabello, R. Llopis, Thermodynamic screening of alternative refrigerants for R290 and R600a, Results in Engineering, 5 (2020) DOI: 10.1016/j.rineng.2019.100081.

[10] International Electrotechnical Commission., IEC 60335-2-89:2019. Household and similar electrical appliances - Safety - Part 2-89: Particular requirements for commercial refrigerating appliances and ice-makers with an incorporated or remote refrigerant unit or motor-compressor, in, 2019.

[11] ASHRAE, ANSI/ASHRAE Standard 34-2019. Designation and safety classification of refrigerants, in, American Society of Heating, Refrigerating and Air-Conditioning Engineers, Inc., Atlanta, USA, 2019.

[12] A. International, E681 - 09(2015) Standard Test Method for Concentration Limits of Flammability of Chemicals (Vapors and Gases), in, 2015, DOI: 10.1520/E0681-09R15.

[13] D. Clodic, T. Jabbour, Method of test for burning velocity measurement of flammable gases and results, Hvac&R Research, 17 (2011) 51-75 DOI: 10.1080/10789669.2011.543252.

[14] C.-C. Chen, C.-P. Lai, Y.-C. Guo, A novel model for predicting lower flammability limits using Quantitative Structure Activity Relationship approach, Journal of Loss Prevention in the Process Industries, 49 (2017) 240-247 DOI: 10.1016/j.jlp.2017.07.007.

[15] Z. Li, M. Gong, J. Wu, Y. Zhou, Flammability limits of refrigerant mixtures with 1,1,2,2-tetrafluoroethane, Experimental Thermal and Fluid Science, 35 (2011) 1209-1213 DOI: 10.1016/J.EXPTHERMFLUSCI.2011.04.008.

[16] K. Zhang, X. Meng, J. Wu, Flammability limits of binary mixtures of dimethyl ether with five diluent gases, Journal of Loss Prevention in the Process Industries, 29 (2014) 138-143 DOI: 10.1016/j.jlp.2014.02.008.

[17] S. Kondo, K. Takizawa, A. Takahashi, K. Tokuhashi, A. Sekiya, Flammability limits of five selected compounds each mixed with HFC-125, Fire Safety Journal, 44 (2009) 192-197 DOI: 10.1016/j.firesaf.2008.06.001.

[18] G. Linteris, V. Babushok, Laminar burning velocity predictions for C1 and C2 hydrofluorocarbon refrigerants with air, Journal of Fluorine Chemistry, 230 (2020) DOI: 10.1016/j.jfluchem.2019.05.002.

[19] K. Takizawa, N. Igarashi, K. Tokuhashi, S. Kondo, On simple method for predicting burning velocities for lower flammability refrigerants using quenching distance measurement, International Journal of Refrigeration, 120 (2020) 370-377 DOI: 10.1016/j.ijrefrig.2020.08.027.

[20] G.T. Linteris, I.H. Bell, M.O. McLinden, An empirical model for refrigerant flammability based on molecular structure and thermodynamics, International Journal of Refrigeration, 104 (2019) 144-150 DOI: 10.1016/j.ijrefrig.2019.05.006.

[21] Author, Cantera: An object-oriented software toolkit for chemical kinetics, thermodynamics, and transport processes. , 2021 DOI: 10.5281/zenodo.4527812.

[22] J.S. Brown, P.A. Domanski, REFLEAK: NIST Leak/Recharge Simulation Model for Refrigerant Blends Version 5.1; User's Guide, (2018) DOI: 10.6028/nist.Nsrds.73-2018.

[23] A. Kazakov, M.O. McLinden, M. Frenkel, Computational Design of New Refrigerant Fluids Based on Environmental, Safety, and Thermodynamic Characteristics, Industrial & Engineering Chemistry Research, 51 (2012) 12537-12548 DOI: 10.1021/ie3016126.

[24] W. Zhou, Z. Gan, A potential approach for reducing the R290 charge in air conditioners and heat pumps, International Journal of Refrigeration, 101 (2019) 47-55 DOI: 10.1016/j.ijrefrig.2019.02.030.

[25] A. Pisano, S. Martínez-Ballester, J.M. Corberán, A.W. Mauro, Optimal design of a light commercial freezer through the analysis of the combined effects of capillary tube diameter and refrigerant charge on the performance, International Journal of Refrigeration, 52 (2015) 1-10 DOI: 10.1016/j.ijrefrig.2014.12.023.

[26] W. Cho, D.S. Jang, S.H. Lee, S. Yun, Y. Kim, Refrigerant charge reduction in R600a domestic refrigerator-freezer by optimizing hot-wall condenser geometry, International Journal of Refrigeration, 117 (2020) 295-306 DOI: 10.1016/j.ijrefrig.2020.05.012.

[27] W. Zhou, X. Bi, Z. Gan, Performance investigation of a domestic freezer with micro-bare-tube evaporators, Applied Thermal Engineering, 174 (2020) DOI: 10.1016/j.applthermaleng.2020.115306.

[28] H.Y. Afeefy, J.F. Liebman, S.E. Stein, Neutral Thermochemical Data, in: NIST Chemistry WebBook, NIST Standard Reference Database Number 69, National Institute of Standards and Technology, DOI: 10.18434/T4D303.

[29] A. Burcat, B. Ruscic, Third Millennium Ideal Gas and Condensed Phase Thermochemical Database for Combustion with Updates from Active Thermochemical Tables, in, 2005, DOI: doi.org/10.2172/925269.

[30] K.G. Joback, R.C. Reid, Estimation of Pure-Component Properties from Group-Contributions, Chemical Engineering Communications, 57 (2007) 233-243 DOI: 10.1080/00986448708960487.

[31] IPCC, Climate Change 2013: The Physical Science Basis. Contribution of Working Group I to the Fifth Assessment Report of the Intergovernmental
Panel on Climate Change [Stocker, T.F., D. Qin, G.-K. Plattner, M. Tignor, S.K. Allen, J. Boschung, A. Nauels, Y. Xia, V. Bex and P.M. Midgley
(eds.)]. Cambridge University Press, Cambridge, United Kingdom and New York, NY, USA, 1535 pp., in, 2013.

[32] S. Kondo, K. Takizawa, A. Takahashi, K. Tokuhashi, A. Sekiya, A study on flammability limits of fuel mixtures, Journal of Hazardous Materials, 155 (2008) 440-448 DOI: 10.1016/j.jhazmat.2007.11.085.

[33] S. Kondo, K. Takizawa, A. Takahashi, K. Tokuhashi, Extended Le Chatelier's formula for carbon dioxide dilution effect on flammability limits, Journal of Hazardous Materials, 138 (2006) 1-8 DOI: 10.1016/j.jhazmat.2006.05.035.

[34] S. Kondo, K. Takizawa, A. Takahashi, K. Tokuhashi, A. Sekiya, Flammability limits of isobutane and its mixtures with various gases, Journal of Hazardous Materials, 148 (2007) 640-647 DOI: 10.1016/j.jhazmat.2007.03.021.

TABLES

Table 4.1. Investigations to reduce refrigerant charge and achieved capacity vs. charge ratios.

Reference	Refrigerant	System	Ratio capacity vs. charge ($W \cdot g^{-1}$)	Capacity with 150 g (W)	Capacity with 500 g (W)
Zhou & Gan [24]	R-290	Split air conditioning with micro bare-tube heat exchangers	14.70	2200	7350
Pisano et al. [25]	R-290	Commercial freezer with finned-tube evaporator and tubeless condenser	6.94	1041	3470
Cho et al. [26]	R-600a	Domestic refrigerator-freezer with hot-wall condenser and finned-tube evaporators	2.19	328	1095
Zhou et al. [27]	R-600a	Domestic freezer with micro-bare-tube evaporators and wired-tube condenser	1.42	213	710

Table 4.2. Fractionation analysis of the refrigerant mixture R-465A.

R-465A														
Components in the blend	Nominal Composition (mass %)	Tolerances (mass %)	WCF1 (mass %)	WCFF 1 (mass %)					WCF 2 (mass %)	WCFF 2 (mass %)				
				WCFF 1 leak storage (T_i= 54.4ºC)	WCFF 1* leak storage (T_i= -40ºC)	WCFF 1 leak equipment (T_i= -40 ºC)	WCFF 1 leak equipment (T_i= 10 ºC)	WCFF 1 leak/ recharge (T_i= 23 ºC)		WCFF 2 leak storage (T_i= 54.4 ºC)	WCFF 2 leak storage (T_i=-40 ºC)	WCFF 2 leak equipment (T_i=-40 ºC)	WCFF 2 leak equipment (T_i=10 ºC)	WCFF 2 leak/ recharge (T_i=23 ºC)
R-32	21.0	(+0.5 /-1.5)	21.5	31.35	44.30	43.50	34.01	27.39	19.9	29.68	42.96	42.09	32.25	25.66
R-290	7.9	(+0.1 /-0.9)	8.0	9.88	16.36	15.86	11.02	9.36	8.0	9.90	16.24	15.76	11.03	9.4
R-1234yf	71.1	(±1.0)	70.5	58.76	39.34	40.64	54.97	63.25	72.1	60.42	40.80	42.15	56.72	64.95
F/F+H	0.462		0.460	0.425	0.346	0.351	0.409	0.436	0.461	0.427	0.348	0.353	0.411	0.437
T_{ad} (K)	2295.26		2294.7	2284.5	2272.5	2273.1	2281.7	2288.3	2296.1	2285.9	2273.5	2274.2	2283.1	2289.7
Π	59.15		59.23	60.78	65.14	64.83	61.62	60.34	59.19	60.76	65.05	64.75	61.58	60.32

* Worst-Case Fractionated Formulation

Table 4.3. Flammability characteristics of R-440A (most flammable A2 blend) and R-430A (lest flammable A3 blend) at the NC and at the WCFF

	Composition (by mass %)		$\left(F/_{F+H}\right)$	T_{ad} (K)	Π (º)
R-440A	Nom. Comp.	R-290/R-134a/R-152a (0.6/1.6/97.8)	0.316	2228.2	65.66
	WCFF	R-290/R-134a/R-152a (4.0/0.9/95.1)	0.293	2233.1	67.37
R-430A	Nom. Comp.	R-152a/R-600a (76.0/24.0)	0.196	2252.1	74.88
	WCFF	R-152a/R-600a (68.6/31.4)	0.167	2256.9	77.10

Table 4.4. Pure fluids considered for the screening and products of combustion reaction. Enthalpy of formation at 298 K.

Reactants		
Component	Δh_f (kJ·kmol^{-1})	Reference
R-290	-104.70	[28]
R-1270	20.41	[28]
R-600a	-134.20	[28]
R-E170	-184.10	[28]
R-152a	-497.00	[28]
R-1132a	-344.00	[28]
R-32	-452.21	[28]
R-143a	-748.70	[28]
R-1234yf	-813.20	[29]
R-1234ze(E)	-781.82	[30] (estimated)
R-134a	-877.80	[30] (estimated)
R-125	-1120.00	[29]
R-218	-1784.70	[28]
R-744 (CO_2)	-393.51	[28]

Products		
Component	Δh_f (kJ·kmol^{-1})	Reference
HF	-273.30	[28]
COF_2	-638.90	[28]
H_2O	-241.83	[28]
R-744 (CO_2)	-393.51	[28]

Table 4.5. Pure components used to determine A2 blends. GWP on a 100-year horizon value in brackets [31]

A3 base component	A2 pure fluids	A2L pure fluids	A1 pure fluids
R-1270 (2)	R-1132a (1)	R-1234yf (1)	R-744 (1)
R-600a (3)	R-152a (138)	R-1234ze(E) (1)	R-134a (1300)
R-290 (3)		R-32 (677)	R-125 (3170)
		R-143a (4800)	R-218 (8900)

Table 4.6. Composition limits of HC blends with A2, A2L and A1 fluids, resulting in A2 safety classification and GWP lower than 150

	Environmental criteria	Flammability criteria						Composition limit (% mass)
Binary blend	**GWP < 150**	**WCFF**				**WCF**		**NC (A2 & GWP < 150) (Neglecting tolerances in composition)**
		HOC=19000 kJ·kg^{-1} (% mass)	LFL=0.1 kg·m^{-3} (% mass)	LFL reference	$\Pi = 67.37º$ (% mass)	WCF	Limiting leakage test	
Propane blends								
R-290/R-152a	n.e.	8.9 / 91.1	12.3 / 87.8	[32]	n.n.	1.6 / 98.4	a	**1.6 / 98.4**
R-290/R-1132a	n.e.	11.4 / 88.6	12.4 / 87.6	[32]	n.n.	0.7 / 99.3	b	**0.7 / 99.3**
R-290/R-32	78.3 / 21.7	26.0 / 74.0	-	n.a.	n.n.	n.n.	-	n.p.
R-290/R-143a	97.0 / 3.0	24.3 / 75.7	-	n.a.	n.n.	n.n.	-	n.p.
R-290/R-1234yf	n.e.	23.3 / 76.7	-	n.a.	21.2 / 78.8	11.0 / 89.0	a	**11.0 / 89.0**
R-290/R-1234ze(E)	n.e.	22.7 / 77.3	-	n.a.	21.2 / 78.8	5.0 / 95.0	a	**5.0 / 95.0**
R-290/R-125	95.4 / 4.6	34.5 / 65.5	-	n.n.	n.n.	n.n.	-	n.p.
R-290/R-134a	88.7 / 11.3	29.6 / 70.4	-	n.n.	n.n.	n.n.	-	n.p.
R-290/R-218	98.4 / 1.6	36.5 / 63.5	-	n.a.	n.n.	n.n.	-	n.p.
R-290/R-744	n.e.	41.0 / 59.0	40.0 / 60.0	[33]	n.n.	4.6 / 95.4	b	**4.6 / 95.4**
Isobutane blends								

R-600a/R-152a	n.e.	9.1 / 90.9	13.7 / 86.3	[32]	n.n.	4.7 / 95.3	a	**4.7 / 95.3**
R-600a/R-1132a	n.e.	11.7 / 88.3	13.5 / 86.5	[32]	n.n.	0.3 / 99.7	b	**0.3 / 99.7**
R-600a/R-1234yf	n.e.	23.8 / 76.2	-	n.a.	22.1 / 77.9	8.4 / 91.6	c	**8.4 / 91.6**
R-600a/R-1234ze(E)	n.e.	23.2 / 76.8	-	n.a.	22.1 / 77.9	17.6 / 82.4	b	**17.6 / 82.4**
R-600a/R-744	n.e.	41.6 / 58.4	39.5 / 60.5	[34]	n.n.	0.9 / 99.1	d	**0.9 / 99.1**
Propylene blends								
R1270/R-152a	n.e.	9.0 / 91.0	13.7 / 86.3	[32]	n.n.	1.8 / 98.2	a	**1.8 / 98.2**
R1270/R-1132a	n.e.	11.6 / 88.4	15.7 / 84.3	[32]	n.n.	1.0 / 99.0	b	**1.0 / 99.0**
R1270/R-1234yf	n.e.	23.6 / 76.4	-	n.a.	23.0 / 77.0	10.0 / 90.0	a	**10.0 / 90.0**
R1270/R-1234ze(E)	n.e.	23.0 / 77.0	-	n.a.	23.0 / 77.0	4.7 / 95.3	a	**4.7 / 95.3**
R1270/R-744	n.e.	41.5 / 58.5	48.9 / 51.1	[33]	n.n.	4.2 / 95.8	b	**4.2 / 95.8**

Notes about Table 6:

- Table 6 presents the nominal composition (NC) of refrigerant blends that would be classified at least A2 by ASHRAE standard 34 according to the methodology presented in this paper. Any blend with a mass proportion of hydrocarbon less than the value specified in ‘Composition limit’ would be classified as A2 or with a lower flammability class. Furthermore, any blend included in this table will present a GWP below 150.

- Compositions in column ‘Composition limit’ coincide with compositions of column ‘WCF’ which corresponds to the worst case of formulation for flammability. They coincide because this work omits tolerances in the blend manufacturing.
- Values in column ‘WCF’ are obtained considering the most flammable composition in column ‘WCFF’. Composition identified in ‘WCFF’ has been evaluated using REFLEAK under the different leak conditions stablished by ASHRAE standard 34. Compositions in column ‘WCF’ are the results of the fractionation of ‘WCFF’ compositions under the most restrictive leak test (a, b, c or d). The most restrictive leakage test is also identified.

n.e.: limit non existing.

n.n.: calculation not needed.

n.a.: data not available.

n.p.: not possible A2 blend with GWP<150.

a: leak under storage/shipping conditions. Vapor 2% leakage.

b: leak under storage/shipping conditions. Liquid 95% leakage.

c: leak from equipment. Liquid 95% leakage.

d: leak from equipment. Liquid 84.2% leakage.

CHAPTER 5.

DROP-IN SUBSTITUTES FOR R-600a. EXPERIMENTAL EVALUATION AND OPTIMIZATION OF A COMMERCIAL FRIDGE

Chapter adapted from the paper:

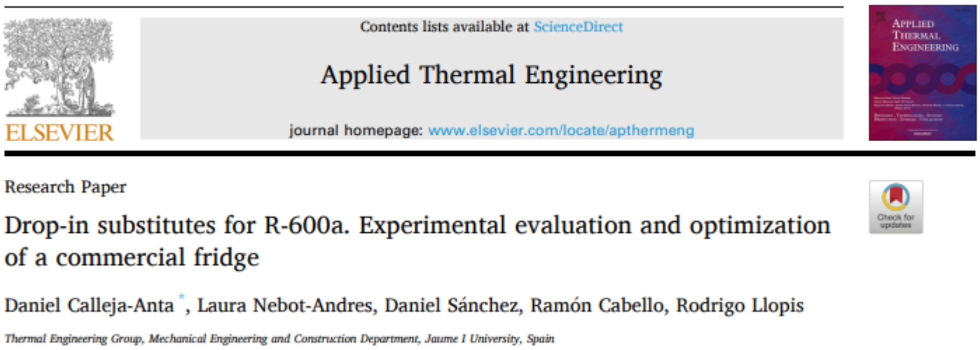

Contents lists available at ScienceDirect

Applied Thermal Engineering

journal homepage: www.elsevier.com/locate/apthermeng

Research Paper

Drop-in substitutes for R-600a. Experimental evaluation and optimization of a commercial fridge

Daniel Calleja-Anta *, Laura Nebot-Andres, Daniel Sánchez, Ramón Cabello, Rodrigo Llopis

Thermal Engineering Group, Mechanical Engineering and Construction Department, Jaume I University, Spain

Calleja-Anta, D., Nebot-Andrés, L., Sánchez, D., Cabello, R., Llopis, R., Drop-in substitutes for R-600a. Experimental evaluation and optimization of a commercial fridge (2022) Applied thermal Engineering, 211, art. no. 118490. DOI: 10.1016/j.applthermaleng.2022.118490

Journal Impact Factor QUARTILE: Q1.

Cited 3 times.

5 Drop-in substitutes for R-600a. Experimental evaluation and optimization of a commercial fridge.

Calleja-Anta, D., Nebot-Andrés, L., Sánchez, D., Cabello, R., Llopis, R.

Thermal Engineering Group, Mechanical Engineering and Construction Department,
Jaume I University, Spain

Abstract

This work aims to validate the hypothesis that refrigerant blends could allow energy savings in real refrigeration systems. For that purpose, five selected blends have been evaluated as drop-in substitutes in a domestic fridge for fresh food designed for R-600a under laboratory conditions. Mixtures, selected from an initial theoretical work, were subjected to a charge optimization process following the standard EN 62552-2:2020. At their optimum refrigerant charge, three offered energy savings: 2.15% is obtained with the mixture R-600a/R-1234yf [92.5/7.5%]; 3.84% with R-1234ze(E)/R-600 [10.5/89.5%] and 1.31% with R-600/R-290 [89.0/11.0%]. This work discusses the experimental procedure and the operating parameters of the selected mixtures in relation to R-600a. Thus, it has been verified that energy savings could be obtained with refrigerant blends. However, understanding the operation of the mixtures requires further investigation not covered in this work.

Keywords

Domestic refrigeration; R-600a, refrigerant mixture; drop-in; energy saving.

5.1 Introduction

Release of the 6th Assessment Report of the IPCC [1] has warned humanity about the acceleration of climate change, predicting that the increase of the planet temperature will reach 1.5 K by the early 2030s, ten years early than forecasted. Refrigeration is one of the culprits of the climate change, realising 7.8% of the overall GHG in 2018, a figure that is expected to grow quickly [2]. This sector has been immersed in profound changes during the last two decades, with the Kigali Amendment to the Montreal Protocol being the most recent global commitment that expects to phase-down 80% of hydrofluorocarbon (HFC) refrigerants by 2047 and avoid up to 0.5 K global temperature by the end of the century [3]. However, the 6th Assessment Report warns that it would not be enough and further effort is required to enlarge the energy efficiency of all refrigeration appliances.

Domestic refrigerators and freezers, with estimated annual production of 170 million units and approximately an inventory of 2.3 billion units [4] consume nearly 4% of the world's electricity [2]. New appliances are predominantly built with HC-600a, but HFC-134a still remains in North America [4]. Their efficiency level has increased notably pushed by energy labelling regulations in many countries, but they remain as high-consuming electricity devices.

Replacement of HFC-134a by other fluids to fulfil F-Gas restrictions [Global Warming Potential (GWP) >150] [5] was an intense line of research during the last decade. HFC-152a allowed energy consumption reductions between 4% [6] and 7% [7]. HFO-1234ze(E) was measured to have between 5% [8] to 16% [9] lower energy consumption, but suffered a reduction in capacity. HFO-1234yf offered similar performance than HFC-134a [10] or even worse [9]. Surprisingly, binary mixtures of HFC-134a with HFOs were the fluids that offered better energy performance. Blends with HFO-1234yf offered 3.5% {HFO-1234yf/HFC-134a [44/56%] [11]} and up to 6% energy consumption reduction {HFO-1234yf/HFC-134a [90/10%] [12]}. Mixtures with HFO-1234ze(E) resulted in 14.1% less consumption than HFC-134a and in 8.92% than pure HFO-1234ze(E) [13]. In the same way, hydrocarbon mixtures were also tested to replace HFC-134a. Wongwises and Chimres [14], Fatouh and El Kafafy [15], Mohanraj, et al. [16] and Rasti, et al. [17] experimentally evaluated mixtures of propane, butane and isobutane, all of them obtaining reductions in energy consumption with respect HFC-134a and even pure HC-600a [17].

Little attention has been given to the search of new blends to compete with HC-600a, since mixtures in general provide lower heat transfer coefficients (HTC) than pure components [18]. Non-linear shift in equilibrium phase concentrations and different volatility of mixture components generate a temperature glide along evaporation and condensation, leading to a reduction of the HTC. These reductions were verified experimentally in boiling by Oliveira, et al. [19] and Zou, et al. [20]; and in condensation by Chang, et al. [21] and Moreira, et al. [22]. However, as highlighted by Moreira, et al. [18], the reduction of the HTC may become marginal when the heat exchanger is a refrigerant-to-air one, since the main thermal resistance is on the airside. Thus, as verified experimentally by several authors, it is reasonable to think that refrigerant blends could be a good opportunity to reduce the energy consumption in refrigerators, even against HC-600a.

This opportunity was considered theoretically by Calleja-Anta, et al. [23], who performed a systematic screening of ternary blends that having a GWP below 150 offered higher energy performance than HC-600a and HC-290. A small set of blends was identified to replace the former fluids, most of them belonging to an A3 ASHRAE security classification, since the identified mixtures were based mainly on HCs. Later, Calleja-Anta, et al. [24] extended the search including flammability restriction, where compositions limits belonging to an A2 ASHRAE security classification were obtained.

As reflected in the introduction, the possibility to reduce the energy consumption of domestic refrigerators by using refrigerant blends is feasible. However, there are few experimental studies and most of them deal with replacing HFC-134a. Authors aim to contribute to the hypothesis that there are fluids that could be energetically more advisable than pure HC-600a for domestic appliances. Therefore, this work presents the experimental optimization of a domestic fridge using HC-600a as reference fluid against five binary blends identified theoretically by Calleja-Anta, et al. [23]. The possibility is demonstrated in this work.

5.2 Thermodynamic approach

5.2.1 Thermophysical properties of mixtures

Five refrigerant blends were selected from the theoretical studies of Calleja-Anta et al. [23] for evaporating and condensing temperatures of -30 ºC and 40 ºC respectively, whose compositions and main properties are summarised in Table 5.1. Figure 5.1depicts the pressure-enthalpy diagram and 40 ºC and -30 ºC isotherms. The binary blends present a high proportion of hydrocarbons, being classified as A3 ASHRAE security classification according to the results of Calleja-Anta, et al. [24]. They have all similar Normal Boiling Point (NBP) and critical point to R-600a. In reference to the latent heat of phase-change at evaporating conditions, variations with respect R-600a are from -2.6% to 15.6%; and considering the specific volume from -9.6% to 43.8%. The main difference from the reference fluid is the existence of an important temperature glide, both in evaporating and condensing conditions. Table 5.1 reflects that the largest glide in the evaporator would be up to 12.0 K for the mixture of R-600/R-1270.

Table 5.1. Physical, environmental and safety characteristics of refrigerant mixtures used as drop-ins R-600a

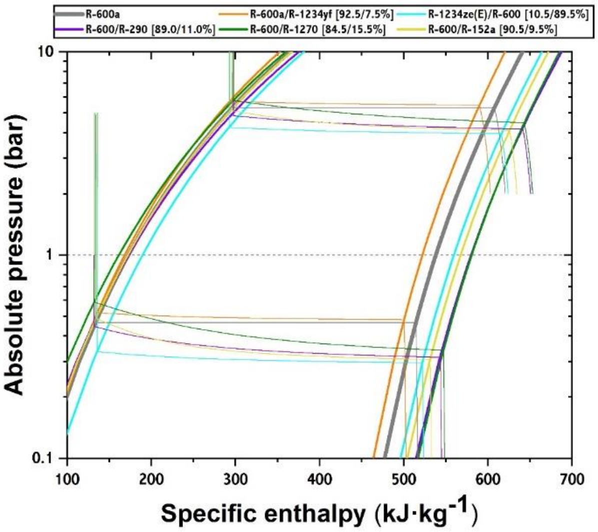

Figure 5.1. Pressure-enthalpy diagram of considered refrigerants and isotherms (-30 ºC, 40 ºC)

5.2.2 Ideal performance of mixtures

The thermodynamic performance of a cycle using the mixtures was evaluated according to the model presented by Calleja-Anta, et al. [23], simulating an ideal-single stage cycle with adiabatic capillary tube. The cycle was evaluated at -30 ºC of evaporating temperature with 20 K evaporating superheat (SH) and 40 ºC of condensing temperature with 2 K subcooling (SUB). The condensation pressure was evaluated for the reference temperature and a vapour title of 50%, Eq.(5.1); whereas the evaporation pressure was calculated through an iteration process for the reference temperature and the medium enthalpy in the evaporator, Eq.(5.2). At these pressures, the VCC, Eq.(5.3); the coefficient of performance, Eq.(5.4); and the vapour title at the evaporator inlet, Eq.(5.5), were evaluated using the default mixing parameters of REFPROP v.10 [25]. More information about the model can be found in Calleja-Anta, et al. [23].

$$p_K = f(t_K, x_v = 0.5) \qquad \text{Eq.(5.1)}$$

$$p_O = f\left(t_O, \frac{h_{O,in}+h_{O,out}}{2}\right) \qquad \text{Eq.(5.2)}$$

$$VCC = \frac{h_{O,out} - h_{O,in}}{v_{O,out}} \qquad \text{Eq.(5.3)}$$

$$COP = \frac{h_{O,out} - h_{O,in}}{h_{dis,s}(p_K, s_{O,out}) - h_{O,out}} \qquad \text{Eq.(5.4)}$$

$$x_{v,O,in} = f(p_O, h_{O,in}) \qquad \text{Eq.(5.5)}$$

Figure 5.2 contrasts the expected performance of the ideal single-stage cycle of the selected mixtures against the operation with R-600a. The selected mixtures present higher COP and variations in the VCC. Mixture of R-600a/R-1234yf predicts 0.5% increment in COP and an enhancement in capacity of 5.7%. The other mixtures show reductions in the predicted capacity between 12.2% (R-600/R-1270) to 27.2% (R-1234ze(E)-R-600) but predict COP increments between 3.2% (R-600/R-290) and 6.0% (R-600/R-152a). However, it needs to be mentioned that these figures do not include the effects of the compressor behaviour.

Finally, Figure 5.3 contrast the expected working pressures of the mixtures in relation to R-600a ones. Except for the R-600a/R-1234yf mixture which will operate at higher pressure, the other mixtures will present a pressure reduction in evaporation between 0.10 to 0.16 bar, still working under vacuum condition; and in condensation between 0.85 to 1.20 bar. In any case, due to their similarity to those of isobutane, the predicted pressures are compatible with the operation of a R-600a compressors.

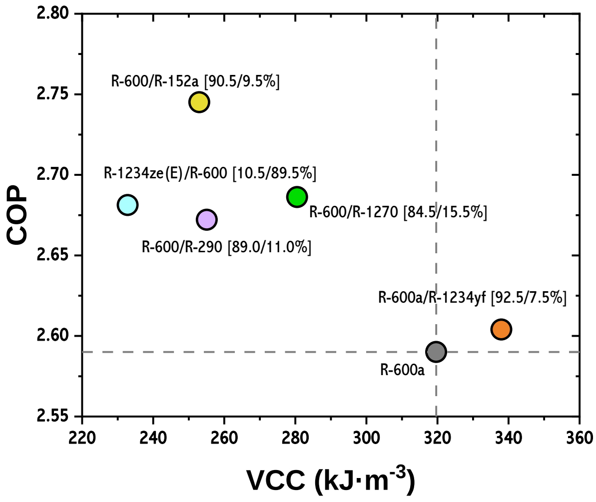

Figure 5.2. Ideal COP and VCC at t_O=-30 °C, t_K=40 °C, *SH*=20 K, *SUB*=2 K

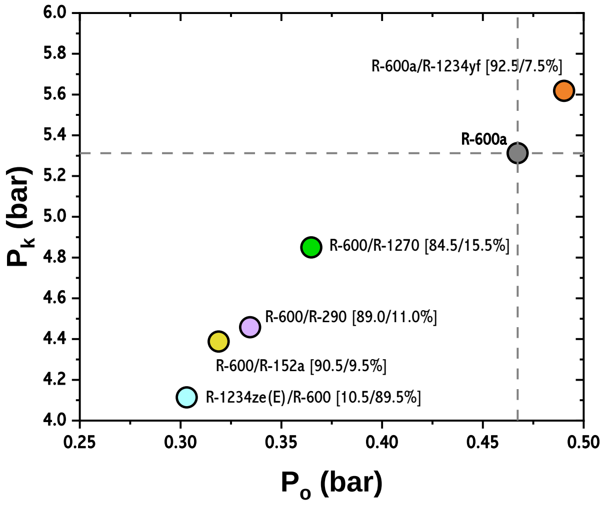

Figure 5.3. Ideal working pressures at t_o=-30 °C, t_k=40 °C, SH=20 K, SUB=2 K

5.3 Methods and materials

5.3.1 Experimental system

Experimental evaluation was done using a 340-litre domestic fridge for fresh food (Figure 5.4). The system is run by a 6.6 cm^3 1/8 HP LBP R-600a hermetic compressor using mineral lubricant. The evaporator is of roll bond type, condenser is a wire-tube (1052 mm height and 557 mm width) and the expansion system is an adiabatic capillary tube.

The fridge was placed inside a climatic chamber with temperature and humidity controlled according to the standard IEC 60335-2-89:2019 [26]. Variables were measured with a thermo-hygrometer, with uncertainty of ±2% RH and ±0.2 K.

The system was only modified to install pressure gauges: one at the compressor discharge (-1 to 15 bar), one at exit of the condenser (-1 to 15 bar) and two at the compressor suction (-1 to 8 bar). Uncertainty of pressure gauges is of ±1%. Three T-type surface thermocouples were placed at compressor suction, compressor discharge and condenser outlet since other parts of the circuit were not accessible. Surroundings (left, right and bottom), upper and lower temperatures inside the fridge were measured with T-type thermocouples immersed in 25 g brass cylinders, and the reference product temperature was obtained as average temperature of 7 M-Test packages with an immersion T-type thermocouple. Uncertainty of all thermocouples is of ±0.5 K. Power consumption was registered with a digital wattmeter, with an uncertainty of ±0.5 %.

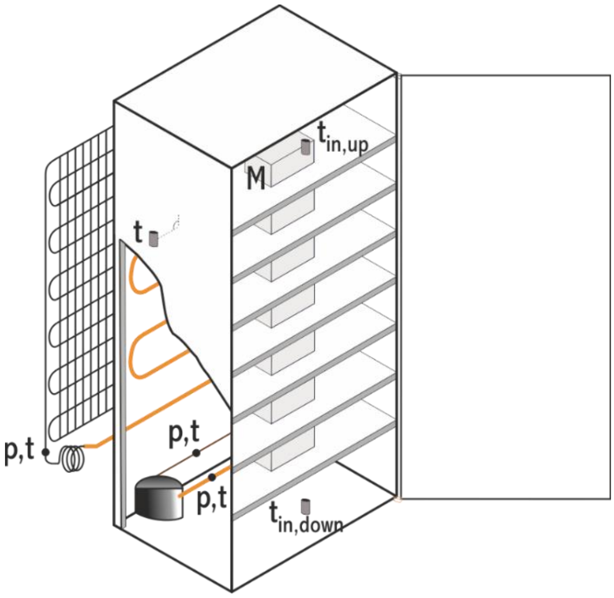

Figure 5.4. Schematic view of the fridge used in the experimental evaluation

5.3.2 Experimental procedure and mixtures preparation

The objective was to verify that the selected mixtures were able to reduce the energy consumption of the fridge with minimal modifications. To do this the fridge, always closed, was tested inside the climatic chamber at 25.4 ± 0.3 ºC and relative humidity below 60%. Its behaviour was registered for 24 hours according to the following restrictions:

- Product temperature: reference product temperature for all the tests was 5.0 ºC, which corresponds to the average temperature of the 7 M-test packages. The compressor was operated with ON/OFF operation with a programmed control in the data acquisition system. The control adjusted the inner temperature set-point automatically with a hysteresis of 3 K.
- Defrosting: the fridge uses manual defrosting. For each test the fridge was stopped until it reached the chamber temperature, then it was dried and later performed the pull-down until the reference temperature was achieved. Then the test could start.

Figure 5.5 details a 24-h test with 26 g of R-600a and Figure 5.6 with 28 g of the mixture R-1234ze(E)/R-600 [10.5/89.5%]. Table 5.2 summarizes the reference parameters and the main energy results of all the performed tests.

Refrigerant mixtures were prepared in our laboratory using certified 99.9% purity gases. For each fluid, 100 g of mixture was prepared using a 5-litre tank, ensuring that all the mixture was in vapour phase. For the mixture preparation, the tank was firstly filled with the calculated quantity of the pure component with lowest NBP. Then, the tank was filled with the calculated quantity of the component with highest NBP. Authors assume that the mixture between both components was good, since the mixture was in vapour phase. Refrigerant charge was done through the service valve of the compressor using a precision balance with an uncertainty of ±0.1 g. Maximum mass composition uncertainty was calculated using the method described by Milton, et al. [27], resulting in an uncertainty below 1.25%. The composition uncertainty is considered adequate for the purpose of the work. The composition uncertainty is considered adequate for the purpose of the work. Then, this mixture was used to perform the charge optimization process. The first test was carried out with an initial charge that allowed obtaining the desired product temperature. Then, after vacuum in each charge process, the charge was increased in steps of 2 g to record the energy consumption as function of the charge. For most of the fluids the charge optimization process was done at least twice to check the consistency of the measurements. Number of repetitions for each charge of refrigerant is presented in Table 5.2. Authors assumed that compatibility of the mixtures with the lubricant oil was good, since the refrigerant that mainly constitutes the mixture is butane or isobutane and they are compatible with mineral oil; and no operating problems occurred during the whole experimental process.

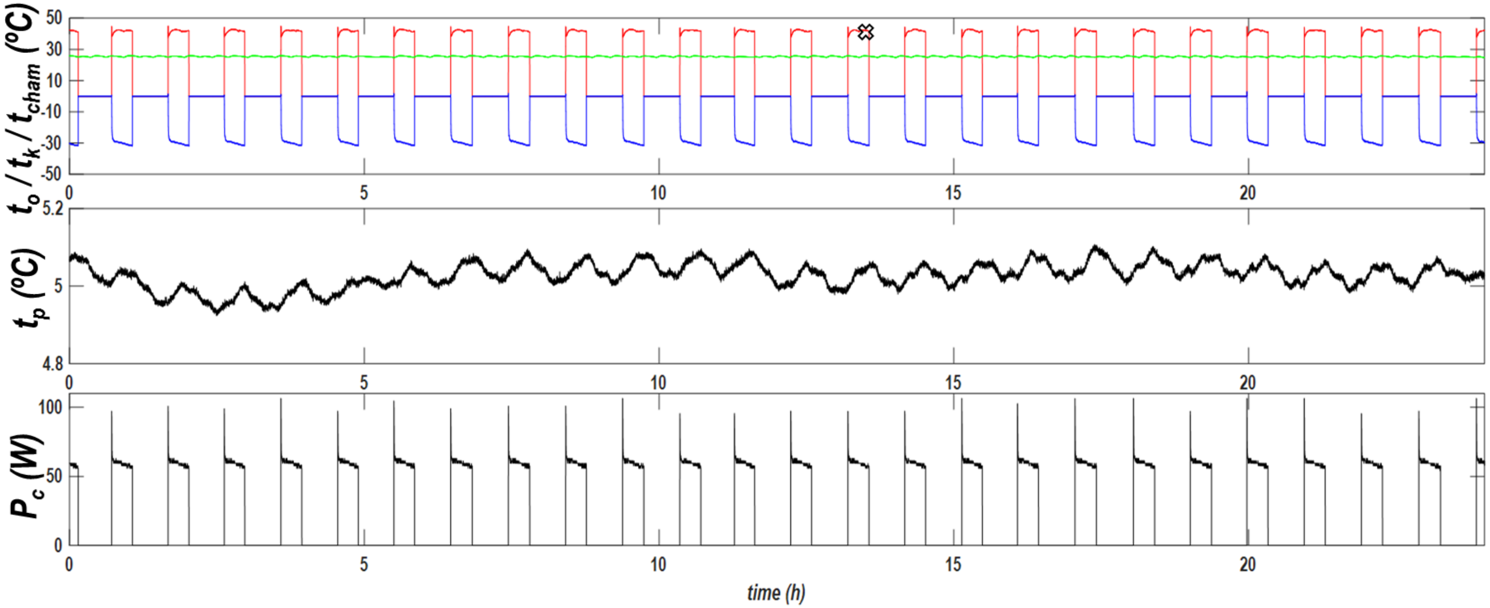

Figure 5.5. R-600a (26 g) 24 h reference test.

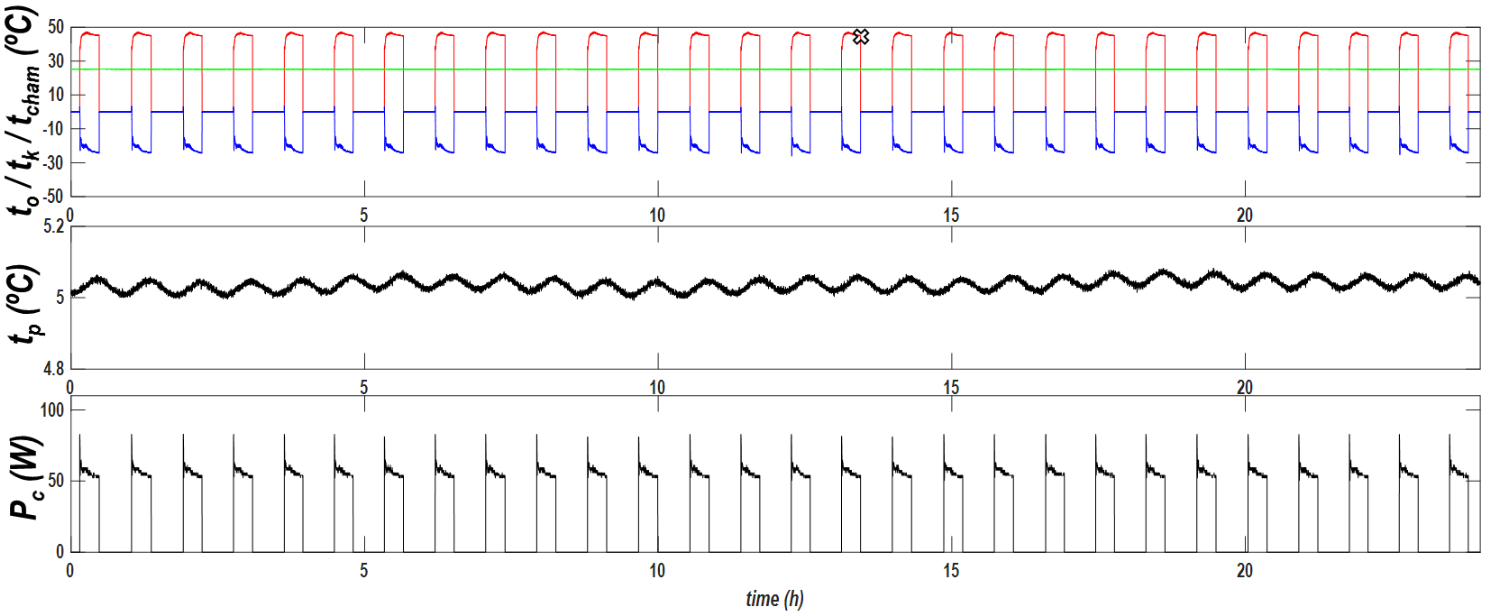

Figure 5.6. R-1234ze(E) / R-600 [10.5/89.5%] (28 g) 24 h reference test.

5.4 Experimental results

This section presents first the charge optimization process of the fridge with the different fluids and then presents a detailed analysis of the energy performance at the optimum refrigerant charges.

5.4.1 Charge optimization

As mentioned, the optimization was done only adjusting the refrigerant charge. Capillary tube was unaltered. The initial refrigerant charge was that that allowed the fridge to reach an average product temperature of 5 ºC. Then, the refrigerant charge was raised in steps of 2 g until the optimum point was determined (which is the charge with the lowest energy consumption).

The energy consumption during the 24 h test was calculated from the power consumption measurement, which was recorded every 5 seconds. Eq.(5.6) details the expression used to compute this parameter, where the energy consumption is expressed in W·h. Calculated energy consumption presents an uncertainty below 0.5%.

$$E_i = \frac{1}{3600} \cdot \int_0^{24h} P_C(t) \cdot dt = \frac{1}{3600} \cdot \sum_{j=1}^{24h} \left\{ \left[\frac{P_C(j) + P_C(j-1)}{2} \right] \cdot [t(j) - t(j-1)] \right\} \qquad \text{Eq.(5.6)}$$

First, the fridge was subjected to the optimization using the certified R-600a. Evolution of energy consumption, which is depicted in Figure 5.7, resulted in a 24-h energy consumption of 536.92 W·h for an optimum refrigerant charge of 26 g. The optimum refrigerant charge coincides with the manufacturer one.

Then the fridge was evaluated for all the mixtures selected for the study, which main properties are detailed in Table 5.1. Figure 5.7 summarizes the energy consumption of each fluid for the different refrigerant charges. Details about repetitions are collected in Table 5.2.

As it is observed in Figure 5.7 three refrigerant mixtures resulted in lower energy consumption than the reference fluid. Mixture R-600a/R-1234yf [92.5/7.5%] reduced by 2.15% the energy consumption at an optimum refrigerant charge of 28 g; blend R-1234ze(E)/R-600 [10.5/89.5%] by 3.84% at 28 g; and mixture R-600/R-290 [89.0/11.0%] by 1.31% at 28 g. However, the other two mixtures were not able to stay below R-600a.

Accordingly, this experiment validates the hypothesis that refrigerant blends could offer energy consumption reductions in relation to pure fluids, as launched by Calleja-Anta, et al. [23].

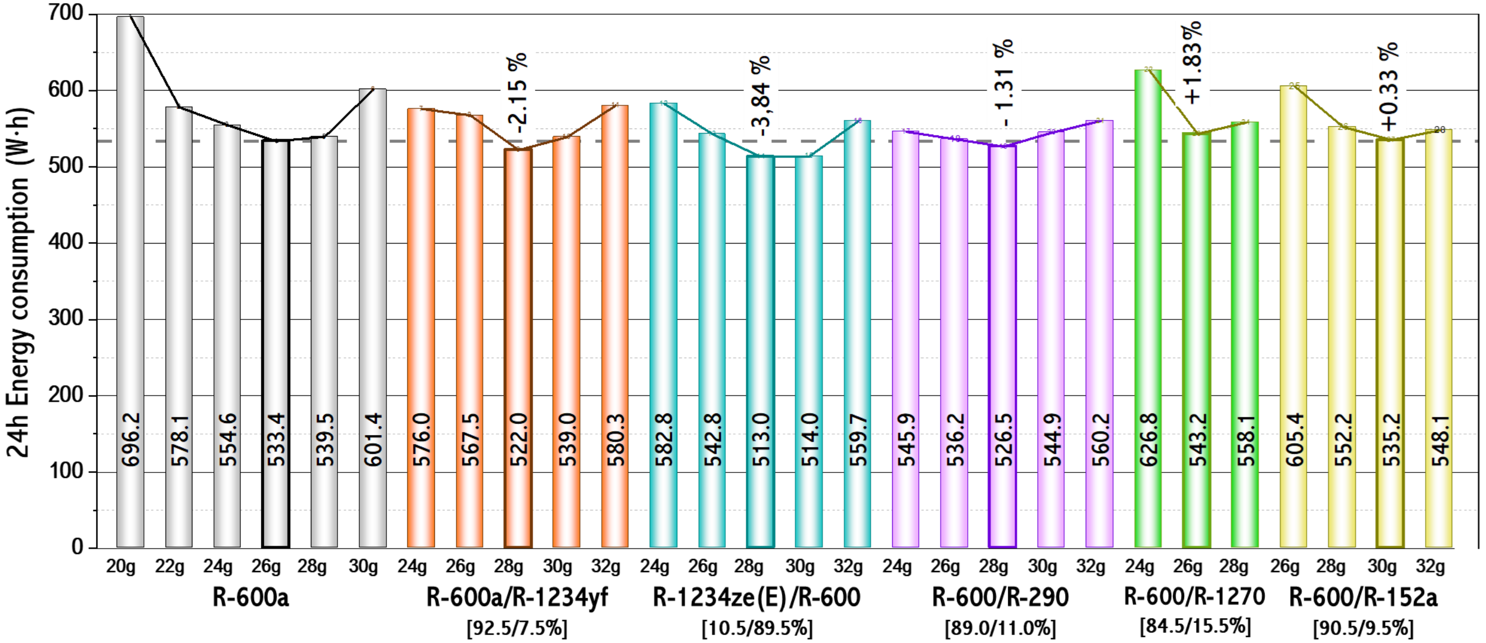

Figure 5.7. 24 h energy consumption vs. refrigerant charge. Charge optimization procedure.

5.4.2 Optimized configurations

Although experimentation does not allow analysing the exact performance of the refrigerant mixtures along the cycle, this section presents a comparison of the operation of the different mixtures at the optimum refrigerant charge in reference to R-600a. Detailed analysis about the behaviour of the fluids in the heat exchangers, in the compressor or even the dynamic performance of the system require specific test benches.

Averaged indicators

Figure 5.8 presents the average power consumption during the 24 h test (only when the compressor is in operation) versus the duty cycle of the compressor (see Table 5.2 for detailed information). Mixtures of interest have small deviations from the operation with R-600a: Blend of R-600a/R-1234yf presents 11.3% increment in the average power consumption but the duty cycle is reduced by 4.4%, what indicates that the mixture operates with larger capacity. Mixture R-1234ze(E)/R-600 allows to reduce the power consumption by 6.3% and the duty is enlarged by 0.9%. And blend R-600/R-290 presents close performance to R-600a since the average power consumption is reduced only by 1.5% and the duty only increases by 0.9%.

Figure 5.8 summarizes the average evaporation and condensation temperatures when the compressor is in operation. Condensing temperature is evaluated as function of pressure at the inlet of the condenser for a vapour title of 50%, as detailed by Eq.(5.7); and the evaporating temperature as function of pressure at compressor suction and the mean enthalpy between saturated vapour (at suction pressure) and at the evaporator inlet, as expressed by Eq.(5.8). It can be observed that all the blends, at optimum condition, present higher evaporating temperatures, which could imply an improved thermal effectiveness of the evaporator; but they also present an increased condensing level, which could imply the opposite for the condenser. Although variations in the condensing level are not much relevant, the increments of the for the mixtures with interest reach: 2.6 K for R-600a/R-1234yf, 6.8 K for R-600/R-290 and 8.1 K for R-1234ze(E)/R-600, which obviously help to increase the performance of the cycle. In any case, these values only indicate that the evaporator performance is enhanced, but they do not quantify the improvement, since specific analysis are needed.

$$t_K = f\left(p_{K,in}, x_v = 0.5\right) \qquad \text{Eq.(5.7)}$$

$$t_O = f\left(p_{suc}, \frac{h_{O,in} + h_{O,v}}{2}\right) \qquad \text{Eq.(5.8)}$$

Since the differences in operating parameters do not deviate largely from the original fluid, these fluids are expected to perform adequately with R-600a systems, and an improvement in evaporator heat transfer characteristics could also be expected.

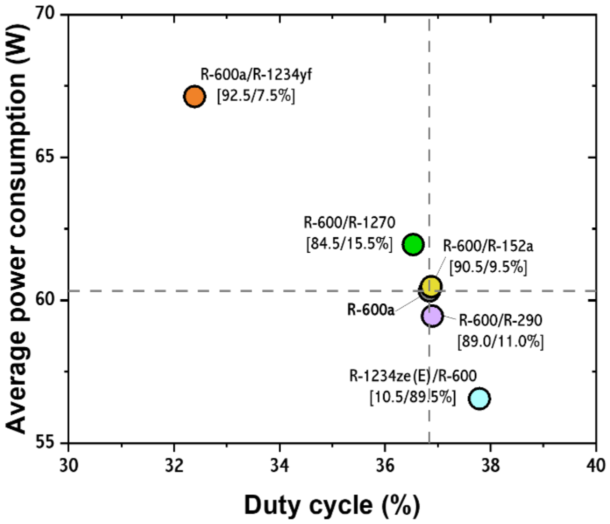

Figure 5.8. Average power consumption vs. duty cycle of the compressor for optimized charges during 24 h (compressor ON)

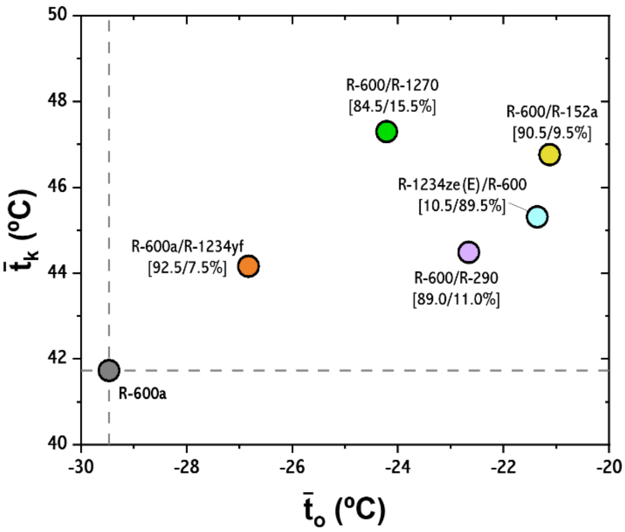

Figure 5.9. Average phase-change temperatures during 24 h for optimized charges (compressor ON)

Cycle indicators

To provide a closer analysis to the behaviour of the mixtures in the cycle, this section discusses some thermodynamic characteristics at the end of the cycling period. Reference period corresponds to the averaged properties during 30 seconds before the compressor stops the operation, which is the most stable period during the operation of the fridge and the closest to steady state conditions. The period is highlighted with an '*X*' in Figure 5.5 and Figure 5.6, and all data is collected in Table 5.3 for reference.

First, Figure 5.10 presents the estimation of the COP* and VCC* of the mixtures the from measured data. COP* is evaluated using Eq.(5.9), as quotient of the enthalpy difference in the evaporator (expansion process considered as isenthalpic) and the enthalpy difference during compression, where the discharge enthalpy is assumed to be ideal (no better approximation can be done). VCC* is calculated with Eq.(5.10) as the quotient of the enthalpy difference in the evaporator and the specific volume of the mixture at the compressor inlet. All properties are evaluated using standard mixing rules with REFPROP v.10. [25].

$$COP^* = \frac{h_{o,out} - h_{k,out}}{h_{dis,s} - h_{suc}} \qquad \text{Eq.(5.9)}$$

$$VCC^* = \frac{h_{O,out} - h_{O,in}}{v_{suc}} \qquad \text{Eq.(5.10)}$$

For the considered period, we observe that mixtures perform with higher COP* and higher VCC* than R-600a, which is consistent with the theoretical approach (Figure 5.2). However, we observe that the increments in the COP* are larger than predicted, because the evaporating temperature rises with the mixtures, as well as the vapour title at the inlet of the evaporator, which is reduced in relation to R-600a (Table 5.3). Mixtures of interest present a COP* increment between 1.7 to 17.4% in relation to R-600a. In addition, all mixtures present larger VCC* than the reference, due to the higher evaporation temperature.

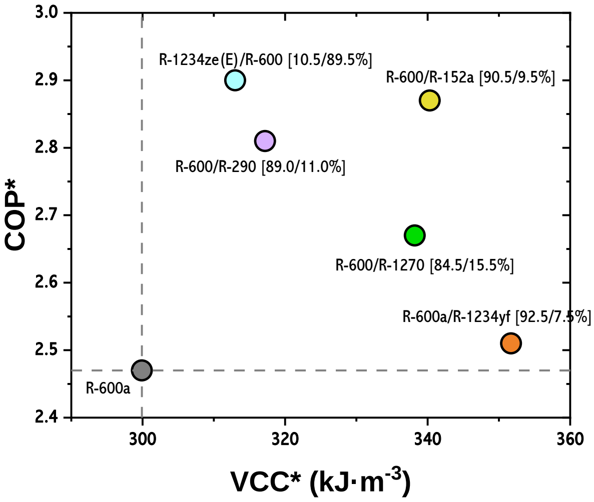

Figure 5.10. Estimated *COP* and *VCC* at the end of cycling period

Secondly, Figure 5.11 depicts the evaporator superheat and condenser subcooling for the considered period. It is observed that at optimum refrigerant charge, mixtures perform with lower superheat at the evaporator (enhancement of the thermal effectiveness of the evaporator) and higher subcooling degree at condenser. These values could be influenced by the glide in the heat exchangers (Table 5.3). Mixtures that obtain energy consumption reduction perform with low effective glides in condenser and evaporator, but mixtures with large glide (R-600/R-152a and R-600/R-1270) are not able to provide energy benefits, even that at stable conditions present a higher COP*.

$$RU = t_{o,out} - t_v|_{p_{suc}} \qquad \text{Eq.(5.11)}$$

$$SUB = t_l|_{p_{k,out}} - t_k \qquad \text{Eq.(5.12)}$$

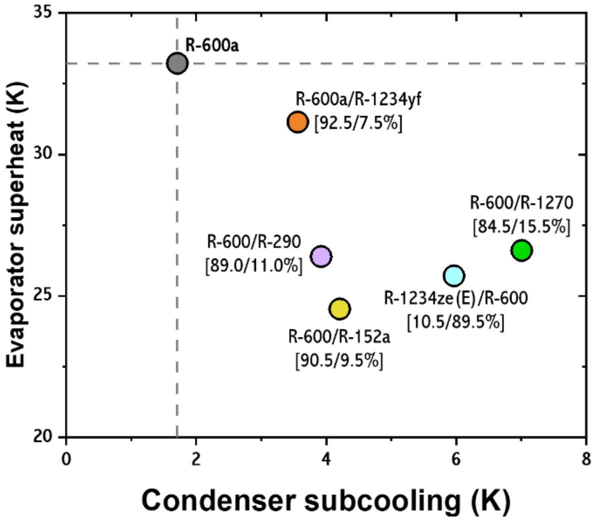

Figure 5.11. Estimated evaporator superheat and condenser subcooling at the end of on period for optimized charges

5.5 Conclusions

This work has addressed the hypothesis that refrigerant mixtures could offer energy consumption savings in reference to pure fluids in real systems. Blends selected to operate in R-600a refrigeration systems were experimentally tested in a real domestic fridge under laboratory conditions.

The mixtures R-600a/R-1234yf [92.5/7.5%], R-1234ze(E)/R-600 [10.5/89.5%], R-600/R-290 [89.0/11.0%], R-600-1270 [84.5/15.5%] and R-600/R-152a [90.5/9.5%] were selected as candidates to replace R-600a in refrigeration systems operating at -30 ºC and 40 ºC of evaporation and condensation levels respectively. Performance of an ideal single-stage vapour compression system with adiabatic capillary tube operating at these conditions predicted COP increments in relation to R-600a between 0.5 to 6.0% with variations in the volumetric cooling capacity from -27.0 to 5.7%. Differences of the theoretical working pressures versus R-600a were not large.

An experimental evaluation was done using a 340-litre commercial fridge for fresh food run by an LBP R-600a hermetic compressor. Test were performed in a climatic chamber according to the standard EN 62552-2:220 at 25.4 ºC and relative humidity below 60%. Average product temperature in the tests was fixed at 5 ºC and the 24-hour energy consumption was considered as objective parameter. For each refrigerant, fridge was subjected to a charge optimization process with a 2 g step. Only three refrigerant mixtures presented 24-h energy consumption lower than R-600a:

- R-600a/R-1234yf [92.5/7.5%] reduced by 2.15% at an optimum refrigerant charge of 28 g.
- R-1234ze(E)/R-600 [10.5/89.5%] by 3.84% at 28 g.
- R-600/R-290 [89.0/11.0%] by 1.31% at 28 g.

At optimum charges, it was observed that the mixtures operated at higher averaged evaporating and condensing temperatures versus R-600a. R-600a/R-1234yf had an increment of evaporating temperature in relation to R-600a of 2.4 K, R-600a/R-290 of 3.6 K and R-1234ze(E)/R-600 of 3.6 K, indicating that the overall performance of the evaporator increased. Finally, it was estimated the experimental performance of the blends at the end of the cycling period of the compressor. It was observed that all mixtures presented estimated increments of COP and volumetric cooling capacity in relation to R-600a. However, no more specific analysis could be done due to the simple experimental set-up.

In summary, this paper confirms the hypothesis that refrigerant blends could offer energy savings in relation to pure fluids in real refrigeration systems, although the heat transfer coefficients of refrigerant blends are reduced in reference to pure refrigerants. Authors invite researchers to perform specific analysis of mentioned blends to investigate the performance in heat exchangers and other experimental systems.

5.6 Acknowledgements

Authors gratefully acknowledge Jaume I University (grant PREDOC/2019/19 and project UJI-B2021-10), Ministry of Science, Innovation and Universities of Spain (RTI2018-093501-B-C21) and Ministry of Education, Culture and Sport of Spain (grant FPU16/00151) for financing this research work.

5.7 Author contribution statements

R. Ll, D. C. and D.S. developed idea, methods and realized experimental process. R. Ll. wrote the manuscript and D.C, D.S, L.N. made final proofreading. R. Ll, D.S. and R.C. helped to get funds.

5.8 Nomenclature

COP	Coefficient of performance
E	Energy consumption, W·h
GWP	Global warming potential
h	Specific enthalpy, kJ·kg^{-1}
HC	Hydrocarbon molecule
HFC	Hydrofluorocarbon molecule
HFO	Hydrofluoroolefin molecule
NBP	Normal boiling point, ºC
M	Molecular mass, kg·kmol^{-1}
p	Absolute pressure, bar
P_C	Compressor power consumption, W
q_O	Specific cooling capacity, kJ·kg^{-1}
RH	Relative humidity, %
s	Specific entropy, KJ·kg^{-1}·K^{-1}
SH	Degree of superheat in evaporator, K
SUB	Degree of subcooling in condenser, K
t	Temperature, ºC
VCC	Volumetric cooling capacity, kJ·m^{-3}
w_s	ideal compression work, kJ·kg^{-1}
x_v	Vapour title

Greek symbols

λ	latent heat of phase change, kJ·Kg^{-1}
v	Specific suction volume, m^3·kg^{-1}

Subscripts

c	at critical conditions
cham	refers to climatic chamber
comp	refers to the compressor
dis	compressor discharge
down	at the bottom of the fridge
in	inlet
K	refers to condensing conditions
O	refers to evaporating conditions
out	outlet
p	refers to product
s	isentropic
suc	compressor suction
up	at the upper part of the fridge

5.9 References

[1] IPCC, Climate Change 2021: The Physical Science Basis. Contribution of Working Group I to the Sixth Assessment Report of the Intergovernmental Panel on Climate Change [Masson-Delmotte, V., P. Zhai, A. Pirani, S. L. Connors, C. Péan, S. Berger, N. Caud, Y. Chen, L. Goldfarb, M. I. Gomis, M. Huang, K. Leitzell, E. Lonnoy, J. B. R. Matthews, T. K. Maycock, T. Waterfield, O. Yelekçi, R. Yu and B. Zhou (eds.)]. in: C.U.P.I. Press (ed.) IPCC, 2021: , 2021.

[2] International Institute of Refrigeration, 38th Note on Refrigeration Technologies. The Role of Refrigeration in the Global Economy (2019). in, International Institute of Refrigeration, 2019, DOI: 10.18462/iif.NItec38.06.2019.

[3] UNEP, Report of the Twenty-Eighth Meeting of the Parties to the Montreal Protocol on Substances that Deplete the Ozone Layer, in, Kigali, Rwanda, 2016.

[4] UNEP, Refrigeration and air conditioning and heat pumps technical options committee. 2018 Assessment Report, in, United Nations Environment Programme, Kenya, 2018.

[5] European Commission, Regulation (EU) No 517/2014 of the European Parliament and of the Council of 16 April 2014 on fluorinated greenhouse gases and repealing Regulation (EC) No 842/2006., in: E. Commission (ed.), Official Journal of the European Union, 2014.

[6] B.O. Bolaji, Experimental study of R152a and R32 to replace R134a in a domestic refrigerator, Energy, 35 (2010) 3793-3798 DOI: http://dx.doi.org/10.1016/j.energy.2010.05.031.

[7] A. Maiorino, C. Aprea, M.G. Del Duca, R. Llopis, D. Sánchez, R. Cabello, R-152a as an alternative refrigerant to R-134a in domestic refrigerators: An experimental analysis, International Journal of Refrigeration, 96 (2018) 106-116 DOI: https://doi.org/10.1016/j.ijrefrig.2018.09.020.

[8] C. Aprea, A. Greco, A. Maiorino, C. Masselli, The drop-in of HFC134a with HFO1234ze in a household refrigerator, International Journal of Thermal Sciences, 127 (2018) 117-125 DOI: https://doi.org/10.1016/j.ijthermalsci.2018.01.026.

[9] Karber K. M., Abdelaziz O., Vineyard E.A., Experimental Performance of R-1234yf as a Drop-in Replacement for R-134a in Domestic Refrigerators, in: International Refrigeration and Air Conditioning Conference at Purdue, Purdue, EEUU, 2012.

[10] C. Aprea, A. Greco, A. Maiorino, An experimental investigation on the substitution of HFC134a with HFO1234YF in a domestic refrigerator, Applied Thermal Engineering, 106 (2016) 959-967 DOI: 10.1016/j.applthermaleng.2016.06.098.

[11] M. Yang, H. Zhang, Z. Meng, Y. Qin, Experimental study on R1234yf/R134a mixture (R513A) as R134a replacement in a domestic refrigerator, Applied Thermal Engineering, 146 (2019) 540-547 DOI: 10.1016/j.applthermaleng.2018.09.122.

[12] C. Aprea, A. Greco, A. Maiorino, An experimental investigation of the energetic performances of HFO1234yf and its binary mixtures with HFC134a in a household refrigerator, International Journal of Refrigeration, 76 (2017) 109-117 DOI: 10.1016/j.ijrefrig.2017.02.005.

[13] C. Aprea, A. Greco, A. Maiorino, Comparative performance analysis of HFO1234ze/HFC134a binary mixtures working as a drop-in of HFC134a in a domestic refrigerator, International Journal of Refrigeration, 82 (2017) 71-82 DOI: https://doi.org/10.1016/j.ijrefrig.2017.07.001.

[14] S. Wongwises, N. Chimres, Experimental study of hydrocarbon mixtures to replace HFC-134a in a domestic refrigerator, Energy Conversion and Management, 46 (2005) 85-100 DOI: 10.1016/j.enconman.2004.02.011.

[15] M. Fatouh, M. El Kafafy, Assessment of propane/commercial butane mixtures as possible alternatives to R134a in domestic refrigerators, Energy Conversion and Management, 47 (2006) 2644-2658 DOI: 10.1016/j.enconman.2005.10.018.

[16] M. Mohanraj, S. Jayaraj, C. Muraleedharan, P. Chandrasekar, Experimental investigation of R290/R600a mixture as an alternative to R134a in a domestic refrigerator, International Journal of Thermal Sciences, 48 (2009) 1036-1042 DOI: 10.1016/j.ijthermalsci.2008.08.001.

[17] M. Rasti, S. Aghamiri, M.-S. Hatamipour, Energy efficiency enhancement of a domestic refrigerator using R436A and R600a as alternative refrigerants to R134a, International Journal of Thermal Sciences, 74 (2013) 86-94 DOI: http://dx.doi.org/10.1016/j.ijthermalsci.2013.07.009.

[18] T.A. Moreira, G. Furlan, G.H.d.S.e. Oliveira, G. Ribatski, Flow boiling and convective condensation of hydrocarbons: A state-of-the-art literature review, Applied Thermal Engineering, 182 (2021) 116129 DOI: https://doi.org/10.1016/j.applthermaleng.2020.116129.

[19] G.H.S. Oliveira, T.A. Moreira, Z.H. Ayub, G. Ribatski, Flow boiling of hydrocarbons and their zeotropic binary mixtures under pre- and post-dryout conditions, Applied Thermal Engineering, 198 (2021) 117483 DOI: https://doi.org/10.1016/j.applthermaleng.2021.117483.

[20] X. Zou, M.Q. Gong, G.F. Chen, Z.H. Sun, Y. Zhang, J.F. Wu, Experimental study on saturated flow boiling heat transfer of R170/R290 mixtures in a horizontal tube, International Journal of Refrigeration, 33 (2010) 371-380 DOI: 10.1016/j.ijrefrig.2009.10.013.

[21] Y.S. Chang, M.S. Kim, S.T. Ro, Performance and heat transfer characteristics of hydrocarbon refrigerants in a heat pump system, International Journal of Refrigeration, 23 (2000) 232-242 DOI: https://doi.org/10.1016/S0140-7007(99)00042-0.

[22] T.A. Moreira, Z.H. Ayub, G. Ribatski, Convective condensation of R600a, R290, R1270 and their zeotropic binary mixtures in horizontal tubes, International Journal of Refrigeration, 130 (2021) 27-43 DOI: https://doi.org/10.1016/j.ijrefrig.2021.06.031.

[23] D. Calleja-Anta, L. Nebot-Andrés, J. Catalán-Gil, D. Sánchez, R. Cabello, R. Llopis, Thermodynamic screening of alternative refrigerants for R290 and R600a, Results in Engineering, 5 (2020) 100081 DOI: https://doi.org/10.1016/j.rineng.2019.100081.

[24] D. Calleja-Anta, L. Nebot-Andres, R. Cabello, D. Sánchez, R. Llopis, A3 and A2 refrigerants: Border determination and hunt for A2 low-GWP blends, International Journal of Refrigeration, 134 (2022) 86-94 DOI: 10.1016/j.ijrefrig.2021.11.012.

[25] Author, NIST Standard Reference Database 23: Reference Fluid Thermodynamic and Transport Properties-REFPROP, Version 10.0, National Institute of Standards and Technology, 2018 DOI: dx.doi.org/10.18434/T4JS3C.

[26] International Electrotechnical Commission., IEC 60335-2-89:2019. Household and similar electrical appliances - Safety - Part 2-89: Particular requirements for commercial refrigerating appliances and ice-makers with an incorporated or remote refrigerant unit or motor-compressor, in, 2019.

[27] M.J.T. Milton, G.M. Vargha, A.S. Brown, Gravimetric methods for the preparation of standard gas mixtures, Metrologia, 48 (2011) R1-R9 DOI: 10.1088/0026-1394/48/5/r01.

[28] IPCC, Climate Change 2014: Synthesis Report. Contribution of Working Groups I, II and III to the Fifth Assessment Report of the Intergovernmental Panel on Climate Change [Core Writing Team, R.K. Pachauri and L.A. Meyer (eds.)]. IPCC, Geneva, Switzerland, 151 pp., (2014).

TABLES

Table 5.1. Physical, environmental and safety characteristics of refrigerant mixtures used as drop-ins R-600a [25]

	R-600a	R-600a/ R-1234yf [92.5/7.5%]	R-1234ze(E)/ R-600 [10.5/89.5%]	R-600/R-290 [89.0/11.0%]	R-600/R-1270 [84.5/15.5%]	R-600/ R-152a [90.5/9.5%]
M (g·mol^{-1})	58.1	60.3	61.3	56.2	54.9	58.8
NBP (ºC)	-11.75	-16.47	-6.98	-11.5	-16.43	-15.12
t_C (ºC)	134.7	132.4	149.6	146.35	144.9	146.7
p_C (bar)	36.3	36.9	39.6	39.6	41.5	40.3
Glide at 40 ºC (K) $^{\alpha}$	0	0.54	2.62	6.34	9.6	8.6
Glide at -30 ºC (K) $^{\alpha}$	0	1.73	2.59	8.34	12.0	10.0
λ a t = 40 °C (kJ · kg^{-1}) $^{\alpha}$	311.5	302.4	332.2	357.9	366.8	354.4
λ a t = -30 °C (kJ · kg^{-1}) $^{\alpha}$	380.7	370.9	395.4	428.3	438.9	422.3
v at t = -30 °C (m^3 · kg^{-1}) $^{\alpha}$	0.73	0.66	1.05	1.02	0.94	1.02
GWP100 years [28]	20	19	18	20	20	31
ASHRAE 34 safety group	A3	A3 $^{\beta}$	A3 $^{\beta}$	A3 $^{\beta}$	A3 $^{\beta}$	A3 $^{\beta}$

$^{\alpha}$ Calculated for pressure evaluated at the corresponding temperature and 50% of vapour quality

$^{\beta}$ Mixture without ASHRAE 34 security classification, but according to Calleja-Anta et al.[24], it is assumed to belong to the A3 safety group.

Table 5.2. Summary of energy tests with the different refrigerants and reference parameters

Refrigerant	Charge (g)	Repetitions	$\bar{t}_p$ (ºC)	$\bar{t}_{cham}$ (ºC)	$\overline{RH}_{cham}$ (%)	$\bar{P}_C$ (W)	Duty cycle (%)	E (W·h)	E deviation repetitions (%)
R-600a	20	2	5.04	25.4	41	48.1	60.4	696.2	0.3
	22	3	5.02	25.5	41	56.2	42.9	578.1	0.9
	24	3	5.03	25.7	42	60.2	38.4	554.6	1.3
	26	**3**	**5.03**	**25.4**	**40**	**60.3**	**36.8**	**533.4**	1.3
	28	2	5.04	25.5	34	66.4	33.8	539.5	0.5
	30	2	5.04	25.5	42	65.9	38.0	601.4	0.9
R-600a/ R-1234yf [92.5/7.5%]	24	3	4.99	25.1	57	60.0	40.0	576.0	0.5
	26	2	5.05	25.2	59	60.8	38.9	567.5	0.3
	28	**2**	**5.07**	**25.2**	**48**	**67.1**	**32.4**	**522.0**	0.7
	30	1	5.00	25.2	51	70.3	31.9	539.0	-
	32	1	5.03	25.4	58	70.0	34.6	580.3	-
R-600/R-152a [90.5/9.5%]	26	2	4.96	25.5	39	51.4	49.1	605.4	1.3
	28	2	4.95	25.4	49	57.3	40.1	552.2	0.9
	30	**5**	**5.02**	**25.7**	**37**	**60.5**	**36.9**	**535.2**	1.4
	32	3	4.98	25.3	33	63.2	36.1	548.1	1.3
R-600/R-290 [89.0/11.0%]	24	2	5.01	25.4	56	56.1	40.5	545.9	0.5
	26	3	5.02	25.6	34	56.1	39.8	536.2	0.3
	28	**2**	**5.03**	**25.6**	**48**	**59.5**	**36.9**	**526.5**	0.7
	30	1	5.02	25.7	46	62.5	36.3	544.9	-
	32	2	5.04	25.7	44	63.0	37.1	560.2	1.1
R-1234ze(E)/ R-600	24	1	5.04	25.5	39	48.6	50.0	582.8	-
	26	4	5.03	25.2	40	52.0	43.5	542.8	1.2
	28	**3**	**5.04**	**25.2**	**39**	**56.6**	**37.8**	**513.0**	0.9

[10.5/89.5%]	30	4	5.06	25.6	41	57.4	37.3	514.0	0.3
	32	2	5.00	25.5	40	59.9	38.9	559.7	0.9
R-600/R-1270 [84.5/15.5%]	24	1	4.93	25.4	37	55.6	47.0	626.8	-
	26	**1**	**5.08**	**25.2**	**30**	**62.0**	**36.5**	**543.2**	-
	28	1	5.02	25.7	29	66.2	35.1	558.1	-

Table 5.3. Summary of fridge's main operation indicators at optimum refrigerant charge

		R-600a (26 g)	R-600a/ R-1234yf [92.5/7.5%] (28 g)	R-600/ R-152a [90.5/9.5%] (30 g)	R-600/ R-290 [89.0/11.0%] (28 g)	R-1234ze(E)/ R-600 [10.5/89.5%] (28 g)	R-600/ R-1270 [84.5/15.5%] (26 g)
Measured variables	$p_{k,in}$ (bar)	5.58	6.35	5.27	5.01	4.74	5.95
	$p_{k,out}$ (bar)	5.54	6.28	5.20	4.94	4.68	5.89
	p_{suc} (bar)	0.44	0.51	0.44	0.42	0.40	0.44
	$\bar{t}_p$ (ºC)	5.0	5.1	5.0	5.0	5.0	5.1
	$t_{p,min}$ (ºC)	3.7	3.7	3.7	3.7	3.7	3.7
	$t_{p,max}$ (ºC)	7.4	7.3	7.3	7.5	7.4	7.2
	$t_{in,up}$ (ºC)	9.7	9.9	9.8	10.1	9.8	9.5
	$t_{in,down}$ (ºC)	1.8	2.4	1.9	1.9	2.0	2.1
	$t_{k,o}$ (ºC)	39.9	38.5	33.6	35.5	35.2	33.8
	$t_{comp,in}$ (ºC)	24.7	23.3	8.7	13.8	13.8	20.0
	$t_{comp,out}$ (ºC)	48.1	48.6	46.4	46.1	45.7	48.2
	P_c (W)	57.6	63.2	57.7	56.2	53.4	59.6
Calculated / Estimated*	t_O (ºC)	-31.4	-29.0	-23.4	-25.4	-24.1	-25.9
	t_k (ºC)	41.6	44.3	46.3	43.8	44.7	47.3
	$t_{dis,s}{}^*$ (ºC)	72.3	72.7	71.9	72.0	69.1	78.3
	SUB (K)	1.7	3.6	4.2	3.9	6.0	7.0
	RU^* (K)	33.2	31.1	24.5	26.4	25.7	26.6
	$x_{v,O,in}$ (-)	0.43	0.44	0.36	0.36	0.38	0.35

	$Glide_k$ (K)	0.00	3.51	11.26	6.72	5.15	9.33
	$Glide_O$ (K)	0.00	0.79	2.85	2.73	1.40	4.27
	$q_O{}^*$ (kJ·kg^{-1})	266.5	256.6	298.1	306.0	286.2	286.2
	$w_s{}^*$ (kJ·kg^{-1})	107.7	102.0	103.8	109.1	98.5	117.4
	VCC^* (kJ·m^{-3})	299.9	351.7	340.3	317.2	313.0	338.2
	COP^* (-)	2.47	2.51	2.87	2.81	2.90	2.67

CHAPTER 6.

ALTERNATIVE MIXTURES TO R-600a. THEORETICAL ASSESSMENT AND EXPERIMENTAL ENERGY EVALUATION OF BINARY MIXTURES IN A COMMERCIAL COOLER.

Chapter adapted from the paper:

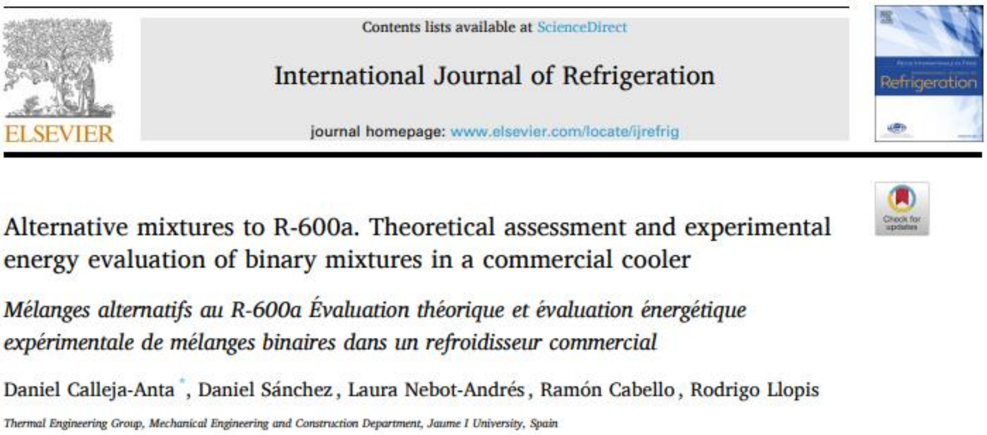

Contents lists available at ScienceDirect

International Journal of Refrigeration

journal homepage: www.elsevier.com/locate/ijrefrig

ELSEVIER

Alternative mixtures to R-600a. Theoretical assessment and experimental energy evaluation of binary mixtures in a commercial cooler

Mélanges alternatifs au R-600a Évaluation théorique et évaluation énergétique expérimentale de mélanges binaires dans un refroidisseur commercial

Daniel Calleja-Anta [*], Daniel Sánchez, Laura Nebot-Andrés, Ramón Cabello, Rodrigo Llopis

Thermal Engineering Group, Mechanical Engineering and Construction Department, Jaume I University, Spain

Calleja-Anta, D., Sánchez, D., Nebot-Andrés, L., Cabello, R., Llopis, R., Alternative mixtures to R-600a. Theoretical assessment and experimental energy evaluation of binary mixtures in a commercial cooler (2023) International Journal of Refrigeration, 152, 83-92. DOI: 10.1016/j.ijrefrig.2023.05.009

Journal Impact Factor QUARTILE: Q2 (2022 quartile).

Cited 1 times.

6 Alternative mixtures to R-600a. Theoretical assessment and experimental energy evaluation of binary mixtures in a commercial cooler.

Daniel Calleja-Anta[1, *], Daniel Sánchez[1, *], Laura Nebot-Andres[1], Ramón Cabello[1], Rodrigo Llopis[1]

[1]Thermal Engineering Group, Mechanical Engineering and Construction Department, Jaume I University, Spain

Abstract

This work focuses on the exploration of binary mixtures as alternative to isobutane (R-600a) from a theoretical and experimental point of view. To predict the most energy efficient blends, a theoretical model was used that analysed 5445 different blends consisting of 11 pure refrigerants. Three blends were selected for experimental testing in a commercial cabinet: R-1234ze(E)/R-600 $(8/92)_{\%mass}$, R-152a/R-600 $(8/92)_{\%mass}$ and R-32/R-600 $(2/98)_{\%mass}$. The results of the 16-hour tests showed that, at their optimum refrigerant charge, the R-1234ze(E)/R-600 $(8/92)_{\%mass}$ and R-152a/R-600 $(8/92)_{\%mass}$ blends achieved energy consumption reductions of -2.69% and -5.04%, respectively, while the R-32/R-600 $(2/98)_{\%mass}$ blend showed an increase of +0.36%. All blends reduced compressor consumption, but increased duty cycles. The results demonstrate the existence of alternative blends that can significantly reduce isobutane energy consumption with similar thermodynamic properties.

Keywords

Commercial refrigeration; R-600a; Refrigerant mixture; energy savings; experimental tests

6.1 Introduction

The growing concern to confront the Global Warming has affected to the layers of our society. The refrigeration sector is one of the main contributors to the temperature increment that the planet is facing, as it was the responsible of 7.8% of global GHG emissions in 2018 [1]. To mitigate this impact, the European Commission, via the Regulation Nº 517/2014 [2], focused on limiting the use of refrigerants with high GWP. Among other measures, the use of refrigerants with GWP higher than 150 were banned for the domestic subsector and for the majority of commercial stand-alone applications from January 2015 and January 2022 respectively. The use of hydrocarbon as refrigerants has become as one of the best options for these two subsectors, since they have reduced GWP, excellent thermodynamic properties, low cost, high availability and are natural.

The stand-alone appliances dedicated for refrigeration and food counted with more than 2.12 billion of units in 2010 (2 billion related with domestic purposes and 120 million with commercial ones) [1]. Globally, the main refrigerants used are R-22 and R-134a, however in Europe the new equipment is related with the use of hydrocarbons, being R-600a for small capacities and R-290 for higher capacities the most common [3].

R-600a has become the standard in Europe in many stand-alone applications. However, previously to it, the use of other refrigerants has been deeply discussed in the research community to substitute R-134a. Mota-Babiloni, et al. [4] analysed experimentally the refrigerants R-1234yf and R-1234ze(E) as R-134a drop-ins in a vapour compression test bench, obtaining COP reductions between 3% and 11% and between 2% and 8% respectively. Similarly, Aprea, et al. [5] tried R-1234yf as drop-in in a domestic refrigerator originally design for R-134a, concluding that the plant was functionally and provided energy saving of 3% in 24 hours. R-152a is another refrigerant that has attracted the attention of researchers. Firstly Sánchez, et al. [6] tested it in a vapour compression test bench, obtaining a slight increase in COP of between 1% and 4.8%. Later, Maiorino, et al. [7] and Sánchez, et al. [8] analysed R-152a in a domestic refrigerator and a commercial cabinet respectively, reducing the energy consumption by 7.4% and 13.7% respectively. In the same work, Sánchez, et al. [8] additionally analysed the refrigerants R-290, R-1270 and R-744, all of them providing energy savings in relation to R-600a. But not only have pure refrigerants been studied. Saravanakumar and Selladurai [9] and Yu and Teng [10] analysed mixtures formed by R-290/R-600a in different proportions as substitute of R-134a, resulting in savings up to 5%. Aprea, et al. [11] also analysed the mixture R-134a/R-1234yf (10/90) in a domestic refrigerator with an energy save of 16% in 24 hours. Oliveira, et al. [12] did an experimental evaluation of the heat transfer of the hydrocarbons R-600a, R-290 and R-1270, demonstrating that the R-600a presented the highest heat transfer coefficient among all of them, and concluded that it could be a reasonable substitute for R-134a in residential and commercial refrigeration. Similar conclusions were obtained by Solanki and Kumar [13], in which the heat transfer coefficients of R-600a were between 64% and 132% higher than those of R-134a under different conditions.

However, little attention has been paid to the search for alternative mixtures to isobutane through mixtures. For first time in 2020, Calleja-Anta, et al. [14] addressed the possibility of raising COP of the isobutane-based systems via mixtures with similar thermodynamic properties. In that study, a theoretical thermodynamic screening was launched, in which a total of 55440 ternary mixtures were analysed considering an ideal vapour compression cycle with different typologies and different temperatures ranges. The most promising mixtures were R-1270/R-600, R-152a/R-600, R-1234zeE/R-600 and R-290/R-600, foreseeing theoretical COP increments up to 8.6% in relation to R-600a. Subsequently, based on the mixtures obtained in the cited study, Calleja-Anta, et al. [15] experimentally analysed the drop-in of the mixtures R-600a/R-1234yf [92.5/7.5%], R-1234ze(E)/R-600 [10.5/89.5%], R-290/R-600 [89.0/11.0%], R-600/R-1270 [84.5/15.5%] in a commercial fridge for fresh food originally designed to work with isobutane, measuring energy consumption reductions in the first three mixtures (-2.15%, -3.84% and -1.31% respectively). However, the main purpose of that work was the validation of the hypothesis that existed mixtures with better energy consumption behaviour than isobutane but with similar thermodynamic properties, as the appliance did not allow any kind of retrofit, not allowing to show the real potential of the mixtures. Latterly, Calleja-Anta, et al. [16] took a step forward and evaluated the possibility of creating binary mixtures with isobutane as component but with reduced flammability. The results showed that few mixtures could accomplish with the requirements and with many limitations in terms of mass composition.

The aim of this paper is to continue exploring alternative mixtures to isobutane that can reduce its energy consumption but maintaining similar thermodynamic properties. First, a theoretical screening is conducted to identify mixtures that predict an increment of COP respect isobutane. The most promising fluids are experimentally tested in a stand-alone commercial cabinet initially designed to work with isobutane but upgraded for the selected mixtures by modifying only the expansion system. Energy tests were conducted during 16 h to demonstrate the convenience of using mixtures in a real application under the same operating conditions of heat rejection conditions and cooling demand. Results corroborate the existence of mixtures with better energy performance than R600a that can be used as an alternative achieving energy savings of up to 5.04%.

The novelty that this work present is to prove the real applicability of alternative mixtures to isobutane. The experimental unit used is a commercial plant with higher cooling demands that other plants tested in other works, which allows to obtain more stable test results in which the external disturbances have barely importance. In addition, this unit is equipped with an electronic expansion valve with the capability to adapt its operation to the tested refrigerants, allowing a better adjustment of the system to the refrigerant. These two facts, that might seem minor, have a significant impact in the evaluation of the alternative mixtures, since they allow to evaluate more closely the actual potential of the alternative mixtures analysed.

6.2 Theoretical obtention of the mixtures

This section describes the model used to foresee mixtures that can provide theoretically higher COP than R-600a. The results obtained are discussed and the mixtures that will be tested are selected.

6.2.1 Description of the theoretical assessment

Simulations were carried out considering an ideal simple vapour compression refrigeration cycle with an internal heat exchanger (IHX) connecting the outlet of the condenser with the outlet of the evaporator. The intention was to replicate as close as possible the conditions in which the experimental plant worked. For that, the conditions obtained from the reference test carried out with R-600a at the optimum mass charge were took as reference and maintained constant for the rest of fluids (the analysis of the test and how the conditions are obtained are explained in detail in the following section and can be seen in Table 6.4). The evaporation and condensation temperatures (t_o and t_k) were fixed at -10.2 ºC and 33.25 ºC, with a superheating (SH) and a subcooling (SUB) of 13.5 K and 1.3 K respectively. The efficiency of the IHX (ε_{IHX}) was considered as 0.85. To lighten the calculation process, pressure drops were neglected. Calculations were performed using the latest version of the Refprop v.10 software [17], using the program's default interaction coefficients.

Evaporation pressure of the mixtures (p_o), corresponding to the evaporation temperature, was calculated with an iterative method by using the mean enthalpy in the evaporator [Eq.(6.1) and Eq.(6.2)]. Following the same criteria, condensing temperature (p_k) was calculated according with a vapor quality (x_v) of 50%, since it coincides with the mean enthalpy [Eq.(6.3)].

$$h_m = \left(\frac{h_{o,in}+h_{o,out}}{2}\right) \qquad \text{Eq.(6.1)}$$

$$p_o = f(t_o, h_m) \qquad \text{Eq.(6.2)}$$

$$p_k = f(t_k, x_v = 0.5) \qquad \text{Eq.(6.3)}$$

Temperatures at the outlet of the evaporator and the condenser were calculated according to the Eq.(6.4) and Eq.(6.5) respectively, in which t_{sat,vap,p_o} and t_{sat,liq,p_k} are the saturations temperatures in vapor ($x_v = 1$) and liquid state ($x_v = 0$) for the given pressure.

$$t_{o,out} = t_{sat,vap,p_o} + SH \qquad \text{Eq.(6.4)}$$

$$t_{k,out} = t_{sat,liq,p_k} - SUB \qquad \text{Eq.(6.5)}$$

Finally, suction enthalpy and inlet evaporator enthalpy were calculated following Eq.(6.6), Eq.(6.7) and Eq.(6.8).

$$t_{suc} = t_{o,out} + \varepsilon_{ihx} \cdot \left(t_{k,out} - t_{o,out}\right) \qquad \text{Eq.(6.6)}$$

$$h_{suc} = f(t_{suc}, p_o) \qquad \text{Eq.(6.7)}$$

$$h_{o,in} = h_{k,out} - h_{suc} + h_{o,out} \qquad \text{Eq.(6.8)}$$

The theoretical model to predict the binary blends is sketched in Figure 6.1, which is similar to the one used in Calleja-Anta, et al. [14].

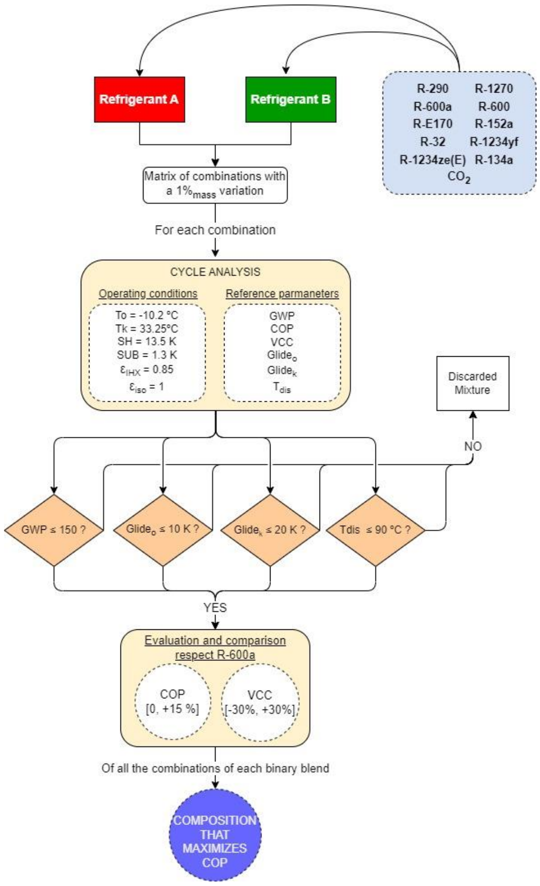

Figure 6.1. Sketched of the theoretical model used to evaluate alternative mixtures.

Firstly, the different thermodynamic states through the cycle were calculated according with the cycle previously described. To classify the mixture as “acceptable” to substitute the isobutane, some requirements were set. The mixture must have a GWP bellow 150 [according to the fifth assessment report [18]], an effective evaporation glide ($Glide_{o,e}$) and a condensation glide ($Glide_k$) lower than 10 K and 20 K respectively and a discharge temperature (t_{dis}) lower the 90 ºC. Mixtures not accomplishing these requirements were discarded. Formulas used to calculate these parameters can be seen from Eq.(6.9) to Eq.(6.12).

$$GWP = \sum_i^n (m_i \cdot GWP_i) \qquad \text{Eq.(6.9)}$$

$$Glide_{o,e} = t_{f(p_o, x_v=1)} - t_{f(\, p_o, x_{v,o,in})} \qquad \text{Eq.(6.10)}$$

$$Glide_k = t_{f(P_k, x_v=1)} - t_{f(p_k, x_{v,}=0)} \qquad \text{Eq.(6.11)}$$

$$t_{dis} = f(s = s_{suc,}\, p_k) \qquad \text{Eq.(6.12)}$$

For the “accepted” mixtures, a second filter based on energy parameters was set. Mixtures with a Volumetric Cooling Capacity (VCC) within a range between 0.7 and 1.3 respect VCC obtained by isobutane are considered as acceptable. Since the unit used for the experimental tests is equipped with a R-600a compressor, higher deviations on this parameter may lead to a lack of cooling capacity and an excessive duty-cycle. Additionally, only mixtures with a Coefficient Of Performance (COP) between 1 and 1.2 times respect isobutane were considered. Blends with lower values are not of interest for this study and higher values of 1.2 isobutane COP are thought to be unrealistic and may be caused by punctual errors in the mixing rules of Refprop.Eq.(6.13) and Eq.(6.14) show how these two parameters are calculated.

$$VCC = \frac{h_{o,out} - h_{o,in}}{v_{suc}} \quad \text{Eq.(6.13)}$$

$$COP = \frac{\Delta \mathrm{h_o}}{\Delta \mathrm{w_{comp}}} = \frac{h_{o,out} - h_{o,in}}{h_{dis,s_{\mathrm{f}(s_{suc},p_k)}} - h_{suc}} \quad \text{Eq.(6.14)}$$

11 pure refrigerants were considered as possible constituents of the mixtures (R-290, R-1270, R-600a, R-600, R-E170, R-152a, R-32, R-1234yf, R-1234ze(E), R-134a and CO_2). All of them were mixed together to form binary blends, creating a total of 55 different combinations. For each combination of two refrigerants, the mass composition of the refrigerants was varied in 1%, resulting in a total of 99 different compositions. For all the 99 compositions of each binary blend, it was selected the one which offered a higher COP. In total 5445 different mixtures were analysed in this screening.

6.2.2 Theoretical results and mixtures selected to be tested

For each pair of refrigerants, the compositions that maximize COP and accomplish with the requirements are chosen. The resultant mixtures can be seen Figure 6.2. Highlighted in a red circle are the mixtures which will be tested in the experimental unit. In the same line as the study Calleja-Anta, et al. [14], two different patterns can be observed. At the right of the graph are placed mixtures mainly formed by isobutane and a second refrigerant, while at the left are the mixtures with butane as principal constituent. Mixtures with isobutane, despite of presenting similar VCC than isobutane, are considered of less interest due to their low increments of COP respect isobutane. On the other side, mixtures with butane present increments in COP around 2%. Of all the mixtures, four blends highlight, which are the ones with R-32 and R-744 as constituents in a very small fraction. These results may be due to the uncertainty associated with the calculation program used. In any case, to validate this hypothesis, the mixture R-32/R-600 (2/98) is chosen to be experimentally tested.

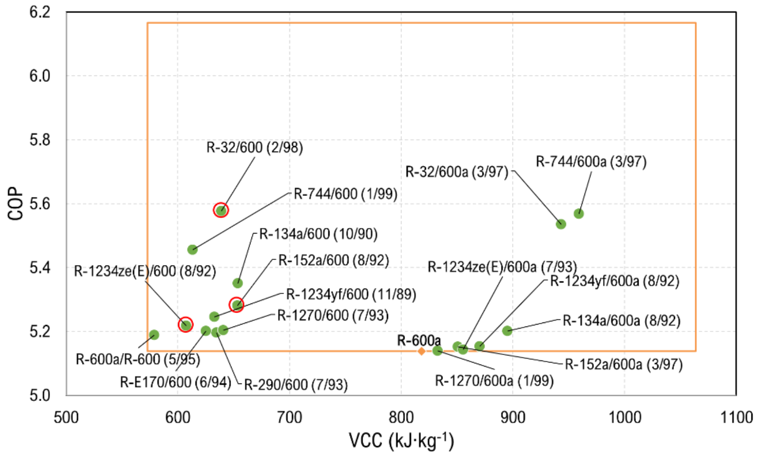

Figure 6.2. Results obtained in the thermodynamic screening. For each pair of refrigerants, the composition with higher COP was chosen.

A total of three mixtures are chosen to be tested in the experimental unit: R-1234ze(E)/R-600 (8/92), R-152a/R-600 (8/92) and R-32/R-600 (2/98). The reason for choosing the first two mixtures was that it had already been demonstrated in previous work that they could offer energy reductions, while R-32/R-600 (2/98) is chosen for the reason previously explained.

The thermodynamic properties of the selected mixtures and GWP obtained in the theoretical process can be seen in Table 6.1, as well as their comparison respect R-600a. The three mixtures present a significant VCC reduction and slight COP increments, which may lead to duty cycle increments in the plant.

Table 6.1. Properties and GWP of the mixtures selected to be tested.

Refrigerant (Mass %)	COP [-] (ΔCOP)	VCC [kJ/kg] (ΔVCC)	$Glide_{o,e}$ [K]	$Glide_{k}$ [K]	Tdis [ºC]	GWP $_{100years}$
R-600a	5.14	818.15	-	-	69.12	3
R-1234ze(E)/ R-600 (8/92)	5.22 (+ 1.54%)	607.49 (- 25.75%)	2.17	3.87	68.2	3.27
R-152a/ R-600 (8/92)	5.28 (+ 2.78%)	653.42 (- 20.13%)	5.21	10.08	65.06	13.8
R-32 /R-600 (2/98)	5.58 (+ 8.52%)	638.85 (- 21.92%)	3.02	16.01	58.28	9.75

Figure 6.3 represents the pressure-enthalpy diagram and 35 ºC and -10 ºC isotherms. The tree mixtures present similar pressure levels to isobutane. In reference to the latent heat of phase-change at evaporating conditions, all the three mixtures present higher values, as it can be seen in the diagram. Concretely, isobutane present a latent heat of 363.53 kJ/kg, while the mixtures of 374.99 kJ/kg, 381.4 kJ/kg and 390.54 kJ/kg, which represents increments of +3.15%, +4.92% and 7.43% respectively. The main difference can be observe in the tempearture glides in both temperatures levels. The glide occurs mainly at low vapor quality values, while at high values is much smaller and tend to stabilize. It can be see by the flow of the isotherms that the glide is higher in the mixtures R-152a/R-600 (8/92) and R-32/R-600 (2/98), as the effective glide in Table 6.1 shows.

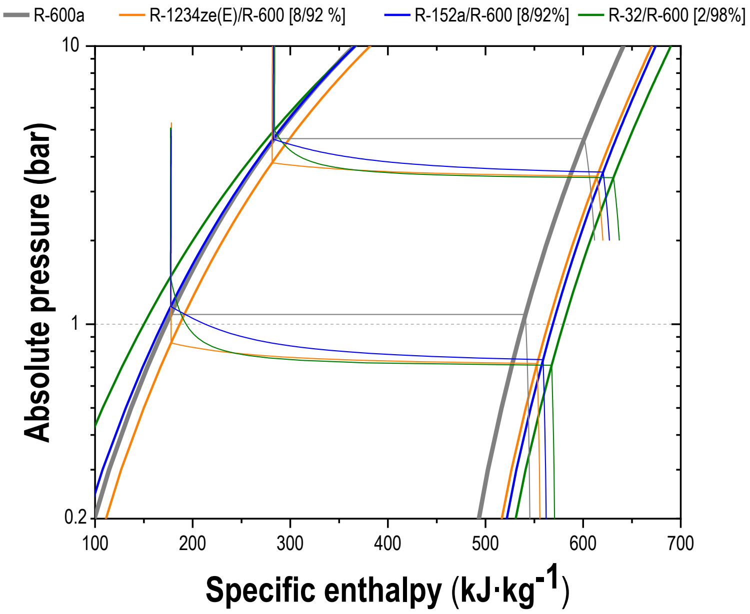

Figure 6.3 .Pressure-enthalpy diagram of considered refrigerants and isotherms (-10 ºC, 35 ºC)

6.3 Methods and materials

This section describes the experimental unit used to perform the experimental tests, as well as the experimental procedure followed and the mixture preparation process.

6.3.1 Experimental system

The experimental tests were performed in a stand-alone commercial cabinet used for the refrigeration of fresh beverage. Its dimensions are 620 (L)x 2000 (H)x 655 (D) mm with a total inner volume of 440 litres. The schematic refrigeration circuit can be seen in Figure 6.4, as well as a picture of the appliance. It consists in a hermetic reciprocating compressor, two condensers (one wired-tube and another finned-tube) in series (to ensure a complete condensation of the refrigerant), an internal heat exchanger (IHX), an electronic expansion valve (whose driver can be configurable to work accordingly with each mixture) and a finned-tube evaporator. The characteristics of each element can be seen in Table 6.2.

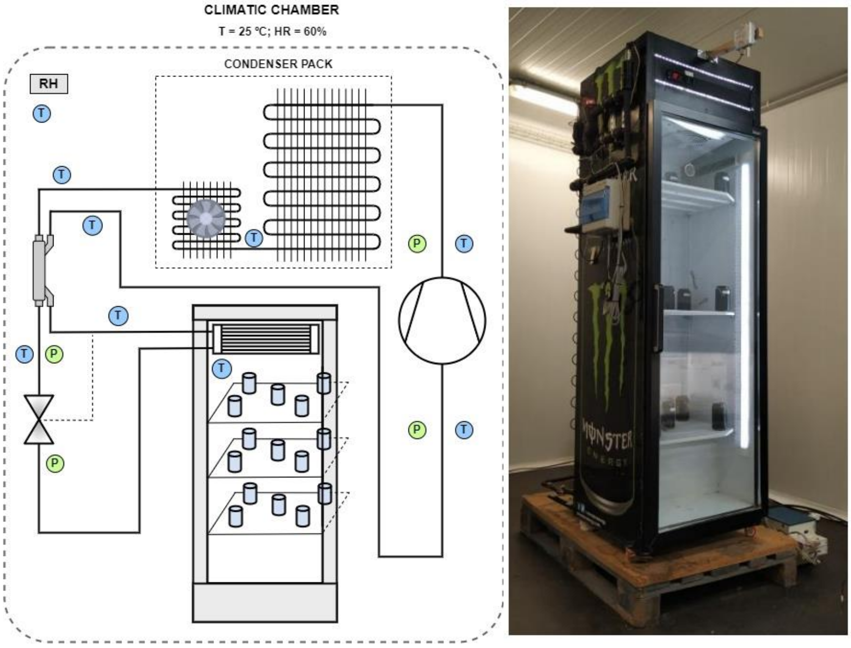

Figure 6.4 Picture of the appliance where the experimental tests are conducted(right) and frigorific scheme of its refrigeration cycle with the position of the different sensors installed (left).

Table 6.2. Description of the cabinet elements.

ID	Element	Characteristics	
1	Compressor	Hermetic reciprocating compressor originally designed to work with isobutane. Displacement: 14.3 cm^3, 2900 rpm, 1/4 horsepower, HBP. Model: Embraco NE K6170Y.	
2	Condenser pack	1st condenser	Wire-on-tube heat exchanger. Natural convection. Heat transfer area: 0.186 m^2
		2nd condenser	Finned-tube heat exchanger. Forced convection. Heat transfer area: 0.089 m^2
3	IHX	Concentric tube heat-exchanger Heat transfer area: 0.01 m^2	
4	Electronic valve	Used as thermostatic expansion valve. Driver configurable to each refrigerant mixture with bubble and dew temperatures.	
5	Evaporator	Finned-tube heat-exchanger. Forced convection. Heat transfer area: 0.186 m2	

The regulation of the cabinet was done with an ON/OFF control system which activated and deactivated the compressor to adjust the internal temperature of the appliance to the set-point specified temperature by the user, with a hysteresis of 3.5 K. The ON/OFF system also commanded the function of the fans of the evaporator and the second condenser, being their power consumption of 60 W in total. The lights of the appliance and its different controllers were always demanding a constant electric power of 17.7 W. The defrosting periods were programmed each 8 hours and finished when the temperature in the surface of the evaporator reached 5 ºC. In that period the evaporator fan was activated.

To obtain the different thermodynamic parameters of the refrigerants, the refrigeration circuit was instrumented with 7 T-type surface thermocouples (T) and 4 pressure gauges (P) [2 high-pressure (0-16 bar) and 2 low-pressure (0-9 bar)]. Additionally, three thermocouple probes at the inlet and outlet of the evaporator airflow were installed. To simulate the product behaviour, 15 test cans filled with a mixture of water/propylene-glycol (67/33%$_v$) were homogeneously placed inside the cabinet with an immersion T-type thermocouple in them. The position of the sensors can be seen in Figure 6.4 (except the evaporator airflow ones, which are not represented). The uncertainty of the T-thermocouple is of ±0.5 K and of the pressure gauges is of ±1% of the full measuring range. To measure the electric power demanded, a digital wattmeter was used with an uncertainty of ± 0.5% of measurement.

The cabinet was placed in a climatic chamber with control of the temperature and the relative humidity. Both parameters were measured with a thermohydrometer with an accuracy of ±2% RH and ±0.2 K.

6.3.2 Experimental procedure and mixtures preparation

The objective of the work is to verify experimentally that the mixtures identified in the theoretical study are able to reduce the energy consumption of the isobutane and quantify it. For that, the standard ISO 23953-2:2015 [19] is used as the reference method to conduct the tests. The tests were performed during 16 hours in the cabinet previously presented (Sánchez, et al. [8] demonstrated that, for this particular appliance, the energy consumption recorded during 16 hours was proportionally the same than 24 hours). The experimental unit was placed inside a climatic chamber at the conditions of 25 ± 0.3 ºC and 60 ± 4% of RH.

The set-point of the ON/OFF controller was adjusted to obtain an average product temperature for all tests of 3.1 ºC.

Refrigerant mixtures were prepared in our laboratory installations using fluids with 99.5% guarantied purity. The mixtures were done in an 8-litre tank, ensuring always that the mixture was in gaseous state. The first refrigerant added in the tank was the one with lower Normal Boiling Point (NBP), followed by the other component, whose quantity was adjusted to match with the desired proportions. A balance with an uncertainty of ±0.1 g was used.

The valve was adapted to work with each refrigerant, configuring the controller according to the bubble and dew temperatures of each mixture. The set-point of the SH of the expansion valve was set at 6 K.

The refrigerant charge of the cabinet was done via the service valve of the compressor. The initial charge was around 90 g for each refrigerant (except isobutane, which required a lower initial charge of 72 g). Once the test finished, the cabinet was charged a quantity between 6 and 8 g. This process was repeated still an optimum charge is clearly reached (charge with the lowest energy consumption respect the rest). A reasonable amount of time was left between charges, never less than 4 hours, until the device stabilized to the new conditions. The effective test sample chosen for the analysis comprise one whole period between two defrosting periods, the last part of one cycle and the beginning of the other, as it can be seen in Figure 6.5. Figure 6.5 represents the evolution of the discharge and aspiration pressures, the product temperature (as the average of the 15 test cans inside the cabinet) and the power consumption during by the unit during 16 hours of the test R-600a 115 g.

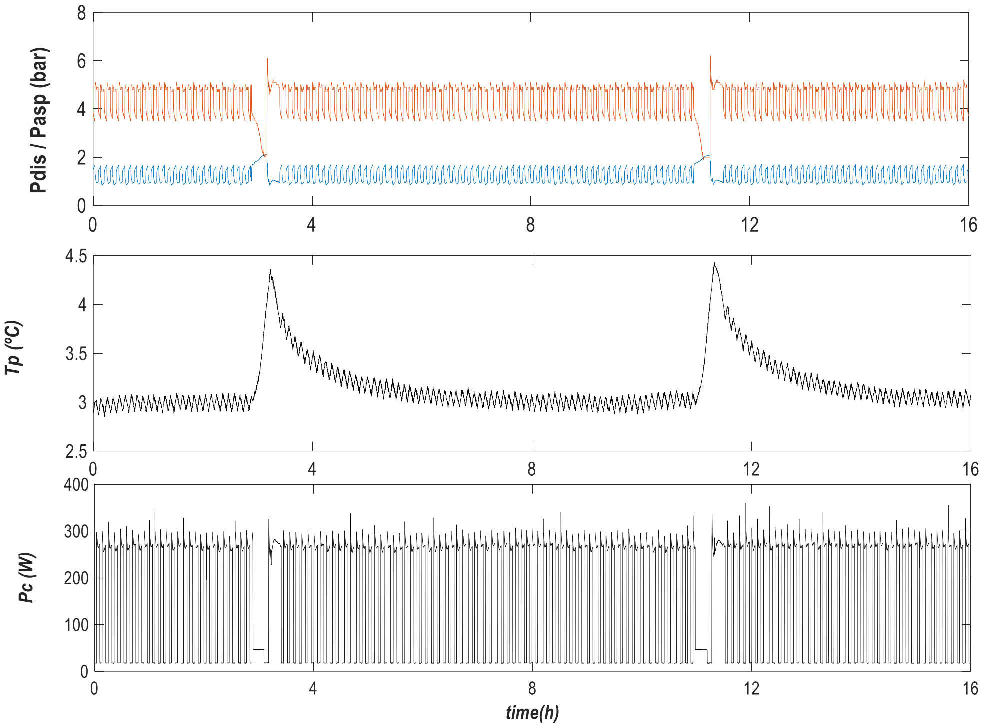

Figure 6.5. Evolution of power consumption (Pc), average product temperature (t_p), discharge pressure (p_{dis}) and aspiration pressure (p_{asp}) during 16 hours of the test R-600a with 115 g.

6.4 Experimental results

6.4.1 Mass charge optimization

For each refrigerant there is an optimum in the mass charge in which the energy consumption is lower. Each blend is subject to mass charge optimization process, as explained in the previous section. The energy consumption of the appliance for 16 hours is calculated with Eq.(6.15), in which $P_c(t)$ is the total power demanded by the experimental unit in the instant t. Each sample is taken every 5 seconds. Calculated energy consumption has an uncertainty below 0.5%.

$$E_i = \frac{1}{3600} \cdot \int_0^{16h} P_c(t) \cdot dt = \frac{1}{3600} \cdot \sum_{j=1}^{16h} \left\{ \left[\frac{P_c(j) + P_c(j-1)}{2} \right] \cdot [t(j) - t(j-1)] \right\} \qquad \text{Eq.(6.15)}$$

The energy consumption results obtained for each mixture during the optimization process can be seen in Figure 6.6. For the four refrigerants tested there is an optimum charge at which the energy consumption is minimum. From that charge, the energy consumption tends to stabilize and increase slightly respect the optimum. When charged with isobutane, at its optimum charge (115 g), the plant consumes 2.627 kW·h during 16 h. With the mixture R-1234ze(E) / R-600 (8/92)$\%_{\mathrm{mass}}$ at 159 g, the energy consumption of the experimental unit is reduced by -2.69%, consuming a total of 2.556 kW·h in the test period, whereas with the mixture R-152a/ R-600 (8/92)$\%_{\mathrm{mass}}$ at 165 g, the total energy consumption is 2.495 kW·h, a reduction of -5.04% with respect R-600a. As expected, the R-32/R-600 (2/98)$\%_{\mathrm{mass}}$ mixture does not provide a reduction on the energy consumption, consuming in practice the same energy as isobutane. Detailed parameters of the tests can be seen in Table 6.4.

These results verify the conclusions obtained in the theoretical section and even improve the improvement predicted for two of the three mixtures. In the following section, the thermodynamic properties of the refrigerants are analysed at the optimum operating conditions in order to try to explain the results obtained in Figure 6.6.

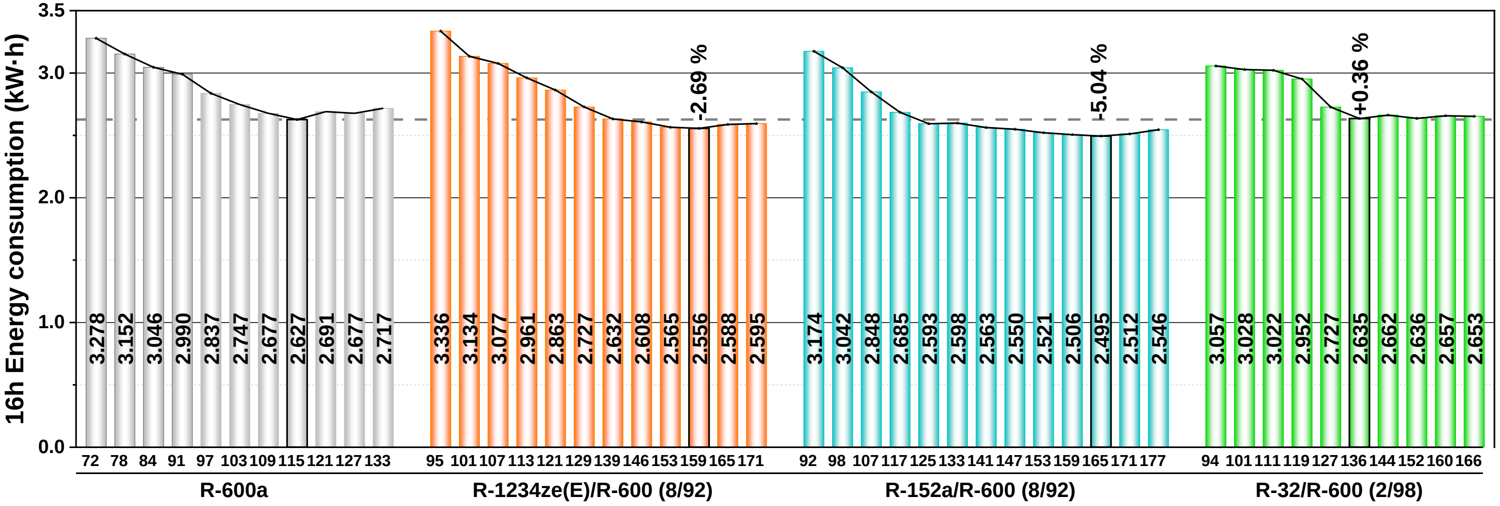

Figure 6.6. Energy consumption in 16 hours of the isobutane (R-600a) and the alternative mixtures.

6.4.2 Optimized configurations

This section aims to analyse the different operating parameters obtained with the experimental unit during the 16-h test. The results analysed here corresponds to the optimum charge of each refrigerant analysed.

Differentiated consumptions

The energy consumption shown in Figure 6.6. is the combination of all the energy consumed by the compressor (variable), the fan in the evaporator (28.8 W) and in the condenser (31.2 W) and the lights and electronics (17.7 W). Figure 6.7 shows the energy consumption during the 16-h test differentiated by the compressor and by the rest of elements (called "auxiliary power" in the figure). As explained priorly, electronics and lights were demanding a constant power nearly independently to other variables. When the compressor was ON, both fans were activated, while OFF, both were deactivated. During defrosting periods (programmed each 8 hours), only the evaporator fan switched on.

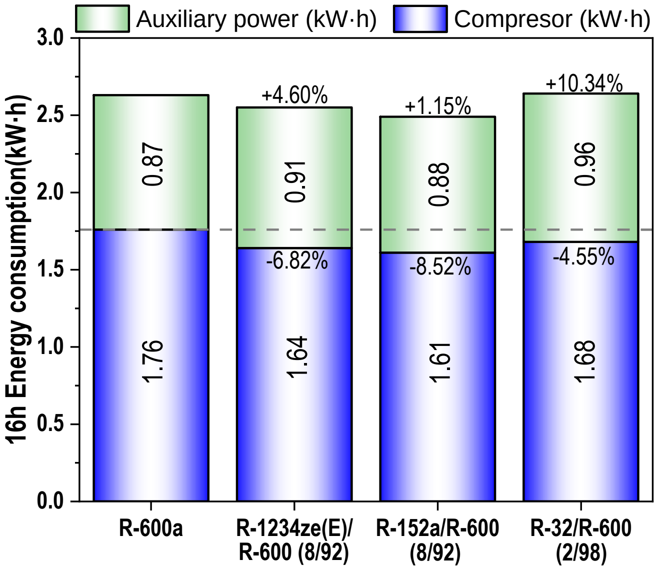

Figure 6.7. Energy consumption of each refrigerant differentiated by compressor and the rest.

It can be observed that for the three alternative mixtures the compressor consumption is lower than isobutane one and the energy reductions are even greater than the observer in Figure 6.6.. The reductions are 6.82% for R-1234ze(E)/R-600 (8/92), 8.52% for R-152a/R-600 (8/92) and 4.55% for R-32/R-600 (2/98). This indicates that, just considering the refrigeration cycle, the energetic behaviour is better than the isobutane one. However, the consumption by the auxiliary power is higher in all cases, which penalises the overall energy consumption of the plant. This fact can be directly explained through the duty cycle, in Figure 6.8.

Duty Cycle vs Power consumption

Figure 6.8 shows the comparison of the duty cycle and the average compressor power consumption when the compressor is ON. As expected, the alternative mixtures, principally due to their lower density, require a lower power input by the compressor. While R-600a require a 191.79 W, the other three mixture present a consumption of 170.55 W, 164.12 W and 156.42 W.

However, presenting a lower density has the drawback that, for a given volume, the circulating mass flow is lower, which has impact in the duty cycle. The duty cycles are 57.3% for isobutane, while for the alternative fluids are 59.12% for R-152a/R-600, 62.6% for R-1234ze(E)/R-600 and 67.09% for R-32/R-600. The duty cycle has a high impact on the overall energy consumption in this particular appliance and can be extrapolated to similar ones. As mentioned above, when the compressor is ON, also the fans are ON, adding 60W of extra power. Thus, for high operation times, the energy consumption by this “auxiliary” power is higher. This can be seen from the fact that refrigerants with lower duty cycles present lower auxiliary power consumption in Figure 6.7 and vice versa. This fact goes so far that, for the R-32/R-600 (2/98) mixture, even though the compressor presents a 4.55% reduction in energy consumption with respect to R-600a, the overall consumption for 16 h is even slightly higher.

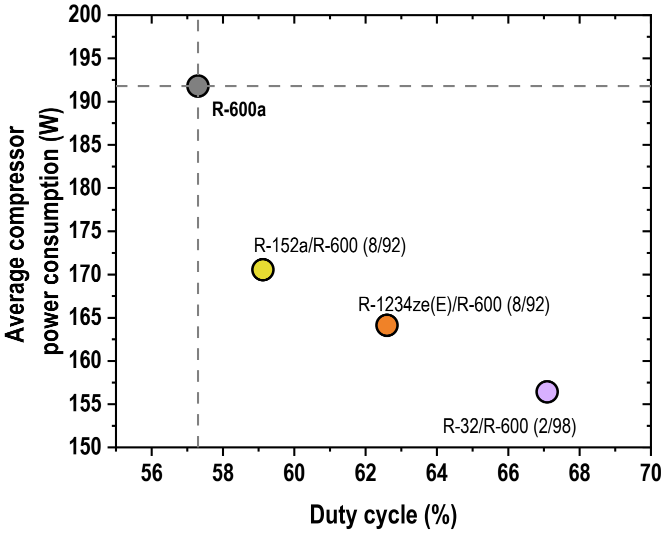

Figure 6.8. Average compressor power demand vs duty cycle.

Operation pressure and temperatures

The operation pressure at the optimum charges is represented in Figure 6.9. Two pressure gauges were installed in each pressure level, allowing the measure of the pressure drops. In the figure, each colour corresponds to a different refrigerant. The point at the right and at the top represents the p_{oin} (should be read at $\bar{p}_o$) and p_{dis} (should be read at $\bar{p}_k$), whereas the point at the left and bottom are p_{asp} and p_{exp} (same form of reading it). The lines connecting the dots correspond to the pressure drops.

All the fluids present similar pressure levels to isobutane, not implying any compatibility problem. Due to the big presence of butane (Normal Boiling Point of 0.5 ºC), all the alternative mixture present evaporation pressures slightly below 1 bar, being the mixture R-32/R-600 (2/98) the one with lower pressure levels in general. In relation with the pressure drops, isobutane has a pressure drop in the liquid line of 0.9 bar, while the alternative mixtures reduce this value significantly (values vary from 0.41 to 0.53 bar). Similar happens at the vapour line, presenting reductions on the pressure drops. This reduction in pressure drop is probably related to the lower mass flow rate of the mixtures, which is ultimately a consequence of their lower density.

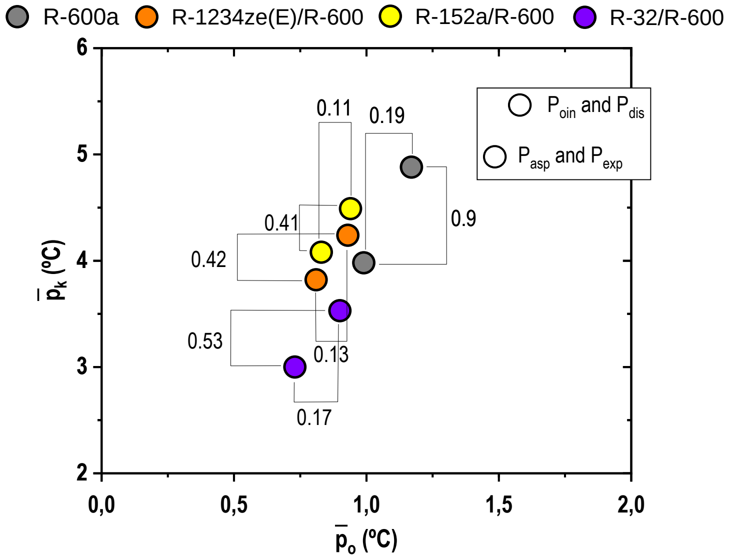

Figure 6.9. Representation of the operating pressures of each mixture. Two gauges were installed in each pressure line. The lines connecting the dots represent the pressure drops.

Phase change temperatures are calculated along the activation period of the compressor, according to Eq.(6.16) to Eq.(6.18). Evaporation temperature is calculated with the mean evaporation pressure and with the mean enthalpy between evaporator inlet and vapor saturated conditions. A similar procedure is used with condensation temperature.

$$\bar{t}_o = f\left[{(p_{o,in} + p_{asp})}/{2}, {(h_{o,in} + h_{sat,vap})}/{2} \right] \qquad \text{Eq.(6.16)}$$

$$h_{sat,sat} = f(p_{asp}, x = 1) \qquad \text{Eq.(6.17)}$$

$$\bar{t}_k = f\left[{(p_{des} + p_{exp})}/{2}, x_v = 0.5 \right] \qquad \text{Eq.(6.18)}$$

Figure 6.10 shows the results obtained with each refrigerant. Perpendicular blue line has a slope of 1:1, in such matter that the fluids at its right present a lower difference between temperatures than the reference and vice versa. R-152a/R-600 (8/92) and R-1234ze(E)/R-600 (8/92) present higher condensation temperature and lower evaporation temperature, probably due to fact that the optimum charge is higher what tends to elevate the pressure levels. However, both fluids are near the blue line, which shows that in practice the relation between both operation temperatures are similar to isobutane. However, the mixture R-32/R-600 present lower condensation and evaporation temperature.

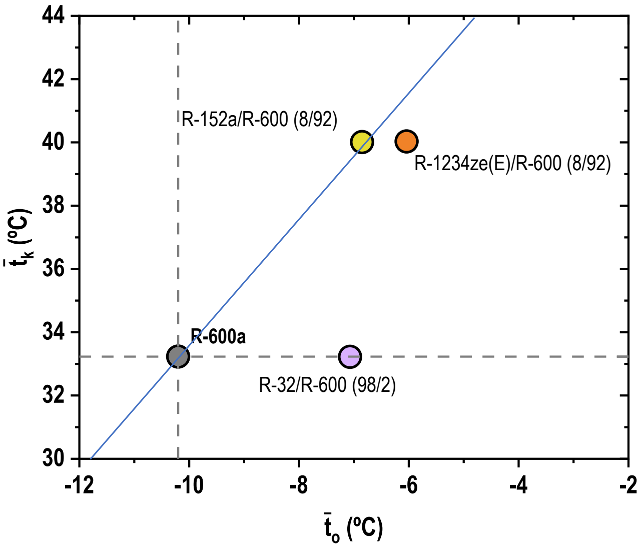

Figure 6.10. Operation temperatures of the refrigerants.

COP Estimation

The COP in an experimental compression vapour cycle is the ratio between the cooling capacity and the power demanded by the compressor for a given time. However, this unit does not count with a mass flow meter that allow to measure the mass flow rate and determine the cooling capacity, so an estimation of COP should be done. For this purpose, the hour before the second defrost period is chosen to be analysed, as it is long and stable enough to be representative.

COP estimation is performed according Eq.(6.19), in which E_o is the cooling energy to be supplied for one hour and E_{comp} is the compressor energy consumption for the same period. E_o can be divided into the thermal load that comes from the enclosures of the cabinet (E_{enc}) and from the fan of the evaporator ($E_{f,o}$) [Eq.(6.20)]. Assuming that E_{enc} is equal for all fluids [Eq.(6.21)] (the inner cabinet and climatic chamber temperatures are equal for all fluids), we can arrive at Eq.(6.22) and Eq.(6.23), in which the relation existing between the COP of a mixture and the isobutane depends on the relation of compressors power consumptions and the difference between the consumption of the fans. Eq.(6.23) can be develop into Eq.(6.24) in which the difference in fan power consumption is directly related to the difference in duty cycles (DC) ($P_{f,o}$refers to the power demanded by the fan).

$$COP = \frac{E_o}{E_{comp}} \qquad \text{Eq.(6.19)}$$

$$E_o = E_{f,o} + E_{enc} \qquad \text{Eq.(6.20)}$$

$$E_{enc}|_{R600a} = E_{enc}|_{MIX} \qquad \text{Eq.(6.21)}$$

$$COP_{R600a} \cdot E_{comp_{R600a}} - E_{f,o_{R600a}} = COP_{MIX} \cdot E_{comp_{MIX}} - E_{f,o_{MIX}} \qquad \text{Eq.(6.22)}$$

$$COP_{MIX} = COP_{R600a} \cdot \frac{E_{comp_{R600a}}}{E_{comp_{MIX}}} + \left(\frac{E_{f,o_{MIX}} - E_{f,o_{R600a}}}{E_{comp_{MIX}}}\right) \qquad \text{Eq.(6.23)}$$

$$COP_{MIX} = COP_{R600a} \cdot \frac{E_{comp_{R600a}}}{E_{comp_{MIX}}} + (DC_{MIX} - DC_{R600a}) \cdot time \cdot \frac{P_{f,o}}{E_{comp_{MIX}}} \qquad \text{Eq.(6.24)}$$

The results of the analysis can be seen in Table 6.3. Since having similar duty cycles, the term associated with the fans is negligible for the mixtures R-1234ze(E)/R-600 (8/92) and R-152a/R-600 (8/92), having relative COP increments of 11% and 13%

respectively. However, in the mixture R-32/R-600 (2/98) the last term is relevant, increasing a 0.0255 the ratio between two COPs, which is 1.05.

COP increments are consistent with the 16-h energy tests, the duty cycles and compressor power consumptions observed. The energy consumption is a trade-off between the COP and the required compressor operation time (duty cycle), resulting in the results in Figure 6.6. The mixtures R-1234ze(E)/R-600 (8/92) and R-152a/R-600 (8/92) have a duty cycle that exceed in 5.3% and 1.8% respect R-600a and 11% and 13% relative COP increments. Therefore, the expected energy consumption should be lower than the COP increments and closer to them when lower the duty cycle is, which is the case. However, the mixture R-32/R-600 (2/98) have a significant increment in the duty cycle (10% higher) and a lower COP increment than the other two mixtures (around 5%), thus penalizing its overall performance.

Compared with the theoretical analysis, COP results obtained experimentally are higher than the predicted theoretically. I any case, the results are coherent with the expected and help to contribute to the hypothesis that the high COP predicted with the mixture R-32/R-600 was not realistic and may be caused by errors in the interaction coefficients of Refprop.

It is important to mention that the results presented in this section are based on estimations. Results are therefore an approximation and should be interpreted as such. Other perspectives should be considered to obtain a more accurate value.

Table 6.3. Estimation of COP of the alternives mixtures.

	R-600a	R-1234ze(E)/R-600	R-152a/R-600	R-32/R-600
$P_{comp}\ (W \cdot h)$	112.66	101.07	99.31	107.62
$E_{f,o}\ (W \cdot h)$	17.11	17.59	16.75	19.86
$COP_{MIX} =$	---	$1.11 \cdot COP_{R600a} + 0.0047$	$1.13 \cdot COP_{R600a} - 0.0036$	$1.05 \cdot COP_{R600a} + 0.0255$

6.5 Conclusions

Previous works have demonstrated the existence of mixtures that, having similar thermodynamic properties, allow to decrease the energy consumption in relation to isobutane refrigeration systems. This paper addresses that possibility. The aim is the exploration of binary mixtures based on butane as principal component and a second refrigerant from a theoretical and experimental point of view.

To predict the possible mixtures with better energy performance, a theoretical model was launched. 11 pure refrigerants were considered as possible constituents of the mixture. All of them were combined to forms all the possible combinations (55 in total) and their mass composition was varied in steps if 1% (99 possibilities for each pair of refrigerants). In total 5445 different mixtures were analysed. The model simulated an ideal simple vapour compression cycle, operating at t_o = -10.2 ºC and t_k = 33.25 ºC, and a SH = 13.5 K and a SUB = 1.3 K. After some filters in terms of glide, t_{dis}, GWP and VCC, the mass composition for each combination of two refrigerants which maximizes COP is chosen. Mixtures R-1234ze(E)/R-600 (8/92), R-152a/R-600 (8/92) and R-32/R-600 (2/98) are chosen to be experimentally tested, as they offered theoretical COP increments of 1.54%, 2.78% and 8.52% respect isobutane.

Experimental tests were conducted in a stand-alone commercial cabinet used for the refrigeration of fresh beverage. The unit was equipped with an electronic expansion valve which was programmed to work specifically with each refrigerant according to its saturation lines. Tests were performed during 16 hours in a climatic chamber at 25 ºC and 60% RH. For each mixture, an optimization charge process was conducted.

The 16-hours tests showed that the cycle charge with isobutane presented an energy consumption of 2.627 kW·h at a charge of 115 g, while mixtures R-1234ze(E)/R-600 (8/92) accomplished a reduction of 2.69% at 159 g and R-152a/R-600 (8/92) of -5.04% at 165 g. The mixture R-32/R-600 (2/98) showed an increment of +0.36% at 136 g. Compressor consumption was reduced in all mixtures (-6.82%, -8.5% and -4.55% respectively), but duty cycles were higher (+5.3%, +1.82% and +9.79%, respectively). The pressures of the alternative mixtures were compatible with the application.

The COP of the fluids was compared by assuming that the thermal loads by the enclosures were equal for all the tests, showing that the mixture R-1234ze(E)/R-600 (8/92) had an increment of COP of +11%, R-152a/R-600 (8/92) of +13% and R-32/R-600 (2/98) of around +5%.

This paper proves the existence of alternative mixtures that can significantly reduce the power consumption of isobutane with similar thermodynamic properties.

6.6 Acknowledgments

Authors gratefully acknowledge for the economic support to this study to Jaume I University (grant PREDOC/2019/19), the European Union – “NextGenerationEU” (L. Nebot, Margarita Salas postdoctoral contract MGS/2022/15); and the Ministerio de Ciencia e Innovación of Spain (project PID2021-126926OB-C21 and TED2021-130162B-I00).

6.7 Author contribution statements

D.C developed idea and methods, realized experimental process and wrote the manuscript. R. Ll developed idea and methods and supervised the work. D.S developed idea and methods, realized experimental process and supervised the work. L. N. helped to develop the methods and made final proofreading. R.C. helped to get funds and helped in the experimental process.

6.8 Nomenclature

COP	Coefficient of performance
DC	Duty cycle
GHG	Greenhouse gases
GWP	Global warming potential (referred to 100 years)
IHX	Internal heat exchanger
NBP	Normal boiling point, ºC
RH	Relative humidity, %
VCC	Volumetric cooling capacity, kJ·m^{-3}
SH	Degree of superheat in evaporator, K
SUB	Degree of subcooling in condenser, K
E	Energy consumption, kW·h
h	Specific enthalpy, kJ·kg^{-1}
m	Mass, kg
p	Absolute pressure, bar
P_c	Total power consumption, W
s	Specific entropy, kJ·kg^{-1}·K^{-1}
t	Temperature, ºC
v	Specific volume, m^3· kg^{-1}
w	specific work, kJ· kg^{-1}
x_v	Vapour title

Subscripts

comp	refers to compression
dis	compressor discharge
e	effective
enc	related to enclosures
f	related to fans
in	inlet
iso	isenthalpic transformation
k	refers to condensing conditions
liq	liquid conditions
m	medium conditions
o	refers to evaporating conditions
out	outlet
sat	saturation conditions
suc	compressor suction
vap	vapour conditions

Greek symbols

ε	efficiency

6.9 References

[1] International Institute of Refrigeration, 38th Note on Refrigeration Technologies. The Role of Refrigeration in the Global Economy (2019). in, International Institute of Refrigeration, 2019, DOI: 10.18462/iif.NItec38.06.2019.

[2] European Commission, Regulation (EU) No 517/2014 of the European Parliament and of the Council of 16 April 2014 on fluorinated greenhouse gases and repealing Regulation (EC) No 842/2006., in: E. Commission (ed.), Official Journal of the European Union, 2014.

[3] UNEP, Refrigeration and air conditioning and heat pumps technical options committee. 2018 Assessment Report, in, United Nations Environment Programme, Kenya, 2018.

[4] A. Mota-Babiloni, J. Navarro-Esbrí, Á. Barragán, F. Molés, B. Peris, Drop-in energy performance evaluation of R1234yf and R1234ze(E) in a vapor compression system as R134a replacements, Applied Thermal Engineering, 71 (2014) 259-265 DOI: 10.1016/j.applthermaleng.2014.06.056.

[5] C. Aprea, A. Greco, A. Maiorino, An experimental investigation on the substitution of HFC134a with HFO1234YF in a domestic refrigerator, Applied Thermal Engineering, 106 (2016) 959-967 DOI: 10.1016/j.applthermaleng.2016.06.098.

[6] D. Sánchez, R. Cabello, R. Llopis, I. Arauzo, J. Catalán-Gil, E. Torrella, Energy performance evaluation of R1234yf, R1234ze(E), R600a, R290 and R152a as low-

GWP R134a alternatives, International Journal of Refrigeration, 74 (2017) 269-282 DOI: http://dx.doi.org/10.1016/j.ijrefrig.2016.09.020.

[7] A. Maiorino, C. Aprea, M.G. Del Duca, R. Llopis, D. Sánchez, R. Cabello, R-152a as an alternative refrigerant to R-134a in domestic refrigerators: An experimental analysis, International Journal of Refrigeration, 96 (2018) 106-116 DOI: https://doi.org/10.1016/j.ijrefrig.2018.09.020.

[8] D. Sánchez, A. Andreu-Nácher, D. Calleja-Anta, R. Llopis, R. Cabello, Energy impact evaluation of different low-GWP alternatives to replace R134a in a beverage cooler. Experimental analysis and optimization for the pure refrigerants R152a, R1234yf, R290, R1270, R600a and R744, Energy Conversion and Management, 256 (2022) DOI: 10.1016/j.enconman.2022.115388.

[9] R. Saravanakumar, V. Selladurai, Exergy analysis of a domestic refrigerator using eco-friendly R290/R600a refrigerant mixture as an alternative to R134a, Journal of Thermal Analysis and Calorimetry, 115 (2014) 933-940 DOI: 10.1007/s10973-013-3264-3.

[10] C.C. Yu, T.P. Teng, Retrofit assessment of refrigerator using hydrocarbon refrigerants, Applied Thermal Engineering, 66 (2014) 507-518 DOI: 10.1016/j.applthermaleng.2014.02.050.

[11] C. Aprea, A. Greco, A. Maiorino, An experimental investigation of the energetic performances of HFO1234yf and its binary mixtures with HFC134a in a household refrigerator, International Journal of Refrigeration, 76 (2017) 109-117 DOI: 10.1016/j.ijrefrig.2017.02.005.

[12] G.H.S. Oliveira, T.A. Moreira, Z.H. Ayub, G. Ribatski, Flow boiling of hydrocarbons and their zeotropic binary mixtures under pre- and post-dryout conditions, Applied Thermal Engineering, 198 (2021) DOI: 10.1016/j.applthermaleng.2021.117483.

[13] A.K. Solanki, R. Kumar, Two-phase flow condensation heat transfer characteristic of R-600a inside the horizontal smooth and dimpled helical coiled tube in shell type heat exchanger, International Journal of Refrigeration, 107 (2019) 155-164 DOI: 10.1016/j.ijrefrig.2019.07.017.

[14] D. Calleja-Anta, L. Nebot-Andres, J. Catalan-Gil, D. Sánchez, R. Cabello, R. Llopis, Thermodynamic screening of alternative refrigerants for R290 and R600a, Results in Engineering, 5 (2020) DOI: 10.1016/j.rineng.2019.100081.

[15] D. Calleja-Anta, L. Nebot-Andres, D. Sánchez, R. Cabello, R. Llopis, Drop-in substitutes for R-600a. Experimental evaluation and optimization of a commercial fridge, Applied Thermal Engineering, 211 (2022) DOI: 10.1016/j.applthermaleng.2022.118490.

[16] D. Calleja-Anta, L. Nebot-Andres, R. Cabello, D. Sánchez, R. Llopis, A3 and A2 refrigerants: Border determination and hunt for A2 low-GWP blends, International Journal of Refrigeration, 134 (2022) 86-94 DOI: 10.1016/j.ijrefrig.2021.11.012.

[17] Author, NIST Standard Reference Database 23: Reference Fluid Thermodynamic and Transport Properties-REFPROP, Version 10.0, National Institute of Standards and Technology, 2018 DOI: dx.doi.org/10.18434/T4JS3C.

[18] IPCC, Climate Change 2013: The Physical Science Basis. Contribution of Working Group I to the Fifth Assessment Report of the Intergovernmental Panel on Climate

Change [Stocker, T.F., D. Qin, G.-K. Plattner, M. Tignor, S.K. Allen, J. Boschung, A. Nauels, Y. Xia, V. Bex and P.M. Midgley (eds.)], in, Cambridge University Press, Cambridge, United Kingdom and New York, NY, USA, 1535 pp., 2013.

[19] I. 23953-2:2015, ISO 23953-2:2015 Refrigerated display cabinets - Part 2. Classification, requirements and test conditions, in, 2015.

TABLES

Table 6.4. Reference, operation and energy parameters of the refrigerants evaluated.

	Reference parameters				Operating parameters		Duty cycle	Fractioned energy parameters		Total energy parameters		
Charge (g)	t_P (ºC)	$\pm\sigma_{t,P}$ (K)	t_{cam} (ºC)	$\pm\sigma_{t,cam}$ (K)	$t_{K,on}$ (ºC)	$t_{O,ON}$ (ºC)	(%)	$E_{compressor,16h}$ (kWh)	$E_{aux,16h}$ (kWh)	P_{C_ON} (W)	E_{16h} (kWh)	$(E-E_{ref})/E_{ref}\,100$ (%)
R-600a												
72	3.15	0.25	24.79	0.08	31.68	-11.24	77.61	2.23	1.05	257.36	3.28	n.c.
78	3.06	0.29	24.76	0.08	32.25	-9.84	72.49	2.15	1.00	263.28	3.15	n.c.
84	3.11	0.21	24.77	0.06	32.74	-8.21	67.98	2.08	0.96	269.41	3.05	n.c.
91	3.09	0.26	24.74	0.08	33.03	-7.78	65.62	2.05	0.94	272.55	2.99	n.c.
97	3.16	0.27	24.72	0.08	33.22	-7.83	61.37	1.93	0.90	274.55	2.84	n.c.
103	3.12	0.25	24.76	0.10	33.21	-7.91	59.25	1.86	0.89	274.16	2.75	n.c.
109	3.14	0.27	24.79	0.10	33.23	-8.05	57.55	1.80	0.87	273.90	2.68	n.c.
115	**3.16**	**0.28**	**24.81**	**0.08**	**33.23**	**-10.20**	**57.30**	**1.76**	**0.87**	**269.42**	**2.63**	**n.c.**
121	3.10	0.29	24.88	0.10	33.09	-8.93	58.60	1.81	0.88	270.63	2.69	n.c.
127	3.13	0.29	24.70	0.05	33.72	-8.93	57.82	1.80	0.87	272.60	2.68	n.c.
133	3.15	0.27	24.75	0.06	33.79	-9.01	58.71	1.84	0.88	273.21	2.72	n.c.
R-1234ze(E) /600 (8/92)												
95	3.31	0.36	24.94	0.09	38.36	-6.26	86.11	2.21	1.13	237.97	3.34	26.99
101	3.16	0.32	25.20	0.08	38.09	-6.82	82.23	2.04	1.09	232.98	3.13	19.31
107	3.25	0.31	25.09	0.08	38.26	-6.91	78.96	2.01	1.06	237.08	3.08	17.13

113	3.15	0.32	25.07	0.09	38.37	-6.95	76.15	1.92	1.04	235.60	2.96	12.71
121	3.12	0.33	25.11	0.07	38.46	-6.89	72.86	1.86	1.01	237.00	2.86	8.99
129	3.17	0.30	25.10	0.06	38.79	-6.20	67.69	1.77	0.96	240.89	2.73	3.83
139	3.13	0.30	25.08	0.06	39.01	-5.42	64.40	1.70	0.93	242.87	2.63	0.18
146	3.11	0.29	24.96	0.06	38.94	-5.10	63.87	1.68	0.93	242.31	2.61	-0.73
153	3.19	0.29	24.93	0.06	38.99	-4.99	63.25	1.65	0.92	240.43	2.57	-2.35
159	**3.14**	**0.30**	**24.93**	**0.08**	**40.03**	**-6.04**	**62.60**	**1.64**	**0.91**	**241.75**	**2.56**	**-2.69**
165	3.16	0.29	25.16	0.08	41.26	-4.69	62.15	1.68	0.91	246.29	2.59	-1.49
171	3.08	0.30	25.09	0.08	42.26	-4.66	62.07	1.68	0.91	247.19	2.59	-1.22
R-152a /600 (8/92)												
92	3.28	0.33	25.14	0.08	36.57	-7.89	80.64	2.10	1.08	240.11	3.17	20.84
98	3.15	0.29	25.18	0.08	36.66	-8.24	77.11	2.00	1.04	239.55	3.04	15.80
107	3.14	0.30	25.02	0.10	36.64	-8.00	71.26	1.85	1.00	237.89	2.85	8.42
117	3.25	0.27	25.00	0.08	36.87	-7.01	65.93	1.74	0.94	242.69	2.68	2.21
125	3.10	0.28	25.00	0.08	37.18	-6.33	62.98	1.68	0.92	244.16	2.59	-1.28
133	3.07	0.27	24.98	0.08	37.22	-6.11	62.58	1.68	0.91	245.91	2.60	-1.09
141	3.18	0.28	24.95	0.08	37.25	-5.92	61.61	1.66	0.90	245.88	2.56	-2.44
147	3.13	0.27	24.98	0.08	37.19	-6.05	61.99	1.64	0.91	243.22	2.55	-2.94
153	3.14	0.28	25.53	0.29	37.30	-6.30	61.02	1.62	0.90	244.00	2.52	-4.02
159	3.12	0.27	25.54	0.20	38.49	-6.03	59.82	1.62	0.89	246.72	2.51	-4.60
165	**3.07**	**0.27**	**24.92**	**0.14**	**40.01**	**-6.85**	**59.12**	**1.61**	**0.88**	**248.18**	**2.49**	**-5.04**
171	3.09	0.26	25.23	0.26	39.91	-5.78	59.44	1.63	0.89	248.63	2.51	-4.38
177	3.11	0.27	24.98	0.08	40.92	-5.54	59.78	1.66	0.89	250.94	2.55	-3.10

R-32 /600 (2/98)													
94	3.09	0.24	24.62	0.20	32.69	- 6.36	79.57	1.99	1.06	234.25	3.06	16.36
101	3.09	0.25	24.61	0.17	32.70	-6.83	77.92	1.98	1.05	236.37	3.03	15.27
111	3.09	0.26	25.17	0.15	32.59	-7.19	76.63	1.98	1.04	239.31	3.02	15.05
119	3.15	0.24	24.96	0.26	32.83	-7.16	74.46	1.93	1.02	239.72	2.95	12.37
127	3.12	0.29	24.75	0.10	32.77	-7.11	70.61	1.74	0.99	231.87	2.73	3.82
136	**3.07**	**0.33**	**24.44**	**0.05**	**33.22**	**-7.07**	**67.09**	**1.68**	**0.96**	**234.05**	**2.63**	**0.29**
144	3.10	0.33	24.90	0.12	33.61	-6.86	67.78	1.70	0.96	234.50	2.66	1.34
152	3.12	0.36	25.00	0.15	34.16	-8.03	67.65	1.68	0.96	232.63	2.64	0.36
160	3.06	0.34	24.94	0.16	34.13	-6.71	67.28	1.70	0.96	235.46	2.66	1.15
166	3.09	0.35	24.96	0.13	35.68	-6.51	66.45	1.70	0.95	237.77	2.65	0.98

Notes about the table:

- n.c. stands for “not considered”

CHAPTER 7.

OPTIMIZING R152a/R600 AND R290/R600 MIXTURES FOR SUPERIOR ENERGY PERFORMANCE IN VAPOR COMPRESSION SYSTEMS: PROMISING ALTERNATIVES TO ISOBUTANE (R600a).

Chapter adapted from the paper:

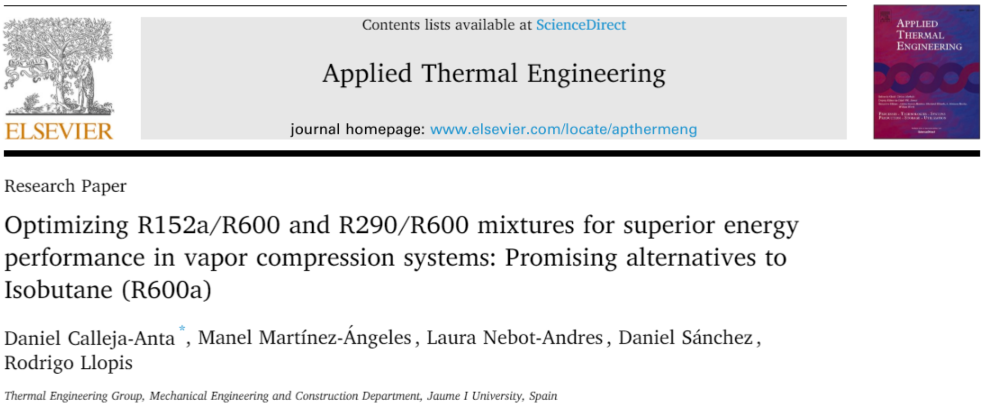

Contents lists available at ScienceDirect

Applied Thermal Engineering

journal homepage: www.elsevier.com/locate/apthermeng

Research Paper

Optimizing R152a/R600 and R290/R600 mixtures for superior energy performance in vapor compression systems: Promising alternatives to Isobutane (R600a)

Daniel Calleja-Anta [*], Manel Martínez-Ángeles, Laura Nebot-Andres, Daniel Sánchez, Rodrigo Llopis

Thermal Engineering Group, Mechanical Engineering and Construction Department, Jaume I University, Spain

Calleja-Anta, D., Martínez-Angeles, M., Nebot-Andrés, L., Sánchez, D., Llopis, R., Optimizing R152a/R600 and R290/R600 Mixtures for Superior Energy Performance in Vapor Compression Systems: Promising Alternatives to Isobutane (R600a) (2023), Applied Thermal Engineering, art. no. 247, 123070, DOI: 10.1016/j.applthermaleng.2024.123070

Journal Impact Factor QUARTILE: Q1 (2022 quartile).

Cited 0 times.

7 Optimizing R152a/R600 and R290/R600 Mixtures for Superior Energy Performance in Vapor Compression Systems: Promising Alternatives to Isobutane (R600a)

Daniel Calleja-Anta[1,*], Manel Martínez-Ángeles[1], Laura Nebot-Andres[1], Daniel Sánchez[1], Rodrigo Llopis[1]

[1]Thermal Engineering Group, Mechanical Engineering and Construction Department, Jaume I University, Spain

Abstract

This study presents an experimental investigation into the optimal composition of R152a/R600 and R290/R600 mixtures as potential alternatives to isobutane (R600a) in a single-stage vapor compression cycle. The research involved testing eight different mass compositions for R152a/R600 and ten mass compositions for R290/R600, comparing their performance with that of R600a. After careful analysis, the "optimum" mass compositions were identified as (10/90)% for both R152a/R600 and R290/R600, achieving a balanced trade-off among coefficient of performance (COP), volumetric cooling capacity (VCC), and cooling output ($\dot{Q}_o$). Further tests were conducted on the "optimum" compositions at nine different secondary fluid temperature inlets. The results indicated an average COP increase of +7.3% for the R152a/R600 mixture, with decreases of -11.4% in VCC and -9.7% in $\dot{Q}_o$. Similarly, the R290/R600 (10/90)% mixture showed a COP increase of +10.3%, accompanied by VCC and $\dot{Q}_o$ decreases of -8.8% and -6.6%, respectively. Notably, both mixtures exhibited superior energy performance compared to isobutane while maintaining similar thermodynamic properties, particularly the R290/R600 (10/90)% mixture. These findings suggest that the R152a/R600 and R290/R600 mixtures could serve as long-term, high-efficiency alternatives to R600a in vapor compression cycles.

Keywords

Domestic refrigeration; R600a alternatives; R152a/R600; R290/R600; Refrigerant mixtures; Energy efficiency

7.1 Introduction

In the realm of low cooling capacity refrigeration applications, it is possible to distinguish between two subsectors: the domestic subsector, primarily consisting of refrigerators and freezers, and the commercial subsector formed by sealed equipment. Both of these subsectors were significantly impacted by the implementation of European Regulation No. 517/2014 [1], which imposed restrictions on the use of refrigerants with a maximum GWP of 150, being effective from the beginning of 2015 for the domestic sector and from the start of 2022 for the commercial one.

While it might appear that the low cooling capacity refrigeration sector does not require extensive research efforts to enhance its efficiency due to its low unitary energy consumption, it is essential to note that, according to the UNEP [2], the domestic subsector alone sees an annual production of around 170 million refrigerators and freezers. In 2018, the total number of units in use within this subsector ranged between 2 billion and 2.3 billion, collectively consuming approximately 4% of the world's electric energy.

Since the early 2000s, there has been a notable adoption of R-600a (isobutane) as the predominant refrigerant in the low-power refrigeration sector in Europe, and this trend has been steadily growing in other regions of the world as well. In 2018, it was estimated that out of the 170 million units produced annually, approximately 100 million were already being manufactured with isobutane [2]. Considering the upward trajectory observed until that year and the regulatory updates that have made the use of flammable refrigerants more flexible (such as the IEC 60335-2-89: 2019, which increased the flammable refrigerant charge in commercial equipment from 150 g to 500 g for A3 refrigerants and to 1200 g to A2 and A2L [3]) it is highly likely that this percentage has increased significantly in recent years.

R-600a replaced R-134a in these applications mainly due to the efforts to combat climate change. According to the 6th IPCC Assessment Report [4], R-134a has a Global Warming Potential (GWP) of 1530, whereas R-600a's GWP is nearly negligible (3). In addition to the reduction of emissions of direct origin, the indirect reduction must also be taken into account, since it is estimated that the energy reductions provided by isobutane with respect to R-134a are 5%, according to different authors and in different applications. For instance, Rasti, et al. [5] conducted tests using a domestic refrigerator and found that energy savings with R-600a compared to R-134a were 7% with the original compressor and reached 18.7% when using a compressor designed specifically for isobutane. In a separate study, Sánchez, et al. [6] conducted 16-hour tests comparing several pure refrigerants as substitutes for R-134a, using specific compressors with the displacement adjusted for each of them in a beverage cooler, where isobutane showed an energy reduction of 1.2%.

In addition to reducing environmental impact, isobutane offers several advantages over other refrigerants. One notable advantage is the lower operating pressure of isobutane compared to most commercial refrigerants. The pressure levels at which it works are lower than most commercial refrigerants, which helps to create exchangers that require less robustness and therefore are significantly cheaper than refrigerants operating at higher pressures [7]. Another positive side effect related to the pressures is the reduction of noise, which in domestic installations is an important parameter; and the reduction of peak electrical power required at the beginning of the compression process, lower requirement of installed power and fewer electrical windings in the compressor [8]. These combined benefits make isobutane an attractive choice in various refrigeration applications.

However, previous to the adoption of the isobutane, several refrigerants were evaluated as potential alternatives. These candidates, however, often had drawbacks or failed to match the advantages offered by R-600a. For instance, R-1234yf and R-1234ze(E) boast an A2L flammability classification [9], but they are synthetic refrigerants with higher operating pressures compared to isobutane. Moreover, certain studies have reported energy performance that is similar to or even worse than R-134a when using these alternatives. Aprea, et al. [10] addressed the possibility to do a R-600a drop-in replacement with the R-1234yf, obtaining higher condensation pressures, increment of the cooling capacity and 3% of energy savings. Similarly, in a complementary study conducted with other domestic appliance, Aprea, et al. [11] demonstrated energy reductions when using the R-1234ze(E) respect to R-134a of 9%. Sánchez, et al. [8] also studied these two refrigerants in a single-stage vapor compression plant reporting COP reductions between 8.3% and 11% for R-1234yf and between 2.8% and 13% for R-1234ze(E). These reductions were accompanied by cooling capacity decreases of 4.5% to 8.6% for R-1234yf and 23.1% to 26.6% for R-1234ze(E). R-152a (also a synthetic refrigerant) has also been examined as a potential alternative for domestic refrigeration. Bolaji [12] conducted an investigation into its use in a domestic refrigerator, where they observed COP increases of 4.7% and energy consumption reductions of 4%. Similarly, Maiorino, et al. [13], using a similar experimental system, demonstrated energy reductions of up to 7.4% and an 8% decrease in the time required for pull-down in a commercial refrigerator.

Refrigerant blends have also been the subject of study and debate. In the study mentioned earlier by Rasti, et al. [5], the R-436A mixture (46% R-600a and 54% propane) was examined, resulting in energy reductions of up to 8%, lower than those achieved with isobutane. In a different study, Mohanraj, et al. [14] tested a mixture consisting of 45.2% R-290 and 54.8% R-600a in a domestic refrigerator, achieving energy reductions of 3.6% compared to isobutane, being a potential alternative.

Isobutane has emerged as the standard choice among alternatives due to its numerous advantages. However, there is a potential possibility for improving its energy characteristics while retaining its benefits at the same time by developing refrigerant blends with thermodynamic properties similar to R-600a.

This research direction was initially explored by Calleja-Anta, et al. [15], through a thermodynamic screening process. 55440 possible ternary mixtures were theoretically analysed to identify those with higher COP than isobutane, similar Volumetric Cooling Capacity (VCC), discharge temperatures, effective evaporator glide below 10 K, and a GWP lower than 150. The study revealed several promising binary mixtures primarily composed of butane (R-600) and a secondary refrigerant. These mixtures were supposed to offer COP increases ranging from 8.6% to 1.7%, with VCC reductions between 28.4% and 8.2%. The most favourable mixtures featured the refrigerant pairs R-1270/R-600, R-152a/R-600, R-1234zeE/R-600, and R-290/R-600, with varying compositions depending on boundary conditions, but generally consisting of around 90% butane by mass proportion.

Building on this foundation, subsequent research in 2022 [16] involved drop-in tests of some previously identified mixtures in a domestic refrigerator over a 24-hour period to verify energy savings. At optimized charges, the mixture R-1234yf/R-600a (7.5/92.5)% achieved an energy reduction of 2.15% compared to R-600a, R-1234ze(E)/R-600 (10.5/89.5)% achieved a reduction of 3.84%, and R-290/R-600 (11/89)% exhibited a reduction of 1.31%, all while maintaining similar or even lower operating pressures and with similar duty cycles.

The potential for enhancing the energy performance of isobutane through mixtures was further explored in a recent study by Calleja-Anta, et al. [17]. Experimental tests were conducted in a stand-alone commercial refrigeration cabinet over 16 hours, with the capability to adapt its operation to the tested refrigerants. Two of the tested mixtures, R-1234ze(E)/R-600 (8/92)% and R-152a/R-600 (8/92)%, achieved energy reductions of 2.69% and 5.04%, respectively, compared to R-600a.

Nonetheless, these previous studies had certain limitations. The mass compositions were optimized based on simplified theoretical models, which allowed for predictions regarding the behaviour of a large number of mixtures. However, these models did not account for critical factors such as heat transfer and compressor performance.

Furthermore, the experimental setups used did not facilitate a comprehensive thermodynamic analysis of the mixtures.

The objective of the present work is to perform an experimental optimization of the composition of the mixtures R-152a/R-600 and R-290/R-600, two of the mixtures that have shown a better energetic performance in the previous studies. To achieve this, experiments using varying composition proportions of these two mixtures have conducted within a single-stage vapor compression bench. This experimental setup was developed and fully monitored, allowing to measure key parameters including COP, VCC and $\dot{Q}_o$. The objective is to identify the "optimum" composition that achieves the most favorable balance among these three parameters.

It is important to note that the goal here is not to find a mixture that can directly replace isobutane (drop-in) but rather to identify a mixture that can enhance the overall energy performance of R-600a while preserving the advantages previously described. This research also features a novel heat exchanger design to facilitate the measurement of the refrigerant's internal evolution during the phase-change process.

7.2 Methods and materials

This section describes the thermodynamic properties of the considered refrigerants, the experimental plant used to perform the tests, the measurement system and the methodology followed.

7.2.1 Fluids and mixtures

Table 7.1 presents the properties of the four refrigerants considered in this study. Notably, the only refrigerant that exceeds the limit of GWP of 150 is R-152a, but it will be used in proportions whose resulting GWP will be below this threshold. Comparing butane and isobutane, butane exhibits a higher Normal Boiling Point (NBP), critical temperature (t_{crit}), and critical pressure (P_{crit}) than isobutane. The increased NBP correlates with a lower evaporation pressure required to achieve a similar evaporation temperature. Furthermore, butane demonstrates a significantly higher latent heat of phase change (+10.88% at 40°C and +7.74%) and suction specific volume (+57.83%) in comparison to isobutane. On the other hand, both R-152a and R-290, which will be combined with R-600 to form the mixtures, exhibit lower NBPs, t_{crit}, and P_{crit} than isobutane. Specifically, R-152a has a lower latent heat of phase change compared to the base refrigerant (-16.57% at -40°C and -12.79% at -10°C), while R-290 shows a similar latent heat at -40°C (-1.41%) and a higher latent heat at -10°C (+6.82%). The properties of the resulting mixtures, formed by mixing butane with R-152a and R-290, are expected to fall within the range of properties exhibited by each individual refrigerant, depending on the proportion of each fluid in the mixture.

Table 7.1. Physical and environmental characteristics of the 4 refrigerants involved in this work (obtained with Refprop 10 [18]).

	R-600a	R-600	R-152a	R-290
M (g·mol-1)	58.1	58.1	66.1	44.1
NBP (ºC)	-11.8	-0.5	-24.0	-42.1
t_{crit} (ºC)	134.7	152	113.3	96.7
p_{crit} (ºC)	36.2	37.9	45.2	42.5
λ at t = 40 °C (kJ·kg^{-1})	311.5	345.4	259.9	307.1
λ at t = -10 °C (kJ·kg^{-1})	363.5	394.0	317.0	388.3
v_{suc} at t =-10 ºC & x_v = 1 (m^3·kg-1)	0.332	0.524	0.171	0.131
GWP$_{100\text{-years}}$ [4]	3	3	164	3

7.2.2 Description of the experimental plant and measurement system

The test bench where the experimental tests are performed is represented through its refrigeration diagram in Figure 7.1. It is a single-stage vapor compression cycle, using a variable speed hermetic reciprocating compressor, a condenser, a liquid vessel of 1.2 L that could be bypassed if needed, an expansion valve (whose driver can be configurable to work accordingly with each mixture) and an evaporator. Table 7.2 shows the characteristics of the main elements.

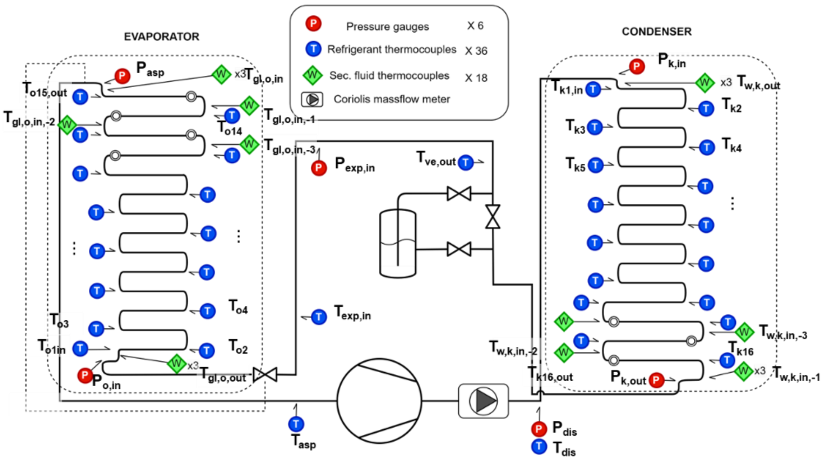

Figure 7.1. Diagram of the plant with the position of the sensors installed and their names.

Table 7.2. Characteristics of the main elements of the refrigeration circuit.

Element	Characteristics
Compressor	R600a Variable speed hermetic reciprocating compressor Displacement: 11.14 cm^3, 1/4 horsepower, LBP. Speed can be adjustable from 1300 RPM to 4500 RPM. Model: EMBRACO VES D11C.
Condenser	Tube-in-tube heat exchanger, self-made. Countercurrent flow. 16 steps per 23.5 cm pipe. Outer tube intended for water flow. Ø_i = 16 mm. Inner tube intended for refrigerant flow. Ø = ¼”. Thickness= 0.8 mm. Total heat exchange area = 750 cm^2
Electronic valve	Used as thermostatic expansion valve. Driver configurable to each refrigerant mixture with bubble and dew temperatures.
Evaporator	Tube-in-tube heat exchanger, self-made. Countercurrent flow. 14 steps per 23.5 cm pipe. Outer tube intended for water flow. Ø_i= 16 mm. Inner tube intended for refrigerant flow. Ø = 3/8”. Thickness= 0.8 mm. Total heat exchange area = 984.5 cm^2

The compressor chosen is a variable speed hermetic reciprocating one, with the characteristics shown in Table 7.2. We control the compressor speed using a wave generator instead of the manufacturer driver.

The geometry of the evaporator and condenser is based on a tube-in-tube configuration, as can be seen in Figure 7.2. The secondary fluid flows through the outer tube while the refrigerant through the inner one, counter current. The heat exchangers (HX) are made with a system of elbows and “T” in which the refrigerant tube passes through the secondary fluid tube different times, with a length of 23.5 cm each step. The condenser has 16 refrigerant-water pitches, while the evaporator has 14. At each pass the inner and outer tube were ensured to be concentric, as shown in Figure 7.2, right.

The selection of this particular geometry for the heat exchangers was motivated by the desire to establish a configuration that is both simple and readily accessible, in which the total heat exchange area was easy to be measured and were able the integration of sensors at various key locations, as explained in the following paragraphs.

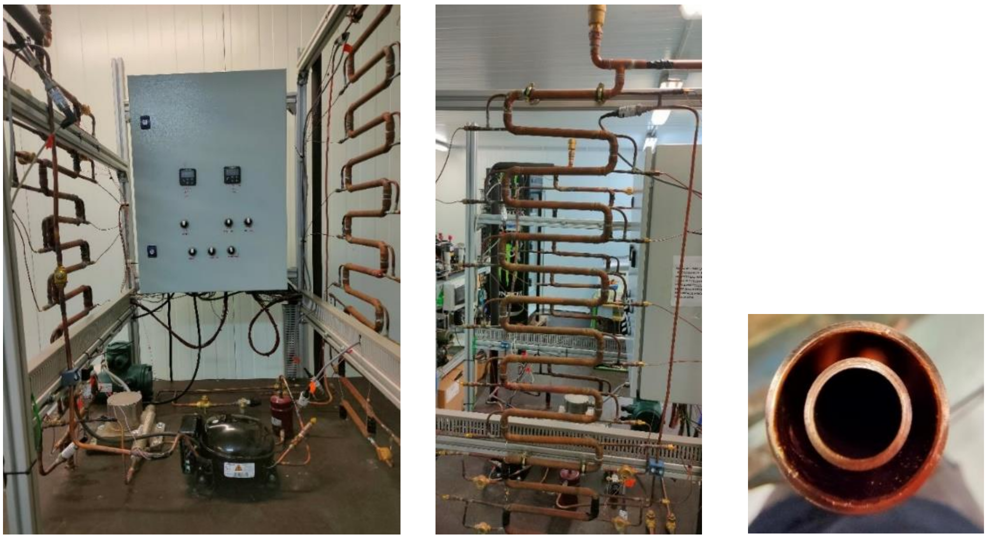

Figure 7.2. Different pictures of the test bench before the application of heat insulation. From left to right: a general picture of the machine, followed by a focused view of the condenser, and finally, the cross section of the evaporator.

To absorb the heat power generated by the condenser and provide thermal load to the evaporator, two auxiliary thermal systems (ATS) were installed. They consist of a loop with circulating secondary fluid, in which its inlet temperature is controlled by a PID controller. Distilled water was used for the condenser loop while a mixture of propylene glycol and water (50/50%$_v$) was used for the evaporator one.

In order to capture the various thermodynamic states experienced by the refrigerant throughout the cycle, the plant was instrumented with different sensors all along the installation, whose location is shown in Figure 7.1. 6 pressure gauges (P) were installed [3 high-pressure (1-30 bar), 1 medium-pressure (0-16 bar) and 2 low-pressure (0-9 bar)]. 36 T-type thermocouples (T) were installed to measure the refrigerant temperatures. 32 of the refrigerant thermocouples were aimed to measure the evolution of the refrigerant temperatures through the two heat exchangers, placed as immersion thermocouples at the outlet of each step of 23.5 cm of pipe in which there is heat exchange between the refrigerant and the secondary fluid (see Figure 7.2, center). In that way, 16 thermocouples were installed at the condenser and 15 in the evaporator. 4 additional surface thermocouples were placed in different points of the cycle (suction, discharge, liquid vessel outlet and expansion valve inlet). The uncertainty of the T-thermocouple is of ±0.5 K and of the pressure gauges is of ±1% of the full measuring range. A Coriolis mass-flow meter was installed at the compressor outlet with an accuracy of ± 0.15% of the measurement. To measure the electric power demanded, a digital wattmeter was used with an uncertainty of ± 0.5% of measurement.

The loops with secondary fluids were also equipped with 18 surface T-type thermocouples (W) to measure the evolution of the fluid temperature at different points (9 in each HX, with 3 thermocouples at the inlet, 3 at the outlet and 3 more at the indicated points). One mass-flow meter was installed at the evaporator loop and one volumetric-flow meter at the condenser one, with uncertainties of ± 0.55% and ± 2.1% respectively.

The plant was conveniently thermally insulated and placed in a climatic chamber with control of the temperature.

7.2.3 Experimental procedure

One of the objectives of this study is to determine experimentally the "optimum" composition of the binary mixtures R-152/R-600 and R-290/R-600 which can be used as R-600a alternatives. To achieve this objective, the mixtures were evaluated in a bench test at varying compositions in order to identify the composition that provides the best balance between the COP, VCC and the $\dot{Q}_o$ relative to isobutane.

The "optimum" composition was selected in base of a commitment between COP, VCC $\dot{Q}_o$ in comparison to R-600a, as in the following sections will be seen.

To obtain the "optimum" composition of each mixture, different compositions were tried, starting from 97.5% in mass basis of R-600 and 2.5% of the other refrigerant. The composition of the second refrigerant was incremented in steps of 2.5% until one "optimum" was reached. Also, tests were conducted with pure butane (R-600) as well as with R-600a, which will be used as the reference. Between each composition tested, a complete vacuum of the refrigeration plant was done and then the plant was charged accordingly with each composition. Firstly, the plant was charged directly from the R-600 bottle (as it is the fluid with less NBP and since with less pressure) and later with the correspondent charge of the second fluid. The plant was tested with the liquid vessel open to avoid that different refrigerant charges could affect in the overall operation of the plant, fluctuating all refrigerant charges between 141 g and 160 g. A weight scale with a ± 0.5 g of uncertainty was used and all the fluids used were certified with 99.5% of purity. For each composition, the electronic expansion valve of the evaporator was adapted to work with each mixture, configuring the controller according to the bubble and dew temperatures of each mixture (evaluated with REFPROP). This optimization process was repeated twice, being the average parameters of each compositions the one used to analyze.

The optimization process was conducted maintaining the same inlet secondary fluid temperatures and secondary fluid mass flows for all the tests. The water loop intended for condenser was set at an inlet temperature of 30 ºC ± 0.8 ºC and a mass flow of 90 kg·h^{-1} ± 0.42 kg·h^{-1}, while the inlet conditions for the loop dedicated for the evaporator was 0 ºC ± 0.06 ºC and 80 kg·h^{-1} ± 0.85 kg·h^{-1}.

Once the “optimum” composition was chosen, the plant was again subjected to another vacuum and recharge with the selected proportions to analyse their performance under different inlet secondary fluid temperatures. Three inlet loop condenser temperatures (25 ºC, 30 ºC and 35 ºC) and three different inlet loop evaporator temperatures (-5 ºC, 0 ºC and 5 ºC) were tested, resulting in a total of 9 tests. R-600a was also tested under these conditions as reference. During this process, the rest of parameters were maintained as in the optimization process.

All the experimental tests described were performed with a useful superheating of expansion valve set at 8 K and with the compressor speed set at 4500 RPM. The selected period to be tested was 8 minutes, once steady-state conditions were clearly reached. To maintain constant the energy losses with the environment, the experimental unit was placed inside a climatic chamber with a temperature of 25 ºC, which was measured with a thermohydrometer with an accuracy of ±2% RH and ±0.2 K.

7.3 Data validation and discussion of the calculation methodology

In this section, the data validation process and the discussion of the calculation methodology are addressed.

The data validation is conducted in both the condenser and the evaporator for the 9 different tests of isobutane that were performed under varying inlet secondary fluid temperature conditions, as explained in the previous section. Validation consists of checking the heat transfer in evaporator and condenser of refrigerant and secondary fluids

The heat power absorbed by the secondary fluid circuits ($\dot{Q}_{sec,fluid}$) is calculated according to Eq.(7.1), where $\dot{m}_{fluid,sec}$ is the mass flow rate, c_p is the specific heat at constant pressure and Δt the temperature difference between the inlet and outlet of the heat exchanger. c_p of the water-propylene glycol mixture is calculated according with Conde [19].

$$\dot{Q}_{secfluid} = \dot{m}_{secfluid} \cdot c_p \cdot \Delta t \qquad \text{Eq.(7.1)}$$

Eq.(7.2) to Eq.(7.4) are used to calculate the heat power absorbed by the refrigerant in the evaporator ($\dot{Q}_{o,ref}$), in this study. The enthalpy value at the outlet of the evaporator ($h_{o,out}$) is determined as a function of the suction pressure and temperature. The inlet enthalpy ($h_{o,in}$) is determined as a function of the measured pressure with the gauge positioned before the expansion valve and the temperature prior to the valve, isenthalpic lamination is considered.

$$\dot{Q}_{o,ref} = \dot{m}_{ref} \cdot (h_{o,out} - h_{o,in}) \qquad \text{Eq.(7.2)}$$
$$h_{o,out} = f(p_{asp}, t_{asp}) \qquad \text{Eq.(7.3)}$$
$$h_{o,in} = f(p_{exp,in}, t_{exp,in}) \qquad \text{Eq.(7.4)}$$

Similarly, the heat power rejected by the refrigerant in the condenser ($\dot{Q}_{\mathrm{k},ref}$) is calculated using Eq.(7.5) to Eq.(7.7), in which the inlet condenser enthalpy is function of the discharge pressure and the inlet condenser temperature (measured with the first immersion thermocouple in the condenser) and the outlet enthalpy is calculated with the value of the pressure gauge and the outlet condenser temperature (last immersion thermocouple).

$$\dot{Q}_{\mathrm{k},ref} = \dot{m}_{ref} \cdot (h_{k,\mathrm{in}} - h_{k,out}) \qquad \text{Eq.(7.5)}$$
$$h_{\mathrm{k,in}} = f(p_{dis}, t_{k,in}) \qquad \text{Eq.(7.6)}$$
$$h_{k,\mathrm{out}} = f(p_{k,out}, t_{k,out}) \qquad \text{Eq.(7.7)}$$

Figure 7.3 displays the results obtained from the 9 tests conducted with isobutane, indicating the inlet temperature secondary fluid of each test. To evaluate the acceptability of the results, a discrepancy tolerance of ±6% between the two calculations considered adequate. All values obtained are inside this acceptable range. In the condenser, deviations observed across all tests remain below 3% (with the exception of the "35ºC, -5ºC" test, which exhibits a 4.65% deviation). In the evaporator, deviations tend to be more pronounced when the inlet temperature of the secondary fluid is lower. The deviation reaches approximately 5% at an inlet temperature of -5ºC, around 3.5 % at 0ºC, and approximately 0.5% at 5ºC.

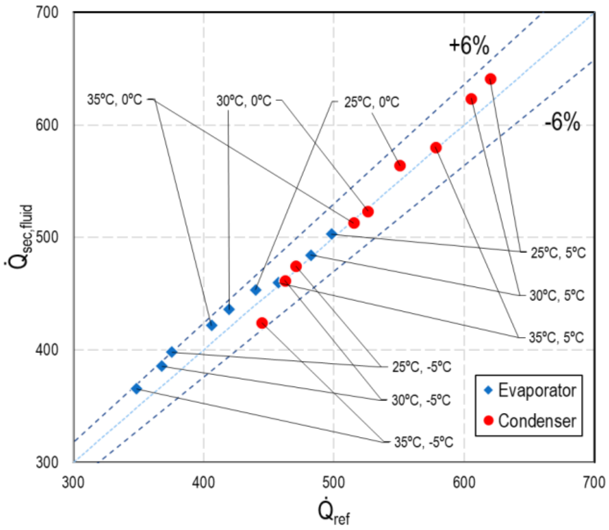

Figure 7.3. Data validation for the isobutane tests. The inlet secondary fluid temperature for each test is indicated, being the first value the one related to the condenser and the second value the evaporator.

Based on the obtained results, it can be concluded that the level of agreement achieved between the calculations conducted from the two distinct perspectives is considered satisfactory.

However, in contrast with isobutane, a less optimal agreement was observed in the tests conducted with the remaining mixtures when performing heat balances between the data obtained from the refrigerant and the secondary fluid. Figure 7.4 shows the data validation of all the tests performed with the mixtures R-152a/R-600 and R-290/R-600 at different mass compositions and different temperature inlet secondary fluid temperatures. This discrepancy between both calculations occurs principally with the mixture R-290/R-600, exhibiting differences higher than ±6% for 8 of the tests in the condenser and for 11 in the evaporator of a total of 20 tests considered. According to the authors' perspective, these variations can be attributed to uncertainties and inaccuracies inherent to the thermodynamic property calculations of new mixtures.

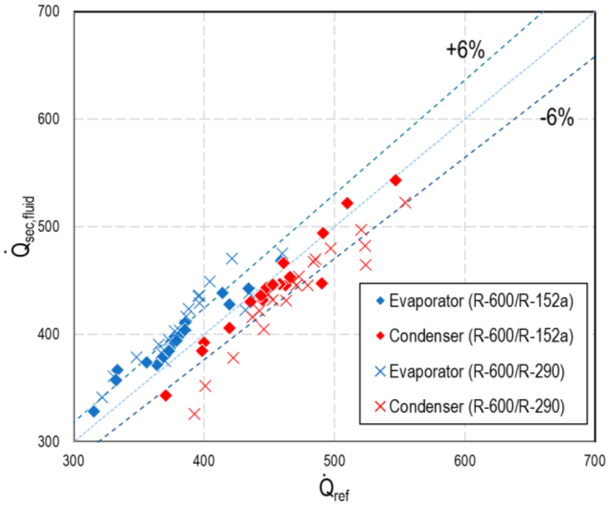

Figure 7.4. Heat exchange of the all the tests performed with the mixtures R-152a/R-600 and R-290/R-600, with different mass compositions and different secondary fluid inlet temperatures.

The assumption done by the authors is reinforced by the comparison of the PT curves obtained by REFPROP 10 and the saturation points obtained experimentally as shown in Figure 7.5. The figure represents with a solid line the saturation curves of the isobutane and the two mixtures with the “optimum” composition, as seen in the following sections. For each fluid, a total of 9 tests are available at different operating temperatures conditions. In the case of the two mixtures, a liquid saturation line and a vapor one can be differentiated, due to the existing glide. The data points in the figure represent the pressure-temperature values obtained experimentally, measured from points known to be in saturation conditions. The condenser and evaporator are both equipped with thermocouples, with 16 and 15 thermocouples respectively. This instrumentation enables the identification of the points where the phase change begins, as seen in following sections. Generally, in the condenser, the process begins at the 3rd thermocouple and concludes at the 16th thermocouple, while in the evaporator, the 12th thermocouple indicates the start of superheating. The corresponding pressures for these points are $p_{k,in}$, $p_{k,out}$ and p_{asp}, respectively. Furthermore, as isobutane does not exhibit glide, it is possible to represent the points of the evaporator inlet, which are measured by the 1st thermocouple in the evaporator, along with the pressure $p_{o,\text{in}}$.

The comparison between the experimental data obtained with isobutane and the theoretical saturation curves provided by REFPROP 10 reveals a good agreement. The mean absolute error (MAE) between the experimental values and the predicted ones is 0.5 K, which is considered a favorable approximation and falls within the range of sensor uncertainties. Furthermore, the observed trend aligns well with the theoretical curves.

However, the comparison of the saturation states for the mixtures between the experimental data and the predictions obtained with REFPROP 10 is not as favorable. For the mixture R-152a/R-600 (10/90)%, the MAE is calculated to be 1.43 K (0.82 K for the saturated liquid curve and 1.73 K for the vapor curve). Similarly, for the mixture R-290/R-600 (10/90)%, the MAE is found to be 1.9 K (1.89 K for the liquid curve and 2.01 K for the vapor curve).

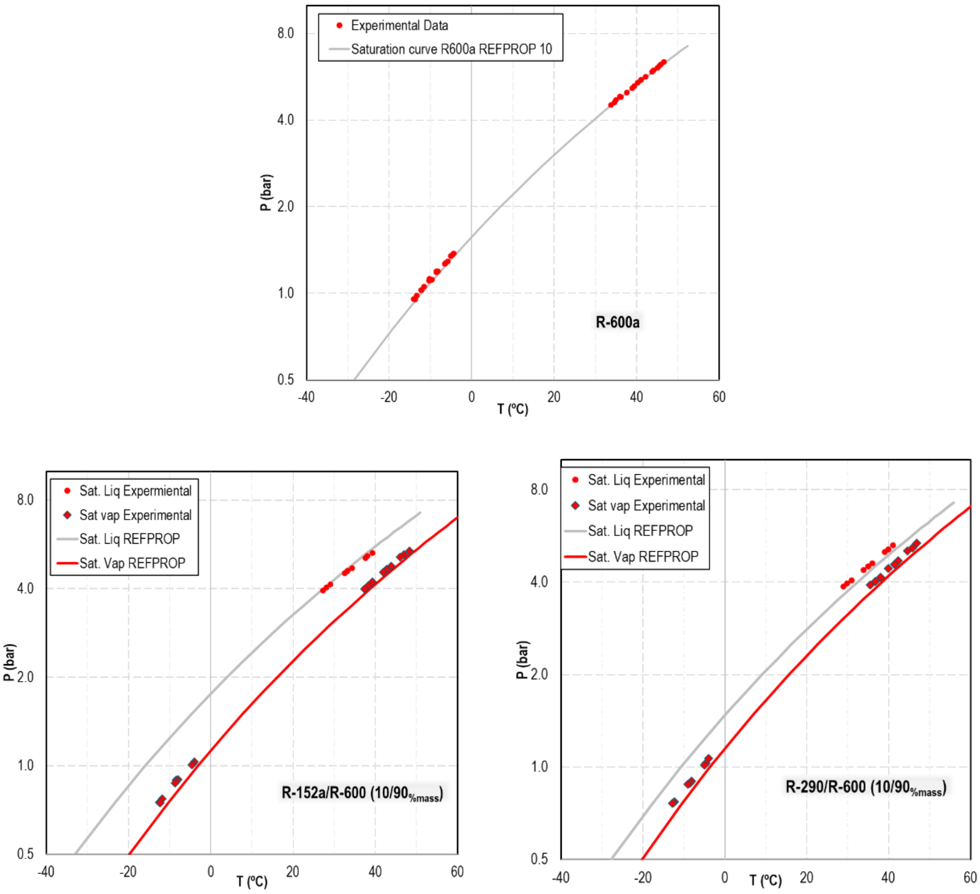

Figure 7.5. Comparison of saturation curve values obtained by REFPROP 10 (solid lines) and experimental saturation values for each fluid (points).

The findings presented in Figure 7.4 and Figure 7.5 indicate a strong agreement between the calculated parameters obtained with REFPROP 10 and the data acquired through various sensors for R-600a. However, this agreement does not hold true for the two alternative mixtures tested. This observation leads to two significant conclusions: i) the calibration of the plant is considered adequate since the results obtained data from the sensors present in the plant for isobutane, align well with the provided by REFPROP, which are known to be reliable; ii) the data obtained for the mixtures does not correspond to the data predicted by REFPROP. This suggests that parameters obtained through direct measurements (collected from various sensors throughout the plant) are more reliable compared to indirect parameters that involve calculations utilizing REFPROP, as it necessitates the utilization of mixing rules, which are based on estimations [20].

Overall, these findings highlight the importance of relying on direct measurements when possible for increased reliability in the determination of parameters, as opposed to relying solely on calculations involving REFPROP and its associated mixing rules. It is worth noting that the authors have adjusted the mixing coefficients for each mixture to the most recent coefficients available in the bibliography [21], but not a significant improvement was observed.

7.4 Composition optimization process - Thermodynamic analysis

7.4.1 Composition optimization process

As previously mentioned, the "optimization" process involves conducting tests on a range of mass compositions within the mixture. This range starts from 97.5% butane (with 2.5% of the second fluid) and progresses incrementally in 2.5% intervals until an "optimum" composition is determined. Throughout these tests, a constant inlet secondary fluid temperature of 30 ºC is maintained for the condenser (with a secondary fluid mass flow rate of 90 kg·h^{-1}), while an inlet temperature of 0 ºC is maintained for the evaporator (with a mass flow rate of 80 kg·h^{-1}).

The selection of the "optimum" composition is based on the evolution of the COP, VCC and $\dot{Q}_o$ parameters. These two parameters are calculated through the secondary fluid [Eq.(7.1)], since yields satisfactory precision for the purpose of this work.

The COP is calculated according to Eq.(7.8), considering the cooling capacity as the heat absorbed by the evaporator loop ($\dot{Q}_{o,secfluid}$) and the power consumption of the compressor ($\dot{P}_c$). VCC is determined using Eq.(7.9), which considers the specific cooling capacity and the specific suction volume ($v_{asp}{}^*$), which is calculated with REFPROP, as there are no direct measurements available for this parameter.

$$COP = \frac{\dot{Q}_{o,secfluid}}{\dot{P}_c} \qquad \text{Eq.(7.8)}$$

$$VCC = \frac{\dot{q}_{o,secflud}}{v_{asp}{}^{*}} = \frac{\frac{\dot{Q}_{o,secfluid}}{\dot{m}_{ref}}}{v_{asp}{}^{*}} \qquad \text{Eq.(7.9)}$$

Figure 7.6, Figure 7.7 and Figure 7.8 depict the evolution of the COP, the VCC and the cooling capacity of the two alternative mixtures analyzed in this work as the proportion of the less dominant refrigerant increases while the proportion of butane decreases. In a red line the isobutane value (considered the reference) is represented. Isobutane presents a COP of 2.51 a VCC of 827.4 kJ·m^{-3} and a $\dot{Q}_o$ of 435.9 W. Pure butane presents values of 2.74, 640.4 kJ·m^{-3} and 366.25 W respectively.

The COP evolution of the two analyzed mixtures differs significantly between the two mixtures. The mixture consisting of refrigerants R-152a and R-600 exhibits the highest COP values at compositions of 2.5/97.5% and 5/95% (2.76), followed by a slight but noticeable decrease as the R-152a composition increases. On the other hand, the mixture R-290/R-600 achieves its maximum COP at a composition of 10/90% (2.81), maintaining a similar value until the proportion reaches 20/80%, after which it starts to decrease.

Regarding the evolution of VCC, it is evident that both mixtures exhibit a similar trend. As anticipated, pure butane demonstrates a considerably lower VCC compared to isobutane (-22.77%). This difference arises because, despite having a greater enthalpy difference, the specific volume at the compressor inlet is significantly lower for butane, as detailed in Table 7.1. As the proportion of the secondary refrigerants increases, it is observed that the VCC rises. This is due to the fact that secondary refrigerants have higher densities than butane, leading to a rapid reduction in the specific volume at the compressor inlet, subsequently increasing the VCC. The recorded values for both mixtures remain similar across the entire mass range tested and surpass those of isobutane proportions of R-152a exceed 20% and R-290 surpasses 77.5%.

The trend in the evolution of cooling capacity closely mirrors that of Volumetric Cooling Capacity, with the key distinction being that the mixture containing propane consistently exhibits higher values across the entire mass range. Similarly to the VCC, the $\dot{Q}_o$ increases as the density of the mixture increases. In both mixtures, cooling capacity surpasses the value of isobutane when the proportion of the secondary fluid exceeds 20%.

It is worth noting that throughout the entire range of compositions examined, both mixtures present an A3 flammability classification, according with Calleja-Anta, et al. [22] considering the fractionation in the classification.

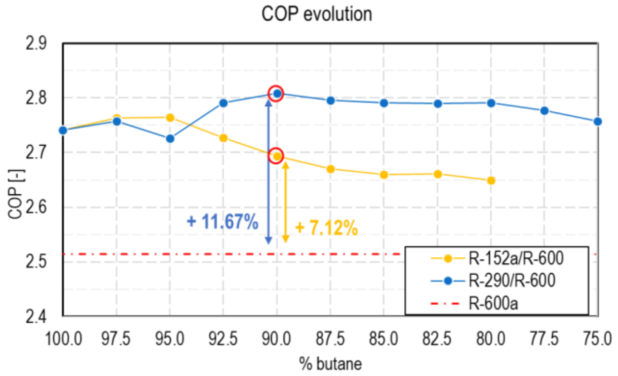

Figure 7.6. Evolution of the COP when varying the composition of the alternative mixtures. The COP obtained with isobutane is represented by the red line.

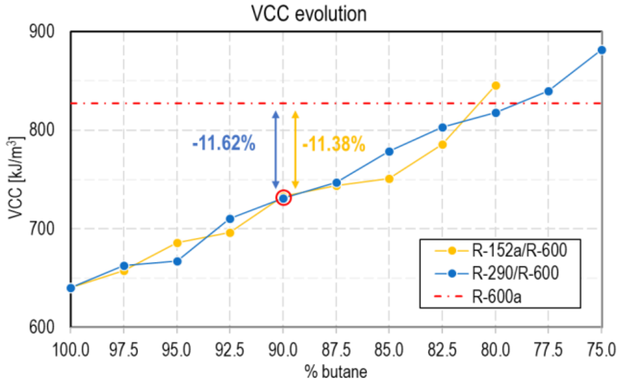

Figure 7.7. Evolution of the VCC when varying the composition of the alternative mixtures. The VCC obtained with isobutane is represented by the red line.

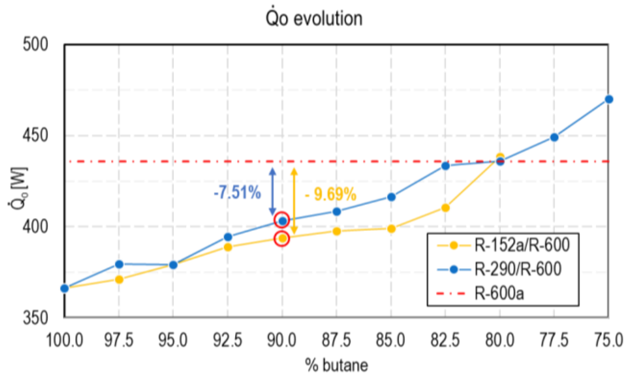

Figure 7.8. Evolution of the cooling capacity when varying the composition of the alternative mixtures. The cooling capacity obtained with isobutane is represented by the red line.

The "optimum" composition for the mixtures has been determined by carefully considering the trade-offs among the three discussed parameters. For the R-152a/R-600 mixture, the composition selected as the most advantageous is 10/90%. Lower proportions of R-152a result in a significant reduction in VCC compared to isobutane (-15.8% at 7.5/92.5% versus -11.4% for the chosen composition), while higher proportions do not yield substantial improvements (-10.1% at 12.5/87.5%). At the selected composition, there is a notable increase COP by +7.1%, along with a decrease in VCC by -11.4% and cooling capacity by 9.7%.

Similarly, for the R-290/R-600 mixture, the same composition of 10/90% has been identified as the "optimum". This composition achieves the maximum COP (+11. 7% compared to isobutane) and incurs relatively modest reductions in VCC and $\dot{Q}_o$ (-11.6% and -7.5%, respectively).

The calculated uncertainty for the three parameters determined for R-600a is less than 3.8%. For the R-152/R-600 and R-290/R-600 mixtures, the average uncertainty is 3.9%, with all compositions and parameters having uncertainties less than 4.2%. It is important to note that none of the parameter values calculated during the composition evolution of the mixtures fall within the uncertainty region of R-600a.

It is important to emphasize that this choice has been done taking into account the authors' opinion and based on quantitative and qualitative decisions, since it is difficult to unite all three parameters into one that designates which is the “best” composition.

The authors acknowledge that the determination of the "optimum" composition can be subject to debate and may vary depending on the specific application. Different researchers may hold differing opinions on what constitutes the ideal composition. However, it is essential to note that while selecting the right "optimum" composition may appear crucial, the values around these compositions exhibit similarity, and minor fluctuations in proportions would not significantly affect the overall performance of the system. In any case, these compositions have been chosen by the authors as the most favorable options based on their evaluation, considering the trade-offs and objectives at hand.

7.4.2 Thermodynamic analysis of the “optimum” compositions

Phase change temperatures and glide

Figure 7.9 represents the evolution of the refrigerant temperature within both the condenser and the evaporator for the isobutane, R-152a/R-600 (10/90)% and R-290/R-600 (10/90)% at the “optimization” conditions ($t_{w,in}$=30ºC and $t_{gly,in}$=0ºC). Each heat exchanger is equipped with immersion thermocouples at 23.5 cm intervals along the pipe (which corresponds to an area of 46.88 cm^2 for the condenser and 70.32 cm^2 for the evaporator). This configuration enables a total of 16 temperature data points for the condenser and 15 for the evaporator, facilitating a detailed analysis based on direct measurements of their respective thermal evolutions.

In the condenser, two different regions can be differentiated. Initially, there is a pronounced temperature decrease, attributed to the desuperheating process that involves the removal of sensible heat from the vapor after the compression is completed, up to the point where condensation begins. Generally, this process finishes at the 3rd thermocouple, marked by a transition in the temperature trend, resulting in a smoother slope. This phase corresponds to the extraction of latent heat during the condensation process, persisting until the end of the condenser. It is noteworthy that no subcooling occurs, probably due to the use of a liquid vessel at the outlet condenser.

A comparable pattern is evident in the evolution of evaporator temperatures. The refrigerant enters the evaporator in two-phase state, which persists until the 12th thermocouple, at which point there is a notable shift in the temperature trend. This abrupt change signifies the beginning of superheating.

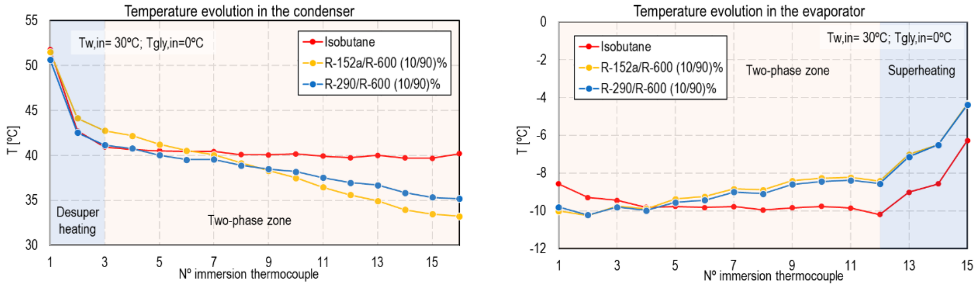

Figure 7.9. Refrigerant temperature evolution in the condenser (left) and in the evaporator (right) of the three refrigerants tested.

Figure 7.9 shows the evolution of the three refrigerants tested. It must be noted that all along the condenser there is a pressure drop of 102 mbar for the R-600a, 60 mbar for the R-152a/R-600 (10/90)% and 62 mbar for R-290/R-600 (10/90)%, being 68 mbar, 64 mbar and 54 mbar in the evaporator respectively. The differences in these values compared to isobutane and the two mixtures, especially in the condenser, can be attributed to variations in mass flow, primarily due to isobutane's higher density (as seen in Table 7.1). Specially in the evaporator, observing the isobutane temperature pattern, it suggests that the pressure drop mainly occurs in the initial part of the heat exchanger, as initially a decrease of the temperature is observed, which stabilizes latter in the process.

In the condenser, the phase-change temperature ($\bar{t}_k$), calculated as the mean temperature of the thermocouples within the two-phase zone, is 40.19 ºC for the R-600a (at an average pressure of 5.45 bar), 37.83 ºC for the R-152a/R-600 (10/90)% (4.64 bar) and 38.17ºC for the R-290/R-600 (10/90)% (at 4.44 bar). The evaporation temperature ($\bar{t}_o$), evaluated equally as the condensing temperature, shows a value of -9.67 ºC for R-600a (at 1.16 bar), -9.13 ºC for the R-152a/R-600 (10/90)% (at 0.92 bar) and -9.23ºC for the R-290/R-600 (10/90)% (at 0.9 bar). While the evaporation temperatures are similar among the evaluated fluids, the condensing one presents lower values for the alternative mixtures, being the difference between both temperatures lower with the mixtures than with R-600a. This could contribute to a reduction on the compressor ratio expected and partly explain the COP increment seen with the alternative mixtures.

Reading the temperature difference between the starting and ending of the phase-change process (Δt_{pc}), two factors contribute to it: the pressure drop and the glide. The existing pressure drop, despite not presenting high values, may be significant, especially in the evaporator. R-600a exhibits a measured $\Delta t_{pc,k}$ of 0.76 K and a measured $\Delta t_{pc,o}$ of 1.62 K. Interestingly, and differently that happens whit the two alternative mixtures, these values align closely with those predicted by REFPROP (0.72 K and 1.55 K), supporting the authors' hypothesis of relying on direct measurements when feasible. For the two mixtures, the primary contribution to Δt_{pc} is attributed to their glide in addition to the pressure drop effect being cumulative for the condenser and subtractive for the evaporator. The mixture R-152a/R-600 (10/90)% present a measured $\Delta t_{pc,k}$ of 9.51 K and a $\Delta\ t_{pc,o}$ of -1.58 K, while for the mixture R-290/R-600 (10/90)% of 5.98 K and -1.23 K, respectively.

The two fluids with glide follow the typical glide temperature evolution, where the temperature variation is higher at lower vapor quality and diminishes as the vapor proportion increases. This could explain the different values between the glide measured in the condenser and in the evaporator, since while in the condenser the entire glide is measured, in the evaporator only the effective glide is, as the inlet is in a two-phase state, skipping the zone with the most significant temperature variations.

Table 7.3 provides comprehensive data, including evaporation and condensation temperatures as well as Δt_{pc} values for all the compositions considered, including butane. It's noteworthy that butane exhibits a higher evaporation temperature compared to isobutane (-7.94 ºC at 0.82 bar). In contrast, the two alternative mixtures experience a reduction in temperature as the proportion of the lesser proportion refrigerant increases. This temperature reduction may be attributed to a decrease in the overall heat transfer coefficient, a characteristic feature of the mixtures. A similar trend can be observed in the condensing temperature, where butane displays a lower temperature than isobutane (37.86 ºC at 3.64 bar). However, unlike the evaporation temperature, the fluctuations in temperature with changing compositions are less pronounced in the condenser, with all values remaining below that of isobutane.

In the supplementary information, the evolution of the temperature of the exchangers of the rest of the tests is available to represent their evolution, as well as the recorded pressures.

Compressor power consumption and mass flow rate

The evolution of the refrigerant mass flow and the compressor electric power use when varying the composition is presented in Figure 7.10.

The mass flow rate of butane is lower than that of isobutane, with values of 5.69 $kg \cdot h^{-1}$ and 4.25 $kg \cdot h^{-1}$, respectively. Presenting a lower density has the advantage that the power required for the compression is lower but, for a given volume, the mass flow circulating is lower, requiring higher compression volumes to satisfy the same cooling capacities. As the proportion of the secondary fluid increases in the mixture, the mass flow rate also increases, as expected, since the density increases accordingly. Interestingly, the mixture containing R-152a exhibits a higher mass flow rate than the one with R-290. This unexpected result may be attributed to the fact that the evaporation temperature is higher with R-152a for the same composition than with R-290. It could be also related to better volumetric efficiency characteristics of the mixture with R-152a.

The trend in $\dot{P}_c$ evolution follows a similar pattern to that observed in Volumetric Cooling Capacity (VCC) and Cooling Capacity ($\dot{Q}_o$). As the refrigerant mass flow rate increases, $\dot{P}_c$ also increases. It is worth noting that for all the compositions tested, the power consumption is lower than that required by R-600a. Specifically, R-600a exhibits a $\dot{P}_c$ of 173.4 W. In contrast, at the "optimum" compositions, the mixture R-152a/R-600 (10/90)% demonstrates an energy reduction of 15.7%, while the R-290/R-600 (10/90)% mixture achieves an even greater reduction of 17.2%.

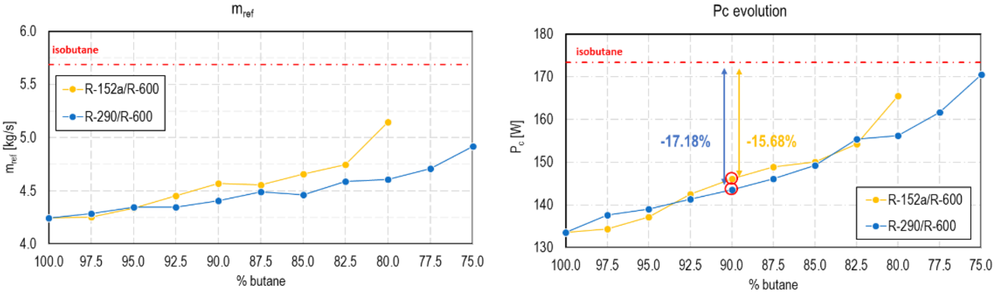

Figure 7.10. Evolution of the refrigerant mass flow (left) and $\dot{P}_c$ (right) when varying the composition of the alternative mixtures. The m$_{ref}$ and $\dot{P}_c$ obtained with isobutane are represented by the red line.

7.5 Optimum compositions at varying temperature conditions.

Finally, the "optimum" compositions were evaluated under different inlet secondary fluid temperatures. Figure 7.11 to Figure 7.13 show the evolution of the COP, VCC and $\dot{Q}_o$ respectively of the R-600a, R-152a/R-600 (10/90)% and R-290/R-600 (10/90)%, together with the percentage increment of each test of the alternative mixtures with respect to the equivalent with isobutane. Three different water inlet and three different glycol inlet temperatures are considered, giving as a result nine different conditions.

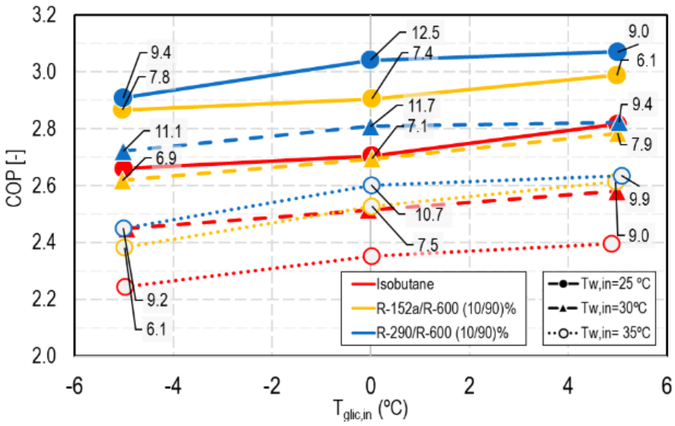

Figure 7.11. COP evolution of the R-600a, R-152a/R-600 (10/90)% and R-290/R-600 (10/90)% at different inlet secondary fluid temperatures. Additionally, labels indicating the percentage increase relative to the equivalent R-600a test for the alternative mixtures are included. These labels are organized in pairs, with the upper label corresponding to R-290/R-600 and the lower one to R-152a/R-600.

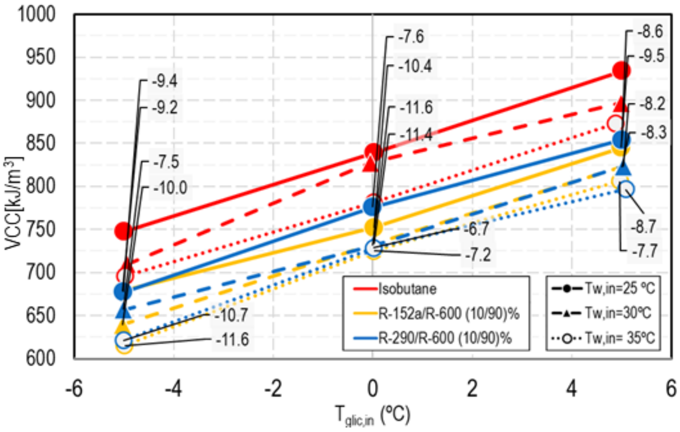

Figure 7.12. VCC evolution of the R-600a, R-152a/R-600 (10/90)% and R-290/R-600 (10/90)% at different inlet secondary fluid temperatures.

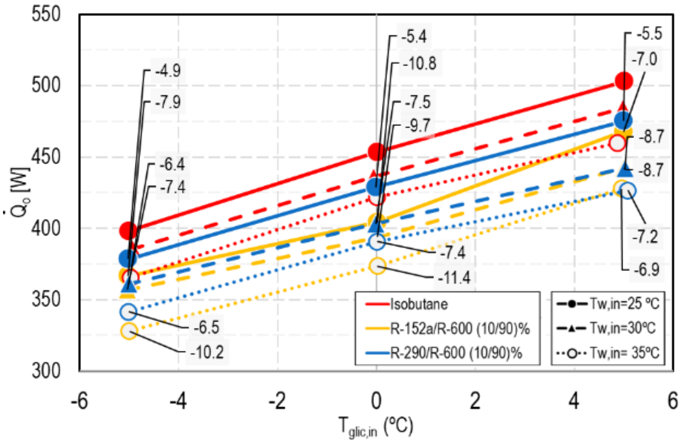

Figure 7.13. $\dot{Q}_o$ evolution of the R-600a, R-152a/R-600 (10/90)% and R-290/R-600 (10/90)% at different inlet secondary fluid temperatures.

The two considered mixtures exhibit significant increments in COP compared to isobutane in all tested points. Notably, the mixture R-290/R-600 (10/90)% outperforms the mixture R-152a/R-600 (10/90)% in terms of COP improvements. On average, R-290/R-600 (10/90)% demonstrates a 10.32% increase across the 9 test cases, with percentage increments ranging from +12.5% (at $t_{gly,in}$ = 0 ºC and $t_{w,in}$ = 25 ºC) to 9.0% (at $t_{gly,in}$ = 5 ºC and $t_{w,in}$ = 25 ºC). Conversely, R-152a/R-600 (10/90)% achieves an average increase of 7.31%, with fluctuations between 9% (at $t_{gly,in}$ = 5 ºC and $t_{w,in}$ = 35 ºC) and 6.1% (at $t_{gly,in}$ = -5 ºC and $t_{w,in}$ = 35 ºC).

A similar trend is observed for the other two considered parameters, with both mixtures generally showing percentage reductions compared to R-600a. Notably, these reductions tend to be more pronounced in the case of the R-152a/R-600 (10/90)% mixture. Specifically, in terms of VCC, the propane mixture exhibits an average reduction of -8.8% (ranging from -10.7% to -6.7%), while the R-152a-containing mixture shows an average reduction of -9.5% (ranging from -11.6% to -7.2%). Regarding $\dot{Q}_o$ values, the observed average reductions are -6.6% (ranging from -8.7% to -4.9%) and -8.9% (ranging from -11.4% to -7%) for the two mixtures, respectively.

In summary, the results presented in this section corroborate the findings from the "optimization" process, highlighting a substantial COP improvement in the alternative mixtures compared to isobutane, with R-290/R-600 (10/90)% showing superior energy performance, regardless of external conditions. No clear patterns emerge to suggest that any mixture exhibits better performance under specific conditions, indicating a relatively consistent performance across different scenarios. It can be concluded that, in terms of energy performance, the R-290/R-600 (10/90)% mixture is a preferable alternative to R-152a/R-600 (10/90)% as a an alternative for R-600a, considering also that the both refrigerants constituting this mixture are natural.

The supplementary information contains a table analogous to Table 7.3, presenting the most important thermodynamic parameters of the mixtures discussed in this section under varying conditions.

7.6 Conclusions

In this study, an experimental optimization of the composition of the mixtures R-152a/R-600 and R-290/R-600 was conducted as an alternative to isobutane (R-600a) in a simple vapor compression cycle. A novel heat exchanger design, based on a tube-in-tube configuration with immersion thermocouples, was employed to monitor the refrigerant temperature evolution during the phase-change process.

The methodology involved testing all possible mass composition combinations of the two considered mixtures in steps of 2.5%, ranging from 2.5% to 20% of R-152a (resulting in a total of 8 different mass compositions) and from 2.5% to 25% of R-290 (10 compositions). Results were compared to those obtained with R-600a under fixed boundary conditions. These conditions included an inlet water temperature of 30 ºC, an inlet glycol temperature of 0 ºC, a water flow rate of 90 $kg \cdot h^{-1}$, and a glycol flow rate of 80 $kg \cdot h^{-1}$.

At those conditions, R-600a demonstrated a COP of 2.51, a VCC of 827.4 $kJ \cdot m^{-3}$, and a $\dot{Q}_o$ of 435.9 W. In comparison, R-600 exhibited values of 2.74, 640.4 $kJ \cdot m^{-3}$, and 366.25 W, respectively. The mixture R-152a/R-600 achieved the highest COP values at compositions of 2.5/97.5% and 5/95% (2.76), with a slight decrease as the R-152a composition increased. Similarly, the mixture R-290/R-600 reached its maximum COP at a composition of 10/90% (2.81), maintaining a similar value until the proportion reached 20/80%, after which it decreased. VCC and $\dot{Q}_o$ increased linearly as the secondary fluid proportion increased. R-152a/R-600 surpassed R-600a's VCC and $\dot{Q}_o$ values at a composition of (20/80)%, whereas R-290/R-600 did so at (22.5/77.5)% and (20/80)%, respectively.

The "optimum" compositions were chosen as (10/90)% for both mixtures, striking a balance between the three parameters. The mixture R-152a/R-600 (10/90)% exhibited a COP increase of +7.1%, with a decrease in VCC by -11.4% and cooling capacity by -9.7%. The mixture R-290/R-600 (10/90)% showed a COP increase of +11. 7%, along with a decrease in VCC by -11.6% and cooling capacity by -7.5%.

At these compositions, the R-152a-containing mixture presented an average condensing temperature of 37.8 ºC at 4.64 bar, with a measured glide of 9.5 K. In the evaporator, the phase change temperature was -9.1 ºC at 0.92 bar, with an effective glide of 1.6 K. The mixture R-290/R-600 (10/90)% exhibited condensing conditions of 38.2 ºC at 4.4 bar, with a glide of 5.98 K, and evaporating conditions of -9.2 ºC at 0.91 bar, with an effective glide of 1.2 K. As a reference, R-600a had condensing and evaporating temperatures of 40.2 ºC and -9. 7 ºC, respectively.

Furthermore, the performance of the "optimum" compositions was tested under nine different secondary fluid inlet temperatures, resulting in average increments and reductions compared to isobutane in the nine tests as follows:

- R-152a/R-600 (10/90)%: +7.3% of COP, -9.45% of VCC, and -8.9% of $\dot{Q}_o$.
- R-290/R-600 (10/90)%: +10.3% of COP, -8.77% of VCC, and -6.6% of $\dot{Q}_o$.

In summary, R-290/R-600 (10/90)% exhibits superior energy performance compared to R-152a/R-600 (10/90)% as an alternative for R-600a. R-290/R-600 (10/90)% can be considered as an interesting long-term alternative to R-600a, since the energy improvements respect to isobutane are significant, its thermodynamic properties are similar to those of R-600a and the two refrigerants constituting this mixture are natural.

7.7 Acknowledgments

Authors gratefully acknowledge for the economic support to this study to Jaume I University (grant PREDOC/2019/19). This article is part of the project TED2021-130162B-I00, funded by MCIN/AEI/10.13039/501100011033 and by the European Union

- NextGenerationEU “NextGenerationEU”/PRTR.; and of the project PID2021-126926OB-C21 funded by the Ministerio de Ciencia e Innovación of Spain.

7.8 Author contribution statements

Daniel Calleja-Anta: Methodology, Writing - Original Draft, Conceptualization, Investigation **Manel Martínez-Ángeles:** Investigation, Writing - Review & Editing **Laura Nebot-Andrés:** Writing - Review & Editing **Daniel Sanchez:** Supervision, Funding acquisition, Writing - Review & Editing **Rodrigo Llopis:** Supervision, Funding acquisition, Conceptualization, Writing - Review & Editing

7.9 Nomenclature

ATS	Auxiliary Thermal System
c_p	specific heat at constant pressure, kJ·kg^{-1}·K^{-1}
COP	Coefficient of Performance
C_r	Compression rate
GWP	Global Warming Potential over 100-year, $kg_{co2,eq}$ / kg_{ref}
h	specific enthalpy, kJ·kg^{-1}
HX	Heat Exchanger
m	mass flow rate, kg·s^{-1}
M	Molar mass, g·mol^{-1}
MAE	Mean Absolute Error
NBP	Normal Boiling Point, ºC
p	absolute pressure, bar
$\dot{P}_c$	compressor power consumption, W
$\dot{Q}_o$	cooling capacity, W
$\dot{q}_o$	specific cooling capacity, kJ·kg^{-1}
RH	Relative Humidity, %
t	temperature, ºC
V	volume flow rate, L·s^{-1}
VCC	Volumetric Cooling Capacity, kJ·m^{-3}
x_v	vapor tittle

Subscripts

suc	refers to compressor suction conditions
crit	at critical conditions
dis	refers to compressor discharge conditions
exp	refers to the expansion device
gly	refers to propylene glycol-water mixture
in	inlet
k	related to condensation
o	related to evaporation
out	outlet

pc	refers to the phase change
ref	related to the refrigerant
sec,fluid	related to the secondary fluid
w	related to the water

Greek symbols

λ	latent heat of phase change, $kJ\cdot Kg^{-1}$
Ø	diameter, cm

7.10 References

[1] European Commission, Regulation (EU) No 517/2014 of the European Parliament and of the Council of 16 April 2014 on fluorinated greenhouse gases and repealing Regulation (EC) No 842/2006., in: E. Commission (ed.), Official Journal of the European Union, 2014.

[2] UNEP, Refrigeration and air conditioning and heat pumps technical options committee. 2018 Assessment Report, in, United Nations Environment Programme, Kenya, 2018.

[3] International Electrotechnical Commission., IEC 60335-2-89:2019. Household and similar electrical appliances - Safety - Part 2-89: Particular requirements for commercial refrigerating appliances and ice-makers with an incorporated or remote refrigerant unit or motor-compressor, in, 2019.

[4] IPCC, Climate Change 2023: Synthesis Report. Contribution of Working Groups I, II and III to the Sixth Assessment Report of the Intergovernmental Panel on Climate Change [Core Writing Team, H. Lee and J. Romero (eds.)]. IPCC, Geneva, Switzerland, pp. 35-115, (2023) DOI: 10.59327/IPCC/AR6-9789291691647.

[5] M. Rasti, S. Aghamiri, M.-S. Hatamipour, Energy efficiency enhancement of a domestic refrigerator using R436A and R600a as alternative refrigerants to R134a, International Journal of Thermal Sciences, 74 (2013) 86-94 DOI: http://dx.doi.org/10.1016/j.ijthermalsci.2013.07.009.

[6] D. Sánchez, A. Andreu-Nácher, D. Calleja-Anta, R. Llopis, R. Cabello, Energy impact evaluation of different low-GWP alternatives to replace R134a in a beverage cooler. Experimental analysis and optimization for the pure refrigerants R152a, R1234yf, R290, R1270, R600a and R744, Energy Conversion and Management, 256 (2022) DOI: 10.1016/j.enconman.2022.115388.

[7] E. Granryd, I. Ekroth, P. Lundqvist, A. Melinder, B. Palm, P. Rohlin, Refrigerating Engineering, Royal Institute of Technology, KTH, Department of Energy Technology, Division of Applied Thermodynamics and Refrigeration, 2009.

[8] D. Sánchez, R. Cabello, R. Llopis, I. Arauzo, J. Catalán-Gil, E. Torrella, Energy performance evaluation of R1234yf, R1234ze(E), R600a, R290 and R152a as low-GWP R134a alternatives, International Journal of Refrigeration, 74 (2017) 269-282 DOI: http://dx.doi.org/10.1016/j.ijrefrig.2016.09.020.

[9] ASHRAE, ANSI/ASHRAE Standard 34-2019. Designation and safety classification of refrigerants, in, American Society of Heating, Refrigerating and Air-Conditioning Engineers, Inc., Atlanta, USA, 2019.

[10] C. Aprea, A. Greco, A. Maiorino, An experimental investigation on the substitution of HFC134a with HFO1234YF in a domestic refrigerator, Applied Thermal Engineering, 106 (2016) 959-967 DOI: 10.1016/j.applthermaleng.2016.06.098.

[11] C. Aprea, A. Greco, A. Maiorino, C. Masselli, A. Metallo, HFO1234ze as Drop-in Replacement for R134a in Domestic Refrigerators: An Environmental Impact Analysis, Energy Procedia, 101 (2016) 964-971 DOI: http://dx.doi.org/10.1016/j.egypro.2016.11.122.

[12] B.O. Bolaji, Experimental study of R152a and R32 to replace R134a in a domestic refrigerator, Energy, 35 (2010) 3793-3798 DOI: http://dx.doi.org/10.1016/j.energy.2010.05.031.

[13] A. Maiorino, C. Aprea, M.G. Del Duca, R. Llopis, D. Sánchez, R. Cabello, R-152a as an alternative refrigerant to R-134a in domestic refrigerators: An experimental analysis, International Journal of Refrigeration, 96 (2018) 106-116 DOI: https://doi.org/10.1016/j.ijrefrig.2018.09.020.

[14] M. Mohanraj, S. Jayaraj, C. Muraleedharan, P. Chandrasekar, Experimental investigation of R290/R600a mixture as an alternative to R134a in a domestic refrigerator, International Journal of Thermal Sciences, 48 (2009) 1036-1042 DOI: 10.1016/j.ijthermalsci.2008.08.001.

[15] D. Calleja-Anta, L. Nebot-Andres, J. Catalan-Gil, D. Sánchez, R. Cabello, R. Llopis, Thermodynamic screening of alternative refrigerants for R290 and R600a, Results in Engineering, 5 (2020) DOI: 10.1016/j.rineng.2019.100081.

[16] D. Calleja-Anta, L. Nebot-Andres, D. Sánchez, R. Cabello, R. Llopis, Drop-in substitutes for R-600a. Experimental evaluation and optimization of a commercial fridge, Applied Thermal Engineering, 211 (2022) DOI: 10.1016/j.applthermaleng.2022.118490.

[17] D. Calleja-Anta, D. Sánchez, L. Nebot-Andrés, R. Cabello, R. Llopis, Alternative mixtures to R-600a. Theoretical assessment and experimental energy evaluation of binary mixtures in a commercial cooler, International Journal of Refrigeration, 152 (2023) 83-92 DOI: 10.1016/j.ijrefrig.2023.05.009.

[18] Author, NIST Standard Reference Database 23: Reference Fluid Thermodynamic and Transport Properties-REFPROP, Version 10.0, National Institute of Standards and Technology, 2018 DOI: dx.doi.org/10.18434/T4JS3C.

[19] M. Conde, Thermophysical properties of brines, in, 2011.

[20] O. Kunz, W. Wagner, The GERG-2008 Wide-Range Equation of State for Natural Gases and Other Mixtures: An Expansion of GERG-2004, Journal of Chemical & Engineering Data, 57 (2012) 3032-3091 DOI: 10.1021/je300655b.

[21] I.H. Bell, E.W. Lemmon, Automatic Fitting of Binary Interaction Parameters for Multi-fluid Helmholtz-Energy-Explicit Mixture Models, Journal of Chemical & Engineering Data, 61 (2016) 3752-3760 DOI: 10.1021/acs.jced.6b00257.

[22] D. Calleja-Anta, L. Nebot-Andres, R. Cabello, D. Sánchez, R. Llopis, A3 and A2 refrigerants: Border determination and hunt for A2 low-GWP blends, International Journal of Refrigeration, 134 (2022) 86-94 DOI: 10.1016/j.ijrefrig.2021.11.012.

Declaration of generative AI and AI-assisted technologies in the writing process

During the preparation of this work the authors used “OpenAI. (2023). ChatGPT 3.5” in order to improve language and readability. After using this tool/service, the authors reviewed and edited the content as needed and take full responsibility for the content of the publication.

Table 7.3. Summary of the reference test conditions, various thermodynamic aspects and energy parameters during the optimization process.

	Reference parameters					High pressure cycle section				Low pressure cycle section				Compression process				Energy parameters			
Refrigerant and mass composition	$t_{w,k,in}$ (ºC)	$t_{gly,o,in}$ (ºC)	$\dot{V}_{w,k}$ (L/h)	$\dot{m}_{gl,o}$ (kg/h)	Ref. charge(g)	$p_{k,in}$ (bar)	$p_{k,out}$ (bar)	$\bar{t}_k$ (ºC)	$\Delta t_{pc,k}$ (ºC)	$p_{o,in}$ (bar)	p_{suc} (bar)	$\bar{t}_o$ (ºC)	$\Delta t_{pc,o}$ (ºC)	p_{dis} (bar)	t_{dis} (ºC)	C_r (-)	m_{ref} (kg/s)	P_c (W)	Q_o (W)	COP (-)	VCC (kJ/m^3)
R-600a																					
	30.02	-0.05	90.23	80.68	160	5.50	5.40	40.19	0.76	1.19	1.12	-9.67	1.62	5.60	59.66	4.98	5.69	173.4	435.9	2.51	827.4
R-600																					
	30.03	0.01	90.16	79.82	154	3.68	3.61	37.86	0.71	0.85	0.79	-7.94	1.44	3.75	59.34	4.75	4.25	133.6	360.8	2.74	640.4
R-152a/R-600																					
2.5/ 97.5	29.95	0.04	89.72	79.78	155	3.87	3.81	37.97	3.97	0.86	0.80	-8.26	0.66	3.93	60.13	4.93	4.25	134.4	371.3	2.76	657.9

5/95	30.01	0.03	89.93	79.53	141	4.18	4.12	37.77	6.91	0.89	0.83	-8.64	-0.44	4.24	61.08	5.11	4.34	137.2	379.2	2.76	686.3
7.5/ 92.5	29.92	0.01	89.77	79.54	146	4.37	4.31	37.80	8.25	0.90	0.84	-8.87	-0.88	4.43	62.15	5.28	4.46	142.6	388.8	2.73	696.5
10/ 90	**30.00**	**0.02**	**90.35**	**80.85**	**150**	**4.66**	**4.61**	**37.83**	**9.51**	**0.95**	**0.89**	**-9.13**	**-1.58**	**4.72**	**63.39**	**5.29**	**4.57**	**146.2**	**393.7**	**2.69**	**733.2**
12.5/87.5	29.98	0.01	89.90	79.52	152	5.02	4.96	37.68	11.00	0.96	0.89	-9.53	-2.79	5.06	64.09	5.68	4.56	148.9	397.5	2.67	743.7
15/85	30.00	-0.01	90.08	80.02	153	5.19	5.13	37.69	11.18	0.98	0.91	-9.61	-3.09	5.24	65.14	5.74	4.66	150	399.1	2.66	750.8
17.5/82.5	30.03	0.04	90.25	79.74	154	5.52	5.46	37.74	11.84	1.01	0.95	-9.93	-4.09	5.56	65.87	5.88	4.75	154.2	410.4	2.66	785.7
20/80	30.00	0.01	89.95	80.40	150	5.70	5.62	37.70	10.65	1.10	1.03	-9.36	-3.84	5.78	68.38	5.62	5.15	165.5	438.5	2.65	845.4
R-290/R-600																					
2.5/97.5	29.98	0.00	90.20	79.71	160	3.89	3.83	38.03	2.64	0.85	0.80	-8.57	0.70	3.95	60.57	4.93	4.29	137.6	379.5	2.76	662.7

5/95	29.96	0.00	90.29	80.10	140	3.96	3.89	37.84	3.17	0.88	0.83	-8.46	0.41	4.03	60.79	4.88	4.35	139.1	379.1	2.73	667.6
7.5/92.5	29.96	-0.03	90.06	80.09	147	4.27	4.21	38.11	5.16	0.90	0.85	-9.13	-0.65	4.33	61.58	5.09	4.35	141.4	394.6	2.79	710.4
10/90	**29.98**	**0.00**	**89.72**	**80.14**	**150**	**4.47**	**4.40**	**38.17**	**5.98**	**0.93**	**0.88**	**-9.23**	**-1.23**	**4.53**	**62.12**	**5.17**	**4.41**	**143.6**	**403.2**	**2.81**	**731.3**
12.5/87.5	29.96	0.02	89.87	80.03	152	4.71	4.65	38.23	6.92	0.96	0.91	-9.58	-1.92	4.76	63.15	5.26	4.49	146.1	408.4	2.80	747.3
15/85	29.98	0.02	90.01	80.01	154	4.93	4.87	38.29	7.84	0.98	0.93	-9.85	-2.56	4.98	63.26	5.37	4.46	149.3	416.7	2.79	778.9
17.5/82.5	29.97	0.05	89.72	80.23	154	5.19	5.13	38.56	8.52	1.01	0.95	-10.18	-3.16	5.24	64.83	5.50	4.59	155.4	433.6	2.79	803.4
20/80	29.95	0.00	89.63	79.43	150	5.35	5.29	38.57	8.89	1.03	0.97	-10.32	-3.46	5.40	64.79	5.54	4.61	156.2	435.9	2.79	818.1
22.5/77.5	29.98	-0.03	90.31	80.09	152	5.61	5.55	38.75	9.39	1.06	1.00	-10.58	-3.98	5.66	65.79	5.67	4.71	161.7	449.1	2.78	839.8
25/75	30.06	0.06	90.42	79.50	148	6.00	5.93	38.99	9.74	1.12	1.05	-10.85	-4.65	6.05	66.99	5.74	4.92	170.5	470.2	2.76	881.6

CHAPTER 8.

CONCLUSIONS AND FUTURE RESEARCH

8 CONCLUSIONS

This thesis deals with the investigation of alternative refrigerant blends to isobutane (R-600a), which is used as the standard refrigerant in Europe since the early 2010s in sealed domestic appliances and low-capacity sealed commercial refrigeration. R-600a is attributed to its low GWP and good energy efficiency, enabling compliance with industry regulations. However its disadvantage is its high flammability, which in practice limits the refrigeration capacity that can be handled by a single system.

However, before writing this thesis, a review of the bibliography showed that there were mixtures that have been proven to improve the energetic characteristics of pure refrigerants, but there has been no in-depth study to find the best mixtures with respect to R-600a and exploit their potential.

The present thesis therefore focuses on the search for alternative blends to R-600a as a refrigerant fluid in vapor compression systems for cold production. Specifically, the search for blends is carried out by looking for an improvement of the energetic properties of isobutane on the one hand and a reduction of the flammability on the other hand and, if possible, a combination of both properties.

The first step was to carry out a **theoretical thermodynamic screening to identify the mixtures with the highest COP increases compared to isobutane.** All possible ternary mixtures of a total of 10 refrigerants were simulated, varying their composition by 5%. In total, 120 different refrigerant trios and 229 compositions for each of them were evaluated, giving a total of 27480 different mixtures. These mixtures were simulated assuming two different typologies of appliances and two different evaporation temperatures. The following refrigerants were identified as the most promising with the highest COP increases compared to R-600a, being present in the majority of scenarios:

- **R-1270/R-600**. ∆COP between 1.7% and 5.3%.
- **R-152a/R-600.** ∆COP between 3.3% and 7.6%.
- **R-1234yf/R-600.** ∆COP between 2.5% and 4.4%.
- **R-1234ze(E)/R-600.** ∆COP between 2% and 4.5%.
- **R-290/R-600.** ∆COP between 1.6% and 8.6%.

The identified composition of these blends varies according to the considered scenario, but it should be noted that R-600 (n-butane) is present in the majority of all blends (around 90% in mass composition) while the other refrigerant is present in a smaller composition.

This first work served to identify potential mixtures to isobutane and to constitute the initial hypothesis of the existence of mixtures with potential energy improvements to R-600a.

The next study was the **extension of a method for identifying the flammability class to which newly developed refrigerant blends belong.** This work extended Linteris et al. method for determining the boundary between A3 and A2 refrigerants as a function of the F/F+H ratio and the adiabatic flame temperature. The search for the boundary was carried out using an empirical approach based on the existing refrigerants in ASHRAE Standard 34 and completed with an extensive screening based on the HOC index. It was concluded that all blends with an **angle Π greater than 67.37° belong to an A3 safety classification.**

The developed method was used to **define the composition limits of HC refrigerant blends** (R-600a, R-290 and R-1270) with A1, A2 and A2L components that meet the A2 safety classification and have a GWP less than 150. It was concluded that **no blend with A1 fluids meets the criteria** because the amount of A1 component used for inerting causes the GWP to exceed 150 and **it is possible to create A2 blends by blending with A2 and A2L components.** The limits identified are shown in Table 8.1.

Table 8.1. Composition limits for A2 classification.

Composition limits for A2 classification (%mass)					
Propane Mixtures		**Isobutane Mixtures**		**Propylene Mixtures**	
R-290/R-152a	1.6 / 98.4	R-600a/R-152a	4.7 / 95.3	R-1270/R-152a	1.8 / 98.2
R-290/R-1132a	0.7 / 99.3	R-600a/R-1132a	0.3 / 99.7	R-1270/R-1132a	1.0 / 99.0
R-290/R-1234yf	11.0/89.0	R-600a/R-1234yf	8.4 / 91.6	R-1270/R-1234yf	10.0/90.0
R-290/ R-1234ze(E)	5.0 / 95.0	R-600a/ R-1234ze(E)	17.6 / 82.4	R-1270/ R-1234ze(E)	4.7 / 95.3
R-290/R-744	4.6 / 95.4	R-600a/R-744	0.9 / 99.1	R-1270/R-744	4.2 / 95.8

On the basis of what has been seen, it is concluded that the possibilities of creating **alternative binary mixtures with low-GWP to isobutane by combining HCs with lower flammability components are very limited,** mainly due to the strong influence of fractionation on nominal composition. It is also concluded that these mixtures are very far from the results obtained in the thermodynamic screening, so that there are **no binary mixtures that improve the energetic properties of isobutane while reducing its flammability classification.**

From this point on, the efforts of the thesis were focused on the experimental demonstration and accounting of the energy consumption savings with the identified blends in relation to R-600a. For this purpose, two commercial units were adapted and instrumented with different sensors: a domestic refrigerator (fridge) and a commercial stand-alone unit (beverage cooler). The domestic refrigerator was not modified in its circuit (drop-in analysis), while the commercial refrigerator was equipped with an electronic expansion valve configured according to the characteristics of each refrigerant. The tests consisted of steady-state tests in which energy consumption (as well as several other parameters) was recorded for 24 and 16 hours respectively.

The mixtures tested in the domestic refrigerator are those identified in the thermodynamic screening, with the following energy savings compared to R-600a:

- **R-1234yf/ R-600a (7.5/92.5%).** Energy reduced by **2.15%.**
- **R-1234ze(E)/ R-600 (10.5/89.5%).** Reduced by **3.84%.**
- **R-290/ R-600 (11.0/89.0%).** Reduced by **1.31%.**
- R-1270/ R-600 (15.5/84.5%). Increase by 1.83%.
- R-152a/ R-600 (9.5/90.5%). Increase by 0.33%.

The blends tested in the commercial appliance are as follows, with their corresponding energy reductions:

- **R-1234ze(E)/R-600 (8/92%).** Energy reduced by **2.69%.**
- **R-152a/R-600 (8/92%).** Reduced by **5.04%.**
- R-32/R-600 (2/98%). Increased by 0.36%.

Up to this point, the existence of blends with better energy performance than R-600a in stand-alone domestic and commercial appliances has been demonstrated and 4 binary blends with energy savings have been identified.

However, up to this point, the composition in which the mixtures were tested has been obtained from theoretical studies with certain limitations and uncertainties. These studies primarily aimed to conduct a broad screening of blends and did not take into account all variables.

In order to directly measure the thermodynamic properties of the blends and to experimentally determine the optimum composition of the **R-152a/R-600 and R-290/R-600 blends** (the blend with the highest energy reduction obtained and the only blend identified with entirely natural components), a test bench with a highly sensor-equipped vapour compression cycle was built. On the basis of the COP, VCC and $\dot{Q}_o$ parameters, it was concluded that the **optimum composition** for both mixtures was **10/90 %.**

The performance of the optimum blends was tested at nine different secondary fluid inlet temperatures, resulting in the following average increases and decreases with respect to isobutane over the nine tests:

- **R-152a/R-600 (10/90)%: +7.3% COP, -9.45% VCC and -8.9% $\dot{Q}_o$.**
- **R-290/R-600 (10/90)%: +10.3% of COP, -8.77% of VCC and -6.6% of $\dot{Q}_o$.**

In light of the results obtained, there is a notable discrepancy between the theoretical predictions from the original study and the experimental findings. This deviation may be due to several limitations of the theoretical evaluation, but according to my opinion, the two that may have the most impact are:

i) Working pressure and temperature: The theoretical study evaluated the mixtures at fixed evaporation and condensation temperatures, with the working pressure determined through an iterative method using mean enthalpy. Reassessing the mixtures at the temperatures corresponding to the pressures recorded in the experimental plant (-6.5ºC for both mixtures and -8.5ºC for R-600a), the COP increases to +8.45% for the R-152a/R-600 (10/90)% mixture and +9.15% for R-290/R-600 (10/90)%. These results exhibit closer experimental results obtained.

ii) Uncertainties of REFPROP with mixing rules: The experimental results highlight potential calculation uncertainties associated with the mixing rules in REFPROP, which impacts theoretical predictions.

There are also other factors such as the variability of the isotropic, volumetric and mechanical-electrical efficiencies between the different mixtures considered. However, it should be noted that the main objective of the theoretical study was to identify promising blends, while the experimental study was intended to provide reliable results to draw conclusions on energy improvements.

In conclusion, this thesis has identified 4 binary mixtures as energy efficient alternatives to isobutane. Figure 8.1 shows the main results obtained. In addition to the energy savings observed, the operating parameters and thermodynamic properties of the blends are similar to those of R-600a, such as low operating pressures and low density, so that no redesign of these installations and no additional safety considerations are required.

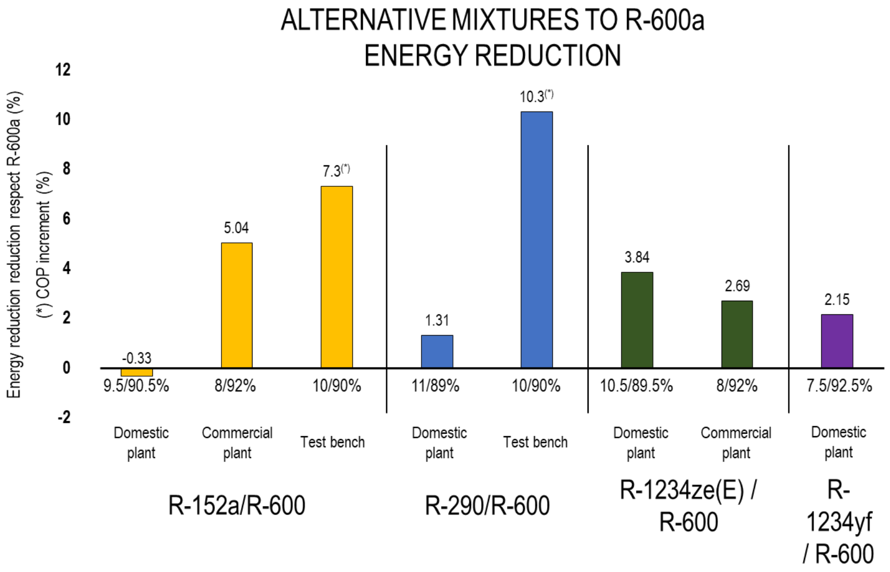

Figure 8.1. Summary of the results obtained with the alternative mixtures to R-600a in different appliances.

This study has highlighted the limited capacity to reduce the flammability classification of HCs by blending them with less flammable refrigerants. Additionally, it has been established that no binary refrigerant mixtures can achieve simultaneous reductions in flammability, increased energy efficiency, and low Global Warming Potential (GWP).

The objectives defined at the beginning of the thesis can be considered to have been met and the results can be considered to be relevant, robust and comprehensive in the search for an alternative to R-600a.

8.1 FUTURE RESEARCH

At the beginning of this thesis, a thermodynamic screening was conducted, which included a theoretical exploration of potential refrigerants to replace R-290. While this line of inquiry was set aside to prioritize the search for R-600a alternatives, a diverse array of refrigerants with significant increases in COP was identified. Similar experimental research as done in this thesis focusing on enhancing R-290 could be highly valuable and present compelling avenues for further investigation.

Moreover, it has to be mentioned that not all the pure refrigerants have been considered in this study to form mixtures. There are refrigerants that have recently attracted a lot of scientific attention, such as R-E170 and R-1233zd(E). These refrigerants have interesting properties. On the one hand, R-E170 has a relatively high LFL compared to other flammable refrigerants, so it can be a good alternative to combine with R-600 to obtain refrigerant blends with lower flammability. On the other hand, in the last part of this thesis it was observed that R-1233zd(E) has the ability to form azeotropic mixtures with R-600a and R-600, so its study may be of great interest.

All of the experimental results in this thesis have been obtained using compressors originally designed for R-600a. Although the blends tested are thermodynamically close to R-600a, it is expected that the use of a compressor specifically designed for each of them will increase their energy efficiency and achieve greater energy reductions. Therefore, a possible line of future research is to analyse the impact of the blends on the compressor behaviour.

Exploring heat transfer in heat exchangers could be a valuable area of research, as it directly impacts phase change temperatures and subsequently influences the energy performance of refrigerants. Given the extensive sensorization of the experimental plant discussed in CHAPTER 7, it could serve as a valuable tool for this purpose. Using its, researchers could gain insight into the heat transfer dynamics within heat exchangers, leading to a better understanding of their performance and potential areas for optimization.

Moreover, the line of future research with the greatest potential is the study of mixtures of 3 or more components with the aim of reducing flammability. As seen in this work, fractionation plays a crucial role in the flammability classification of mixtures, with an extreme effect on binary mixtures. Fractionation in ternary mixtures has not been studied and may be the key to achieving a higher HC presence in mixtures of lower flammability. We believe that it may be possible to create ternary or multi-component blends that, with good component selection, mitigate the effects of fractionation and allow the creation of low GWP blends with lower ASHRAE 34 flammability ratings and at the same time energy efficiencies comparable to R-600a.

CHAPTER 9

SCIENTIFIC CONTRIBUTIONS

9 Scientific contributions

9.1 Journal contributions

21 Rodrigo LLopis, Manel Martínez-Ángeles, Daniel Calleja-Anta, Laura Nebot-Andrés
Optimizing R152a/R600 and R290/R600 mixtures for superior energy performance in vapor compression systems: Promising alternatives to Isobutane (R600a)
Applied Thermal Engineering Year 2024
D.O.I. doi.org/10.1016/j.applthermaleng.2024.123070 Editorial: Pergamon-Elsevier Science LTD
Vol. 247 Art. Num 123070 ISSN: 1359-4311 Cites 0

20 Rodrigo LLopis, Manel Martínez-Ángeles, Daniel Calleja-Anta, Laura Nebot-Andrés
Energy performance assessment of an auto-cascade cycle for ultra-low temperatures with the pair R1150 - R600a
Applied Thermal Engineering Year 2024
D.O.I. doi.org/10.1016/j.applthermaleng.2023.122255 Editorial: Pergamon-Elsevier Science LTD
Vol. 240 Art. Num 122255 ISSN: 1359-4311 Cites 0

19 Manel Martínez-Ángeles, Laura Nebot-Andrés, Daniel Calleja-Anta, Rodrigo LLopis
Experimental assessment of CO2/R-152a mixtures in a refrigeration plant with integrated mechanical subcooling
International Journal of Refrigeration – Revue Internationale de Froid. Year 2022
D.O.I. doi.org/ 10.1016/j.ijrefrig.2023.12.005 Editorial: Pergamon-Elsevier Science LTD
Vol. 158 Pages 288-302 ISSN: 0140-7007 Cites 0

18 Daniel Calleja Anta, Daniel Sánchez, Laura Nebot, Ramón Cabello, Rodrigo Llopis,
Alternative mixtures to R-600a. Theoretical assessment and experimental energy evaluation of binary mixtures in a commercial cooler
Applied Thermal Engineering Year 2023
D.O.I. doi.org/10.1016/j.ijrefrig.2023.05.009 Editorial: Pergamon-Elsevier Science LTD
Vol. Art. Num ISSN: 1359-4311 Cites 1

17 Daniel Calleja Anta, Laura Nebot, Daniel Sánchez, Ramón Cabello, Rodrigo Llopis,
Drop-in substitutes for R-600a. Experimental evaluation and optimization of a commercial fridge
Applied Thermal Engineering Year 2022
D.O.I. doi.org/10.1016/j.applthermaleng.2022.118490 Editorial: Pergamon-Elsevier Science LTD
Vol. 211 Art. Num 118490 ISSN: 1359-4311 Cites 3

16 Ramón Cabello, Daniel Sánchez, Rodrigo Llopis, Alejandro Andreu Nacher, Daniel Calleja Anta,
Energy impact of the Internal Heat Exchanger in a horizontal freezing cabinet. Experimental evaluation with the R404A low-GWP alternatives R454C, R455A, R468A, R290 and R1270
International Journal of Refrigeration – Revue Internationale de Froid. Year 2022
D.O.I. doi.org/10.1016/j.ijrefrig.2022.02.007 Editorial: Pergamon-Elsevier Science LTD
Vol. 137 Pages 22-23 ISSN: 0140-7007 Cites 7

15 **Laura Nebot Andrés, Daniel Calleja Anta, Carlos Fossi, Daniel Sánchez, Ramón Cabello, Rodrigo Llopis**
Experimental assessment of different extraction points for the integrated mechanical subcooling system of a CO2 transcritical plant
International Journal of Refrigeration – Revue Internationale de Froid. Year 2022
D.O.I. 10.1016/j.ijrefrig.2022.01.006 Editorial: Pergamon-Elsevier Science LTD
Vol. 136 Pages 8-16 ISSN: 0140-7007 Cites 5

14 **Daniel Sánchez, Alejandro Andreu Nacher , Daniel Calleja Anta, Rodrigo Llopis, Ramón Cabello**
Energy impact evaluation of different low-GWP alternatives to replace R134a in a beverage cooler. Experimental analysis and optimization for the pure refrigerants R152a, R1234yf, R290, R1270, R600a and R744
Energy Conversion and Management Year 2022
D.O.I. doi.org/10.1016/j.enconman.2022.115388 Editorial: Pergamon-Elsevier Science LTD
Vol. 256 Num 115388 ISSN: 0196-8904 Cites 32

13 **Daniel Calleja Anta, Laura Nebot Andrés, Ramón Cabello, Daniel Sánchez, Rodrigo Llopis**
A3 and A2 refrigerants: Border determination and hunt for A2 low-GWP blends
International Journal of Refrigeration – Revue Internationale de Froid. Year 2022
D.O.I. doi.org/10.1016/j.ijrefrig.2021.11.012 Editorial: Pergamon-Elsevier Science LTD
Vol. 134 Pages 86-94 ISSN: 0140-7007 Cites 6

12 **Laura Nebot Andrés, Daniel Calleja Anta, Daniel Sánchez, Ramón Cabello, Rodrigo Llopis**
Experimental assessment of dedicated and integrated mechanical subcooling systems vs parallel compression in transcritical CO2 refrigeration plants
Energy Conversion and Management Year 2022
D.O.I. doi.org/10.1016/j.enconman.2021.115051 Editorial: Pergamon-Elsevier Science LTD
Volumen 252 Art. 115051 ISSN: 0196-8904 Cites 24

11 **Ramón Cabello, Daniel Sánchez, Rodrigo Llopis, Laura Nebot-Andrés, Daniel Calleja-Anta**
Energy evaluation of a low temperature commercial refrigeration plant working with the new low-GWP blend R468A as drop-in of R404A
International Journal of Refrigeration – Revue Internationale de Froid. Year 2021
D.O.I. doi.org/10.1016/j.ijrefrig.2021.01.012 Editorial: Pergamon-Elsevier Science LTD
Vol. 127 Pages 1 - 11 ISSN: 0140-7007 Cites 6

10 **Laura Nebot-Andrés, Daniel Sánchez, Daniel Calleja-Anta, Ramón Cabello, Rodrigo Llopis**
Experimental determination of the optimum intermediate and gas-cooler pressures of a commercial transcritical CO2 refrigeration plant with parallel compression
Applied Thermal Engineering Year 2021
D.O.I. doi.org/10.1016/10.1016/j.applthermaleng.2021.116671 Editorial: Pergamon-Elsevier Science LTD
Vol. 189 Art. 116671 ISSN: 1359-4311 Cites 25

9 **Laura Nebot-Andrés, Daniel Sánchez, Daniel Calleja-Anta, Ramón Cabello, Rodrigo Llopis**
Experimental determination of the optimum working conditions of a commercial transcritical CO2 refrigeration plant with a R-152a dedicated mechanical subcooling.
International Journal of Refrigeration – Revue Internationale de Froid. Year 2021
D.O.I. doi.org/10.1016/j.ijrefrig.2020.10.002 Editorial: Pergamon-Elsevier Science LTD
Vol. 121 Pages 258-268 ISSN: 0140-7007 Cites 21

8 **Rodrigo Llopis, Daniel Calleja-Anta, Angelo Maiorino, Laura Nebot-Andrés, Daniel Sánchez, Ramón Cabello**
TEWI analysis of a stand-alone refrigeration system using low-GWP fluids with leakage ratio consideration.
International Journal of Refrigeration – Revue Internationale de Froid. Year 2020
D.O.I. https://doi.org/10.1016/j.ijrefrig.2020.05.028 Editorial: Pergamon-Elsevier Science LTD
Vol. 118 Pages 279-289 ISSN: 0140-7007 Cites 26

7 **Daniel Sánchez, Jesús Catalán, Ramón Cabello, Daniel Calleja, Rodrigo Llopis, Laura Nebot**
Experimental analysis and optimization of an R744 transcritical cycle working with a mechanical subcooling system.
Energies Year 2020
D.O.I. https://doi.org/10.3390/en13123204 Editorial: MDPI Open Access Journal
Vol: 13 Art. 3204 ISSN: 1996-1073 Cites 20

6 **Laura Nebot-Andrés, Jesús Catalán-Gil, Daniel Sánchez, Daniel Calleja-Anta, Ramon Cabello, Rodrigo Llopis**
Experimental determination of the optimum working conditions of a transcritical CO2 refrigeration plant with integrated mechanical subcooling
International Journal of Refrigeration – Revue Internationale de Froid. Year 2020
D.O.I. https://doi.org/10.1016/j.ijrefrig.2020.02.012 Editorial: Pergamon-Elsevier Science LTD
Vol. 113 Pages 266-275 ISSN: 0140-7007 Cites 38

5 **Jesús Catalán, Daniel Sánchez, Ramón Cabello, Rodrigo Llopis, Laura Nebot, Daniel Calleja**
Experimental evaluation of the desuperheater influence in a CO2 booster refrigeration facility.
Applied Thermal Engineering Year 2020
D.O.I. doi.org/10.1016/j.applthermaleng.2019.114785 Editorial: Pergamon-Elsevier Science LTD
Vol. 168 Art. 114785 ISSN: 1359-4311 Cites 9

4 **Jesús Catalán, Daniel Sánchez, Ramón Cabello, Rodrigo Llopis, Laura Nebot, Daniel Calleja**
Improvements in CO2 booster architectures with different economizer arrangements
Energies Year 2020
D.O.I. https://doi.org/10.3390/en13051271 Editorial: MDPI Open Access Journal
Vol: 13 Art. 1271 ISSN: 1996-1073 Cites 11

3 **Daniel Calleja-Anta, Laura Nebot-Andrés, Jesús Catalán, Daniel Sánchez, Ramón Cabello, Rodrigo Llopis**
Thermodynamic screening of alternative refrigerants for R290 and R600a
Results in Engineering Year 2020
D.O.I. https://doi.org/10.1016/j.rineng.2019.100081 Editorial: Pergamon-Elsevier Science LTD
Vol: 5 Art. 100081 ISSN: 2590-1230 Cites 40

2 **Laura Nebot, Daniel Calleja, Daniel Sánchez, Ramón Cabello, Rodrigo Llopis**
Thermodynamic Analysis of a CO2 Refrigeration Cycle with Integrated Mechanical Subcooling
Energies Year 2020
D.O.I. https://doi.org/10.3390/en13010004 Editorial: MDPI Open Access Journal
Vol: 13 Art. number: 4 ISSN: 1996-1073 Cites 8

1 **Rodrigo Llopis, Daniel Calleja-Anta, Daniel Sánchez, Laura Nebot-Andrés, Jesús Catalán, Ramón Cabello**
R-454C, R-459B, R-457A and R-455A as low-GWP replacements of R-404A: Experimental evaluation and optimization.
International Journal of Refrigeration – Revue Internationale de Froid. Year 2019
D.O.I. doi.org/10.1016/j.ijrefrig.2019.06.013 Editorial: Pergamon-Elsevier Science LTD
Vol. 106 Pages 133 – 143 ISSN: 0140-7007 Cites 26

Cites updated to 23 de May de 2024. Source: SCOPUS

9.2 Contributions to international conferences

32 **Daniel Calleja Anta, Laura Nebot, Rodrigo Llopis**
Self-evaluation by the students of a laboratory practice of a thermodynamic cycle. Sharing of the correction rubric
13th National and 4th International Conference on Engineering Thermodynamics. CNIT13
29/11/2023 Castellon de la Plana Spain Oral communication Year 2023

31 **Daniel Calleja Anta, Daniel Sanchez, Laura Nebot, Rodrigo Llopis**
Investigation of R-600a alternatives mixtures. COP improving in a test bench
13th National and 4th International Conference on Engineering Thermodynamics. CNIT13
29/11/2023 Castellon de la Plana Spain Oral communication Year 2023

30 **Manel Martínez, Laura Nebot Daniel Calleja, Rodrigo Llopis**
CO2/R152a mixtures as working fluids for single-stage refrigerating plants
13th National and 4th International Conference on Engineering Thermodynamics. CNIT13
29/11/2023 Castellon de la Plana Spain Oral communication Year 2023

29 **Rodrigo Llopis, Manel Martínez, Daniel Calleja, Marc García, Laura Nebot**
Experimental optimization and evaluation of an auto-cascade refrigeration system for ultra-low refrigeration temperature
13th National and 4th International Conference on Engineering Thermodynamics. CNIT13

29/11/2023 Castellon de la Plana Spain Oral communication Year 2023

28 Daniel Calleja Anta, Daniel Sánchez, Laura Nebot Andres, Rodrigo Llopis

Energy consumption reduction of a commercial cooler with the use of alternative mixtures to isobutane.

13th National and 4th International Conference on Engineering Thermodynamics. CNIT13

29/11/2023 Castellon de la Plana Spain Oral communication Year 2023

27 Francisco Vidán, Rafael Larrondo, Daniel Sánchez, Manel Martínez, Daniel Calleja, Laura Nebot, Rodrigo Llopis, Ramón Cabello

Experimental evaluation of alternative CO2-based blends for transcritical refrigeration systems.

26th International Congress Of Refrigeration

22/08/2023 París Francia Oral communication Year 2023

26 Daniel Calleja, Giovanni Napoli, Laura Nebot, Daniel Sánchez, Ramón Cabello, Luca Viscito, William Alfonso Mauro, Rodrigo Llopis

Experimental development of alternative mixtures to isobutane. Energy optimization.

26th International Congress Of Refrigeration

22/08/2023 París Francia Oral communication Year 2023

25 Daniel Sánchez, Daniel Calleja, Alejandro Andreu, Laura Nebot, Francisco Vidán, Rodrigo Llopis, Ramón Cabello

Low-GWP hydrocarbons blends as an alternative for the HFC R134a. Energy assessment in a vertical beverage cooler

XII National and III International Conference on Engineering Thermodynamics. CNIT12

29/06/2022 Madrid Spain Oral communication Year 2022

24 Ramón Cabello, Daniel Sánchez, Rodrigo Llopis, Alejandro Andreu, Daniel Calleja, Laura Nebot, Francisco Vidán

Experimental Energy evaluation of the Internal Heat Exchanger mounted in an horizontal freezing cabinet using R404A and its low-GWP alternatives

XII National and III International Conference on Engineering Thermodynamics. CNIT12

29/06/2022 Madrid Spain Oral communication Year 2022

23 Daniel Calleja, Laura Nebot, Ramón Cabello, Daniel Sánchez, Rodrigo Llopis

Search of new A2 refrigerant mixtures. Possibilities of reducing hydrocarbons flammability via mixtures

15th IIR-Gustav Lorentzen Conference on Natural Refrigerants . GL2022

13/06/2022 Trondheim Noruega Poster Year 2022

22 Laura Nebot, Daniel Calleja, Daniel Sánchez, Ramón Cabello, Manel Martínez, Rodrigo Llopis

Mejora energética de sistemas de subenfriamiento mecánico en plantas de refrigeración con CO2.

XI Congreso Ibérico y IX Congreso Iberoamericano de Ciencias y Técnicas del Frío. CYTEF 2022

19/04/2022 Cartagena Spain Oral communication Year 2022

21 Daniel Sánchez, Alejandro Andreu, Daniel Calleja, Laura Nebot, Francisco Vidán, Rodrigo Llopis, Ramon Cabello, Rafael Larrondo Sancho

Optimización energética de los refrigerantes R152a, R1234yf, R290, R1270. R600a y R744, como alternativa al R134a en un armario de refrigeración vertical.

XI Congreso Ibérico y IX Congreso Iberoamericano de Ciencias y Técnicas del Frío. CYTEF 2022

19/04/2022 Cartagena Spain Oral communication Year 2022

20 **Daniel Calleja, Laura Nebot, Manel Martínez Ángeles, Ramón Cabello, Daniel Sánchez, Rodrigo Llopis**

Hacia la búsqueda de mezclas refrigerantes A2 de bajo PCA

XI Congreso Ibérico y IX Congreso Iberoamericano de Ciencias y Técnicas del Frío. CYTEF 2022

19/04/2022 Cartagena Spain Oral communication Year 2022

20 **Laura Nebot, Daniel Sánchez, Ramón Cabello, Daniel Calleja, Carlos Fossi, Rodrigo Llopis**

Current limits of CO2 compressors working in integrated mechanical subcooling cycles

12th International Conference on Compressors and their Systems

6/09/2021 Londres Inglaterra Oral communication Year 2021

19 **Daniel Calleja, Laura Nebot, Carlos Fossi, Daniel Sánchez, Ramón Cabello, Rodrigo Llopis**

Blends with HFOs as alternative to R-600a. Theoretical and experimental evaluation for domestic appliances.

2nd IIR Conference on HFO Refrigerants and Low GWP Blends

16/06/2021 Osaka Japón Oral communication Year 2021

18 **Rodrigo Llopis, Jesus Catalan, Daniel Sanchez, Laura Nebot, Daniel Calleja, Ramon Cabello**

Worldwide performance of CO2 booster systems with auxiliary compressor

14th IIR-Gustav Lorentzen Conference on Natural Refrigerants . GL2020

07/12/2020 Kioto Japón Oral communication Year 2020

17 **Daniel Sanchez, Patricia Aranguren, Alvaro Casi, Ramón Cabello, David Astrain, Miguel Araiz, Rodrigo Llopis, Daniel Calleja-Anta, Laura Nebot-Andrés**

Energy performance of a CO2 transcritical refrigerating plant with a thermoelectric subcooler system

14th IIR-Gustav Lorentzen Conference on Natural Refrigerants . GL2020

07/12/2020 Kioto Japón Oral communication Year 2020

16 **Daniel Sanchez, Daniel Calleja, Laura Nebot, Ramon Cabello, Rodrigo Llopis**

Experimental analysis of CO2 blends for transcritical refrigeration systems

14th IIR-Gustav Lorentzen Conference on Natural Refrigerants . GL2020

07/12/2020 Kioto Japón Oral communication Year 2020

15 **Laura Nebot, Daniel Sanchez, Ramon Cabello, Daniel Calleja, Rodrigo Llopis**

Experimental evaluation of CO2 refrigeration plant with integrated mechanical subcooling system at optimal working conditions

14th IIR-Gustav Lorentzen Conference on Natural Refrigerants . GL2020

07/12/2020 Kioto Japón Oral communication Year 2020

14 **Daniel Calleja, Daniel Sanchez, Ramon Cabello, Laura Nebot, Rodrigo Llopis**

Experimental evaluation of natural refrigerant blends as substitutes for R-600a in a domestic fridge and freezer

14th IIR-Gustav Lorentzen Conference on Natural Refrigerants . GL2020

07/12/2020 Kioto Japón Oral communication Year 2020

13 **Ramón Cabello, Daniel Sánchez, Laura Nebot, Daniel Calleja, Rodrigo Llopis**

Evaluación energética del refrigerante R468A como alternativa al R404A en aplicaciones comerciales de baja temperatura

X Congreso Ibérico y VIII Congreso Iberoamericano de Ciencias y Técnicas del Frío. CYTEF 2020

11/11/2020 Pamplona Spain Oral communication Year 2020

12 Laura Nebot, Jesús Catalán, Daniel Sánchez, Ramón Cabello, Daniel Calleja, Rodrigo Llopis

Evaluación experimental de un ciclo de subenfriamiento mecánico integrado en una planta de refrigeración con CO_2

X Congreso Ibérico y VIII Congreso Iberoamericano de Ciencias y Técnicas del Frío. CYTEF 2020

11/11/2020 Pamplona Spain Oral communication Year 2020

11 Daniel Calleja, Laura Nebot, Andrea Ariano, Daniel Sánchez, Ramón Cabello, Rodrigo Llopis

Evaluación experimental de mezclas alternativas al R-600a en un frigorífico y un congelador doméstico

X Congreso Ibérico y VIII Congreso Iberoamericano de Ciencias y Técnicas del Frío. CYTEF 2020

11/11/2020 Pamplona Spain Oral communication Year 2020

10 Rodrigo Llopis, Laura Nebot, Daniel Sánchez, Jesús Catalán, Daniel Calleja, Ramón Cabello

Subcooled CO_2 *refrigeration cycles: current status and lines of research*

X Congreso Ibérico y VIII Congreso Iberoamericano de Ciencias y Técnicas del Frío. CYTEF 2020

11/11/2020 Pamplona Spain Oral communication Year 2020

9 Daniel Sánchez, Daniel Calleja, Laura Nebot, Jesús Catalán, Rodrigo Llopis, Ramón Cabello

Experimental analysis of alternative blends of refrigerants for CO2 transcritical refrigeration systems

X Congreso Ibérico y VIII Congreso Iberoamericano de Ciencias y Técnicas del Frío. CYTEF 2020

11/11/2020 Pamplona Spain Oral communication Year 2020

8 Daniel Sánchez, Ramón Cabello, Rodrigo Llopis, Jesús Catalán, Laura Nebot, Daniel Calleja, Eduardo Gil

Energy improvements in a stand-alone transcritical refrigeration system using a low-GWP mixture of CO_2*/R1270*

25th IIR International Congress of Refrigeration

24/08/2019 Montreal Canada Oral communication Year 2019

7 Daniel Calleja, Laura Nebot, Jesús Catalán, Rodrigo Llopis, Daniel Sánchez, Ramón Cabello

Experimental evaluation of low-GWP replacements of R-404A in a stand-alone commercial cabinet for fresh product

25th IIR International Congress of Refrigeration

24/08/2019 Montreal Canada Oral communication Year 2019

6 Laura Nebot, Rodrigo Llopis, Jesús Catalán, Daniel Sánchez, Daniel Calleja, Ramón Cabello

Thermodynamics analysis of CO_2 *refrigeration cycles working with mechanical subcooling systems*

25th IIR International Congress of Refrigeration

24/08/2019 Montreal Canada Oral communication Year 2019

5 Laura Nebot, Daniel Calleja, Rodrigo Llopis, Jesús Catalán, Daniel Sánchez, Ramón Cabello

Mechanical subcooling systems for CO_2 *refrigeration cycles. Thermodynamic analysis.*

XI National and II International Engineering Thermodynamics Congress

14/06/2019 Albacete Spain Oral communication Year 2019

4 Daniel Calleja, Laura Nebot, Jesús Catalán, Rodrigo Llopis, Daniel Sánchez, Ramón Cabello

Thermodynamic screening for alternative refrigerants for R-290 and R-600a.

XI National and II International Engineering Thermodynamics Congress

14/06/2019 Albacete Spain Oral communication Year 2019

3 Daniel Calleja, Jesús Catalán, Laura Nebot, Rodrigo Llopis, Daniel Sánchez, Ramón Cabello

Low-GWP replacements of R-404A for commercial refrigeration. Experimental analysis.

XI National and II International Engineering Thermodynamics Congress

14/06/2019 Albacete Spain Oral communication Year 2019

2 **Jesús Catalán, Laura Nebot, Daniel Calleja, Daniel Sánchez, Rodrigo Llopis, Ramón Cabello**

Experimental comparison of CO_2 Booster architecture for commercial refrigeration

XI National and II International Engineering Thermodynamics Congress

14/06/2019 Albacete Spain Oral communication Year 2019

1 **Daniel Sánchez, Patricia Aranguren, Jesús Catalán, Laura Nebot, Daniel Calleja, Rodrigo Llopis, Ramón Cabello**

Development of a heat transfer test-bench for educational purpose based on Arduino.

XI National and II International Engineering Thermodynamics Congress

14/06/2019 Albacete Spain Oral communication Year 2019